School of Biodiversity, One Health & Veterinary Medicine
College of Medical, Veterinary and Life Sciences

Screening of Malaria Infections Using AI-Powered Infrared Spectroscopy

Submitted in fulfilment of the requirements for the degree of Doctor of Philosophy

By

Issa H. Mshani

Submitted on the 23rd of September 2024

Abstract

Over the past two decades, malaria control efforts have averted 2.1 billion cases and saved 11.7 million lives globally, yet the disease still claims over 600,000 lives annually, mostly in sub-Saharan Africa. Key interventions like insecticide-treated nets, indoor spraying, and antimalarial drugs have driven success, but major challenges persist. Accurate, timely detection of malaria parasites and scalable population screening remain difficult, especially in low transmission areas. Although WHO promotes surveillance as a core pillar of elimination, resource constraints in low-income countries hinder the expansion of effective, affordable surveillance systems. Current malaria screening tools, such as rapid diagnostic tests (RDTs) and microscopy, are essential for detecting parasites but have limitations, particularly in low transmission settings and at low parasite densities, which hampers elimination efforts. While more sensitive methods like polymerase chain reaction (PCR) are available, they are costly and impractical for widespread use in resource-limited areas. As a result, there is an urgent need for sensitive, cost-effective, and scalable tools capable of detecting low-density infections, especially in low transmission contexts.

Recent studies have shown the potential of using artificial intelligence (AI)-powered infrared spectroscopy to detect malaria parasites in human blood. This approach is reagent-free, robust, user-friendly, quick and potentially cost-effective. However, to address the gaps in current methods for malaria screening and diagnosis, it was important to also assess factors such as lowest detectable parasite density and performance in low transmission settings before adoption by malaria control programs.

The primary aim of my PhD research was to improve malaria surveillance by exploring the application of infrared spectroscopy and machine learning (IR-ML) for malaria screening in population surveys. To achieve this, I pursued five complementary objectives: (1) reviewing the potential applications of IR-ML for malaria surveillance, developing a target product profile, and identifying key considerations and research gaps for integrating IR-ML into control efforts; (2) demonstrating the performance of mid-infrared spectroscopy and machine learning (MIRs-ML) across varying parasite densities and anaemic conditions; (3) conducting

cross-sectional surveys to map malaria burden in an endemic setting, assessing the performance of existing methods (RDTs, microscopy, and qPCR) for risk stratification; (4) evaluating MIRs-ML performance in areas with differing prevalence rates; and (5) developing a web-based platform to deliver MIRs-ML results to end users. The ultimate goal was to advance the development of MIRs-ML as a scalable malaria screening tool, adaptable to both high (prevalence rate >30%) and low transmission (prevalence rate <5%) settings, with the potential to transform malaria detection and monitoring.

To achieve the first objective, I reviewed the current state of infrared spectroscopy and machine learning (IR-ML) for malaria surveillance, comparing its advantages and limitations to existing tools like PCR, RDTs, and microscopy. This review identified research gaps and developed a target product profile (TPP) for integrating infrared technology into routine surveillance. For the second objective, I conducted lab experiments using blood from 70 malaria-free volunteers in Tanzania, diluted with cultured *Plasmodium falciparum* to create different parasitemia and anemia levels. These samples were used to create dry blood spots, which were then scanned using ATR-FTIR spectroscopy. Using supervised machine learning classifiers trained on a subset of the samples, we achieved over 90% accuracy in detecting malaria, even at low parasite densities, and across different anemia conditions. Field applications of these models demonstrated over 80% accuracy in predicting natural infections.

The third and fourth objectives involved cross-sectional surveys in 93 sub-villages in southeastern Tanzania, screening 7,628 individuals using RDTs and microscopy, with two-thirds analyzed by qPCR. qPCR consistently detected higher transmission rates, revealing that RDTs and microscopy underestimate malaria prevalence, particularly in fine-scale mapping. I then used the survey data to evaluate MIRs-ML performance in areas with varying malaria prevalence rates from low to high. Again, the ML classifiers achieved over 90% accuracy and sensitivity in both high and low transmission settings. We also observed that performance was slightly lower in low transmission areas when trained exclusively on high transmission data, compared to when the models were trained with data from across all settings.

Finally, to make these models readily available to users in future, we developed a web-based platform that allows scientists and national programs to access pretrained ML models for instant malaria infection predictions. This platform is currently powered by models trained on over 5,000 human blood samples and 40,000 mosquitoes, and will continue to expand with data from Tanzania, Burkina Faso, and the UK. The ultimate goal is to democratize the applications of these models across different user groups in different countries.

In conclusion, through population surveys, I demonstrated the limitations of RDTs and microscopy for mapping malaria risk. I developed MIRs-ML in the lab to overcome these challenges and tested it in the field, showing its promise. This research has significantly advanced our understanding of the potential of MIRs-ML for malaria screening. It has demonstrated that the approach has high sensitivity and is capable of detecting parasite levels as low as one parasite/µl of blood, making it particularly suitable for large-scale population surveys and enhancing risk stratification efforts. The study also highlighted the limitations of current screening tools, such as RDTs and microscopy, which perform poorly in low transmission settings compared to the more sensitive PCR. This underscores the urgent need for new, more sensitive approaches for precise stratification. This PhD research shows that MIRs-ML could meet these needs, making it a valuable complement to existing surveillance methods and a promising tool for malaria screening, even in low transmission areas.

Contents

List of Tables

List of Figures

Declaration of Authorship

I hereby declare that the work written in this thesis is entirely my own, except where otherwise stated. I honestly recognized the contributions of laboratory and field technicians, volunteers and the co-authorship of my supervisors, Dr Simon Babayan, Dr Francesco Baldini, and Professor Fredros Okumu. I further declare that, no part of this work has been submitted as part of any other degree

Acknowledgements

I embarked on my PhD journey in October 2020, during the peak of the COVID-19 pandemic. Despite the uncertainties and difficulties, I am proud to have reached the finish line on time after four demanding years. This journey has been one of the most profound learning experiences of my life, offering lessons I could not have gained elsewhere. It has shaped me as a young man, both academically and personally, in research and in life. Today, at 29 years old, I am grateful to be completing my PhD at this young age. Words cannot fully express my gratitude, but I give all praise to Almighty Allah, the Lord of the universe, for making this possible. It feels like a miracle not only for me but also for my parents, my family, my clan, my village, and even my country.

As the African proverb says, ***"It takes a village to raise a child."*** My PhD journey has been made possible by the support of many. I have achieved this by standing on the shoulders of giants, and I want to raise a heartfelt toast to my supervisors, *Dr. Simon Babayan*, *Dr. Francesco Baldini*, and *Prof. Fredros Okumu*. You are the pillars upon which this accomplishment rests.

To ***Dr. Simon Babayan***, I owe a tremendous debt of gratitude. Thank you, Simon, for agreeing to be my primary supervisor. I remember initially applying for an MSc program, but you and the other supervisors saw potential in me and encouraged me to upgrade to a PhD. Despite the shift, you remained confident in my ability to reach the finish line and took on the role of my primary supervisor. I vividly recall your unwavering support, including the times you would wake up at 7 a.m. UK time to meet with me online for almost two consecutive weeks, discussing analyses and offering guidance. Your insistence that I reach out anytime I faced challenges meant a great deal to me.

I am especially grateful for your words of encouragement. Every time you mentioned, *"Issa, your progress is fantastic",* it fueled my confidence and motivated me to push toward completion. Importantly, Simon, I thank you for the profound impact you've had on my career development, particularly in computational skills. You taught me Python, machine learning, statistics, and technology, all of which have been instrumental in

getting me to the finish line. Your push for me to constantly learn new skills, such as LaTeX and various coding environments, has enriched my professional toolkit, and I am certain these abilities will continue to serve me throughout my career.

One of the most valuable lessons I have learned from you is the power of remaining calm and humble, despite the depth of knowledge one may possess. Simon, thank you for your support and guidance throughout every stage of this journey—from the initial application, research design, and analysis to writing and final completion. I will hold on to your teachings, especially the importance of striving to always be useful, and I promise to carry forward this wisdom with added humility and calmness, as you have so clearly exemplified.

To ***Dr. Francesco Baldini***, I would like to express my heartfelt gratitude. First, thank you for agreeing to be my supervisor and for the tireless support you have provided throughout my PhD journey. In the early days of my studies, during the peak of the COVID-19 pandemic, you sacrificed your time, despite the lockdown, to teach me malaria parasite culture in the university laboratory. The hours we spent calculating dilution formulas to create various parasite concentrations and engineering anemia conditions in the lab were invaluable. Without your technical expertise,these achievements would have been impossible.

I can still hear your voice today regarding the drawings on your office whiteboard, where we discussed how best to present and write our lab paper result section. Francesco, I have preserved pictures of those drawings and voice notes that I will cherish for many years. More importantly, you have been an encouraging supervisor who has tirelessly supported me. I often reflect on the challenging times in Bagamoyo, where we faced nearly seven months of parasite contamination without generating results. Yet, you always believed we would succeed, meeting with me and my colleagues frequently to suggest solutions until we finally overcame those obstacles. Thank you, Francesco.

You consistently believed in the quality of my work throughout this journey, which inspired me to persevere and ultimately reach the finish line. From formulating research questions to writing, I have learned so much from you, including the importance of organizational skills. Your exceptional level of organization and planning is something I aspire to emulate in my career. I will always carry with me your advice to help others achieve their goals in the future. Thank you, Francesco.

To ***Professor Fredros Okumu***, I write this with tears in my eyes. Fredros, you are the architect behind the possibilities and miracles in my career today. It is through you that I met my other remarkable supervisors; it is through you that the funding for this PhD became possible. I can simply say that you made all this possible, and the best way to express my gratitude is to emphasize it in Swahili: Asante Sana, Fredros.

I know you may not remember, but you once asked me and a colleague to escort our guests—Simon, Francesco, Heather, and others—to Mikumi National Park when they visited Ifakara for the closure of one of the infrared projects. That was when I first met Simon, Francesco, and Heather, without imagining they would later become my supervisors alongside you.

Thank you for the trust you placed in me, Fredros, from the first day we met. I remember our meeting in Bagamoyo when you invited me to come to Ifakara. At that time, I could not have imagined my career could be transformed to this level. I even recall the day we sat at the rest house in Ifakara when you encouraged me to register for a PhD program. Accepting this opportunity was daunting, but you had faith that we would succeed together and insisted that I pursue it, assuring me of your unwavering support. I witnessed your tireless dedication, and I believe you are just as happy, if not more so, than I am to see this come to fruition.

Thank you for your encouragement from the very beginning and for the overall support you have provided throughout my PhD journey. This includes inviting me to attend various conferences, providing scientific leadership roles, and giving me opportunities to present our work to guests visiting Ifakara. You have been a positive and supportive presence throughout, always teaching me how to achieve quality work. I am grateful for your time; whenever I sought help, you were even willing to meet on weekends or take calls late at night. I remember receiving your calls and explaining how I should improve my work,analysis,writing, and much more.

Through you, I have learned what it means to be a scientist and how to navigate success with humility. I will always remember your statement that we should make our communities proud and strive to improve people's health and well-being. Honestly, I believe we have a long way to go together, and I will ensure that we take the fight against malaria to the next level for the betterment of our community's health. Fredros, words cannot express what I feel and how thankful I am for your support in my career. Thank you very much, Fredros.

I would also like to express my heartfelt gratitude to Mr. Frank M. Jackson, with whom I led our team in the field. Thank you for your unwavering support during my PhD. I am confident that you will become an excellent scientist, and I wish you all the best.

I must also acknowledge the dedicated individuals who made it possible for us to screen 10,000 individuals for malaria in the remotest villages of Tanzania during my PhD. This achievement would not have been possible without the contributions of Faraja E. Makala, Elihaika G. Minja, Magreth I. Henry, Tumpe G. Mwandyala, Abigael W. Magesa, Magreth C. Magoda, Scolastica N. Hangu, Alex T. Ngonyani, Jiddah A. Ally, Alfred J. Simfukwe, Amisa N. Rajabu, Scolastica A. Ndonde, Rahma S. Kikweo,

Benson B. Makua, Jacob J. Nyooka, Festo I. Tangaliola, Stephen J. Magasa, Joyce Y. Jackson, Idrissa S. Mchola, Fidelis D. Mbena, Sylyakus V. Mlembe, Nasoro S. Lilolime,Said Abbasi and Faraji Abilahi. I would also like to extend special thanks to Dr. Mohammed Mgeni, Dr. Lorenz Hofer, Prisca Kweyamba, and Rehema Mwanga.

I am especially grateful to my flatmate for a year in Glasgow, Mr. Halid S. Salim, whose presence made my stay enjoyable. I will cherish the stories we shared at night and the delightful meals you kindly prepared for me as a surprise after my long days and nights at the university. Thank you for your encouragement and friendship, Halid. To my best friends in Bagamoyo, Said Aziz and Suleiman Liguo, thank you for making my time there enjoyable. With you both, I never felt weary of my surroundings.

I would like to extend my appreciation to our project administrator, Rukia M. Njalambaha, for her support with various challenges, including procurement and payment arrangements. Additionally, I thank the entire Ifakara Health Institute team, the communities in the villages where we conducted this work, the funding bodies (Swiss TPH, Royal Society, and the Bill and Melinda Gates Foundation), and my colleagues at the University of Glasgow, especially the Vectors Glasgow group and the laboratory team, for the knowledge exchange and moments of camaraderie.

I would also like to express my gratitude to Ms. Zuhura Sumbe in countless ways; your presence has been invaluable. Thank you, Zuhura.

Lastly, I would like to thank my family, especially my father, ISP Hassan R. Mshani. Thank you for believing in the value of education and for the investments you have made in my life and the lives of my sisters. I hope this PhD fulfills your aspirations for me, instead of the military salute we used to joke about. I dedicate this thesis to my mother, whose encouragement and positivity have always uplifted me. I also thank my two sisters; your support gives me confidence during the toughest times.

Achievements & Contributions

Published chapters:

1. **Mshani, I.H.**, Siria, D.J., Mwanga, E.P. et al. *Key considerations, target product profiles, and research gaps in the application of infrared spectroscopy and artificial intelligence for malaria surveillance and diagnosis*. Malar J 22, 346 (2023). https://doi.org/10.1186/s12936-023-04780-3.

2. **Mshani, I.H.**, Jackson, F.M., Mwanga, R.Y. et al. *Screening of malaria infections in human blood samples with varying parasite densities and anaemic conditions using AI-Powered mid-infrared spectroscopy*. Malar J 23, 188 (2024). https://doi.org/10.1186/s12936-024-05011-z.

3. **Mshani, I.H.**, Jackson, F.M., Minja, E.G., Abbas, S., Lilolime, N.S., Makala, F.E., Lazaro, A.B., Mchola, I.S., Mukabana, L.N., Kahamba, N. and Limwagu, A., 2024. *Comparison of Fine-Scale Malaria Strata Derived from Population Survey Data Collected Using mRDTs, Microscopy and qPCR in South-Eastern Tanzania*. Malaria J 23, no. 1 (2024): 376.; https://doi.org/10.1186/s12936-024-05191-8

Chapters to be submitted

1. **Mshani, I.H.**, Jackson, F.M., Minja, E.G., Abbas, S., Lilolime, N.S., Makala, F.E., Lazaro, A.B., Mchola, I.S., Mukabana, L.N., Kahamba, N. *Performance of Mid-Infrared Spectroscopy and Machine Learning for Detecting Malaria Infections in High and Low Transmission Settings*.

2. **Mshani, I.H.,** Jackson, F.M., Neema, Z.F, Bazowman, S.B., Rogers S., *A Web-Based AI Platform for Real-Time Analysis of Infrared Spectral Data to Enhance Parasitological and Entomological Surveys of Malaria*.

Scientific awards as a result of this PhD

1. Certificate of Top-performing young scientist of the year 2023, Ifakara Health Institute.
2. American society of tropical medicine and hygiene young investigator award: 2023.

Media coverage

1. Mtanzania ang'ara tuzo za utafiti Marekani 2023 https://www.mwananchi.co.tz/mw/habari/kitaifa/mtanzania-ang-ara-tuzo-za-utafiti-marekani-4411598
2. Tanzanian wins Researcher Award in US https://www.thecitizen.co.tz/tanzania/news/national/tanzanian-wins-young-researcher-award-in-the-us-4411888
3. PROMISING: Meet this rising star in global health, 25 Oct 2023, Ifakara Health Institute; https://ihi.or.tz/our-events/282/details/

List of Abbreviations

- **AI**: Artificial Intelligence
- **ANN**: Artificial Neural Networks
- **API**: Annual Parasite Incidence
- **ATR**: Attenuated Total Reflectance
- **ATR**: Attenuated Total Reflection
- **FTIR**: Fourier Transform Infrared
- **BC**: Bagging Classifier
- **DBS**: Dried Blood Spots
- **DT**: Decision Tree
- **EDTA**:Ethylenediaminetetraacetic Acid
- **ELISA**: Enzyme-Linked Immunosorbent Assays
- **ET**: Extra Tree
- **HEPES**:4-(2-Hydroxyethyl)-1-piperazineethanesulfonic Acid
- **LAMP**:Loop-Mediated Isothermal Amplification
- **LR**: Logistic Regression
- **MIRs**: Mid-Infrared Spectroscopy
- **ML**: Machine Learning
- **NIRs**: Near-Infrared Spectroscopy
- **PCR**: Polymerase Chain Reactions
- ***Pf*PR**: *Plasmodium falciparum* Prevalence Rate
- **RDTs**: Rapid Diagnostic Tests
- **RF**: Random Forest
- **RPMI**:Roswell Park Memorial Institute 1640 Media
- **SVM**: Support Vector Machine
- **XGB**: Gradient Boosting

Chapter 1: Introduction

1.1 Malaria burden

In 2022, the World Health Organization (WHO) reported 249 million cases of malaria globally, making this one of the most important public health challenges of our time [1]. In addition, there were over 600,000 deaths, 94% of which in the WHO-Africa region [1]. Over 50% of these deaths were concentrated in just four countries: Nigeria, the Democratic Republic of Congo, Niger, and the United Republic of Tanzania. While there has been an upward age-shift towards school-age children in many regions [2,3], the most vulnerable populations continue to be pregnant women and children under the age of five [1, 4]. In 2022, approximately 36% of pregnant women in WHO-African region were exposed to malaria, underscoring the critical need for targeted interventions to protect these high-risk groups [1].

Between 2000 and 2015, malaria-caused deaths were notably reduced by half, but this decline has since slowed [1, 5]. For example, the WHO's Global Technology Strategy (GTS) target of reducing malaria incidence to 26 per 1000 population at risk by 2022 has not been met [1]. The disruption caused by COVID-19 significantly contributed to these unmet targets and the increase in burden [6, 7]; and malaria deaths increased by 10% in 2020 compared to 2019 [1, 8]. In the latest WHO report, the challenge of the warming climate was also highlighted alongside other biological threats including insecticide resistance, failing rapid diagnostic tests, drug resistance and invasive vector species [1].

1.2 The epidemiology of malaria

Malaria is transmitted by female mosquitoes of the genus *Anopheles* within the phylum Arthropoda [9, 10]. When an infected female mosquito bites a person to feed on blood, it can pass on the infectious stage of the malaria parasite [11]. In rare instances, malaria can also be transmitted through blood transfusions or organ transplants between infected and uninfected individuals [12, 13]. Malaria infections in humans are caused by five single-celled eukaryotic protozoan parasites: *Plasmodium falciparum*, *Plasmodium ovale*, *Plasmodium malariae*, *Plasmodium vivax*, and *Plasmodium knowlesi* [14, 15]. *P. falciparum* is the predominant cause of

malaria deaths, particularly in Africa. While other malaria-causing parasites have lower mortality rates than *P. falciparum*, their infections can still cause mild to severe malaria and fatalities [1, 16–18]. The taxonomic classifications of malaria parasites are outlined in Figure 1.1.

1.2.1 Malaria parasites

The protozoan parasite *Plasmodium* belongs to the subgenus *Apicomplexa* within the super phylum *Alveolata* [19], the phylum also consist of other parasite of human and veterinary importance such as the *Toxoplasma*,*Theileria*, *Eimeria*, *Babesia*, and *Cryptosporidium* [20, 21]. Like other apicomplexans, *Plasmodium* is an obligate parasite that possesses a non-photosynthetic plastid called the Apicoplast within its cell, Figure 1.1 [22, 23]. This organelle plays a crucial role in the parasite's survival, aiding in various metabolic pathways essential for its lifecycle, including the synthesis of fatty acids, heme, and other biosynthetic products [23, 24]. The parasite also possesses an apical complex, which facilitates its invasion of host cells [24, 25].

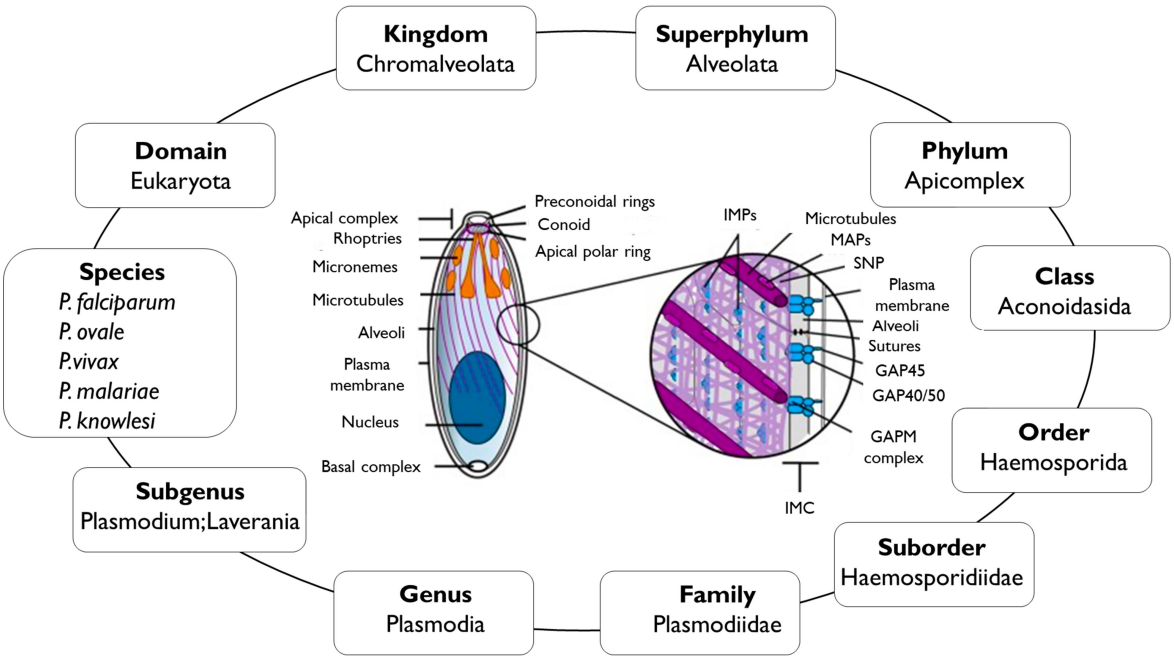

Figure 1.1: Full-spectrum classification of the *Plasmodium* genus, a human protozoan parasite, with a model structure at the centre. Includes the IMC (inner membrane complex), MAP (microtubule-associated protein), SPN (subpellicular network), IMP (inner membrane particle), GAP45, GAP40, or GAP50 (Glycosylphosphatidylinositol (GPI)-anchored proteins 45, 40, or 50), and GAMP (Glycosylphosphatidylinositol (GPI)-anchored membrane protein). Adapted from [19, 26]

1.2.2 Malaria parasite distribution and clinical burden

The distribution of malaria parasites varies significantly across regions, with *P. falciparum* being widespread in most malaria-endemic areas, particularly predominating in tropical Africa [1, 5, 27]. This species is also responsible for the majority of severe malaria cases and deaths [1]. In contrast, *P. vivax* is prevalent in South and Central America, as well as Southeast Asia, but notably absent from most of Africa due to the Duffy-negative blood type among African populations [1, 17, 28, 29].

The Duffy-negative phenotype confers immunity to most Africans against *P. vivax* infections since the parasite requires Duffy antigen receptors to attach to and invade red blood cells [28]. These genetic traits spread among African populations approximately 42,000 years ago, although recent studies have reported instances of *P. vivax* infections in both Duffy-negative and Duffy-positive individuals [30–32]. Additionally, *P. vivax* exhibits resilience in challenging environments by forming dormant stages, hypnozoites, in the liver cells of its hosts, leading to relapses months or years after the initial infection [33]. Clinically, *P. vivax* infections typically present with lower parasitaemia levels compared to *P. falciparum*, targeting reticulocytes, which are smaller than mature red blood cells [34, 35]. Co-infections between *P. falciparum* and *P. vivax* have been reported in over 10% of positive samples in *P. vivax* prevalent areas [36].

P. malariae, although relatively rare globally, co-infects frequently with *P. falciparum*, particularly in sub-Saharan Africa, southeast Asia, and western Pacific where it is more prevalent [37]. This species is characterized by several distinctive clinical features and a notably prolonged parasite life cycle, causing fever every 72 hours [37, 38]. Chronic malaria may result from its extended life cycle and low infection levels, triggering robust immune responses and potentially leading to nephritis due to immune complex deposition in the kidneys [39, 40].

P. ovale is predominantly found in Asia and parts of Africa, particularly West Africa [41]. Initially considered a single species, recent molecular advancements have identified two distinct subspecies: *P. ovale wallikeri* and *P. ovale curtisi* [42]. Both subspecies exhibit similar clinical symptoms and complications, including relapsing malaria due to dormant liver-stage parasites, and they respond to similar antimalarial treatments [42, 43]. Additionally, coinfections of *P. ovale* with *P. falciparum* have been observed [44].

Lastly, *P. knowlesi* is primarily found in the forested regions of southeast Asian countries such as Thailand, Philippines, Malaysia, and Indonesia [45, 46]. Noteworthy for its potential to cause severe malaria cases, including cerebral malaria, acidosis, and severe anaemia, *P. knowlesi* was initially considered to infect only non-human primates like *Macaca fascicularis* and *M. nemestrina* (the long-tailed and pig-tailed macaques respectively) [14, 47, 48]. Human infections were first recorded in Southeast Asia in the 1960s, leading to its recognition as the fifth species capable of causing malaria in humans. Transmission occurs between human and long-tailed macaques when a human host is exposed via mosquitoes that previously fed on *P. knowlesi*-infected long-tailed macaques [45, 49]. Due to its morphological resemblance to *P. malariae* under microscopy, advanced molecular techniques are necessary for accurate identification [46].

Importantly, *P. falciparum* is distinguished from other **Plasmodium** species by its capacity to cause severe and fatal malaria, especially cerebral malaria. It infects a higher proportion of red blood cells than *P. vivax*, *P. ovale*, *P. malariae*, and *P. knowlesi*, and can trigger complications like severe anaemia. A key feature is its sequestration of infected erythrocytes in the microvasculature, particularly in the brain, mediated by proteins such as *P. falciparum* Erythrocyte Membrane Protein 1 (PfEMP1). This process induces inflammatory immune responses and obstructs blood flow, leading to cerebral malaria, characterized by coma and high mortality. Other *Plasmodium* species lack this severe sequestration ability, making *P. falciparum* particularly lethal [50].

Overall, *Plasmodium* parasites that infect humans share similar life cycles and are predominantly transmitted by Anopheline mosquitoes, exhibiting both susceptibility and resistance to various antimalarial drugs [14].

1.2.3 African malaria vectors

Africa has over seven dominant malaria vector species, including *Anopheles arabiensis*, *Anopheles funestus*, *Anopheles gambiae*, *Anopheles melas*, *Anopheles coluzzii*, *Anopheles merus*, *Anopheles moucheti*, and *Anopheles nili* [51–53]. The primary vectors responsible for the majority of malaria transmissions in Africa are *An. gambiae*, *An. arabiensis*, and *An. funestus* [51]. Recently, there have been reports of the invasion of *An. stephensi*, a mosquito native to Asia, in regions of Africa such as Ethiopia, Kenya and more [54–56]. Known for its vector competence, its presence in new regions can affect local malaria dynamics, especially in urban settings [57].

An. gambiae and *An. arabiensis* belong to the *Anopheles gambiae* complex, which also includes *An. melas*, *An. merus*, *An. coluzzii*, *An. bwambae*, *An. quadrimaculatus* and *An. amharicus* [58, 59]. Despite their occasional high population densities, *An. melas* and *An. merus* exhibit lower vectorial capacity compared to *An. gambiae*, *An. coluzzii* and *An. arabiensis*. On the other hand, the *An. funestus* subgroup comprises nearly 13 sibling species: *An. funestus sensu stricto* (often referred to simply as *An. funestus*), *An. funestus*-like, *An. rivulorum*, *An. rivulorum*-like, *An. leesoni*, *An. parensis*, *An. longipalpis* types A and C, *An. vaneedeni*, *An. aruni*, *An. confuses*, *An. brucei*, and *An. fuscivenosus* [60]. Importantly, *An. funestus* s.s is considered the most competent malaria vector in this group [61].

The malaria vector species exhibit different behavioural profiles, which underlie their vectorial capacity across regions. *An. arabiensis* exhibits diverse feeding and resting behaviors influenced by factors like geography and host availability [53,59,62]. Though it commonly bites humans, this species can be zoophilic, preferring to feed on animals over humans compared to *An. gambiae* and *An. funestus*, and it tends to feed and rest outdoors rather than indoors [59, 63]. Although it is predominantly zoophilic and exophilic [63, 64] in areas where cattle are abundant, in certain regions such as West Africa, it has been reported to be anthropophilic, feeding on humans, and endophilic, resting indoors, and endophagic, biting indoors [63]. *An. arabiensis* breeds in various habitats, including shallow, clear, small, and temporary bodies of fresh water [65]. It thrives in habitats like partially shaded streams and man-made environments such as rice farms, especially those exposed to sunlight, this species also exhibits tolerance to dry seasons [58, 65, 66]. Its biting activity typically occurs during the night, with peaks in the early evening hours [67].

An. gambiae is widely recognized as one of the most effective malaria vectors due to its extensive distribution and high behavioral adaptability. This species is particularly successful because of its ability to adapt to various environmental conditions [58, 59, 68]. *An. gambiae* is opportunistic in its feeding habits and has a longer lifespan compared to other species. It primarily feeds on human blood (anthropophilic), although less frequently than *An. funestus* [58, 59].

An. funestus s.s (hereafter referred to simply as *An. funestus*) is the only member of its group recognized for its significant role in malaria transmission [69, 70]. This species breeds in diverse habitats such as swamps, large ponds, and lake edges, thriving in both shaded and sunlit conditions [52, 59, 71]. It prefers permanent and semi-permanent freshwater habitats with emergent vegetation and shaded plant leaves [71–73]. *An. funestus* feeds mostly on humans (anthropophilic) but can also feed on other animals, such as cattle, and tends to bite during the early evening and morning hours [69, 74]. It also prefers to rest indoors (endophilic) and has a notably long lifespan [69]. Morphologically, *An. funestus* can only be distinguished

from other subgroup members at certain stages of its growth [75, 76]. It is considered a primary malaria vector due to its strong preference for human blood and a long life span, which enhances its efficiency in transmitting malaria [69]. In some African regions such as southeastern Tanzania, this species is responsible for the majority of malaria infections, even in settings where the vector has lower abundance than other species [69]. This can be attributed to *An. funestus* harboring a higher proportion of sporozoites infections (the infective stage for malaria transmission) compared to *An. arabiensis* and *An. gambiae*, despite the latter two species having higher population densities [69, 77].

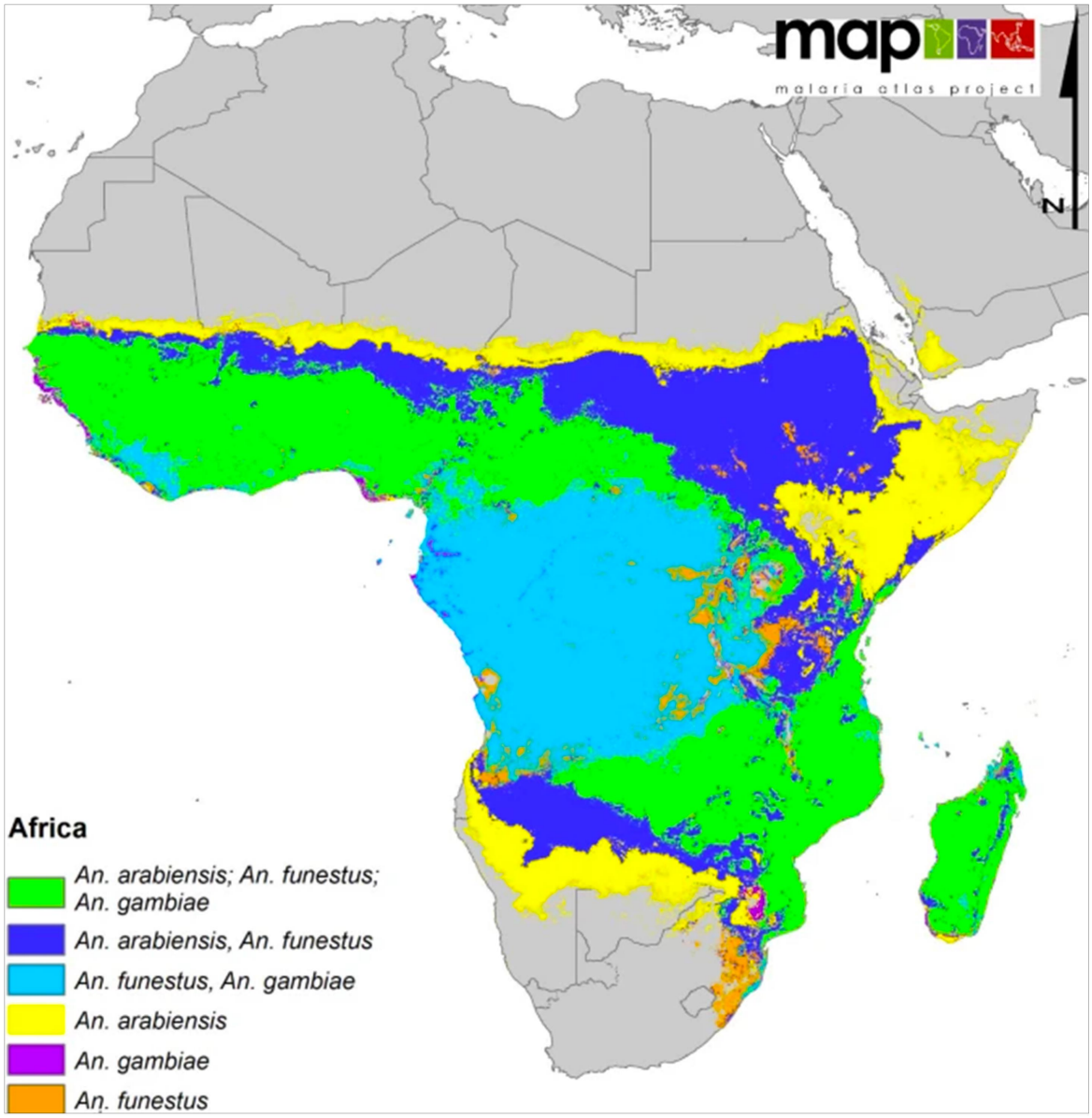

Figure 1.2: Distribution of the major African malaria vector, adopted from [51].

1.3 Malaria transmission

Transmission of malaria primarily involves two steps: (i) Female Anopheles mosquitoes become infected when they feed on the blood of a person infected with malaria, (ii) Subsequently, these infected female mosquitoes transmit the infectious stage of the malaria parasite to a healthy individual during another blood meal [14]. Thus, the malaria parasite completes its life cycle involving two organisms: a vertebrate host, and an arthropod vector, female *Anopheles* mosquitoes [15].

1.3.1 Malaria parasite lifecycle

The motile infective stage of malaria parasites, sporozoites, is injected into the host's skin by an infected female Anophiline mosquito during a blood meal. These sporozoites remain at the inoculation site for up to 30-60 minutes before penetrating the bloodstream using trap-like proteins (TLP) during their gliding motility [15, 78]. However, not all sporozoites successfully enter the bloodstream; some remain in the dermis and are cleared by the host immune response. Once in the bloodstream, the sporozoites travel towards the liver [11, 79], assisted by the sporozoite microneme protein (SPECT), which helps them cross the sinusoidal barrier [80]. They invade liver cells (hepatocytes) using various proteins such as tetraspanin CD81 and scavenger receptor B1 (SR-B1), forming parasitophorous vacuoles that allow entry into the liver cells [15, 81]. In the liver, the sporozoites undergo reproduction outside of RBCs (exoerythrocytic schizogony), where they divide into thousands of merozoites. For example, within six days, a single *P. falciparum* sporozoite can produce up to 40,000 merozoites [82, 83]. This tissue stage can last from 5 to 30 days or more depending on the parasite species. In unfavorable conditions, *P. ovale* and *P. vivax* parasites can delay differentiation into merozoites by entering a dormant stage called hypnozoites (Figure 1.3) [82, 84].

Merozoites are released into the bloodstream and attack red blood cells (RBCs) in three steps: pre-invasion, active invasion, and echinocytosis [25, 85, 86]. In the pre-invasion stage, initial interactions between the merozoites and RBCs cause deformation of the host cell. This is followed by active invasion, where the merozoites irreversibly bind to the RBCs [85]. Lipid-rich parasitophorous vacuoles form at the membrane, allowing the merozoites to propel into the erythrocyte [15, 85]. During this active invasion stage, the parasites successfully enter the erythrocytes, leading to the complete infection of the cells [25, 85]. The erythrocytes then shrink and develop spiky protrusions, a stage known as echinocytosis [86]. Additionally, the released merozoites

can invade both mature RBCs (erythrocytes) and immature RBCs (reticulocytes) [87], though while *P. falciparum* can invade both erythrocytes and reticulocytes, *P. ovale* and *P. vivax* primarily invade reticulocytes (see Figure 1.3).

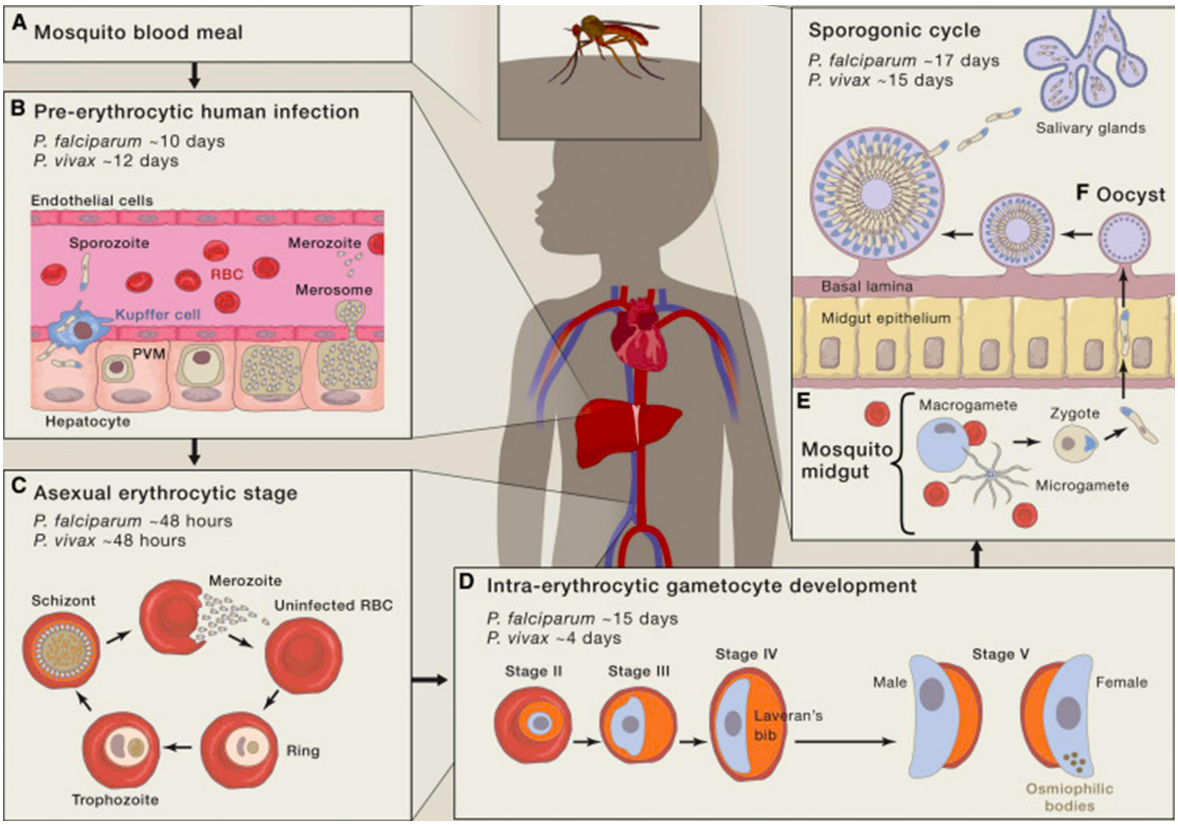

Figure 1.3: Illustration of the malaria parasite life cycle, starting from sporozoite inoculation by the mosquito during a blood meal (A), development in liver cells (B), invasion of red blood cells (C), differentiation into gametocytes (D), and ingestion and development in the mosquito gut (E). Adapted from [15]

1.3.2 Erythrocyte schizogony

During erythrocytic schizogony, merozoites undergo asexual reproduction within red blood cells (RBCs), progressing from ring-shaped forms to trophozoites and then developing into schizonts over approximately 48 hours [38, 82, 88]. For *P. knowlesi*, this cycle is shorter, lasting about 24 hours, whereas for *P. ovale*, *P. falciparum*, and *P. vivax*, it typically spans 48 hours, though *P. malariae* may extend this to up to 72 hours. In *P. falciparum*, erythrocytic schizogony also involves sequestration in the microvasculature of various organs, where schizonts and trophozoites adhere to endothelial cells, which can lead to severe complications such as cerebral malaria. Eventually, the schizonts rupture, releasing daughter merozoites that invade new RBCs, perpetuating the infection cycle. Symptoms of malaria typically manifest 4 to 8 days after the initial invasion of RBCs by merozoites [11, 14]. The entire cycle from

invasion to RBC rupture and release of merozoites into the bloodstream (hemolysis) spans 36 to 72 hours [11]. Hemolysis caused by malaria parasite infections can lead to anaemia (see Figure 1.3) [14, 82, 89].

1.3.3 Gametogenesis

The repeated synchronization of the parasite causes a portion of the merozoites to differentiate into male and female gametes through gametogenesis [14, 15]. This process is triggered by various stimuli such as high parasitemia or drug exposure, which can influence gametocyte production [11, 15, 82]. Gametocytes, which do not cause disease in the infected individual [82, 90], is the parasite stage capable of transitioning from the vertebrate host to female mosquitoes during a blood meal [14,91]. Therefore, gametocyte formation is crucial for malaria transmission and has been considered a potential target for transmission-blocking interventions such as vaccines or drugs [92–94].

It takes over 10 days for mature gametocytes to develop after gametogenesis initiation. There are five stages of gametocyte development, with stages I-IV predominantly found in the bone marrow and stage V circulating in the peripheral blood, increasing the likelihood of transmission to mosquitoes [14, 15, 95]. Mature gametocytes typically evade spleen clearance by sequestering in the bone marrow before entering peripheral blood circulation for uptake by mosquitoes [15, 96]. *P. vivax* and *P. ovale* have shorter sequestration times compared to *P. falciparum*, making them more susceptible to spleen clearance (see Figure 1.3) [15, 89].

1.3.4 Parasite development inside the mosquitoes

In mosquitoes, uninfected females ingest gametocytes when they bite malaria-infected hosts. Inside the mosquito gut, various environmental stimuli, such as changes in temperature and pH levels, trigger each male gametocyte to undergo mitosis and produce eight microgametes, while each female gametocyte forms a single macrogamete [11, 97]. These male and female gametes then fuse to form a zygote, which develops into an ookinete. The ookinete is a motile form that exits the mosquitoes' midgut and develops into an oocyst. Oocysts enlarge and eventually rupture, releasing sporozoites that migrate from the mosquito's abdomen to its salivary glands. Once in the salivary glands, sporozoites are inoculated into a healthy individual during subsequent mosquito blood meals, mixed with

anticoagulant-containing saliva [82, 98]. From the time of ingestion, it takes over 7-10 days for gametocytes to mature into sporozoites, a period known as the extrinsic incubation period (see Figure 1.3), [11, 99].

1.3.5 The pathogenesis of malaria infections

The malaria parasite can cause an infected individual to become ill, prompting them to seek medical care; this is referred to as symptomatic infection. Alternatively, the parasite may be harbored without causing symptoms, resulting in an asymptomatic infection. Symptoms typically manifest when the first schizonts rupture, releasing merozoites into the peripheral circulation. As the parasite progresses through its asexual cycle, merozoite reinvasion, trophozoite development, and schizont rupture every 24-48 hours, the parasite burden in the blood increases, triggering the host's immune response. Fever typically occurs when parasite levels reach 200-1,500 parasites/μL of blood, known as the pyrogenic threshold. Once crossed, the individual becomes symptomatic, and illness severity may increase as the parasite load rises [14, 100].

The rupture of infected cells releases parasite toxins, primarily hemozoin and glycosylphosphatidylinositol (GPI). GPI, a glycolipid that anchors proteins to the red blood cell membrane, is released when infected cells burst. These toxins are recognized by immune cells, leading to the production of inflammatory mediators and cytokines, which stimulate the hypothalamus, causing fever. Various other molecules also including TNF-α, interleukin-10, and interferons, are released during merozoite rupture and trophozoite antigen presentation, contributing to fever. Hemozoin, formed during the degradation of host hemoglobin by parasite, results from the oxidation of ferrous haem into toxic ferric haem, detoxified into insoluble crystals. These processes lead to symptoms such as chills, headaches, fatigue, and loss of appetite, typically appearing 7-18 days after the initial infectious bite [14, 100, 101].

1.3.6 Parasite stages and their importance for diagnosis

Malaria symptoms resemble other diseases. Therefore, the WHO recommends providing treatment only after confirming the presence of malaria parasites in human blood samples. In *P. falciparum* infections, the ring stage is the predominant form in peripheral blood, visualized in Giemsa-stained blood films. Mature stages are sequestered in the deep vasculature and not typically detected in blood smears.

Ring-stage parasites are metabolically inactive, increasing their potential for drug resistance. In contrast, trophozoites and schizonts are metabolically active and more susceptible to treatment. The malaria parasite expresses knob-associated histidine-rich protein (KAHRP), such as small histidine-alanine-rich proteins (SHARP), specific to the parasite and expressed on infected red blood cells. Histidine-rich protein I (HRPI) is associated with knob-like protrusions but is expressed only by mature stages. *P. falciparum* also expresses HRP2 and HRP3, with HRP2 produced by rings and young gametocytes, detectable in blood, serum, and urine. Other markers, like lactate dehydrogenase (LDH) and aldolase, are produced by both sexual and asexual stages across all malaria-causing parasites [102, 103].

1.4 Malaria control, elimination and surveillance

Malaria *control* aims to reduce malaria prevalence, incidence, mortality, and morbidity to acceptable levels at national or subnational scales through well-designed efforts [104]. In contrast, malaria *elimination* aims to bring the burden of malaria to zero within a defined geographic area, typically confirmed by maintaining zero malaria cases for three consecutive years, thereby qualifying for WHO certification as malaria-free [104]. Geographical areas where malaria transmission consistently remains below 1% are often referred to as 'elimination zones'. Both malaria control and elimination strategies involve implementing interventions focused on disrupting the circulation of the malaria parasite and its mosquito vectors [104, 105].

Malaria vector control encompasses a range of strategies aimed at reducing the transmission of malaria by targeting mosquitoes that serve as vectors [106]. Key interventions include the widespread deployment of insecticide treated nets (ITNs), indoor residual spraying (IRS), sometime with supplementary approaches such as larval source management (LSM) [1, 106–108]. IRS involves the application of residual insecticide to the interior surfaces of human dwellings, effectively killing or repelling malaria mosquitoes [106, 109]. Additionally, LSM focuses on meticulously managing mosquito breeding habitats to disrupt their aquatic life stages and prevent their maturation into adult mosquitoes, thus reducing vector densities at source. This approach may involve habitat manipulation, habitat removal, or the application of chemical or biological agents such as larvicides and larvivorous fish [106].

To control circulating malaria parasites, strategies involve administering antimalarial drugs such as Artemisinin combination therapy (ACT) or quinine-based therapy to symptomatic individuals, typically confirmed via diagnostic tests at health centers [106, 110, 111]. ACTs may include artemether-lumefantrine (AL),

artesunate-amodiaquine (AS+AQ), dihydroartemisinin-piperaquine (DHAP), artesunate-sulfadoxine-pyrimethamine (AS+SP), artesunate-mefloquine (ASMQ) and artesunate-pyronaridine (ASPY) [106]. This approach also extends to asymptomatic individuals tested positive during population screening [112]. Additionally, measures to prevent sickness include maintaining therapeutic drug levels in the blood throughout high-risk seasons. This is achieved through chemoprevention methods like Intermittent Preventive Treatment in Pregnancy (IPTp) and Intermittent Preventive Treatment in Infants (IPTi) [113, 114].

1.4.1 Challenges of current malaria control and elimination in Africa

The implication of these control measures have significantly aided the fight against malaria over decades but are notably threatened by various factors, including operational and financial shortages [115], emergence of resistance to commonly used insecticides (typically impregnated on bed nets or applied as IRS) [1], and resistance to antimalarial drugs such as artemisinin, quinine, and chloroquine [116]. Behavioral changes in both vectors and hosts, climate change, and the invasion of new vector species like *An. stephensi* into new areas further compound these challenges [117]. Additionally, malaria control is increasingly threatened by deletions of the histidine-rich protein 2 and 3 (HRP II and III) genes, which code for the protein targets of most *Plasmodium falciparum*-based RDTs [118]. Novel malaria control tools are being developed, including the first two candidates for malaria vaccines, RTS, S / AS01 and R21 / Matrix-mTM, which were approved in 2021 and 2023, respectively, for children in *P. falciparum* endemic areas [119, 120]. Other methods are being developed, including the use of genetically modified mosquitoes (GMM) and gene drive technology for the modification or suppression of the mosquito population [121].

1.4.2 Malaria surveillance

Effective malaria surveillance involves systematic collection of malaria metrics through continuous monitoring, analysis and interpretation of the information collected to track the progress of disease burden and assessing the effectiveness of control measures. The information can be also used for planning, evaluating, and implementing public health measures aimed at malaria control and elimination. The surveillance programs usually include timely entomological and parasitological indicators [104]. For entomological surveillance, data are collected on malaria

vectors, including mosquito species, survival rates, blood meal preferences, breeding sites, biting and resting behaviors, and their resistance status to commonly used insecticides [122–124]. Techniques such as microscopic dissections are used for estimation of mosquito age, morphological species identification, and laboratory methods like ELISA detect sporozoites or PCR confirm species, detect sporozoites, and determine blood meal sources.

In parasitological surveillance, the focus is usually on estimating incidence, understanding malaria endemicity levels and mapping the most impacted demographic groups. This can involve tracking the malaria parasite through routine health information systems at facilities or via community health-care workers (CHWs) for passive surveillance to estimate prevalence (proportion of malaria-positive cases among those tested) or annual parasite incidence (number of malaria-positive cases per 1,000 individuals annually) [125, 126]. Active case detection such as through cross-sectional population surveys can also be done to provide more direct estimates of prevalence across entre populations. For malaria treatment, the parasite presence in human blood must be confirmed using quality-assured microscopy or WHO-recommended RDTs, primarily at health facilities, but also during population surveys where occasionally molecular assays like PCR also serve as detection or confirmation tools for malaria infections [127, 128].

These tools play a crucial role in malaria surveillance and are endorsed as essential components to be integrated into core interventions for malaria control. However, challenges such as sensitivity, costs, and operational implementation remain significant, particularly in malaria-endemic countries. Malaria diagnosis has continuously been advancing from the direct observation of the parasite by microscope to the use of techniques that detect malaria parasite circulating antigens, such as RDTs, and malaria parasite nucleic acids, such as PCR [129–131].

1.5 Introduction to Infrared Spectroscopy

Infrared (IR) radiation is a part of the electromagnetic spectrum between the visible light and microwave regions. This region bridges the energetic ultraviolet (UV) spectrum and the low-energies of microwave and radio frequencies [101, 132, 133]. The discovery of infrared radiation dates back to 1800s, credited to Sir Frederick William Herschel, who was studying the energy levels associated with various wavelengths of light, particularly within the visible spectrum, Figure 1.4A [134, 135]. Herschel's experiment involved passing sunlight through a prism to disperse it into its constituent colors, creating a visible spectrum. Using a mercury-in-glass

thermometer, he measured temperature changes across different colors, Figure 1.4B. As he moved the thermometer from the blue (lower energy) end of the spectrum towards the red (higher energy) end, he noted an increase in temperature. Intriguingly, when he extended his measurements beyond the red region into what was presumed to be the absence of light, he observed a further increase in temperature, Figure 1.4C [134–139]. This led him to identify a new type of radiation, which he initially named as non-colorific rays, later known as infrared radiation, Figure 1.4D. The infrared region, thus identified, encompasses wavelengths longer than those of visible light. Infrared spectroscopy exploits this region to analyze molecular vibrations, providing critical insights into the structural composition and dynamics of various substances [140, 141]

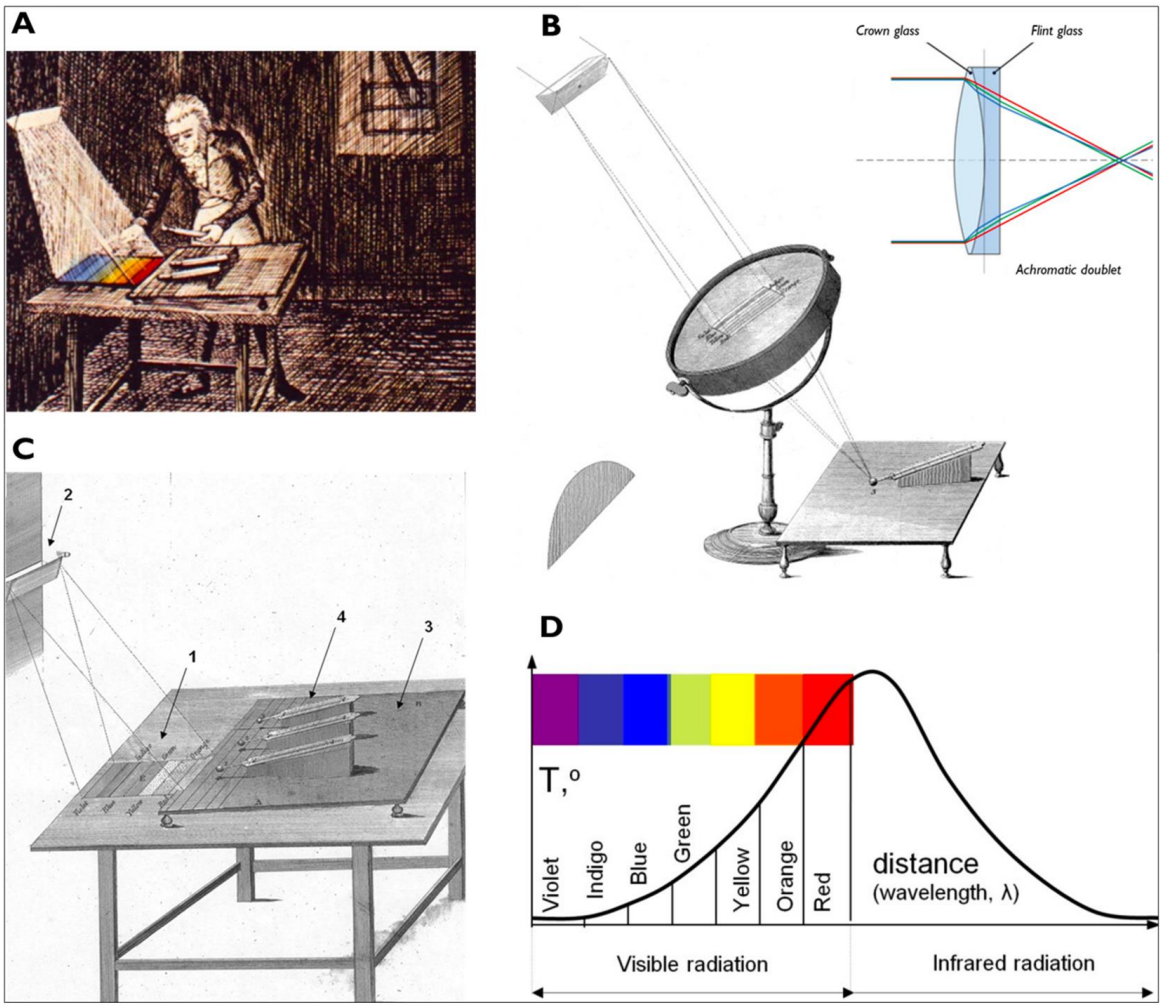

Figure 1.4: Illustrations of Herschel's experiments leading to the discovery of infrared radiation. (A) (B) Shows the setup for the infrared radiation refraction test with the achromat, burning lens, prism, and thermometer. (C) Shows the solar radiation spectrum: 1 marks colors from violet to red, 2 is the prism, and 4 are the mercury thermometers. (D) Indicates the visible light color distribution with infrared radiation discovered next to red. These schematics are adapted from Herschel's original work [135], and from [134].

IR, as other electromagnetic radiations, consists of alternating electric and magnetic fields, explained classically by continuous sinusoidal waves motions Figure 1.5 [133, 142, 143]. Thus, considering a function of time, wavenumber is directly proportional to frequency and inversely proportional to wavelength, as indicated in the equation 1.1 [133, 143].

$$\tilde{\nu} = \frac{\nu}{(\frac{c}{n})} = \frac{1}{\lambda} \tag{1.1}$$

Where $\tilde{\nu}$ is the wavenumber, *C* is the speed of light in a vacuum, *n* is the refractive index of the medium, ν is the frequency, and λ is the wavelength.

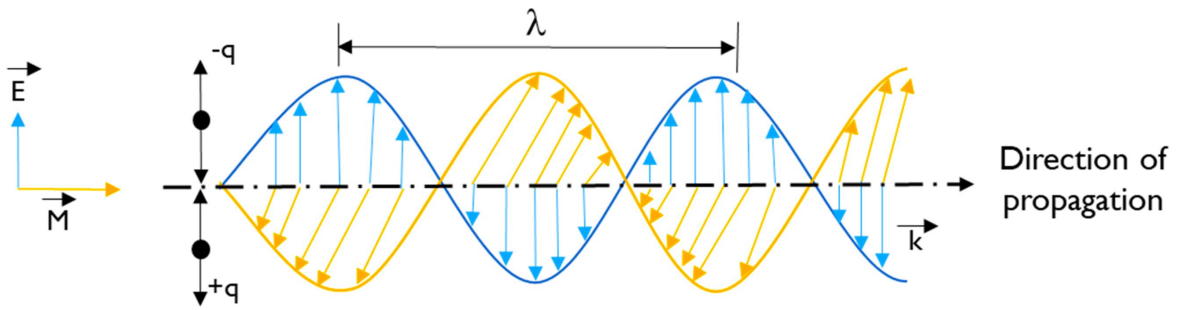

Figure 1.5: The imagined electromagnetic radiations as an oscillating wave of both electric (E) and the magnetic (M) with theoretical propagation of wave from the left toward right, adapted from [132], wavenumber is inversely proportion to the wavelength (λ).

The absorption bands of infrared (IR) spectra are typically reported using frequency and wavelength. Frequency is measured in hertz (Hz) or seconds^{-1} (cycles per second, CPS), and can be expressed as wavenumber, measured in inverse centimeters (cm^{-1}), while the unit of wavelength is the micrometer (µm). The electromagnetic spectrum encompasses a range of electromagnetic radiation frequencies, each corresponding to specific photon energies and wavelengths. Each region of the spectrum is associated with distinct molecular processes: rotational transitions in the microwave region, vibrational transitions in the infrared region, bond breaking and ionization in the x-ray region, and electronic excitation in the ultraviolet/visible region [101, 133, 144, 145]. The energy (E) of electromagnetic radiation, including infrared, is inversely proportional to wavelength (λ) and directly proportional to frequency (f) [133, 145, 146] as shown in equations 1.2 & 1.3:

$$E \propto f \tag{1.2}$$

$$E = hf \tag{1.3}$$

Where E is energy and the h is Planck's constant 6.63×10^{-34} J.s

Additionally, frequency (f) is inversely proportional to the wavelength (λ) as indicated in equation 1.4:

$$f \propto \frac{1}{\lambda} \tag{1.4}$$

Given that, light propagates in a vacuum at a constant speed of light 3×10^{8} m/s, equation 1.5;

$$f = \frac{C}{\lambda} \tag{1.5}$$

Spectroscopy refers to the study of interactions between matter in its various states (solid, liquid, or gas) and electromagnetic radiation. These interactions can manifest as scattering, absorption, emission, transmission, diffraction, and resonance. Thus, the amount of energy absorbed by chemical bonds between molecules is given by the equation 1.6 [133, 145, 146];

$$E = \frac{hC}{\lambda} \tag{1.6}$$

When subjected to infrared (IR) light, molecular bonds absorb infrared energy and produce a spectrum characterized by either absorbance (the amount of light absorbed by the molecular bonds) or transmittance (the amount of light transmitted through the bonds) against wavenumbers (cm^{-1}) [133, 143, 147, 148]. For a molecule to absorb infrared radiation, it must be IR-active, which is a property that allows spectroscopy to determine its chemical functional groups, as molecules with different structures produce distinct spectra [132, 144, 145, 149]. IR-active molecules possess a dipole moment, enabling the covalent bonds to absorb energy and oscillate. Conversely, materials that are IR-inactive have a net zero dipole moment. This differentiation is crucial in spectroscopy for analyzing molecular structures and identifying chemical functional groups [132, 145, 149].

In a molecule, atoms possess partial charges, either positive or negative. The product of these charges (magnitudes) and the distance between the centers of the positive and negative charges is referred to as the dipole moment [133, 144]. The dipole

moment is a vector quantity, having both magnitude and direction. When two atoms with different electronegativities interact, electrons move from the less electronegative atom to the more electronegative one. This movement results in a dipole moment if the magnitudes and directions of the partial charges do not cancel each other [133, 144]. The bond dipole moment, which arises in a chemical bond between two atoms of different electronegativities, can be expressed as equation 1.7:

$$\mu = \delta \cdot d \tag{1.7}$$

Where μ is the bond dipole moment, δ is the magnitude of the partial charges δ^+ and δ^-, and d is the distance between δ^+ and δ^- [133, 144].

Molecules in which all of their atoms have an identical nuclear composition (homonuclear), such as H_2, N_2, and O_2, lack a dipole moment and are therefore IR-inactive. In contrast, heteronuclear (having different nuclear compositions) diatomic molecules like HCl, NO, and CO_2 possess a dipole moment and are IR-active. The IR absorption process occurs when a molecule absorbs energy, causing its dipole to interact with the electric field of the infrared light. This interaction changes the dipole moment and results in a shift in the vibrational energy level of the molecule [145, 150]. This absorption of energy, corresponding to the vibration frequency, induces molecular vibrations by altering the dipole moment [133]. Techniques such as IR spectroscopy and Raman spectroscopy, collectively known as vibrational spectroscopy, can induce these vibrations, making them essential tools widely used for studying, identifying, and detecting the structural, physical, and chemical properties of molecules [133, 140, 151].

1.5.1 Infrared absorptions and molecular vibrations

Infrared-induced molecular vibrations are of two types: Fundamental and non-fundamental vibrations. Fundamental vibrations occur when covalent bonds in molecules, acting like springs between two atoms, exhibit various movements at room temperature. Upon absorbing energy, these bonds demonstrate two primary modes of vibration: stretching and bending. Non-fundamental vibrations occur when electrons within chemical bonds absorb energy and ascend to higher energy levels beyond the fundamental states. Table 1.1 summarizes the types of both fundamental and non-fundamental vibrations.

The vibrational frequency (ν) of a molecule is inversely proportional to the square root of its reduced mass (μ). This relationship is described by the equation 1.8. This illustrates why the fundamental vibrations of organic compounds, which generally involve lighter atoms, are detected in mid-infrared (MIRs) spectroscopy. In contrast, vibrations involving heavier atoms, which have higher reduced masses, fall into the far-infrared (FIR) region. The lower vibrational frequencies of heavier atoms shift their fundamental vibrations to the FIR spectrum, while the higher frequencies of lighter atoms are captured within the MIR range.

$$\nu = \frac{1}{2\pi}\sqrt{\frac{k}{\mu}} \tag{1.8}$$

where ν is the vibrational frequency, k is the force constant of the bond, and μ is the reduced mass of the two atoms involved in the vibration.

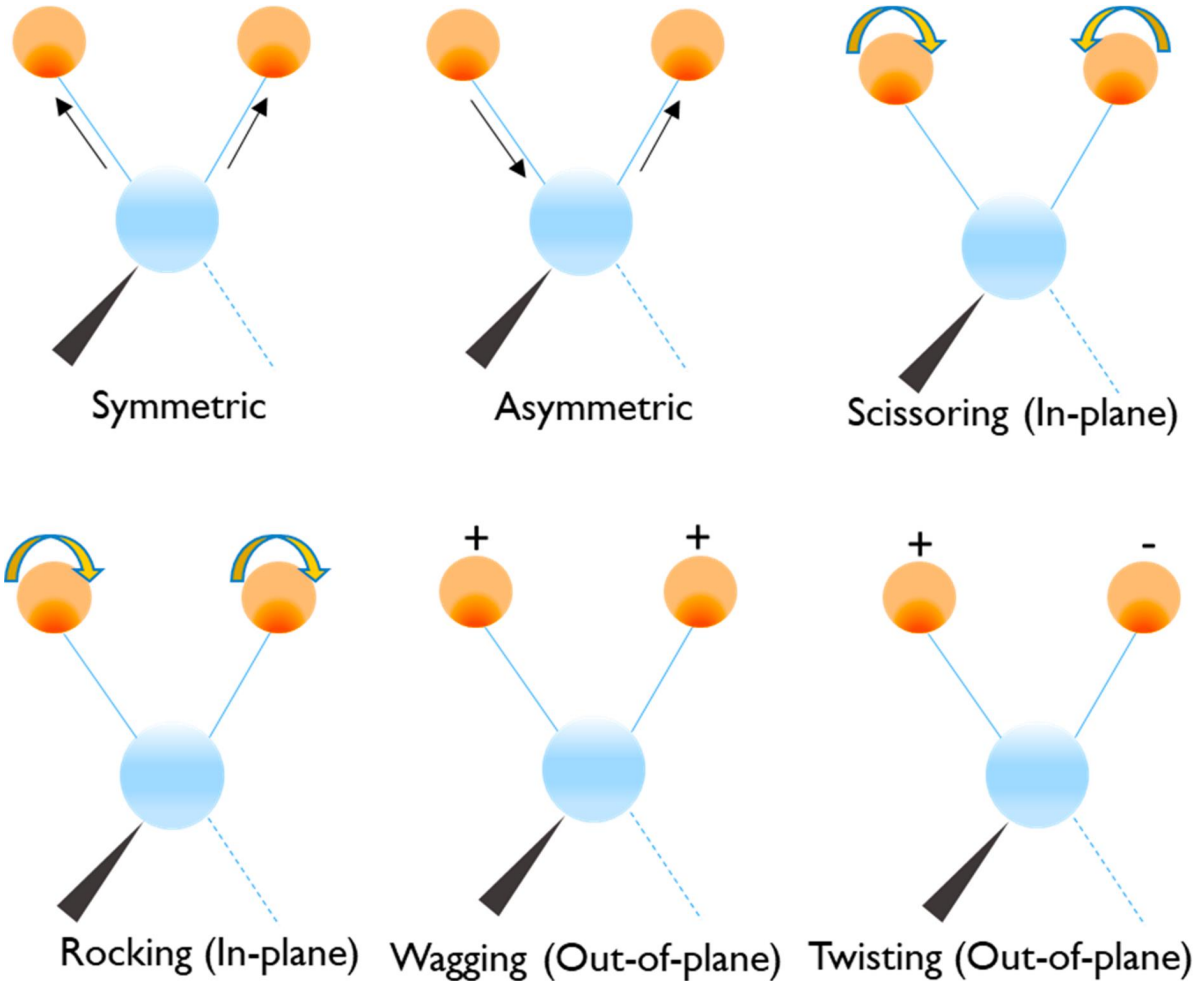

Figure 1.6: Modes of fundamental vibrations in the infrared region primarily include stretching and bending vibrations Modified from [144].

Table 1.1: Fundamental and Non-Fundamental Vibrations in Infrared Spectroscopy with Examples and Wavenumbers, [133, 143–145, 150, 152, 153]

Fundamental Vibrations	**Stretching Vibrations**		
	Type	**Descriptions**	**Examples**
	Symmetrical Stretching	Atoms move simultaneously towards and away from the central atom, altering the bond length.	CH_3 (2870 cm^{-1}), NH_2 (3309 cm^{-1})
	Asymmetrical Stretching	One atom moves away from the central atom (increasing bond length), while the other moves towards it (decreasing bond length).	CH_3 (2960 cm^{-1}), NH_2 (3402 cm^{-1})
	Bending Vibrations		
	Type	**Descriptions**	**Examples**
	Scissoring	Atoms move towards or away from each other within the same plane, deforming the bond angle.	CH_2 (1465 cm^{-1})
	Rocking	Atoms swing side to side within the same plane without altering the bond angle.	CH_2 (720 cm^{-1})
	Wagging	Bond swings back and forth as a unit, moving out of the original plane.	CH_2 (1350 cm^{-1})
	Twisting	Bond rotates out of the plane around a central atom, with bonded atoms moving in opposite directions.	CH_2 (1250 cm^{-1})
Non-Fundamental Vibrations	**Type**	**Description**	**Examples**
	First Overtone	Occurs when electrons jump from the ground state (V=0) to the second energy level (V=2), skipping the first level (V=1).	CH_2 (2700 cm^{-1} - 2900 cm^{-1})
	Combination Vibrations	Occurs when two or more fundamental vibrations combine. These often involve weaker bonds and can shift depending on the molecular environment.	CH_2 stretching and bending combination (2349 cm^{-1})
	Fermi Resonance	Interaction between a fundamental vibration and an overtone or combination band that results in the splitting of absorption bands.	CO_2 (2350 cm^{-1})

1.6 Infrared regions

The infrared spectrum is categorized into three distinct regions based on wavelength: near infrared (wavenumbers $\nu \approx 14000$ cm^{-1} to 400 cm^{-1}, wavelength $\lambda = \frac{1}{\nu} =$ 0.7-2.5 µm), mid-infrared (wavenumbers 4000 cm^{-1} to 400 cm^{-1}, wavelength 2.5-25 µm), and far infrared regions (wavenumbers 400 cm^{-1} to 10 cm^{-1}, wavelength 25-300 µm). Chapter two details the applications of near and mid-infrared spectroscopy for malaria surveillance [144, 150, 154].

1.6.1 Near infrared (NIR)

Near Infrared Spectroscopy techniques rely on wavelengths from 0.7 to 2.5 µm and is distinguished by its higher energy vibrational modes. NIR vibrations were first discovered in the early 1800s and primarily arise from overtones and combination vibrations, resulting in weak bands. Due to its ability to penetrate samples more deeply compared to other infrared regions, NIR is particularly valuable in food science, biomedical applications, and soil sciences Figure 1.7 [150, 155, 156]. NIR spectroscopy provides numerous advantages, including minimal sample preparation, non-destructive measurement capabilities, and the ability to analyze samples in glass containers due to their transparency in the NIR range. Moreover, NIR is less influenced by water content in samples, allowing for direct measurement of aqueous samples. However, the presence of molecular overtone and combination vibrations often leads to broad and overlapping bands in spectra, posing challenges in their interpretation [150].

1.6.2 Mid infrared (MIR)

The spectroscopic region known as mid-infrared spans from 4000 (cm^{-1}) to 400 (cm^{-1}) (2.5 - 25 µm), providing comprehensive qualitative and quantitative insights into the chemical structure and composition of molecules in gas, liquid, and solid phases. MIR spectroscopy is extensively applied across environmental sciences, biotechnology, medicine, and various other fields. Its main vibrational mode, the fundamental vibrations, require less energy compared to NIRs [144, 150, 157].

MIRs are categorized into two primary segments: the fingerprint region (400 – 1400 (cm^{-1})) and the functional groups region (1400 – 4000 cm^{-1}), each further divided into four sub regions. The X-H stretch region (4000-2500 cm^{-1}) exhibits fundamental

vibrations of OH, CH, and NH stretching. In the triple bond region (2500-2000 cm^{-1}), vibrations primarily from C C and C N bonds are observed. The double bond region (2000-1500 cm^{-1}) features vibrations of C=C, C=O, and C=N bonds, while the fingerprint region (1500 – 600 cm^{-1}) provides specific molecular characteristics based on fundamental vibrations [158]. MIR spectroscopy generates strong bands attributed to fundamental vibrations and exhibits particular sensitivity to water bands Figure 1.7 [150]. Integration of MIR spectroscopy with other analytical techniques such as microscopy and gas chromatography is straightforward, facilitating rapid and reagent-free analysis processes [101, 150, 159, 160].

1.6.3 Far infrared (FIR)

The far infrared region, also known as the terahertz (THz) region, encompasses frequencies typically below 400 cm^{-1}, after the MIR range. Historically, FIR spectroscopy has seen slower adoption compared to MIRs due to challenges in instrumentation. However, it has proven invaluable for studying intermolecular interactions, hydrogen bonding, hydration dynamics, and the vibrational modes of various molecules, materials, and tissues, (refer to Figure 1.7) [144, 150, 161].

FIR spectroscopy is particularly suited for probing low-frequency vibrations of heavy atoms, including metal-ligand and lattice vibrations. In some IR region classifications, additional divisions such as long-wave IR (LWIR) or thermal IR (TIR) are included, typically spanning from 8 µm to 15 µm, depending on specific applications. These divisions cater to different analytical needs within the broader infrared spectrum, (refer to Figure 1.7) [132, 144, 150].

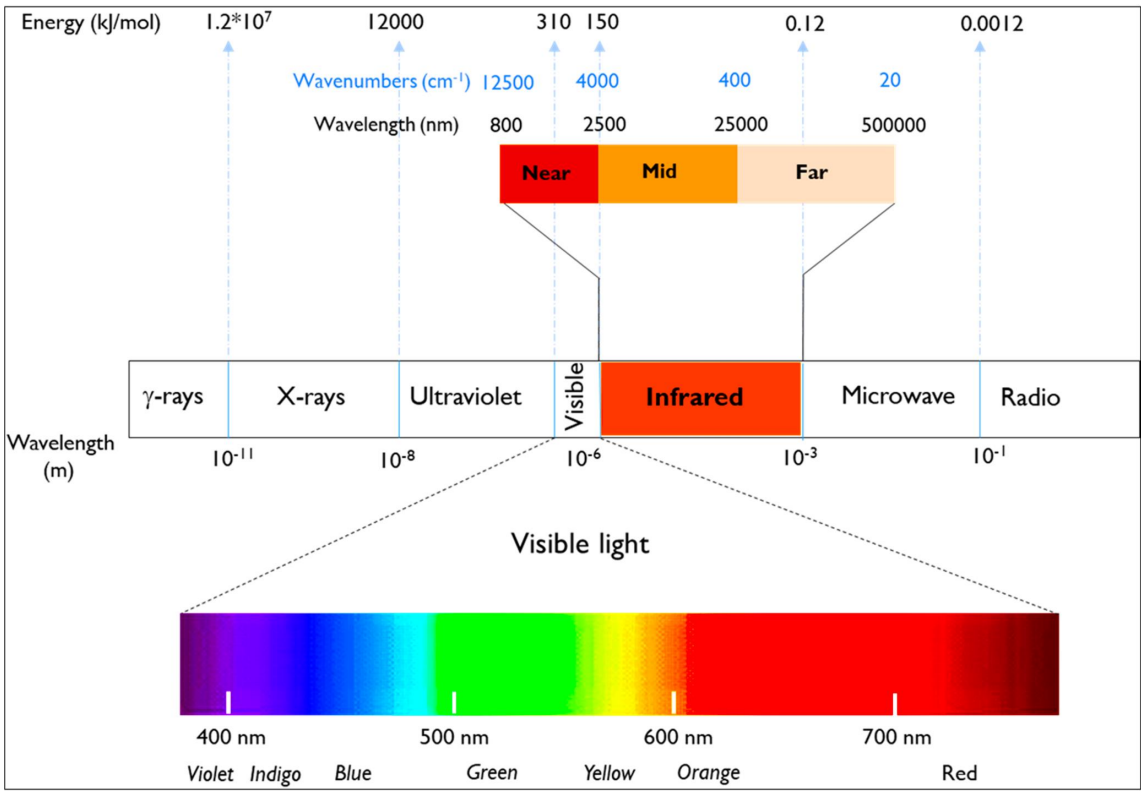

Figure 1.7: The electromagnetic spectrum depicting the full visible light range and the infrared regions with its divisions of near, mid, and far infrared.

1.7 Instrumentation for Infrared Spectroscopy

Infrared spectroscopy has seen significant advancements since the introduction of the first spectrometers, known as dispersive instruments. The evolution of infrared instrumentation can be broadly categorized into classical spectrometers and modern spectrometers, each with distinct features and improvements.

1.7.1 Classical spectrometers

Classical spectrometers, introduced in the 1940s, laid the groundwork for infrared spectroscopy. These instruments primarily differ from modern spectrometers, such as Fourier Transform Infrared (FTIR) spectrometers, in their use of components and operational principles. A classical spectrometer typically includes a light source, a dispersing element (monochromator), a detector, and an optical system composed of mirrors. The monochromator, which could be a diffraction grating or a prism, serves to separate the broad spectrum of infrared radiation into a continuous sequence of individual frequencies. As a result, different frequencies of IR radiation pass to

the detector sequentially, allowing the instrument to record one frequency at a time, (Figure 1.8A). This method, while effective, is time-consuming as it requires scanning the entire frequency range sequentially [132, 143, 162].

1.7.2 Fourier transform infrared (FTIR) spectrometers

The development of modern spectrometers, particularly FTIR spectrometers, in the early 1960s marked a significant leap forward in infrared spectroscopy. The key innovation in FTIR spectrometers is the use of a Michelson interferometer, which allows all frequencies of IR radiation to reach the detector simultaneously [132, 163], (Figure 1.8B). This approach contrasts sharply with the sequential scanning method of classical spectrometers. In an FTIR spectrometer, the interferometer generates an interferogram by splitting a beam of light into two paths, reflecting them off mirrors (one fixed and one movable), and then recombining them (Figure 1.8B). This interferogram, containing information about all wavelengths, is then mathematically transformed into a spectrum using Fourier transform algorithms, which is a mathematical process that converts the time-domain interferogram into a frequency-domain spectrum [138, 139, 149].

The adoption of FTIR technology was greatly facilitated by advancements in electronics and computing. These improvements have made FTIR spectrometers faster, more accurate, and capable of producing high-resolution spectra with an enhanced signal-to-noise ratio. The typical components of an FTIR spectrometer include a light source, a beam splitter, a translating mirror, a fixed mirror, and a detector, all forming an intricate optical system [132, 144, 164].

The transition from classical to modern FTIR spectrometers has brought numerous advantages to infrared spectroscopy. FTIR instruments are not only faster but also more efficient in capturing spectral data. They provide higher resolution and accuracy, making them invaluable tools in various fields such as environmental science, biotechnology, medicine, and material science. The ability to obtain complete spectra in a fraction of the time required by classical spectrometers has expanded the applicability and utility of infrared spectroscopy in research and industry [132, 144, 149].

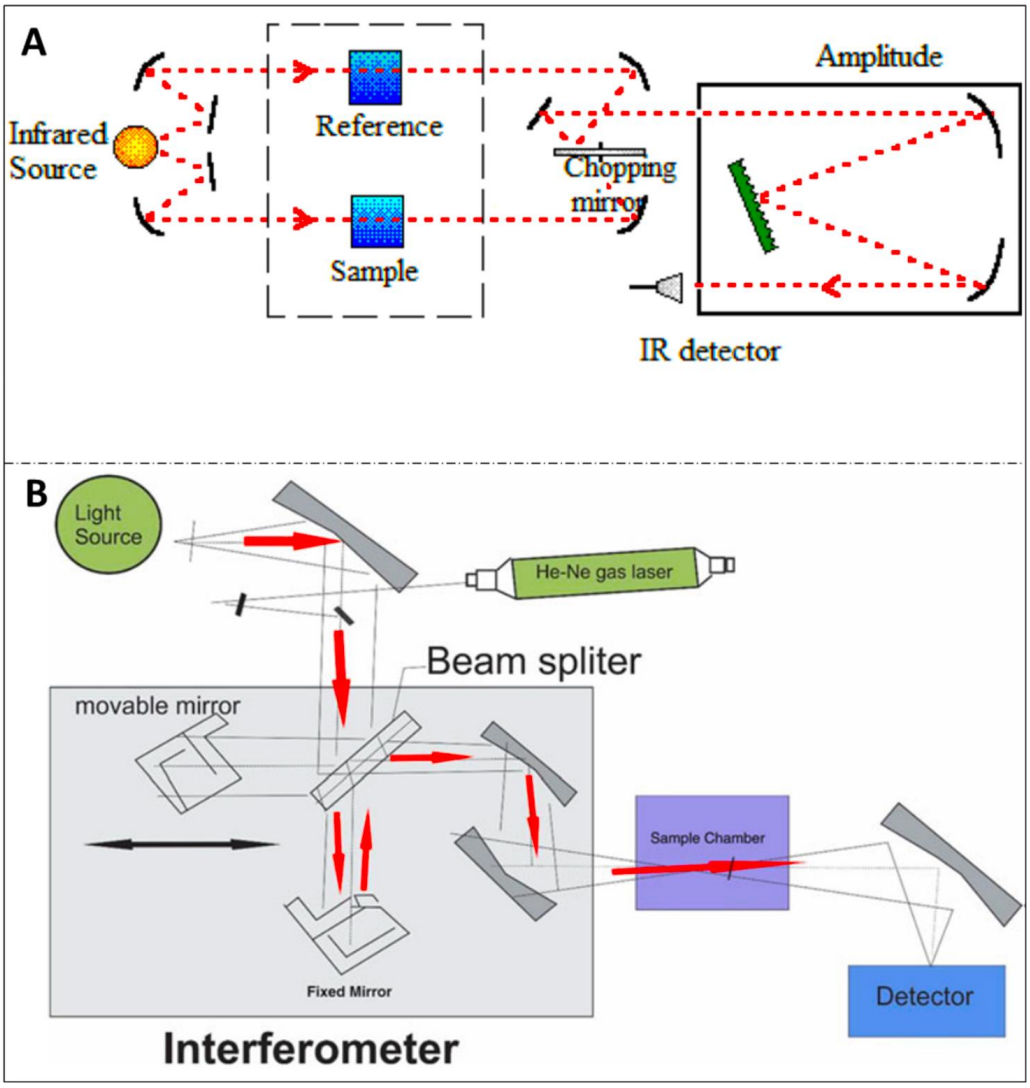

Figure 1.8: Schematic presentations of infrared spectrometers. (A) Depicts the classical spectrometer design, illustrating its traditional components and optical layout. (B) Shows modern spectrometers, highlighting advancements in technology and design features for enhanced performance and versatility in infrared spectroscopy, adopted from [132].

1.8 Sampling techniques and spectra acquisition approaches

1.8.1 Attenuated total reflectance (ATR-IR)

One of the most common modes of reflectance sampling is attenuated total reflectance (ATR-IR), of which light passes through an ATR crystal, which is in contact with the sample, and undergoes multiple internal reflections (Figure 1.9A). During these reflections, a portion of the light, known as evanescent light, penetrates the sample

to a certain depth. This depth depends on the light wavelength, the refractive index of the ATR crystal, the sample contents, and the incidence angle. Common ATR crystals include Zinc Selenide (ZnSe), Diamond, Germanium (Ge), and Silicon (Si) [144, 165–168].

1.8.2 Specular reflection infrared spectroscopy (SRS)

Specular reflection infrared spectroscopy (SRS) involves reflections occurring externally at a specular (mirror-like) surface at well-defined angles, where the angle of reflection equals the angle of incidence of the infrared radiation, (Figure 1.9B). This technique is particularly useful for analyzing thin films, coatings, and surfaces. In SRS, the infrared beam is directed at the sample at a specific angle, and the reflected light is collected and analyzed. It is used more in micro-FT-IR applications, allowing detailed surface analysis with high spatial resolution [140, 144, 162].

1.8.3 Diffuse reflectance spectroscopy (DRS)

Diffuse reflectance spectroscopy (DRS) involves a combination of internal and external reflections, mainly from rough sample surfaces. By collecting scattered light reflected off the sample surface, information about the sample composition and structure is provided. DRS is particularly useful for analyzing powders, heterogeneous materials, and surfaces with irregular textures, (Figure 1.9C). The scattered light is collected using an integrating sphere or other optical arrangements to ensure that both specular and diffuse reflections are captured, providing a comprehensive spectral profile of the sample [169, 170].

Reflectance sampling techniques, particularly ATR-IR, SRS, and DRS, offer versatile and effective methods for acquiring infrared spectra with minimal sample preparation. ATR-IR is highly useful, offering a large depth of penetration into samples, making it ideal for the routine analysis of liquids, solids, and pastes. SRS provides detailed surface analysis capabilities, making it suitable for studying thin films and coatings. DRS excels in analyzing powders and rough surfaces, providing valuable insights into the composition and structure of heterogeneous materials [171, 172].

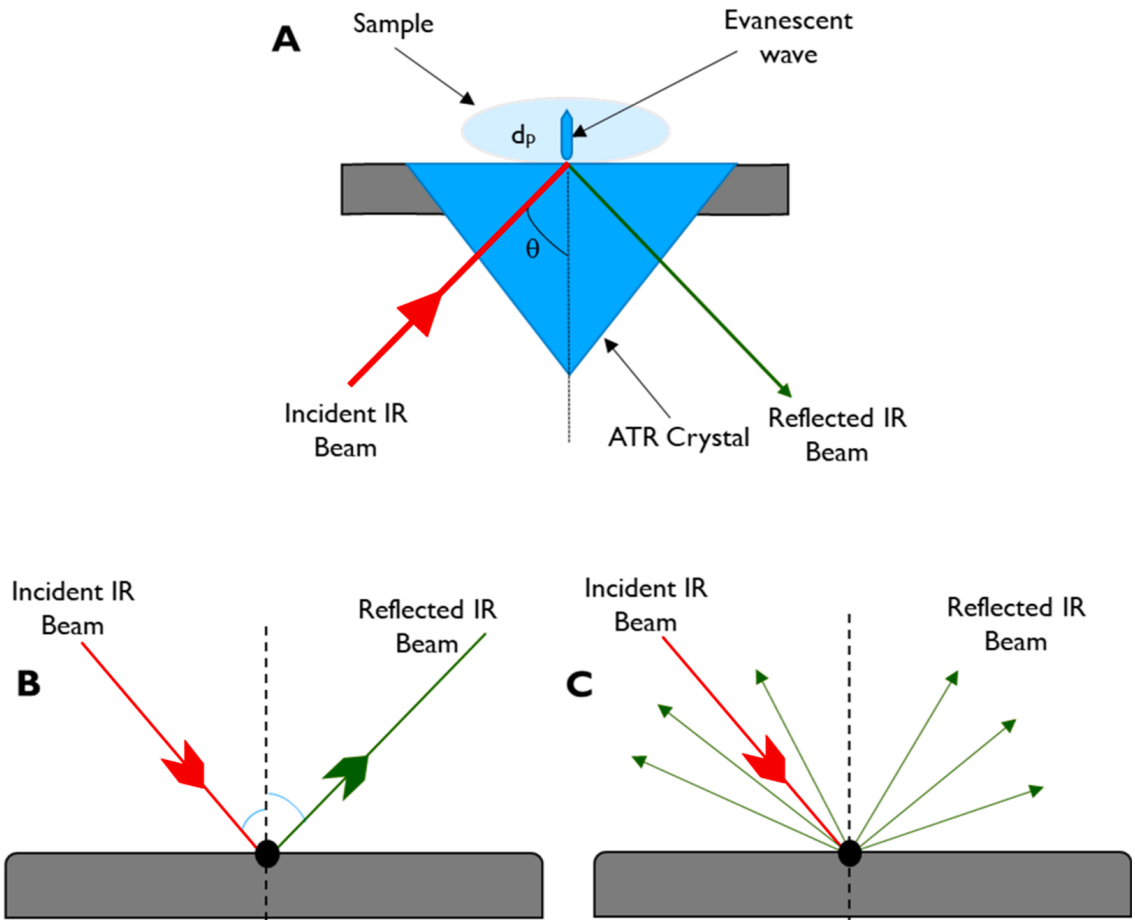

Figure 1.9: Sampling techniques for acquiring spectra with infrared radiation. (A) Attenuated total reflectance (has been widely used for malaria entomology and parasitological studies [173, 174]), (B) Specular reflection infrared spectroscopy, and (C) Diffuse reflectance spectroscopy methods are depicted, modified from [144].

1.9 Applications of artificial intelligence in analysis of infrared spectroscopy data

Artificial intelligence (AI) is the science of simulating and generating computer systems to perform tasks that typically require human intelligence. These tasks may approximate human critical thinking, intelligent behavior such as learning, reasoning, problem-solving, and understanding languages. The concept of AI can be traced back to the pioneering work of English computer scientist, mathematician, and logician Alan Turing. In 1950, Turing posed the seminal question, ***"Can machines think?"*** This inquiry led to the development of the famous Turing Test, a behavioral test designed to evaluate a machine's ability to exhibit intelligent behavior equivalent to, or indistinguishable from, that of a human [175, 176].

1.10 Types of artificial intelligence

Artificial intelligence can be categorized into three main types: Artificial Narrow Intelligence (ANI), Artificial General Intelligence (AGI), and Artificial Super Intelligence (ASI) [177].

Artificial Narrow Intelligence, also known as weak AI, refers to systems that are designed and trained to perform specific tasks. These systems excel in particular domains but lack the ability to generalize knowledge across different areas. ANI systems do not possess consciousness, self-awareness, or general intelligence akin to human cognition. Examples of ANI include facial recognition systems, chess-playing programs, recommendation algorithms on platforms like Amazon, and self-driving car technologies [177].

One class of ANI is Reactive Machines, which do not have the ability to store experiences or use past information to influence future actions. They respond to specific inputs with predefined responses. Another group is Limited Memory AI, which can store and utilize data from previous interactions to inform future decisions and actions, improving performance over time. Overall, ANI is commonly employed in applications such as disease diagnosis, agricultural monitoring, surveillance, transportation, and finance [177].

Artificial General Intelligence, or strong AI, aims to replicate human intelligence comprehensively. AGI systems would possess the ability to understand, learn, and apply knowledge across a broad range of tasks, demonstrating self-awareness and consciousness. However, AGI remains theoretical as no existing systems can fully mimic human cognitive abilities, such as reasoning, problem solving, and learning from past experiences to tackle future challenges autonomously. Current advancements that hint towards AGI include language models like guide partition table (GPT) and supercomputers like IBM's Watson, which can process and analyze large amounts of data to provide insights and recommendations [177].

Artificial Super Intelligence (ASI) represents a hypothetical stage where AI surpasses human intellectual capabilities. ASI systems exhibit superior problem-solving, reasoning, and creative skills beyond any human ability. While ASI remains speculative, advancements in understanding, human brain functions and continuous technological progress suggest the potential for such systems. Current technologies indicating progress towards ASI include advanced neural networks and machine learning algorithms [177].

Within AI, the sub-discipline of machine learning further divides into areas such as statistical learning [178] and deep learning [177]. In the context of this thesis, ANI forms the foundation of current applications and is hereafter referred to simply as AI.

1.10.1 Machine learning

Machine learning (ML), a branch of artificial intelligence (AI), involves the development of mathematical, statistical, and computational approaches known as algorithms. These algorithms enable computers to learn patterns from data and improve their performance based on experience. The ML process begins with input data, from which algorithms learn patterns that link the data's features to the desired outputs. The knowledge derived from these algorithms can be used for various purposes, such as summarization, visualization, grouping, and prediction over datasets [179].

1.10.2 Concept of algorithms

Algorithms in ML are structured mathematical sets designed to solve specific tasks or problems via a logical series of computational steps. The steps enable the algorithms to learn, memorize, and predict based on interactions with data.

The algorithms contain four building blocks, namely the input block, the processing block, the output block, and the termination block. In the presence of computer programs, input data characterized by features (or explanatory variables) and targets (response variables) are presented to the algorithms. The algorithms then perform a series of logical and arithmetic operations to derive a unique function that links the features to the targeted output within the processing block. This successful determination of the mapping function is referred to as decision-making. However, some algorithms require the logical series of computations to be repeated multiple times, a process known as looping, before arriving at a decision. In the output block, after deriving the final decision, the algorithm provides the output to the users. This must be done within a specific time-frame, as the termination block ensures that the logical operations do not run indefinitely [179].

In the machine learning process, algorithms must be trained to perform specific tasks. The data (input) are passed to the ML algorithms, which then learn the patterns and are evaluated based on their performance. Subsequently, the algorithms are tested and

validated before actual use and deployment [179]. Machine learning encompasses various training approaches, including supervised, unsupervised, semi-supervised, and reinforcement learning [180].

Supervised machine learning: Supervised machine learning algorithms learn from labeled data, where input variables are paired with corresponding output labels through human interaction. These algorithms iteratively learn and are tested until they sufficiently perform the task. It is crucial that the labeled data accurately represent population patterns to ensure generalizability. Supervised learning is broadly categorized into two types: classification and regression. In classification tasks, ML models predict categorical output labels such as binary outcomes (e.g., positive/negative) or multiclass scenarios like predicting colors of a rainbow. Common classifiers used include Logistic Regression, Support Vector Machines (SVM), k-Nearest Neighbors (k-NN), and Decision Trees.

In contrast, regression tasks involve learning from datasets with continuous outputs. Regressors use predictor variables to develop regression curves that offer precise predictions. Examples of regression algorithms include Linear Regression and Random Forest Regressors. Advantages of supervised machine learning include achieving high accuracy, lower computational costs, interpretable decision-making processes, and the ability to adapt and improve using pre-trained algorithms. However, supervised learning may face challenges such as underfitting, overfitting, and poor generalizability when the labeled data fail to adequately capture real-world variability and complexity [179, 180].

Unsupervised machine learning: Unsupervised machine learning involves algorithms that operate on unlabeled data to uncover underlying patterns, relationships, and structures. This approach is invaluable for tasks such as discovering hidden patterns in data, identifying similarities between data points, clustering similar data for visualization, and reducing the dimensionality of complex datasets. In practice, unsupervised learning utilizes various techniques such as association, clustering, and dimensionality reduction.

Association techniques aim to find relationships or correlations between variables, which can reveal interesting insights about the data. Clustering methods group similar data points together into clusters based on their characteristics, allowing for the exploration of natural groupings within the data. Dimensionality reduction techniques reduce the number of variables in datasets while preserving essential features, making it easier to analyze and visualize complex data structures.

These unsupervised learning techniques often serve as preprocessing steps before applying supervised learning algorithms like classifiers and regressors. By extracting meaningful patterns and reducing the complexity of data, unsupervised learning facilitates more efficient and effective training of predictive models. Despite its utility, unsupervised learning presents challenges, particularly in predicting and evaluating algorithm performance without labeled data. Since the algorithms operate without predefined output labels, assessing the accuracy and reliability of their results can be more complex compared to supervised learning [179, 180].

Semi-Supervised Learning: Semi-supervised learning integrates aspects of both supervised and unsupervised approaches by leveraging a combination of labeled and unlabeled data for training. This hybrid approach harnesses the benefits of having access to a smaller set of labeled data alongside a larger pool of unlabeled data. By utilizing unlabeled data to augment the learning process, semi-supervised learning can enhance the performance and generalizability of models compared to purely supervised methods. This approach is particularly advantageous in scenarios where acquiring labeled data is costly or time-consuming but unlabeled data is abundant [181].

Reinforcement Learning: often referred to as agents, acquire knowledge and skills by interacting with environments and receiving feedback in the form of rewards or penalties. The goal of reinforcement learning is for the agent to learn optimal strategies that maximize cumulative rewards over time. Through a process of trial, error, and delayed rewards, the agent refines its decision-making capabilities and adapts to changing environments. This iterative learning process emphasizes continuous improvement through repeated actions, allowing the agent to navigate complex scenarios and achieve better outcomes over successive interactions [182].

1.10.3 Infrared spectroscopy and machine learning for medical applications particularly malaria diagnosis.

In medical applications, infrared (IR) spectrometers are used to scan various biological specimens, generating their infrared spectra. These spectra capture unique biochemical signatures, represented by wavenumbers and corresponding absorption intensities. Wavenumbers act as the variables (features), while absorption intensities represent the attributes or values, collectively forming the input data or independent variables. These spectra are then associated with specific labels such as “Positive” or “Negative”, which serve as the dependent variables in subsequent analyses. Studies used classical models based on chemometrics and statistical approaches, such as partial least squares, to classify various malaria indicators.

However, due to the complexity of infrared spectral signals and multicollinearity, these methods had limitations and lacked robustness, performing with limited sensitivity in predicting indicators, particularly when adapting to new datasets beyond those used to build the specific model.

Recently, there has been significant interest in integrating infrared spectroscopy with machine learning techniques (IR-ML) to effectively map the spectral variables (wavenumbers and intensities) to clinically relevant targets. This approach is crucial for estimating various public health parameters, including disease diagnosis and surveillance. In a broader context, IR-ML approaches have demonstrated considerable success in classifying a wide range of diseases [183, 184]. These include bacterial and viral infections, blood disorders, diabetes, heart diseases, autoimmune diseases, respiratory diseases, and neurodegenerative diseases [183]. For instance, IR-ML models have achieved remarkable accuracy in identifying pleural effusion, with reported accuracies exceeding 90% [177]. Similarly, in cancer diagnosis, IR-ML has shown sensitivity rates of up to 90%, distinguishing between cancerous and non-cancerous specimens [185]. The potential of IR-ML extends further into specific types of cancer, such as breast, cervical, colorectal, esophageal, and gastric cancers. Studies have highlighted IR-ML's effectiveness in diagnosing hepatitis C infections with accuracy rates exceeding 90% [186]. Additionally, IR-ML systems have successfully detected conditions like high renin hypertension with accuracies exceeding 89% and thyroid dysfunctions with accuracies over 80% [184]. Moreover, IR-ML demonstrates promising capabilities in identifying dengue viral infections in blood plasma, achieving sensitivity rates above 95% and specificity rates exceeding 90% [187].

Despite being a promising tool for malaria surveillance and surpassing many novel diagnostic methods from proof-of-concept to field validation, there are alternative approaches to IR-ML that have potential to offer greater resolution. One such approach is the Matrix-Assisted Laser Desorption/Ionization Time-of-Flight (MALDI-TOF) technique, which also shows potential for identifying mosquito species and detecting sporozoite infections [188, 189]. While MALDI-TOF is widely used in clinical microbiology for bacterial identification and has been adapted for microbial diagnostics, giving it an advantage in usability and acceptance in clinical settings [190], its application for detecting *P. falciparum* in human blood remains limited to proof-of-concept studies, achieving detection of parasitemia as low as 0.1% (5,000 parasites/µL) under controlled laboratory conditions [191]. In contrast, IR-ML, while not yet clinically applied, outperforms MALDI-TOF in sensitivity, cost-effectiveness, and ease of use, making it especially suited for malaria screening and surveillance.

Firstly, IR-ML offers significant operational advantages. It requires minimal sample preparation and works effectively with whole dried blood samples, whereas MALDI-TOF depends on isolated red blood cells, necessitating extensive laboratory protocols and specialized expertise. Secondly, IR-ML is reagent-free, enhancing affordability, while MALDI-TOF relies on reagents such as α-cyano-4-hydroxycinnamic acid as a matrix to facilitate ionization and absorption of laser energy, adding costs and potentially limiting its use in resource-constrained settings. Thirdly, comparisons of infrared-based approaches and MALDI-TOF for bacterial discrimination have shown infrared approaches to be more sensitive for species identification [192]. This is due to the principle underlying infrared methods, which provide detailed molecular fingerprints associated with species-specific biomarkers in the fingerprint region. In contrast, MALDI-TOF detects protein alterations as mass-to-charge ratios, favoring identification based on peptides and proteins [192]. For malaria screening, IR-ML offers broader metabolic fingerprints of *Plasmodium* infections, enabling the investigation of a wider range of biochemical diversity within infected cells.

Fourthly, IR-ML benefits from robust machine learning integration, enabling real-time adaptability and incremental improvements. This could mitigate future diagnostic threats more effectively than MALDI-TOF, which relies on static spectral libraries as a benchmark databank for pathogen identification. The portability of IR-ML approaches, demonstrated through compact, field-deployable devices, makes it ideal for use in remote, resource-limited areas. In line with WHO's advocacy for sensitive, cost-effective tools in low-transmission settings, IR-ML is better positioned to meet the needs of malaria-endemic regions, balancing sensitivity, affordability, and operational feasibility.

In the context of malaria infection screening and surveillance, IR-ML has demonstrated substantial potential. Chapter Two discusses these demonstrations, highlighting how IR-ML could effectively enhance existing challenges in malaria diagnosis and surveillance. IR-ML stands out for its cost-effectiveness, user-friendly interface, and rapid processing capabilities, all of which enable its deployment even in resource-constrained environments [173]. This project provides scientific evidence of IR-ML applications for malaria screening across large populations. It begins with detailed laboratory demonstrations and progresses to real-world field samples, showcasing IR-ML adaptability and utility in diverse settings.

1.11 Focus of my PhD research

While various studies have demonstrated the potential applications of infrared spectroscopy and machine learning (IR-ML) for malaria screening, evidence supporting their performance in field settings remains limited. Specifically, there is insufficient information on the lowest detectable parasite concentrations using MIRs-ML for malaria detection, as well as on whether the technology is suitable for population surveys or as a point-of-care test. Existing studies have primarily used the MIRs-ML system as a proof of concept, often with samples that do not encompass a broad spectrum of parasite densities, immunological diversity, or account for confounding variables. Additionally, there is a notable absence of field studies evaluating the efficacy of MIRs-ML for malaria screening in low transmission areas, where conventional diagnostic tools, such as rapid diagnostic tests (RDTs) and microscopy, exhibit reduced performance.

Therefore, the main focus of my PhD thesis is to improve malaria surveillance by exploring potential applications of MIRs-ML approaches for screening malaria infections during large population surveys, particularly in low-income settings. To achieve this, I have addressed the following objectives;

1. Reviewing key considerations develop target product profiles and formulate research questions to be addressed for the utilization of IR-ML in malaria surveillance and diagnosis. To achieve this second chapter of my PhD, I wrote and published a comprehensive review identifying key research gaps in exploring the potential of using infrared spectroscopy and machine learning (IR-ML) for malaria surveillance and diagnosis. The chapter also includes the development of a target product profile (TPP), which outlines the essential and desirable characteristics needed for integrating IR-ML into routine malaria surveillance. I led the technical discussions and developed the initial TPP in collaboration with a consortium of experts in IR-ML applications. This consortium includes scientists from the Ifakara Health Institute in Tanzania, the University of Glasgow in the United Kingdom, the University of Queensland in Australia, and institutions in Mozambique and Burkina Faso.

2. Investigating potential of using MIRs-ML for malaria screening in human blood samples in the context of different parasite densities and anaemic conditions. This chapter focuses on establishing the lowest possible parasite concentrations of malaria parasites that can be detected using MIRs-ML approaches. I diluted cultured malaria parasites with blood from 70 malaria-free volunteers recruited for the study. Various dilutions were prepared to create a matrix representing different parasite densities and anemia conditions. Subsequently, dry blood spots (DBS) were generated and scanned using mid-infrared (MIR) spectrometers to acquire spectra. These

spectra were used to train and evaluate the performance of MIRs-ML for screening malaria infections in the context of various parasite densities and anaemia conditions. Additionally, the algorithms developed in the laboratory were tested under real field conditions in southeastern Tanzania.

3. Comparative assessments of the fine-scale malaria strata generated using data collected during population surveys with RDTs, microscopy, and qPCR. In formulating my fourth chapter, I conducted extensive epidemiological surveillance in southeastern Tanzania. The survey covered the Ulanga and Kilombero districts, spanning 93 sub-villages and 35 villages, and screened approximately 8,000 individuals for malaria infections. As malaria stratifications shift from national and subnational levels to fine-scale stratifications (districts, wards, villages) in the context of malaria elimination, the data collected in this survey allowed me to carefully investigate the limitations and strengths of current screening tools particularly RDTs, microscopy, and qPCR for fine-scale mapping of malaria risk. The findings of this objective are useful for alerting national malaria control programs to be aware of the limitations that different screening tools may pose, which could impact precise resource allocation.

4. To evaluate the performance of mid-infrared and machine learning approaches for malaria screening in villages with varying parasite prevalence. I leveraged the extensive stratifications of malaria burden in the Kilombero Valley from objective three. For objective four, I assessed the performance of MIRs-ML in villages with either low or high transmission profiles. The goal was to provide evidence on MIRs-ML performance in low transmission areas, where current tools like RDTs and microscopy exhibit poor performance. I developed ML algorithms using data sets collected from realistic populations in Tanzanian villages (field data). Subsequently, I also developed algorithms using laboratory-based datasets and refined these algorithms by integrating laboratory data with a subset of field data. Building on the objectives outlined in Chapter 3, I rigorously tested and evaluated these algorithms across various malaria transmission strata, including high transmission areas, low transmission areas.

5. To develop a web-based AI platform for real-time analysis of infrared spectral data to enhance parasitological and entomological surveys of malaria. I created a cloud-based system using the Python Django framework. This system allows end-users, including national malaria control programs, healthcare practitioners, and scientists, to upload spectral data and interact with deployed machine learning models. These models provide instant predictions of malaria infections in humans and the age and species of mosquitoes, with potential for further improvement and expansion to additional indicators. Currently, the system is restricted in its use, and predictions

are not authorized for clinical decisions. A deployment roadmap has been prepared to host the system on the Microsoft Azure platform, with plans for public release by December 2024.

Chapter 2: Key considerations, target product profiles, and research gaps in the application of infrared spectroscopy and artificial intelligence for malaria surveillance and diagnosis

Published in Malaria Journal 2023:
https://doi.org/10.1186/s12936-023-04780-3

2.1 Abstract

Studies on the applications of infrared (IR) spectroscopy and machine learning (ML) in public health have increased greatly in recent years. These technologies show enormous potential for measuring key parameters of malaria, a disease that still causes about 250 million cases and 620,000 deaths, annually. Multiple studies have demonstrated that the combination of IR spectroscopy and machine learning (ML) can yield accurate predictions of epidemiologically relevant parameters of malaria in both laboratory and field surveys. Proven applications now include determining the age, species, and blood-feeding histories of mosquito vectors as well as detecting malaria parasite infections in both humans and mosquitoes. As the World Health Organization encourages malaria-endemic countries to improve their surveillance-response strategies, it is crucial to consider whether IR and ML techniques are likely to meet the relevant feasibility and cost-effectiveness requirements - and how best they can be deployed. This paper reviews current applications of IR spectroscopy and ML approaches for investigating malaria indicators in both field surveys and laboratory settings, and identifies key research gaps relevant to these applications. Additionally, the article suggests initial target product profiles (TPPs) that should be considered when developing or testing these technologies for use in low-income settings

2.2 Background

Effective control of malaria requires an in-depth understanding of its transmission. This entails estimating parasitological, entomological and epidemiological parameters in respective communities [193]. Specific activities may include detecting malaria infections in humans, estimating mosquito survival following deployment of interventions, identifying malaria-infected mosquitoes, and characterizing the human populations at risk [193]. As countries move towards malaria elimination in line with the strategic goals of the World Health Organization (WHO) [194], there is a need to develop simple, low-cost and scalable methods for assessing key entomological and parasitological indicators of malaria and for monitoring the impact of interventions [193, 195–198]. Proper management of suspected malaria cases requires confirmation through quality-assured laboratory tests [106, 194]. These tests may also include quantifying the number of asexual malaria parasites in blood samples to determine the severity of the infection, or identifying carriers through the detection of Plasmodium gametocytes [199, 200]. In population surveys, malaria prevalence can be estimated through various methods, such as observing malaria parasites under a microscope, using rapid diagnostic tests (RDTs) to detect parasite-derived proteins and by-products, or detecting parasite nucleic acid sequences through polymerase chain reactions (PCR) [197, 201]. These tools have greatly improved the diagnosis of malaria, guided effective case management, and enhanced the evaluation of key interventions.

In terms of entomological indicators, female *Anopheles* can transmit malaria only if they live long enough to pick up the infective stages of *Plasmodium*, and thereafter incubate those parasites until they mature into the infectious sporozoite stage. This process usually takes 10 – 14 days, but can be slower depending on climatic conditions [202, 203]. Proportions of female mosquitoes that are old enough to transmit malaria can, therefore, be used to estimate vectorial capacity (number of mosquito infective bites produced by a single malaria case) and assess the performance of vector control methods, such as insecticide-treated nets (ITNs) and indoor residual spray (IRS) [204–207].

The primary measure of malaria transmission intensity, the entomological inoculation rate (EIR), is calculated as the product of the human biting rates (number of bites per unit of time) and the proportion of mosquitoes infected with *Plasmodium* sporozoites. Estimating EIR requires detailed assessments of *Anopheles* biting rates, typically through mosquito trapping, and the proportion of female *Anopheles* that carry infective *Plasmodium* sporozoites, typically through enzyme-linked immunosorbent assays (ELISA) or PCR [208, 209]. In addition to these core entomological metrics,

other measures can be used to estimate the natural survival and transmission potential of Anopheles populations. These may include ovarian dissections to assess parous proportions, analysis of vertebrate blood meals to estimate the proportion of mosquitoes biting humans, and estimation of the proportion of mosquitoes biting indoors and outdoors [193, 210].

Although these strategies for monitoring malaria transmission have contributed to progress against the disease [211], there are still considerable obstacles related to operational costs, performance accuracies, scalability, and human resource requirements [124, 196, 198]. In order to align with global priorities for malaria elimination, further advancements in both entomological and parasitological surveillance are just as important as the need for new drugs, vaccines, or vector control approaches [194, 198]..

A recent advancement in malaria monitoring is the use of infrared (IR) spectroscopy in combination with machine learning (ML) techniques to assess key indicators of malaria. These indicators include the chronological age of mosquitoes (e.g. number of days post emergence) [212–215], blood-feeding histories of malaria vectors [216], *Plasmodium* infections in human blood [217–219] or mosquitoes [220], and identification of malaria vector species [212]. In this technique, biological samples are scanned with infrared radiation, and the energy absorbed by the covalent bonds in the target specimen causes its molecules to vibrate. An infrared spectrum generates information about the molecules that absorb the radiation and their intensity of absorption [221]. Despite the subtle biochemical differences between specimens with different biological traits, ML algorithms can disentangle these spectral changes and map them to specific phenotypes [217, 221, 222]. Together, IR and ML-based systems constitute robust, easy-to-use, reagent-free, non-invasive and low-cost approaches, making them attractive in low-income settings [212, 214, 216]. As a result, there has been a significant increase in the number of studies evaluating or validating these techniques for monitoring vector-borne diseases [173, 213, 223].

To ensure maximum benefits going forward, it is important to identify existing gaps and the essential and desirable characteristics that should be met for these technologies to be effectively integrated into routine malaria control programmes. The aim of this article is to review existing IR spectroscopy and ML applications for malaria surveillance and diagnostics, to identify gaps for field use, and to outline a target product profiles for such technologies to be suitable in low-income settings.

2.3 Current methods for measuring malaria transmission

2.3.1 Parasitological methods

The most common method for parasitological assessment of malaria is light microscopy, which is standard practice in many laboratories and relies on direct observations of malaria parasites on thick or thin smears of blood [224–226]. Although light microscopy is accessible even in low-resource settings, it requires highly experienced personnel and can generally detect only parasite densities above 50 parasites/µl of blood with an overall sensitivity of between 50-500 parasites/µl [103, 227]. The method may, therefore, miss individuals with low parasitaemia levels or asymptomatic carriers [103, 226], and may perform poorly in low-transmission settings [228]. The diagnostic accuracy might also be compromised by poor preparation of thick or thin blood smears and visual identification [229, 230].

Another common approach is the use of malaria rapid diagnostic tests (RDTs), which have revolutionized malaria investigations in both clinical settings and community surveys due to their low-cost and promptness [231, 232]. Moreover, they do not require highly-trained or experienced personnel to perform or interpret the tests, and can be used even in hard-to-reach areas, and by community healthcare workers [231, 233]. Most RDTs target the parasite antigen, histidine-rich protein II (HRP-2), which is abundant in *P. falciparum* infected red blood cells [103, 234]. Some RDTs also target glycolytic enzymes, such as *Plasmodium* aldolase and *Plasmodium* lactate dehydrogenase (pLDH) antigens, and can detect non-*falciparum* malaria parasites, such as *Plasmodium ovale*, *Plasmodium malariae* and *Plasmodium vivax* [103, 235].

The main disadvantages of RDTs include the lack of quantitative information and poor performance in asymptomatic cases or low-level parasitaemia, such as those with parasitaemia levels below 100 parasites/µl [197, 233]. In addition, genetic mutations of the HRP-2 genes, which are spreading around the world, also compromise the sensitivity of RDTs [236–243]. These gene deletions, which have so far been detected in nearly 40 countries [118], make the malaria parasites undetectable by the HRP-2 based RDTs even when the patients are severely ill. The WHO currently recommends that countries should withdraw these specific RDTs if more than 5% of malaria infections have HRP-2 mutations [118].

Nucleic acid-based diagnostics, such as PCR, have the highest sensitivity but are often unaffordable in most malaria-endemic settings and are, therefore, rarely used [244–246]. PCR can detect parasitaemia as low as 1-5 parasites/µl of blood, but is used mostly in research settings because of its high cost and the need for specialized facilities and personnel [103, 246, 247]. Epidemiological surveys have also demonstrated that PCR assays can be used to identify areas with unusually high malaria transmission [226, 228]. Moreover, one analysis of methods for detecting malaria hotspots in coastal Kenya concluded that PCR was the most appropriate for mapping asymptomatic cases once overall prevalence had dropped significantly [228]. Lastly, PCR also provides detailed information on *Plasmodium* species based on the small subunit 18S rRNA or circumsporozoite protein genes, and can also detect mixed infections [103, 246]. Unfortunately, as summarized in Figure 2.1A, the techniques require highly-skilled labour, expensive equipment and reagents, making them untenable for regular use in places with poor supply of laboratory materials [197].

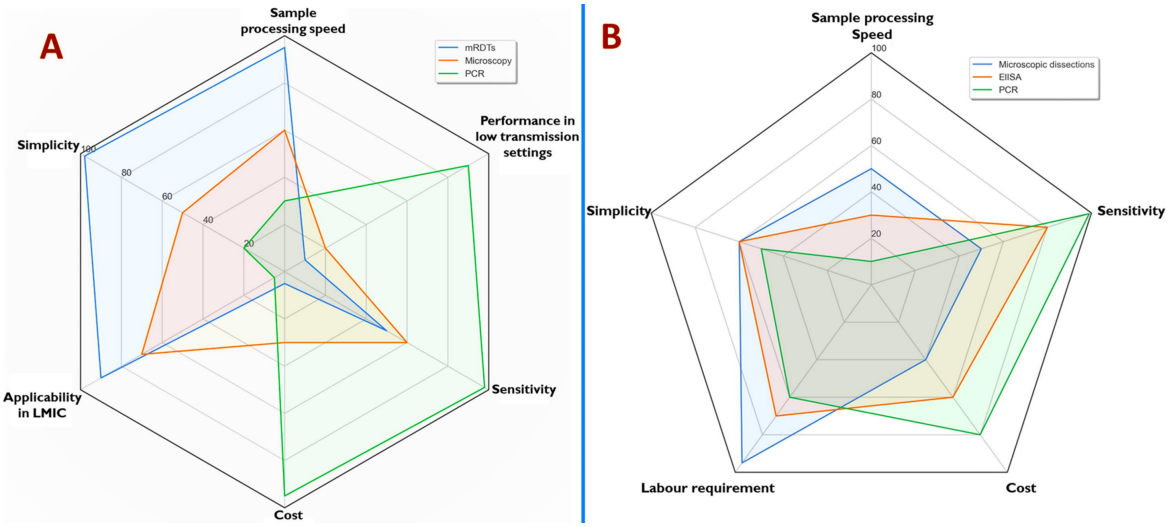

Figure 2.1: Applicability, strengths, and weaknesses of current methods used to measure key malaria indicators. Panel A compares the three most common methods for parasitological assessment [236, 248–256] while panel B compares the three main methods for entomological assessment [257–267], on a proportion score of 1 to 100. These scores are based on expert opinion of the authors of this article.

2.3.2 Entomological methods

The WHO has outlined several entomological indicators that malaria programs may consider for monitoring transmission dynamics, guiding the selection or deployment of control strategies, and evaluating the control efforts [106, 193]. These include: (i) mosquito blood-feeding histories, biting frequencies, and resting behaviours, (ii) vector species presence and densities (iii) insecticide resistance status, (iv)

proportion of mosquitoes with *Plasmodium* sporozoites, and (v) larval habitat profiles [193, 211]. The indicators may be differently prioritized depending on the local capabilities, malaria epidemiological profiles, financial constraints, and prevailing control strategies in the respective countries. However, the most central ones are biting rate, mosquito density and EIR.

Entomological surveys involve different sampling methods, after which the collected mosquitoes are sorted by taxa and physiological features. Adult female mosquitoes are frequently dissected for analysis of their internal organs (e.g. gut, reproductive systems and salivary glands) or retained for other laboratory analyses [210]. Sex and species are initially sorted based on the exterior morphology of the mosquitoes using taxonomic keys [60, 268]; but the indistinguishable members of species complexes, such as *Anopheles gambiae sensu lato* (s.l.) and *Anopheles. funestus s.l*. require further distinction by PCR [76, 269, 270]. As summarized in Figure 2.1B, these methods are time-consuming, expensive, require specialized training, and are not always readily available locally [271].

Depending on the research goals, additional laboratory tests may be performed on the collected mosquitoes. These can include ELISA tests to detect malaria parasite proteins or PCR tests to find *Plasmodium* sporozoites in the heads and thoraces of female *Anopheles* mosquitoes [267, 272, 273]. Additionally, examination of the stomach contents of the mosquitoes, using ELISA [274] or PCR [275], can be performed to identify the vertebrate sources of mosquito blood meals as required to determine their preference for biting humans compared to other animals. The age of field-collected female mosquitoes is generally determined by dissection to examine changes in their ovaries; with age here being estimated in terms of reproductive history (e.g. whether parous or not, and if parous how many gonotrophic cycles have been completed) rather than in terms of chronological age (e.g. number of days post emergence) [210, 261, 276, 277]. Estimates of physiological age derived from these dissection methods are used to approximate chronological age based on fixed assumption of the number of days required to complete a gonotrophic cycle in the field [260, 278]. Finally, a series of bio-efficacy and molecular assays to determine the resistance of the mosquitoes to insecticides, to inform appropriate insecticidal interventions can also be done [279].

Entomological monitoring is complex and costly, and as a result, only a small number of malaria-endemic countries can monitor all the recommended entomological parameters on a large scale [124, 211, 280]. A recent analysis of vector surveillance programmes in malaria-endemic countries found that countries with the highest burden have far less surveillance capacity than countries nearing elimination [211].

Overall, most countries are not well-equipped to establish effective surveillance systems with the minimum essential data necessary to detect changes and adjust public health responses.

2.4 Applications of infrared spectroscopy and machine learning for parasitological and entomological surveys of malaria

The attributes of mosquitoes or human body tissues can be studied by analysing their infrared (IR) spectral signatures. These signatures contain complex biochemical information represented by absorbance intensities at different wavenumbers. Near Infrared (NIR) Spectroscopy specifically measures absorption by vibrational overtones, or vibrations that are excited from the ground state to the second or third energy level, in the 14,000 - 4,000 (cm^{-1}) range. On the other hand, Mid-Infrared (MIR) spectroscopy measures absorption by fundamental vibrations of molecular bonds in the 4,000 - 400 (cm^{-1}) range, which allows for more direct quantification of functional chemical groups present in substances, such as chitin, protein, or wax in the samples of interest [173, 212].

Once the samples have been scanned, ML algorithms can be used to analyse the infrared spectral data and identify specific entomological and parasitological parameters [213–215, 218, 281]. Additional techniques may be used to remove errors and improve the accuracy of the analysis, such as transfer learning [282]. These algorithms can be used to determine features such as mosquito age, species identity, infection status, and blood meal types. Studies have shown that combining IR spectroscopy with machine learning (IR-ML) can provide accurate predictions and estimates of various transmission indicators [173]. For example, this approach has been used to classify malaria-transmitting mosquitoes by chronological age or number of gonotrophic cycles [212, 213], making it useful for studying the effects of vector control on mosquito populations. The potential of IR-ML techniques for measuring malaria transmission should be evaluated based on factors such as robustness, speed, validity, infrastructure needs, scalability, costs, and cost-effectiveness; and should only be adopted if they address the challenges of conventional methods.

The cost of IR spectroscopy equipment used for malaria research can vary greatly. Hand-held versions of NIRS or MIRS spectrometer can cost as little as $2,000 [283], while desktop versions of these spectrometers range from $30,000 to

$60,000 [217, 281]. Most equipment is durable for regular laboratory or field use and requires minimal maintenance. No additional reagents are needed for operation, except standard low-cost maintenance, such as providing desiccants to limit humidity effects.

2.4.1 Parasitological surveys

The use of infrared spectroscopy (IR) for diseases screening and diagnostic purposes has been demonstrated in various branches of medicine, including the histopathological screening of breast cancers and the prediction of infections (e.g. enterococci), leukaemia, Alzheimer's, epilepsy, skin carcinoma, brain oedema, and diabetes [284, 285]. An increasing number of studies are also using IR-ML techniques for parasitological screening [173].

In one study in Tanzania, dried blood spots were scanned using an attenuated total reflection-Fourier Transform Infrared spectrometer (ATR-FTIR) and a logistic regression model was trained using the resulting MIR spectra [217]. This approach achieved 92% accuracy relative to PCR in identifying individuals infected with *P. falciparum*, and 85% accuracy for detecting mixed infections such as those carrying both *P. falciparum* and *P. ovale* [217], which is also common in some parts of Tanzania [286]. Another study used synchrotron MIR Fourier Transform Infrared spectroscopy coupled with artificial neural networks (ANN) to achieve a prediction accuracy of 100% for distinguishing between different stages of the cultured *P. falciparum*, i.e., rings, trophozoites and schizonts [219]. Additionally, support vector machine algorithms fitted with MIR spectra from an ATR-FT spectrometer were used to classify infected and uninfected individuals with a sensitivity of 92% and specificity of 97% [218]. Recently, it has been shown that the near-infrared absorption peaks of malaria parasites can be used for non-invasive detection of malaria infection through human skin using miniaturized hand-held spectrometers [283].

2.4.2 Entomological surveys

Using off-the-shelf hardware, both NIR and MIR spectroscopy can be used to analyse large numbers of mosquito samples at a relatively low cost compared to traditional methods [173, 212, 213, 276]. Studies have demonstrated direct applications to predict mosquito chronological (e.g. number of days post emergence) and physiological age classes (e.g. whether parous or not), blood-feeding histories and species identity [212–216, 287]. They have also been used to detect mosquito

endosymbionts, such as *Wolbachia* [288, 289], and mosquito-borne pathogens, such as Zika [223, 290] and malaria [291, 292]. Scientists have attempted to validate these laboratory findings in the field settings but so far, there has been success in only a small number of studies [213, 293, 294].

There has been a particular interest in evaluating the potential of IR-ML systems for mapping the demographic characteristics of wild mosquito populations and using this to evaluate the performance of vector control interventions, or monitoring transmission risk. Following multiple successes in combining IR spectroscopy and ML for age-grading laboratory and semi-field vector populations [212, 213], field studies are now underway to validate the potential of this tool in malaria-endemic communities. It is expected that these ongoing efforts will deliver a scalable and operationally relevant IR-ML system that integrates off-the-shelf hardware and open-source software to simplify the technologies. Ultimately, IR-ML based approaches will be most desirable only if they constitute a simple set of routine activities that can be performed by researchers and National Malaria Control Programme (NMCP) staff.

Despite advancements in using Infrared-Machine Learning (IR-ML) for malaria surveillance, there remain several challenges that might hinder its full potential. In entomological surveillance, existing algorithms show up to 99% accuracy with laboratory-reared mosquitoes, but this drops significantly in field data, due to variances in mosquito body compositions from dietary, genetic, and environmental factors [173, 212, 213, 293, 295]. Fortunately, recent strides using Convolutional Neural Networks (CNN) have improved accuracy across diverse datasets, with CNNs achieving over 90% accuracy in laboratory and field assessments on specific mosquito species [214]. Transfer learning is also being explored to enhance algorithm generalizability in real-world settings [282]. Additionally, logistical hurdles akin to those faced by existing surveillance methods exist, particularly in hardware maintenance and supply [211]. Moreover, unlike other diagnostic methods with built-in verification, IR-ML lacks this feature [228, 296], indicating a vital area for future research to ensure reliable operations and address these identified gaps. The sections below will discuss these gaps and potential solutions in detail.

2.5 Considerations for research and development of IR-ML approaches for malaria survey and diagnostics

As the WHO encourages malaria-endemic countries to scale up effective surveillance-response strategies for malaria, an important question that remains is what elements should be considered when developing or evaluating new approaches such as IR spectroscopy and ML. Moreover, while IR-ML technologies have the potential to aid in malaria surveillance, several gaps in research and development must be addressed to optimize their utility. This section identifies key research and development gaps in the applications of these technologies for malaria surveys in low-income settings. It further proposes a target product profile (TPP) consisting of both the essential characteristics and desirable characteristics that could improve its uptake, performance, and cost-effectiveness.

2.5.1 Research gaps to be addressed

Table 2.1 provides a summary of the key research gaps for the IR-ML applications relevant to malaria. For each of these gaps, additional details are provided below.

Gap 1: Need for a greater understanding of the biochemical and physicochemical basis of the IR signals relevant for malaria surveys and diagnosis. IR spectral absorption intensities are determined by the chemical bonds within chitin, protein, and wax, which are the three most abundant components of the mosquito cuticle. Recent research has shown that these signals can be used to infer the age and species of mosquitoes [212, 213], as well as distinguish between *Plasmodium*-infected and uninfected human blood [217].

In the case of parasitological observations, it is apparent that the most dominant spectral features that influence ML model predictions are found in the fingerprint region (1730 (cm^{-1}) – 883 (cm^{-1})), where most of the signal from biological samples is expected [217]. The breakdown of haemoglobin into haemozoin crystals may also show up in the IR spectra and can help detect infections in blood samples [217, 297]. The interpretation of IR spectra should, therefore, take into account the sample type and characteristics, and in the case of composite sample types such as parasite-infected blood, considerations on how the parasite interacts with and alters the biochemical makeup of the host tissues should be factored in. For example, changes in the carbohydrate regions at 1144 (cm^{-1}), 1101 (cm^{-1}) and 1085 (cm^{-1})

may be associated with differential glucose levels in infected red blood cells, since *Plasmodium* parasites metabolize glucose faster than normal cells [222, 298]. The presence of these direct and indirect signals of infection raises the possibility of non-specific detection and false positive diagnoses, which should be mitigated with carefully chosen controls when training machine learning (ML) models. Given the many different applications of IR-ML for investigating malaria indicators, a generalized framework is essential and should be derived from an updated understanding of the bio-chemical and physico-chemical features of the samples

Gap 2: Need to validate the performance of the IR-ML in different field settings and laboratories So far, most of the successes in the application of IR-ML have been with laboratory specimens, but it has been difficult to apply these laboratory-trained algorithms to field-collected specimens due to environmental, laboratory, and genetic sources of variation, and/or limited training data. Only a small number of studies have achieved this with partial success [213, 215, 293]. This challenge is compounded by the limited generalizability of many existing ML models. Efforts towards field validation should be integrated with those that seek to improve the generalizability of the models, using more diverse datasets with greater genetic and environmental variability.

Field validation is also essential for IR-based parasitological surveys, as algorithms trained using spectral data from laboratory parasite cultures may not be applicable to other settings, in part due to different immunological and physiological profiles [299–301]. Additionally, cultured parasites mixed with blood may exhibit important differences from natural infections, thus limiting their generalizability to realistic samples unless transfer learning with field data is applied. Consequently, early validation of IR-ML for parasitological surveillance is essential and the training data should capture representative signals associated with immunological and genetic composition from multiple populations [217, 302]. For clinical applications, determining the true effectiveness of these techniques may also require large-scale clinical studies.

Gap 3: Need for appropriate ML-frameworks that achieve maximum predictive accuracies with minimal computational power. While IR-ML approaches for assessing malaria indicators can achieve high accuracies, there are many differences between the analytical methods and algorithms used. Currently, there is no consensus on the best ML frameworks for spectral analysis, either supervised or unsupervised. Ideally, the best framework would be that which provides minimum computational needs while also achieving accurate and generalizable predictions of the target traits.

Initially, multivariate statistics, including partial least squares (PLS) and principal component analysis (PCA) were the most widely used [222, 298, 301, 303, 304]. More recently, IR spectroscopy coupled with different ML classifiers has been used to link the signals of IR biochemical bands to specific biological traits [173]. A general approach is to compare and select from multiple model types. Diverse ML algorithms, such as support vector machines (SVMs), Random Forests (RFs), K-nearest neighbours (KNNs), Naive Bayes (NBs), Gradient Boosts (XGBs), and Multilayer Perceptrons have been tested for their ability to decipher IR spectra associated with malaria indicators [214, 215, 217–219].

Unsupervised learning is often utilized in spectra pre-processing to decrease dimensionality or cluster dominant features before algorithm training [213, 218, 219], but additional statistical techniques can be added to improve generalization. For example, unsupervised PCA was used to reduce the dimensionality of the data set, and an ANN was trained on the pre-processed data to accurately predict malaria parasite stages [219]. Moreover, transfer learning and dimensionality reduction techniques like PCA and t-SNE (t-distributed stochastic neighbour embedding) can significantly reduce computational power while maintaining robust accuracy in models [282].

Gap 4: Need to understand the malaria parasite detection thresholds for the IR-ML systems. As conventional methods have a low likelihood of detecting malaria infections with low parasitaemia [245], it is necessary to understand the lower limits of detection (LLOD) for any novel diagnostic and screening tools. Unfortunately, only a small number of studies have examined such thresholds for IR-based malaria detection. One study which used serially diluted parasites grown in vitro demonstrated that ATR-FTIR data could be used to identify and quantify parasite densities as low as <1 parasite/µl [222]. Other research has shown that NIR spectroscopy coupled with PCA and PLS can detect up to 0.5 parasite/µl and quantify up to 50 parasite/µl parasites in isolated RBCs [300].

Other studies have also shown that using wider spectral ranges, e.g. combining the UV, Visual and IR spectra, can accurately detect and measure malaria without the need for complex preservation methods [300, 305]. Nevertheless, most studies that established the LLODs of the IR did not use ML as the framework for interpreting parasite signals in IR spectra. There has been no investigation of threshold detections for malaria parasites using IR-ML approaches in field settings. Future research should, therefore, establish absolute or the relative LLOD of the IR-ML techniques in both the point-of-care applications and population surveys.

Gap 5: Understanding the performance and validity of the IR-ML techniques in settings with varying epidemiological profiles Malaria screening methods perform differently in settings with varying transmission intensities and parasitaemia. The most sensitive markers of malaria infections at low transmission intensities tend to be nucleic acids or antibodies to *P. falciparum* [306]. One study in coastal Kenya that compared RDTs, light microscopy, and PCR showed that malaria transmission hotspots detectable by PCR overlapped with those detectable by microscopy at a moderate transmission setting but not low transmission settings [228]. Elsewhere, the effectiveness of RDTs and microscopy was greatest in regions with high malaria transmission or in the presence of high parasitaemia [307]. These tests can however miss many infections in low-transmission regions, where microscopy-negative individuals may still contribute 20% - 50% of infections sustaining transmission [308].

According to the WHO-backed “High Burden, High Impact” malaria strategy [4], endemic countries are encouraged to implement sub-nationally tailored plans that differentially address high and low malaria burdens. This requires sensitive, high-throughput, and fast screening tools for malaria with comparable validity across transmission settings [194, 198]. Unfortunately, the performance of new tools such as IR-ML has not been compared across settings. Researchers have been able to identify malaria-positive MIR spectra with models trained on pooled data from both low and high transmission settings or from high transmissions only, but not across strata [217, 218]. Additionally, the positive predictive value (ability to predict true positive cases), and negative predictive value (ability to predict true negative cases) should be clarified. One study in Tanzania estimated the positive and negative predictive values of IR-ML at 92.8% and 91.7%, respectively for detecting malaria infections field-collected dried blood spots relative to PCR [217], but this study had only a small number of samples. Future studies should include broad demonstrations of the performance of IR-ML approaches in different epidemiological strata.

Gap 6: The need for essential human resource training in malaria-endemic countries The implementation of effective malaria surveillance in endemic countries is hindered by inadequacies of trained personnel and facilities. A global survey found that only 8% of malaria-endemic countries had sufficient capacity for vector surveillance and nearly 50% had no capacity to implement core interventions [124]. To effectively implement IR-ML based surveillance at the country level, two forms of training are necessary: one for potential users, including researchers and malaria surveillance officers, and one for higher-level experts capable of tasks such as manipulating infrared and machine learning systems and creating new classification algorithms. Countries may also implement periodic refresher training to boost human resource

capabilities [309]. To ensure sustainability and effectiveness, a comprehensive and strategic training plan involving the development of IR-ML training guidelines and partnerships with research and academic institutions is necessary.

Gap 7: Need to select the most appropriate hardware and software platforms Selecting suitable hardware and software platforms is crucial for enhancing the scalability of IR-ML systems for malaria surveys and diagnostics. A mix of hardware, such as sample collection devices and spectrometers, and software, such as spectral filters and ML models, is necessary. Portable devices are available for field surveys [212, 213, 216], but they are mostly in clinical or research laboratory settings. To implement them on a large scale, spectrometers with hardware systems designed for areas with limited electricity access, such as solar-powered or battery-powered spectrometers, may be necessary. Other options may include the miniaturized IR spectrometers, such as those recently used to detect and quantify malaria parasites in RBCs [305] and for non-invasive parasite detection via the skin of human beings [283].

Spectral data must also be easily interpretable for non-expert users in remote settings. This may require deploying trained algorithms on cloud-based platforms and designing user-friendly interfaces that work with simple internet connectivity. Systems based on mobile phone applications [218] or web interfaces [310] are already being tested, and can be enhanced to remain functional even under limited internet connectivity in remote settings. Lastly, the availability of relevant source codes (preferably via code-sharing platforms such as GitHub) and training in their use should also be ensured.

Gap 8: Need to standardize sample-handling procedures Standardized protocols for sample handling are needed to ensure the comparability of findings and to make IR-ML techniques more widely applicable in parasitological and entomological assessments. Unfortunately, little effort has been devoted to determining the optimal methods for storing and preserving samples for IR-ML investigations. For entomological studies, some protocols have indicated using chloroform to kill specimens and storing them in silica gel for 2-3 days before scanning [212, 216], and also that NIR performs well when samples are stored by either desiccants, RNAlater, or refrigeration [311]. Separately, a study using MIR spectroscopy and ML demonstrated the crucial need for standardized handling (storage or preservation) for both training and validation samples [295].

Proper sample storage and preservation is also essential for reducing spectral noise and preserving the biochemical composition of the specimens. For example, the use of anticoagulant materials can significantly affect model performance when using dried RBCs compared to the wet RBCs or whole blood when scanned using

ATR-FTIR spectroscopy [301]. While some of these challenges can be addressed by statistical approaches, e.g. transfer learning [282], optimal performance requires a level of standardization in methods for handling different sample types destined for IR-ML analysis.

Table 2.1: A summary of key research questions and potential research agenda for IR-ML applications relevant to malaria surveys and diagnostics.

R&D Gaps	Descriptions and Examples	References
Incomplete understanding of the IR spectroscopic signals relative to specific biological traits	There is an insufficient understanding of the IR spectroscopic signals (vibrational absorption bands/wavelengths) and their association with biological traits such as parasite infections, age, species, and blood meals.	[212, 216, 217, 305]
Inadequate field validation of the IR-ML approaches	There is insufficient field validation of the performance of IR-ML methods for assessing important entomological and parasitological indicators.	[212, 213, 218, 302]
Gaps in machine learning frameworks for the IR spectroscopy analysis	There is a need for studies to identify optimal ML objectives such as computational efficiency, prediction accuracy, and model generalizability. This might entail one or a combination of the many existing unsupervised and supervised algorithms.	[212, 213, 218, 305]
Unknown detection thresholds	There has not been sufficient demonstration of the limits of detection of IR-ML techniques for detecting malaria infections in human or mosquito samples.	[222, 300, 305]

R&D Gaps	Descriptions and Examples	References
Uncertain granularity of discretized biological outcomes	It is uncertain which method of classifying mosquito age is the best. For example, comparing classification by specific days (1, 2, 3, 4 days) to using longer ranges of days (1, 3, 5, 7 days) or grouping days into ranges (1-5, 5-7, 7-10 days) is unclear.	[212, 213]
Resolving overlap and interactions between signals	For biological indicators such as blood meal identification, the possibilities of detecting mixed blood sources remain unknown, and how long after feeding, the blood can still be detected.	[212, 213]
Lack of evidence from different epidemiological profiles or settings	There is a need to demonstrate the performance of the IR-ML techniques for detecting malaria parasites in areas with varying epidemiological strata—with low to high transmission or prevalence, and in conditions with varying parasite densities.	[217, 218]
Gaps related to hardware and software for IR and ML	There are limited off-the-shelf portable tools that are completely ready for applications in malaria surveys and diagnostics in both laboratory and field settings.	[216, 218, 300]
Need to standardize sample-handling procedures	There is currently no standardized protocol for sample handling when using IR-ML methods for malaria surveys and diagnostics.	[295, 301, 311]

2.5.2 Target product characteristics of the IR and ML approaches

To guide further development and evaluation of the IR-ML based approaches for parasitological and entomological investigations of malaria, this article proposes an initial outline of key characteristics that should be met. This target product profile (TPP) consolidates the current thoughts and expertise of the authors as experts and early adopters of the application of this technology for malaria surveys. However, this TPP is subject to future modifications and should be considered as a preliminary version. To satisfy the global strategies for malaria monitoring, the draft describes the necessary and desirable qualities of emerging IR and ML-based techniques for use in both field surveys and clinical settings (Tables 2.2 and 2.3).

Different TPPs have previously been proposed for future vector surveillance tools [277] and malaria diagnostic tools [312]. The article complements these by proposing relevant attributes for IR-ML techniques including both parasitological (Table 2.2) and entomological measures (Table 2.3). The proposed profile presents both the core characteristics, which are the minimum basic requirements for a functional system, as well as other desirable characteristics that could further improve the capabilities, scalability, and cost-effectiveness of this technology.

Table 2.2: Proposed Target Product Profile (TPP) for an IR-ML based system for parasitological surveillance of malaria (focusing on detecting parasites in vertebrate host)

	Characteristics	**Parasitological surveillance**			
		Passive case detection in clinical settings (symptomatic cases)		**Active case detection in field screening (asymptomatic cases)**	
		Essential characteristics	**Desired characteristics**	**Essential characteristics**	**Desired characteristics**
Scope	Intended use settings and contexts	As point-of-care test in malaria control settings	As point of care test in elimination and control settings	Malaria screening in moderate to high transmission settings	Can be used in low, moderate and high transmission settings
	Implementation level	District-level health facilities, other centralized facilities & research facilities	Can be used in peripheral health facilities, e.g., dispensaries, health posts & health centres	Used for surveys in research facilities	Routine parasitological surveys in district or regional hospitals
	Types of spectrometers and durability	Bench-top units that require minimum electricity, and can operate 5 years or more with minimal maintenance	Off-the-shelf portable units with long-life battery; can be solar-powered; can operate for up to 10 years with minimal maintenance	Bench-top units that require minimum electricity, and can operate 5 years or more with minimal maintenance	Off-the-shelf portable units with long-life battery; can be solar-powered; can operate for up to 10 years with minimal maintenance

	Characteristics	Parasitological surveillance			
		Passive case detection in clinical settings (symptomatic cases)		**Active case detection in field screening (asymptomatic cases)**	
		Essential characteristics	**Desired characteristics**	**Essential characteristics**	**Desired characteristics**
Technical performance	Sensitivity relative to conventional methods [307, 313, 314]	Can detect >95% of positive *P. falciparum* cases in symptomatic individuals relative to RDT	Can detect >99% of positive *P. falciparum* cases in symptomatic individuals relative to RDT or microscopy	Detects >95% of positive *P. falciparum* cases in moderate to high transmission areas relative to microscopy or RDT or PCR	Detects >95% of positive *P. falciparum* cases in low, moderate or high transmission areas relative to microscopy or PCR
	Specificity relative to current tests [307, 313, 314]	Can identify >95% of malaria-negative cases in febrile individuals relative to RDT	Can identify >99% of malaria-negative cases in febrile individuals relative to RDT or microscopy	Can identify >95% of malaria-negative cases in areas with moderate to high transmission relative to microscopy or RDT or PCR	Can identify >99% of malaria-negative cases in low, moderate to high transmission areas relative to microscopy or PCR.
	Resolution and accuracy of predictions	Achieves at least 95% accuracy compared to RDT or microscopy	Performance equivalent to microscopy or RDTs in detecting *P. falciparum* & other malaria parasites	Has >95% accuracy compared to RDT or microscopy in moderate high transmission sites	Performance matches PCR in detecting malaria parasites under low - high transmission

	Characteristics	Parasitological surveillance			
		Passive case detection in clinical settings (symptomatic cases)		**Active case detection in field screening (asymptomatic cases)**	
		Essential characteristics	**Desired characteristics**	**Essential characteristics**	**Desired characteristics**
Technical performance	Lower limit of parasite detection (LOD)	50-100 parasites/µl of blood; equivalent to microscopy & RDTs in respective settings	<10 parasites/µl of blood; better performance than microscopy in low transmission settings	10-100 parasites/µl of blood; better than microscopy & RDTs in moderate to high transmission settings	1-10 parasites/µl of blood; more accurate than microscopy & RDTs in all settings
	Durability and stability	Stable in ambient temperatures and can withstand increases to 45°C for short periods and varied humidity.	Stable in ambient temperatures and can withstand increases to 45°C for short periods and varied humidity.	Stable in ambient temperatures and can withstand increases to 45°C for short periods and varied humidity.	Stable in ambient temperatures and can withstand increases to 45°C for short periods and varied humidity.
Operational aspects	Equipment & maintenance costs	Less than $ 30,000 per spectrometer; lasts >5 years; costs < $100/yr to maintain	Less than $ 2000 per portable spectrometer; lasts up to 10 years; Costs < $50/Yr to maintain	Less than $ 30,000 per spectrometer; lasts >5 years; costs < $100/yr to maintain	Less than $ 2000 per portable spectrometer; lasts up to 10 years; Costs < $50/Yr to maintain
	Sample handling costs	Costs < $0.1 per test	Costs < $0.01 per test	Costs < $0.1 per test	Costs < $0.01 per test

	Characteristics	Parasitological surveillance			
		Passive case detection in clinical settings (symptomatic cases)		**Active case detection in field screening (asymptomatic cases)**	
		Essential characteristics	**Desired characteristics**	**Essential characteristics**	**Desired characteristics**
	Test duration	<5 minutes	<1 minute	<5 minutes	<1 minute
	Sample preservation and storage	Requires freezing, desiccants, RNAlater Uses must be less than 30 days old.	Can use any preservation method Samples can be older than six months as long as preserved fresh	Freezing, desiccants or RNAlater; Samples must be less than 30 days old	Any preservation method; Samples can be older than six months as long as preserved fresh.
Operational aspects	Human resources: Skills & training	Requires minimal training on sample handling, scanning & data interpretation	No more than 30 minutes training needed to use, conduct the tests and read results	Requires minimal training on sample handling, scanning & data interpretation	No more than 30 mins training needed to use, conduct the tests and read results
	Type of sample	Wet or dry blood samples; presented as glass slides, on filter papers or as blood drops.	Both blood and non-blood samples (saliva, urine, sweat or other samples collected non-invasively e.g. over the skin)	Wet or dry blood samples; presented as glass slides, on filter papers or as blood drops.	Both blood and non-blood samples (saliva, urine, sweat or other samples collected non-invasively e.g. via skin)

Characteristics	Parasitological surveillance			
	Passive case detection in clinical settings (symptomatic cases)		**Active case detection in field screening (asymptomatic cases)**	
	Essential characteristics	**Desired characteristics**	**Essential characteristics**	**Desired characteristics**
Reagents	No reagents needed except for cleaning the instruments or sample collection	No reagents needed except for cleaning the instruments or sample collection	No reagents needed except for cleaning the instruments or sample collection	No reagents needed except for cleaning the instruments or sample collection

Table 2.3: Proposed Target Product Profile (TPP) for an IR-ML based system for entomological surveillance of malaria

	Characteristics	Entomological surveillance	
		Essential characteristics	**Desired characteristics**
Scope	Intended use	Mosquito identification; mosquito age-grading, detection of *Plasmodium*-infected mosquitoes and blood meal identity	One-stop platform for most desired entomological indicators; species IDs, age grading, blood meal identifications, infection detection, and assessment of insecticide resistance status, i.e., ability to predict resistance phenotype as per standard bioassays.
	Implementation level	Can be used in research laboratories and training centres	Used for research and routine surveillance services laboratory and field settings.
	Types of spectrometers and durability	Bench-top units that require minimum electricity, and can operate 5 years or more with minimal maintenance	Off-the-shelf portable units with long-life battery; can be solar-powered; can operate for up to 10 years with minimal maintenance
Technical performance	Sensitivity relative to current methods [208, 209]	*Plasmodium* sporozoites: Sensitivity of > 90% with reference to ELISA	*Plasmodium* sporozoites: Sensitivity of > 90% with reference to PCR
	Specificity relative to current methods [208, 209, 267]	*Plasmodium* sporozoites: Specificity of > 90% with reference to ELISA, Microscopy or PCR	*Plasmodium* sporozoites: Specificity of > 90% with reference to PCR

	Characteristics	Entomological surveillance	
		Essential characteristics	**Desired characteristics**
	Resolution of predictions	*Mosquitoes age:* can classify young (e.g. 1-6 days) vs old (e.g. > 10 days) mosquitoes, with > 90% accuracy *Species identification:* Can distinguish between members of a species complex (e.g. *An. gambiae* vs. *An. arabiensis*) with > 90% accuracy *Mosquito blood meals:* Can distinguish between human blood meal from any other vertebrate blood meals, with >90% accuracy	*Mosquitoes age:* Can classify mosquito ages chronologically at 2-day resolution (e.g 1, 3, 5 days etc) with > 90% accuracy *Species:* Can identify all major malaria vectors (*An. gambiae*, *An. arabiensis*, *An. coluzzii* and *An. funestus*) with >90% accuracy *Blood meal:* Can identify most vertebrate blood meals (i.e. human, cattle, goat, chicken, dog etc) even if the meals are mixed, and with >90% accuracy
	Lower limit of parasite detection	*Plasmodium* sporozoites: has performance equivalent to ELISA or PCR	*Plasmodium* sporozoites: has performance equivalent to PCR
	Temperature and humidity stability	Functions and can be stored in ambient temperature; withstands frequent temperature rises to 35°C for long periods under diverse humidity	Functions and can be stored in ambient temperature; withstands frequent temperature rises to 45°C for long periods under diverse humidity
Operational aspects	Equipment & maintenance costs	Less than $ 30,000 per spectrometer; lasts >5 years; costs < $100/yr to maintain	Less than $ 2000 per portable spectrometer; lasts > 5 yrs; Costs < $50/Yr to maintain
	Sample handling costs	Costs < $0.1 per test	Costs < $0.01per test
	Test duration	<5 minutes	<1 minute

	Characteristics	Entomological surveillance	
		Essential characteristics	**Desired characteristics**
	Sample preservation and storage	Requires freezing, desiccants, RNAlater Uses must be less than 30 days old.	Can use any preservation method Samples can be older than six months as long as preserved fresh
Operational aspect	Human resources: Skills & training	Requires minimal training on sample handling, scanning & data/results interpretation	No more than 30 minutes training needed to use, conduct the tests and read results
	Type of sample	Can analyse dried mosquito body parts	Can analyse either fresh or dried mosquito body parts
	Reagents	No reagents needed except for cleaning the instruments or sample collection	No reagents needed except for cleaning the instruments or sample collection

2.6 Conclusion

The combination of infrared spectroscopy and machine learning is being considered a promising new method for predicting or estimating various entomological and parasitological indicators of malaria. The IR-ML platforms have the added advantage of being simple to use, reagent-free, high-throughput, low-cost, and applicable in rural and remote settings. As malaria-endemic countries seek to enhance their surveillance-response strategies to achieve elimination targets, an important question is how IR-ML-based approaches can complement ongoing processes and be integrated into routine surveillance. This paper has reviewed existing IR and ML applications and their gaps for malaria surveys and parasite screening; with provision of initial suggestions on target product profiles (TPPs) for such technologies in low-income settings. The TPPs outline both essential and desirable attributes to guide further development. The article also outline key research and development gaps that should be addressed in the short and medium term, including the need for field validation, determination of minimum detection threshold, capacity development and training in user countries, assessment of the validity of the tests in different epidemiological strata, and work on robust hardware and software to enable expanded use.

Chapter 3: Screening of malaria infections in human blood samples with varying parasite densities and anaemic conditions using AI-Powered mid-infrared spectroscopy

Published in Malaria Journal 2024:
https://doi.org/10.1186/s12936-024-05011-z

3.1 Abstract

Background: Effective testing for malaria, including the detection of infections at very low densities, is vital for the successful elimination of the disease. Unfortunately, existing methods are either inexpensive but poorly sensitive or sensitive but costly. Recent studies have shown that mid-infrared spectroscopy coupled with machine learning (MIRs-ML) has potential for rapidly detecting malaria infections but requires further evaluation on diverse samples representative of natural infections in endemic areas. The aim of this study was, therefore, to demonstrate a simple AI-powered, reagent-free, and user-friendly approach that uses mid-infrared spectra from dried blood spots to accurately detect malaria infections across varying parasite densities and anaemic conditions.

Methods: *Plasmodium falciparum* strains NF_{54} and FCR_3 were cultured and mixed with blood from 70 malaria-free individuals to create various malaria parasitaemia and anaemic conditions. Blood dilutions produced three haematocrit ratios (50%, 25%, 12.5%) and five parasitaemia levels (6%, 0.1%, 0.002%, 0.00003%, 0%). Dried blood spots were prepared on Whatman^{TM} filter papers and scanned using attenuated total reflection-Fourier Transform Infrared (ATR-FTIR) for machine-learning analysis. Three classifiers were trained on an 80%/20% split of 4655 spectra: (I) high contrast (6% parasitaemia vs. negative), (II) low contrast (0.00003% vs. negative) and (III) all concentrations (all positive levels vs. negative). The classifiers were validated with unseen datasets to detect malaria at various parasitaemia levels and anaemic conditions. Additionally, these classifiers were tested on samples from a population survey in malaria-endemic villages of southeastern Tanzania.

Results: The AI classifier attained over 90% accuracy in detecting infections as low as one parasite per microlitre of blood (0.00003%), a sensitivity unattainable by conventional RDTs and microscopy. These laboratory-developed classifiers seamlessly transitioned to field applicability, achieving over 80% accuracy in predicting natural *P. falciparum* infections in blood samples collected during the field survey. Crucially, the performance remained unaffected by various levels of anaemia, a common complication in malaria patients.

Conclusion: These findings suggest that the AI-driven mid-infrared spectroscopy approach holds promise as a simplified, sensitive and cost-effective method for malaria screening, consistently performing well despite variations in parasite densities and anaemic conditions. The technique simply involves scanning dried blood spots with a desktop mid-infrared scanner and analysing the spectra using pre-trained AI classifiers, making it readily adaptable to field conditions in low-resource settings. In this study, the approach was successfully adapted to field use, effectively predicting natural malaria infections in blood samples from a population-level survey in Tanzania. With additional field trials and validation, this technique could significantly enhance malaria surveillance and contribute to accelerating malaria elimination efforts.

3.2 Background

Malaria control has made significant progress in recent decades but there are still an estimated 600,000 deaths and 250 million cases annually, most of these in sub-Saharan Africa [1]. To accelerate elimination efforts, effective strategies are required, both for control and for surveillance. There is an urgent need for simple, scalable and low-cost methods for monitoring key malaria metrics, so as to establish prevailing risk, evaluate impacts of control measures and assess overall progress against malaria. The World Health Organization (WHO) underscores the need for evidence-based and context-specific control strategies – which require sensitive, rapid, and affordable screening tools that are deployable at scale even in low-income or remote settings [194]. This includes the need for accurate detection of malaria infections – both at clinical points of care settings and in population surveys.

While rapid diagnostic tests (RDTs), microscopy, and polymerase chain reactions (PCR) have played a crucial role in the diagnosis and management of malaria across endemic and elimination situations [103], these approaches still have major limitations in most settings. For example, RDTs have transformed malaria case management across Africa due to their practicality and affordability [231], yet studies

show that as many as half of children in some poor communities still lack access to these tests [197,315]. Their effectiveness is also increasingly threatened by deletions on the histidine-rich protein 2 and 3 (HRP II and III) genes, which code for the protein targets of most *Plasmodium falciparum* RDTs [118,316,317]. Additionally, both microscopy and RDTs have poor sensitivity when parasite densities fall below 50-100 parasites/µL of blood [103,197,227,313,318]; and can miss significant fractions of sub-microscopic infections, which can contribute 20-50% of all human-to-mosquito transmission in low endemicity settings [308]. From an operational perspective, microscopy requires electrical power sources, can take as long as 30 minutes to run, is prone to subjective interpretations of results and can be expensive due to personnel costs and reagents [230]. Unfortunately, even the highly sensitive techniques, such as PCR, enzyme-linked immunosorbent assays (ELISA), and loop-mediated isothermal amplification (LAMP), which detect as few as 5 parasites/µL of blood, with greater accuracy, are expensive, and require highly skilled workers.

In recent years, infrared spectroscopy (IR) in both the near (NIR) and mid (MIR) infrared ranges has shown substantial promise for monitoring key entomological and parasitological indicators of malaria - including detecting malaria infections in human blood [174,217,305]. The technology is rapid, robust, reagent-free, and requires minimum skills to operate. Infrared spectroscopy involves shining infrared light through biological specimens to infer their biochemical composition, which can be analysed using different mathematical techniques to distinguish meaningful traits, such as infection status, age, and species. Given the complexities of assigning spectroscopic bands for interpreting patterns associated with malaria infections, recent studies have been integrating spectroscopy with either multivariate analysis or machine learning (ML) approaches to more effectively interpret the key biological traits [173,174,213]. Infrared spectroscopy combined with machine learning (IR-ML), outperforms the traditional analyses in detecting malaria by efficiently deciphering complex, non-linear, multi-correlated spectral signals and exhibiting high accuracy [174,212]. For example, during the development cycle, malaria parasites generate distinctive biomarkers, which are evident on infrared spectra and can be used to identify infected individuals [173,218,222]. Further, models have been reported to achieve over 90% precision in differentiating infected from uninfected blood samples [217,218].

Despite IR-ML techniques demonstrating potential in identifying malaria infections in whole blood or isolated red blood cells (RBCs), critical gaps remain to be addressed, one of which is the need to evaluate the lower limits of parasite detections and quantifications [174]. One study has shown that MIR coupled with multivariate statistics could detect low density malaria infections at <1-5 parasites/µL of blood in

methanol-fixed RBCs [222]. However, no tests have been done on the actual detection thresholds critical for applications of IR-ML in either point-of-care tests or population surveys using whole blood specimens.

Another key gap is the need to identify and estimate the impacts of confounding factors. In areas with high malaria transmission, infected individuals often exhibit decreased haemoglobin concentrations, other parasitic infections, nutritional deficiencies or other concomitant factors [319–321]; all of which may compromise tools such as IR-ML that are designed to detect biochemical changes resulting from malaria infections. Indeed, previous MIR-ML models trained for malaria detection may have been influenced by the association of co-variates (e.g., anaemia and immune response to parasites) rather than true parasite signals [217]. Immunological variations from persistent asymptomatic infections may also affect performance of IR-ML results for malaria detection, in ways not detectable in studies that use blood bank samples from limited numbers of volunteers. ML algorithms should therefore consider these variabilities, e.g. by incorporating varying anaemic, nutritional or immunologic conditions, but also train models with different parasite ‘contrasts’, to disentangle true infections more effectively from these noise signals.

The aim of this current study was therefore to assess the lower limit of malaria parasite detection on dried blood spots (DBS) using MIR-ML approaches, investigate the impact of anaemic conditions on detecting malaria infections and demonstrate the best ML training approaches, whether utilizing high, low, or combined parasite concentrations, and finally test them on spectra of actual malaria-infected patients. The DBS were generated using whole blood from 70 malaria-free volunteers to capture immunological variations, and were spiked with cultured ring-stage *P. falciparum* at various parasitaemia and haematocrit ratios to mimic anaemia. ML algorithms were then trained on MIR spectra acquired from laboratory-generated DBS, where specific malaria parasite signals could be learned. MIRs-ML, trained with high-contrast parasite concentrations against negatives, demonstrated a detection accuracy of over 90% in laboratory tests across various parasitaemia levels; in field-collected samples, the accuracy consistently remained above 80%.

3.3 Methods

3.3.1 Malaria parasite cultures

Sample collection and parasite cultures were completed at Ifakara Health Institute's laboratories in Bagamoyo, Tanzania using adapted protocols with slight adjustments [322, 323]. Group O+ blood was obtained from four malaria-free volunteers, and kept in tubes containing the anticoagulant, ethylenediaminetetraacetic acid (EDTA) for continuous culturing of *P. falciparum* strains NF_{54} and FCR_3. The blood was centrifuged at 2500 rpm at 24°C for 10 minutes to obtain RBCs. The RBCs were then washed, diluted to 50% haematocrit with uncomplemented media, namely Roswell Park Memorial Institute (RPMI) 1640 media supplemented with hypoxanthine, neomycin and 4-(2-hydroxyethyl)-1-piperazineethanesulfonic acid (HEPES), and stored at 4°C.

The washed RBCs were used to culture *P. falciparum* in vitro for up to seven days. The asexual malaria parasites were grown in uninfected washed O^+ RBCs as host cells at 5% haematocrit, maintained in RPMI-1640 medium supplemented with 25 mM HEPES, 100 µM hypoxanthine, neomycin, 5% Albumax II, and 24 mM sodium bicarbonate. The parasite culture was gassed with a mixture of 5% CO_2, 3% O_2, and 93% N_2 and incubated at 37°C. The culture was examined daily for parasitaemia estimation using field-stained (Hemacolor® rapid staining) thin blood smears under a compound microscope in 10 fields. Two rounds of parasite synchronization were performed to ensure the remaining parasites were only ring-stage *P. falciparum* [324]. The culture was kept until the ring-stage parasitaemia level reached >6% and was used for experimental dilutions. Parallel malaria-free cultures with only media and O^+ RBCs from the same volunteers were kept to create controls. The process was repeated for up to 11 batches until 70 volunteers were recruited and their blood was diluted.

3.3.2 Recruitment of malaria-free volunteers

Malaria-free individuals were recruited from tertiary-level colleges in Bagamoyo, eastern Tanzania, following sensitization meetings, during which the objectives, procedures, potential risks, and benefits of the study were explained. Participants who expressed interest were given a unique identity number, contacted by phone, and requested to provide informed consent. The consenting participants were screened for malaria parasites using RDTs by taking a finger-prick blood sample,

followed by a confirmatory quantitative polymerase chain reaction (qPCR). Participants who tested negative for malaria were enrolled in the study, while those who tested positive were treated following Tanzania's malaria treatment guidelines and excluded from the study [325]. A total of 70 volunteer participants were recruited, all between 20 and 40 years old. A total of 40 mL venous blood was drawn in an EDTA tube from each participant and used for laboratory dilutions of cultured malaria parasites to create different malaria parasitaemia and haematocrit ratios.

3.3.3 Haematocrit dilutions to mimic anaemic conditions

For each participant, two sets of haematocrit dilutions were created to simulate different anaemic conditions for both infected and un-infected blood. One set had malaria-free blood at 50%, 25%, and 12.5% haematocrit content, while the other comprised infected red blood cells (iRBCs) from cultured parasites, adjusted to 50%, 25%, and 12.5% haematocrit ratios using respective plasma. For uninfected blood, 40 ml of venous blood from each participant was split into 5 ml and 35 ml portions and centrifuged to separate plasma from RBCs. After separation, plasma was transferred to empty 1.5mL tubes for haematocrit dilutions. RBCs from the 5 ml portion were used to formulate a 50% haematocrit stock solution by adding plasma from the same volunteer. Serial dilutions was done by transferring 2.5 ml of the stock solution to a second tube, and adding 2.5 ml of previously obtained plasma to simulate moderate anaemia (25% haematocrit) and severe anaemia (12.5% haematocrit) conditions (Figure 3.1). On the other hand, for infected blood, when the culture reached >6% ring stage parasitaemia, it was centrifuged to separate iRBCs from the culture media and washed twice. Washed iRBCs volume was 0.5 ml, which was mixed with an equal volume of participant plasma (0.5 ml) to create a 50% haematocrit ratio stock solution; and serially diluted to 25% and 12.5% solutions (Figure 3.1).

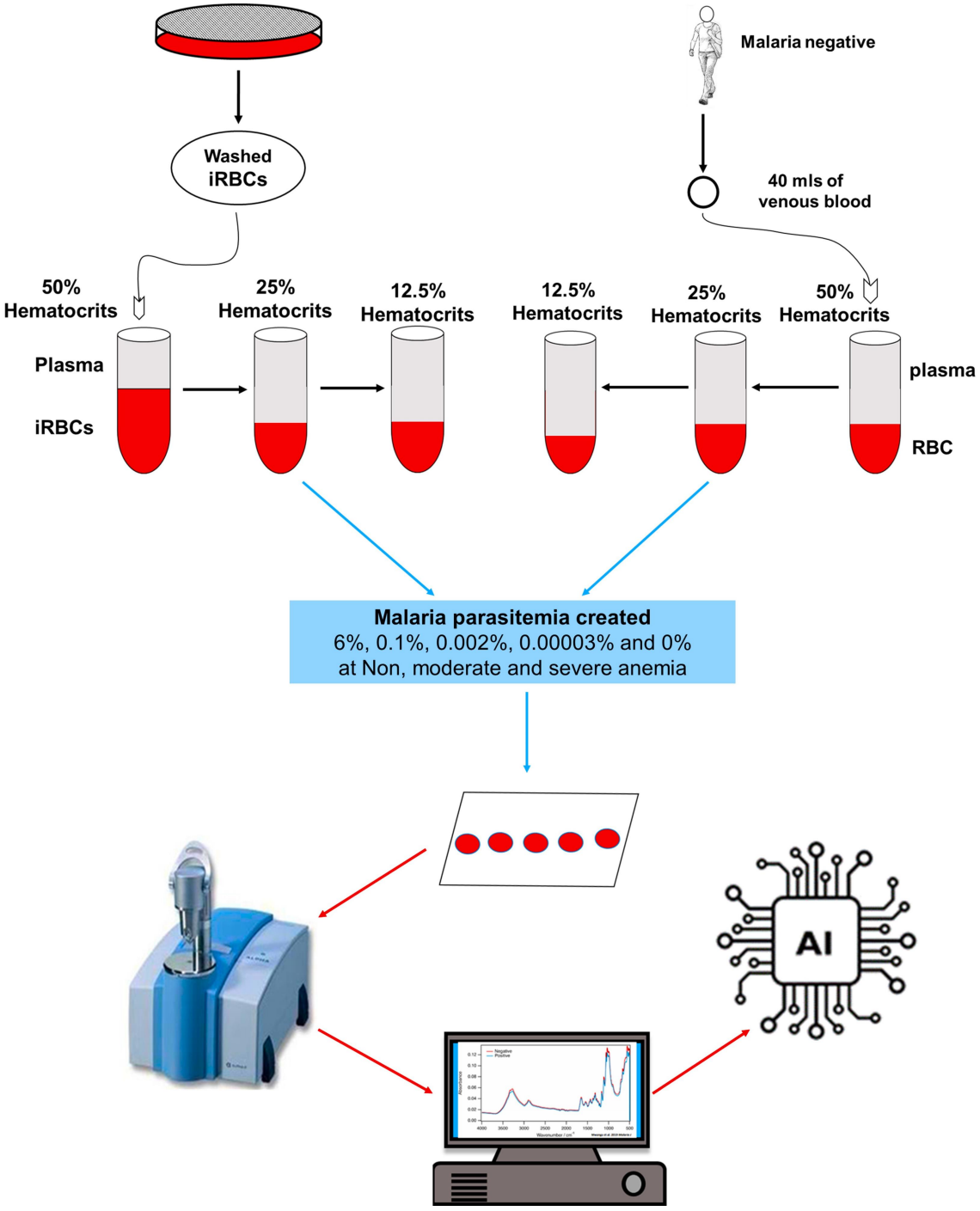

Figure 3.1: Schematic flow of experimental setup used to create DBS of different parasitaemia under non-anaemic (50%), moderate (25%), and severe anaemia (12.5%) and then scanned with MIR Spectrometer for spectra acquisitions and analysis using AI approaches

3.3.4 Serial dilutions for different parasite densities and controls

The parasite dilutions were performed at the respective haematocrit ratios. Initially, the cultured parasitaemia was standardized to 6% stock – and in cases where the initial densities were higher, this was lowered to the 6% densities. Serial dilutions were done to create three additional parasitaemia levels, i.e. 0.1%, 0.002% and 0.00003%, were created from the stock solution.

The control group included malaria-negative samples at haematocrits of 50%, 25%, and 12.5% prepared from uninfected RBC from the culture with plasma from same individual participants. To ensure that the RBC distribution in the control matched that of the malaria parasitaemia dilutions, uninfected haematocrits from the culture were diluted with uninfected haematocrits from participants in volumes equal to the parasitaemia dilutions (Figure 3.1).

3.3.5 Preparation of dried blood spots

For each individual volunteer, five replicates of dry blood spots (DBS) for each parasite density at each haematocrit level were created, resulting in a total of 75 DBS per participant. For each DBS, 50 µL of blood was added on the circular spot on the Whatman^{TM} paper cards. The experimental design ensured that all malaria-positive and negative samples utilized similar filter paper cards to standardize the potential impact of filter paper on ML analysis. The cards were air-dried for up to 3 hours and labelled with batch number, date, parasitaemia levels, haematocrit ratio, and participant ID. To prevent cross-contamination, each card was sealed in a plastic bag. The cards were then grouped by participant ID and stored in a cool environment in a larger bag with desiccant packets and a humidity card, awaiting transportation to another Ifakara Health Institute's facility, the VectorSphere, at Ifakara, Tanzania for infrared scanning. During transport, the bags were kept in a cooler box with ice packs separated by plastic sheeting.

3.3.6 Acquisition and pre-processing of infrared spectra

The DBS were individually scanned using a Fourier transform infrared spectrometer (FT-IR) with a wavenumber range of 4000-500 (cm^{-1}) and a resolution of 2 (cm^{-1}). The instrument employed was a compact Bruker Alpha FTIR interferometer, equipped with a Platinum-Attenuated Total Reflectance (ATR) module that incorporates diamond crystals. Scanning was done after 3-5 days of DBS storage.

Each blood spot was punched and placed on the diamond crystal. For scanning, each blood spot was excised, positioned on the diamond crystal, and subjected to pressure using an anvil to enhance the contact area with the crystal, thereby optimizing the depth of light penetration. Each spot was scanned 32 times to obtain an averaged spectrum, which was labelled by project initial, study site, participant ID, haematocrit ratio, parasitaemia ratio, and dates.

To quantify the depth of light penetration (d) in whole blood, a theoretical approach that considers the wavelength of light (λ), incidence angle (θ), and the refractive indices of whole blood (n_1) and the diamond crystal (n_2) used in the spectrometer was employed. The penetration depth (d) (refer to Fig SS3.1) was calculated using the formula indicated in equation 3.1:

$$d = \frac{\lambda n_1}{2\pi\sqrt{\sin^2\theta - \left(\frac{n_2}{n_1}\right)^2}} \tag{3.1}$$

Given that the incidence angle (θ) was fixed at 45°, the refractive index of whole blood (n_1) was determined using the Sellmeier equation (with λ expressed in micrometres) [326], given as equation 3.2 :

$$n_1(\lambda) = 1 + \frac{0.7960 \times \lambda^2}{\lambda^2 - 1.0772 \times 10^4} + \frac{5.1819 \times \lambda^2}{\lambda^2 - 78301 \times 10^5} \tag{3.2}$$

Similarly, the refractive index of the diamond crystal (n_2) was ascertained through its corresponding Sellmeier equation [326], given as equation 3.3:

$$n_2(\lambda) = 1 + \frac{4.3356 \times \lambda^2}{\lambda^2 - 0.1060^2} + \frac{0.3306 \times \lambda^2}{\lambda^2 - 0.1750^2} \tag{3.3}$$

The acquired spectra were then pre-processed using a Python program to compensate for atmospheric interferences, water vapour, and carbon dioxide (CO_2) and to discard spectra with poor quality as described by González-Jiménez et al. [212]. The pre-processed spectra were subsequently used for training, testing, and validating machine-learning algorithms.

3.3.7 Selection of machine-learning models

Machine learning analysis was conducted using the Python programming language, version 3.9. Employing a supervised ML classification approach, seven classifiers were evaluated: Logistic Regression (LR), Support Vector Machine (SVM), Random Forest (RF), Gradient Boosting (XBG), Decision Tree (DT), Extra Tree (ET) Classifier, and Bagging Classifier (BC). The non-anaemic class (50% haematocrit) was utilized for ML algorithm selection and training, while the two other haematocrit ratios (25% and 12.5%) were kept separate and used to assess the impact of anaemia on the ability of the models to classify infected versus non-infected specimen from sets of previously unseen spectra. To do this, the non-anaemia data was shuffled and split into two portions; 70% for model selection, training, and testing, while 30% were kept separate as an unseen dataset for validating the trained model. Further, 70% portion were divided into 80–20% train-test split, respectively. For model selection, training, and testing, balanced classes were ensured through random under-sampling of the majority class.

Stratified shuffle split, 10-fold cross-validation (SSS-CV) was employed to select the best machine-learning algorithm for identifying malaria infections. The seven mentioned algorithms were evaluated, and the best one was selected based on accuracy scores to distinguish malaria infections within the non-anaemia class using three approaches: (i) Cross-validation using datasets with high contrast (Positive class = 6%, N = 230) against the negative class (Negative = 0%, N = 230); (ii) Cross-validation with all concentrations (6%, 0.1%, 0.002%, and 0.00003%) combined as the positive class (N = 220) against the malaria-negative class (N = 220); and lastly, (iii) Cross-validation with low contrast (positive class = 0.00003%, N = 226) against the negative class (N = 226) datasets. Model selection, training and validation were performed on standardized absorption intensities relative to their wavenumbers.

3.3.8 Training, testing and validation of machine learning models to identify malaria parasite presence in non-anaemic spiked blood

The best ML algorithms selected through SSS-CV were then trained on 80% of the spectra data from non-anaemic blood using three distinct approaches: (i) High Contrast: models were trained using highest parasite densities (6%) as positive samples against negatives (0%); (ii) All Concentrations: models were trained using combined all parasite densities (6%, 0.1%, 0.002% and 0.00003%) as positives,

against negatives (0%); and (iii) Low Contrast: models were trained using lowest parasite densities (0.00003%) as positives, against negatives (0%). The trained models underwent fine-tuning through Grid Search for optimal hyper parameter optimization.

For testing purposes, the final tuned classifiers were tested on a similar parasitaemia class used for training. For instance, the model trained on 80% of the data with high contrast at 6% against negatives was also tested on the remaining 20% of the data at the highest contrast against negative classes. In addition to accuracy, other evaluation measures such as sensitivity, specificity, recall, and F1-score on the test set (20%) were calculated. Finally, the best classifiers were validated on a completely unseen dataset, the 30% kept separate at the start. Beginning with non-anaemic classes at different parasitaemia levels, the total number of DBS included for model validation in the non-anaemic class with various parasitaemia levels were as follows: validated model performance on predicting malaria infections at non-anaemic conditions when positive at 6% parasitaemia (N = 82) against negative 0% (N = 82); then validated positive at 0.1% (N = 82) against negative 0% (N = 82), followed by positive at 0.002% (N = 82) against negative 0% (N = 82), and finally, positive at 0.00003% parasitaemia (N = 82) against negative 0% (N = 82).

3.3.9 Evaluating the effect of anaemia on performance of MIRs-ML for distinguishing between blood samples with and without malaria parasites

The best classifiers developed for predicting malaria infections without considering anaemia were evaluated on a new dataset comprising cases of moderate anaemia (with a haematocrit level of 25%) and severe anaemia (with a haematocrit level of 12.5%). This evaluation was structured across four distinct categories: (i) malaria-positive with a 6% parasitaemia rate (N = 101) versus malaria-negative with a 0% parasitaemia rate (N = 101); (ii) malaria-positive with a 0.1% parasitaemia rate (N = 101) versus malaria-negative (N = 101); (iii) malaria-positive with a 0.002% parasitaemia rate (N = 101) versus malaria-negative (N = 101); and (iv) malaria-positive with a 0.00003% parasitaemia rate (N = 101) versus malaria-negative (N = 101). The accuracy, sensitivity, and specificity of these models computed using a bootstrap method with 100 iterations and establishing a 95% confidence interval for these metrics.

Finally, a generalized linear model was used to test the statistically significant effect of anaemia and parasitaemia on the performance of MIRs-ML approaches in predicting malaria infections.

3.4 Results

3.4.1 Generating samples of different parasite densities and anaemic conditions

In order to identify the lowest detectable concentrations of malaria parasites and assess the impact of anaemia on the predictive accuracy of MIRs-ML for malaria infections, cultured *P. falciparum* ring-stage parasites were diluted with malaria-negative blood from seventy volunteers to generate four different parasite densities (Figure 3.1). The two lowest malaria parasitaemias (0.002% or 50–100 parasites/µL and 0.00003% or 1–3 parasites/µL) were selected to correspond to the approximate detection limits of RDT/microscopy and PCR, respectively. Additionally, parasitaemia levels of 6% and 0.1% were chosen to capture the highest parasite contrasts in the training dataset. Haematocrit was set at 50%, 25%, and 12.5% to represent normal, moderate, and severe anaemia, respectively. Thus, a two-way matrix consisting of four malaria-positive parasitaemia levels (6%, 0.1%, 0.002%, and 0.00003%) and a negative class (0%), along with three anaemic classes, was generated (Table SS3.1). In total, 4,655 DBS were created and scanned using an MIR spectrometer, which were used to train and evaluate ML classifiers. Samples were randomly selected to confirm the success of dilutions (Fig SS3.2 and SS3.2).

3.4.2 Selection and training of machine-learning classifiers

4,559 spectra were analysed with varying malaria parasite densities and haematocrit ratios. Of these, 12 spectra from the non-anaemic samples, 35 from moderately anaemic samples, and 49 from severely anaemic samples were discarded due to excessive water content resulting from plasma and atmospheric interference (Table SS3.2). The mean spectra of each parasitaemia class at different anaemic conditions revealed characteristic biochemical signatures of *P. falciparum* infections such as amide, lipids, and haemozoin (Fig SS3.1) [327]. To ensure ML classifiers would learn features associated with malaria infections, an infrared region without the key

biochemical information (from 2799 to 1801 (cm^{-1})) was eliminated [222], and the regions 3100–2800(cm^{-1}) and 1800–900 (cm^{-1}) were selected to train and validate ML classifiers.

First, using 10-fold stratified shuffle split cross-validation (SSS-CV), LR achieved the highest SSS-CV accuracy score in all three datasets, achieving 97.61%, 71.14% and 70.87% in high contrast, all concentrations combined and low contrast training sets, respectively (Figures 3.2a-3.2c).

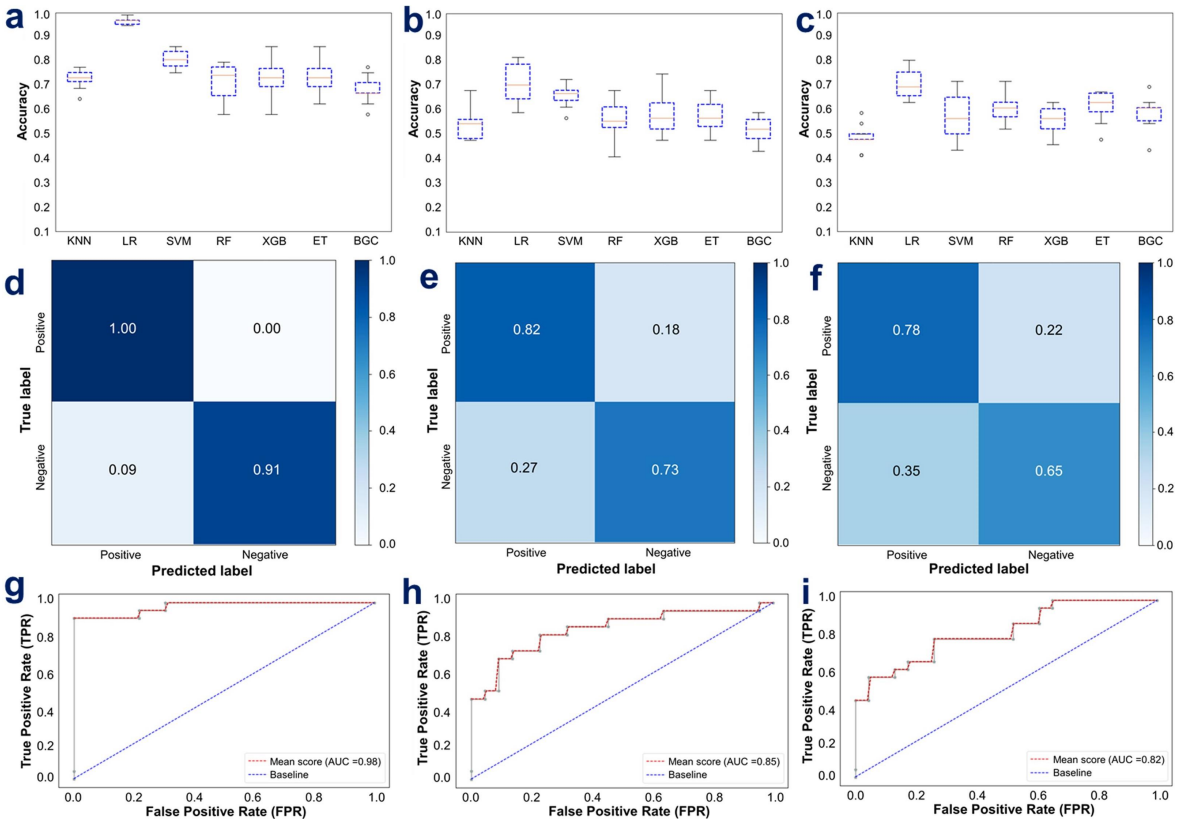

Figure 3.2: The performance of the seven ML classifiers assessed through cross-validation on non-anaemic samples, following three approaches. (a) Accuracy scores of classifiers in high contrast against the negative class. (b) Evaluation with all concentrations, combining all parasite densities as positive against none. (c) Assessment in low contrast against the negative. Confusion matrices for trained and fine-tuned LR models on the 20% test set, with parasitaemia class similar to the training set, are displayed in panels d, e, and f. Receiver Operating Characteristics (ROC) and Area Under the Curve (AUC) of three tuned LR models are presented for high contrast (g), all concentrations (h), and low contrast (i)

LR algorithm was retained for further tuning, utilizing a grid search approach over an extensive range of hyperparameter values. The tuned model, when fitted to high-contrast scenarios characterized by a 6% parasitaemia level versus non-infected samples, demonstrated remarkable capacity to distinguish malaria-positive and -negative samples, achieving accuracies of 100% and 91%, respectively (Figure 3.2d). When evaluating the performance of the tuned models across all

parasitaemia concentrations combined, the accuracy rates for correctly identifying positive and negative samples were 82% and 73%, respectively (Figure 3.2e). Even in the context of low-contrast model, trained with the 0.0003% parasitaemia against negative, the model maintained strong performance, with positive and negative detection accuracies of 78% and 65%, respectively (Figure 3.2f).

Even after tuning the LR to optimize its hyperparameters, training with high contrast had the largest area under the curve (AUC) estimate, 0.98 (Figure Figure 3.2g), outperforming models trained using both the combined concentrations and low contrast data sets, for which the AUC scores were 0.85 and 0.82, respectively (Figures 3.2h-3.2i). The train-test size, precision, recall, and F1-score of the three models on the validation set are summarized in Table 3.1

Table 3.1: Summarized scores (Precision, Recall, and F1-score) for testing the three LR models on the 20% train-test splits using laboratory data

Sample size		Precision score (%)		Recall score (%)	F1-Score (%)
Classifier 01: Trained on High contrast (6%) against 0%					
Train size	460	Positive class	92	100	96
Test size	92	Negative class	100	91	95
Classifier 02: Trained on all concentrations (6%, 0.1%, 0.002%, 0.00003%) against 0%					
Train size	440	Positive class	75	82	78
Test size	88	Negative class	80	73	76
Classifier 03: Trained on Low contrast (0.00003%) against (0%)					
Train size	452	Positive class	69	78	73
Test size	91	Negative class	75	65	70

In addition, to understand the specific biochemical contribution influencing predictions, the wavenumber values were extracted with corresponding coefficients that most influenced the performance of three trained LR classifiers. All three classifiers have learned from wavenumber values associated with biochemical signals associated primarily with lipids (3100-2800 (cm^{-1})) and proteins (1800-600 (cm^{-1})) (Figures 3.3a-3.3c), consistent with signals expected from malaria infections [217, 222].

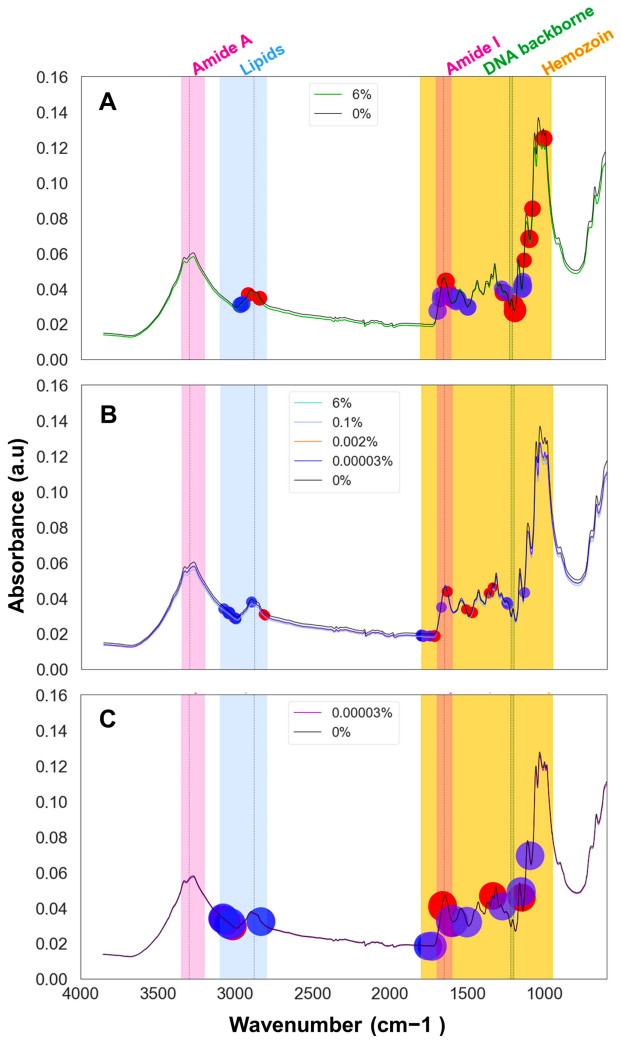

Figure 3.3: Spectral features with the greatest influence on the performance of the three models, a) High contrast, b) All concentrations combined, and c) Low contrast training sets for the prediction of positive class (Red circle) and negative class (Blue circle). The size of the circle represents coefficient scores.

The highest contrast model appears to have primarily learned to classify malaria infections from the wavenumbers associated with proteins, notably amide III and amide I vibrations (1185-1191 (cm^{-1}), 1199-1201 (cm^{-1}), 1619-1617 (cm^{-1}) and 1687-1671 (cm^{-1})), which are indicative of the secondary structure of proteins. Wavenumber values 997, 1125-1139 (cm^{-1}) highlight the models' use of C-N stretching vibrations of proteins (peptides) and phosphodiester stretching (1201, 1071, and 1263 (cm^{-1})) indicative of nucleic acids (Figure 3.3A). The high-contrast model effectively identified wavenumbers linked to lipids, alkanes, and carbohydrates, indicated by key C-H stretching vibrations at 2917(cm^{-1}), 2843(cm^{-1}), 2967 (cm^{-1}), and 2955 (cm^{-1}), and C-H bending vibrations at 1491 (cm^{-1}) and 1493 (cm^{-1}). Optimal wavenumber values for the other LR models, covering all concentrations and low-contrast scenarios, are also visually indicated in Figures 3.3B and Figure 3.3C.

Visualization of blank filters paper revealed distinct peaks in the wavenumbers between 1700 and 1200 (cm^{-1}) in both malaria-positive and malaria-negative blood samples (Figure 3.4), where most of the features of importance for all three classifiers are concentrated (Figures 3.3A-3.3C). Additionally, a similar spectral trend was observed in the 1100–500(cm^{-1}) range across the blank filter paper and both malaria-positive and malaria-negative samples (Figure Figure 3.4). However, of the 40 key features identified by the classifier trained with high contrast samples (Figure 3.3A), only 6 fell within this overlapping region, with 4 out of those 6 having positive coefficients. The other two classifiers—one trained on all concentrations and the other trained with low contrast against negative samples—had fewer features originating from this region (Figures 3.3B-3.3C). This suggests that cellulose, a component of the filter paper, did not significantly affect the accuracy of the classifiers.

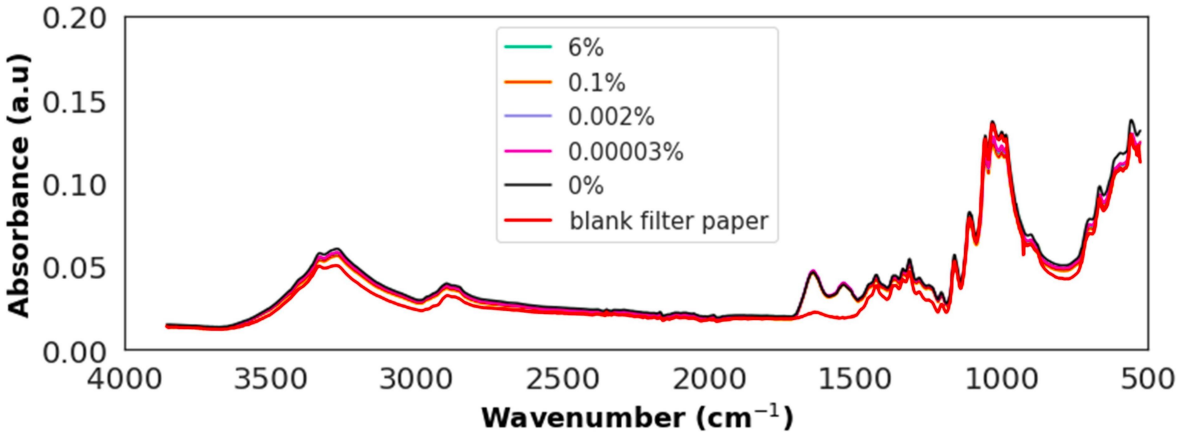

Figure 3.4: Visual comparison of mid-infrared spectra from blank filter paper with those containing varying levels of malaria parasitaemia in malaria-positive blood (6%, 0.1%, 0.002%, and 0.00003%) and malaria-negative blood (0%). The figure represents averaged spectra from 10 filter papers, each scanned 32 times, i.e 320 spectral scans.

3.4.3 Detection of malaria infections at different parasitaemia and anaemic conditions

After establishing that the high contrast training set had the best performance in predicting a dataset of the same parasitaemia levels, the accuracy of the three trained LR algorithms was validated against various parasitaemia and anaemic conditions using 100 bootstrap random resampling. For this purpose, 30% of the full dataset was held out separately before training as unseen data.

The MIRs-ML trained on the high contrast data set against the negative class identified malaria infections in non-anaemic samples with 100% accuracy for the two highest parasitaemia levels tested (6% and 0.1%). Accuracy dropped to 92-91% when classifying intermediate and low-level parasitaemia, and when evaluating combined spectra from all concentrations (Figure 3.5a). Similarly, high accuracies were observed when the high-contrast model was used to predict parasite infections at moderate and severe anaemia (Figures 3.5b-c).

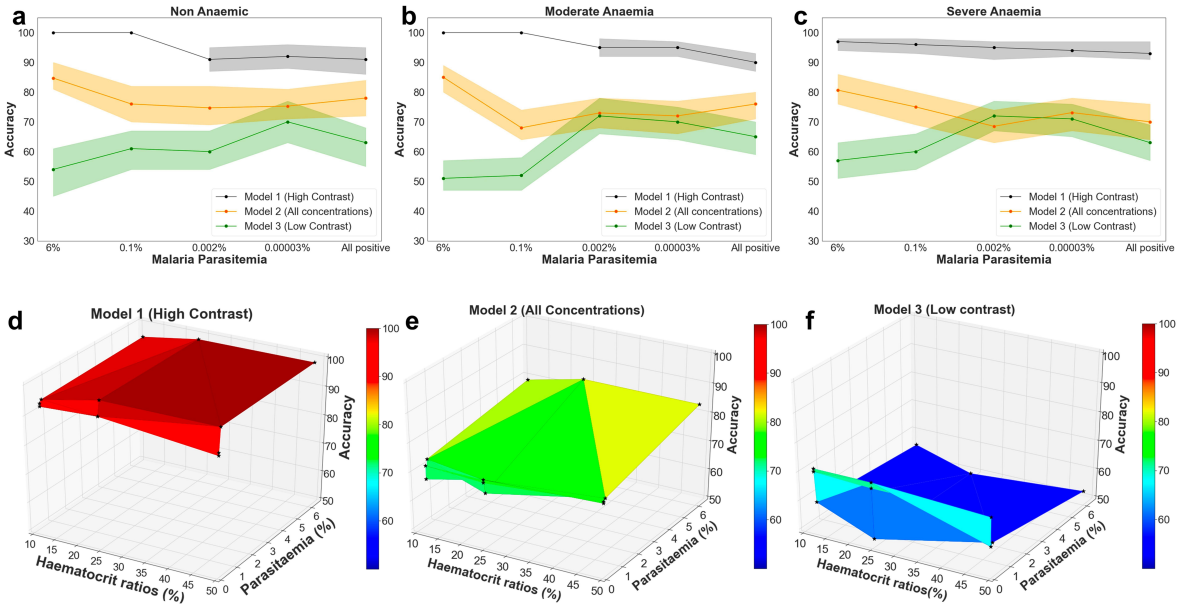

Figure 3.5: Performance of three LR models on a completely unseen dataset held out prior to training, for non-anaemic (a), moderate (b), and severe anaemia (c). d-f represent the three-dimensional representation of the LR performance on the validation set for high contrast, all concentrations, and low contrast models, respectively.

Models trained on all combined concentrations and those trained using low contrast were also validated for predicting various parasitaemia in an unseen dataset. Regardless of anaemia, MIRs-ML trained on all concentrations accurately classified different parasitaemia, achieving an average accuracy of 75.33% [70.07-80.8%] (Figures 3.5a-3.5c). The model trained on the lowest contrast demonstrated an average accuracy of 62.73% [56.53-74.00%] across different parasitaemia and anaemia. When validating the low-contrast model on different parasitaemia and anaemic conditions in new data, an increased accuracy was noticed in predicting parasitaemia levels resembling those in the training set (moderate and low parasitaemia) (Figures 3.5a-3.5c)).

Overall, the high-contrast model outperformed the other two models in predicting malaria infections at all tested parasitaemia and anaemic conditions (Figures 3.5d-3.5f), suggesting that this approach is the most robust for achieving generalizability.

A generalized linear model was fitted to estimate the impact of training methodologies, levels of parasitaemia, and the presence of anaemia on the predictive accuracy of MIRs-ML in diagnosing malaria infections. The analysis revealed that neither anaemia nor the different levels of parasitaemia significantly affected the capabilities of the MIRs-ML models for distinguishing between infected and non-infected samples (anaemic conditions: $\chi^2 = 0.01$, $p = 0.99$; parasite intensities: $\chi^2 = 0.24$, $p = 0.99$). However, the choice of training methodology significantly affected model performance ($\chi^2 = 201.62$, $p < 0.001$). Further analysis using Post-Hoc Tukey's test to compare the three training methodologies showed that training with high-contrast samples notably enhanced the predictive accuracy of MIRs-ML, yielding a mean difference of 19.93% ($p < 0.001$) compared to training with all concentrations, and a mean difference of 32.53% ($p < 0.001$) compared to training with low-contrast samples. Additionally, training with all concentrations demonstrated a significant positive effect, with a mean difference of 12.59% ($p < 0.001$), when compared to training with low-contrast samples.

3.4.4 Validation of the MIRs-ML for identifying malaria infections using spectra from field-collected dry blood spots

The performance of laboratory-trained models was evaluated using realistic samples collected from patients. To facilitate comparison, the created models were tested under two scenarios. Firstly, by employing laboratory data as detailed in the preceding sections. Secondly, by utilizing a realistic dataset obtained from the field (see Figure 3.6a). In simulations resembling field conditions, where all parasitaemia levels generated in the laboratory were combined and treated as positive, the high-contrast trained model distinguished positive from negative samples with accuracies of 88% and 92%, respectively (Figure 3.6b).

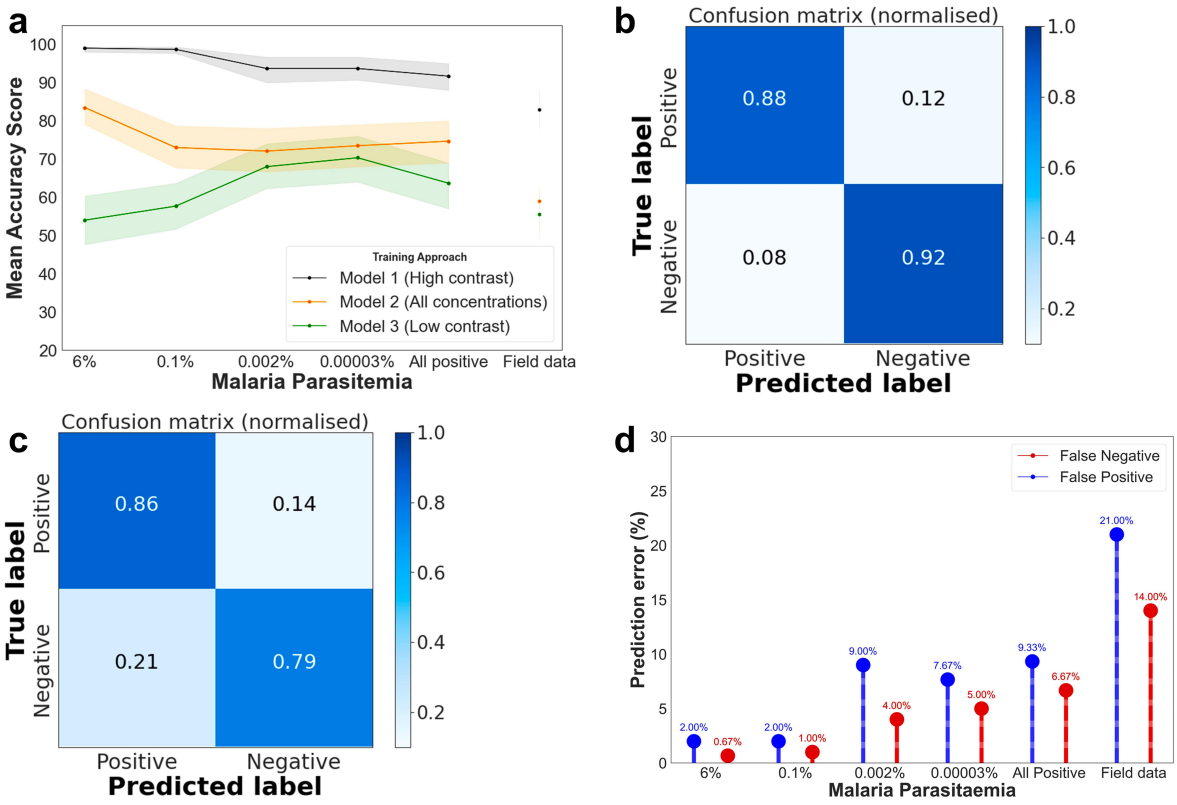

Figure 3.6: Evaluation of three trained logistic regression (LR) models for classifying malaria infections in laboratory and patient samples. (a) Mean accuracy for each anaemia level across various parasitaemia levels using laboratory and field-collected DBS. (b) Confusion matrix of the high-contrast model predicting laboratory-combined parasitaemia against negative in non-anaemic conditions, simulating realistic field collections. (c) Confusion matrix indicated the high-contrast model's performance in detecting malaria infections in realistic field-collected DBS. (d) False positive and false negative predictions by the high-contrast model averaged by anaemic conditions using both laboratory and field samples.

Next, 252 DBS samples collected from a previous field survey in southeastern Tanzania were scanned [217]. The malaria infection status in these samples had been confirmed using nested PCR [217]. In these tests, the model with the highest contrast predicted malaria infections with an accuracy of 83%, achieving 86% accuracy for the positive class and 79% accuracy for the negative class (refer to Figure 3.5c). The precision, recall, and F1-score of the three trained models when tested with these field-collected dataset are summarized in Table 3.2.

To understand the potential applications of MIRs-ML for either point-of-care or population surveys, false negatives and false positives of the highest contrast model were computed in predicting all parasitaemia in laboratory specimens and field datasets (Figure 3.6d). The model exhibited a prediction error of 14% for false negatives and 21% for false positives in field samples, preliminary suggesting that this approach could be most useful in population surveys, especially in low transmission settings, due to the lower rate of false negatives.

Table 3.2: Summarized scores (Precision, Recall, and F1-score) for validating the three LR models on field-collected samples

	Precision score (%)	**Recall score (%)**	**F1-Score (%)**
Classifier 01: Trained on High contrast (6%) against 0%			
Positive class	84	86	85
Negative class	81	79	80
Classifier 02: Trained on combined positive (6%, 0.1%, 0.002%, 0.00003%) against 0%			
Positive class	58	59	58
Negative class	51	50	50
Classifier 03: Trained on Lowest parasitaemia (0.00003%) against (0%)			
Positive class	57	58	57
Negative class	57	56	57

3.5 Discussion

Effective malaria screening is crucial for guiding elimination efforts, especially in detecting low-density parasitaemia. However, current methods often face trade-offs between cost and sensitivity. Alternatively, infrared spectroscopy coupled with machine-learning (MIRs-ML) is showing great promise, particularly in laboratory settings. Here, the findings suggest that the MIRs-ML approach can detect as few as 1–3 parasites/µL of blood with an overall accuracy exceeding 90% under laboratory settings even with presence of anaemia. Furthermore, this study demonstrates that ML algorithms trained with the highest plausible parasite concentrations against negative samples (“high contrast” training set) can yield a potent and robust classifier capable of predicting malaria infections at various parasitaemia levels, regardless of the presence of anaemia. Although anaemia is highly correlated with malaria infections, this study reports for the first time that it does not impact the performance of the ML approach in predicting malaria infections. Notably, the ML model trained with laboratory-generated high contrast dataset accurately classified over 80% of field-collected specimens obtained from malaria-infected patients. Since these specimens were entirely unseen by the model, this indicates good generalizability of this approach and holds great promise for its future optimization in malaria detection, especially for field surveys.

This study demonstrates the ability of MIRs-ML to detect low parasite concentrations (1–3 parasites/µL), which are often missed by methods such as microscopy and RDTs [328, 329], the latter of which is also compromised by HRPII gene deletions [102, 330]. Additionally, this study improves upon earlier studies that applied multivariate analysis, including partial least squares and classical regression approaches, to detect and quantify malaria infections in isolated infected and uninfected RBCs by revealing that the integration of MIRs-ML can detect as low as 1 parasite/µL of blood with an accuracy exceeding 90% in DBS, even in the presence of anaemia, and requiring minimal sample handling.

While malaria is the primary cause of anaemia in regions with high transmission risks, other infections, including gastrointestinal helminths, can also cause anaemia, especially in children and the elderly [331–333]. If MIRs-ML detects anaemia (e.g. where anaemia may be confounded with malaria presence), there could be a risk of misdiagnosis disproportionality affecting children, who are more vulnerable to the effects of misdiagnosed malaria [319]. Therefore, experimentally anaemia levels were simulated by adjusting plasma to RBC ratios using blood from volunteers. MIRs-ML trained on the high contrast dataset predicted malaria infections in the presence of severe anaemia, with accuracy exceeding 90% even at the lowest parasitaemia, indicating that the predictive capabilities of IR-ML are not affected by anaemia.

A further potential problem for IR-ML technologies is poor generalizability to new datasets, as observed in entomological traits of malaria vectors due to genetic, environmental, and dietary variation [174, 213]. Previous studies involving the training of IR approaches for malaria detection used low contrast or less immunologically diverse blood to spike with parasite culture [174]. Here, models were trained on blood samples from 70 individuals to capture population immunological variability, experimentally spiked with cultured ring-stage *P. falciparum* parasites. This allowed models to achieve over 80% accuracy in diagnosing malaria infections with field data without further calibrations. To further improve generalizability, techniques, such as transfer and partial learning [213, 282] could be useful for improving the predictive accuracy of this approach, especially in diverse population surveys.

The trained algorithms in this study learned from peaks associated with the biochemical signatures of malaria-infected samples, particularly those suggested to be linked with the by-products of the malaria ring-stage parasite, such as lipids, proteins (haemozoin) [327], and parasite DNA. In this study, the blood sample was prepared by removing the buffy coat and white blood cells by suction when separating plasma from RBCs for anaemic adjustment. Therefore, the host cells present in the sample were RBCs, which are enucleated. Thus, the signal observed corresponding to phosphodiester stretching (997, 1201, 1071, and 1263 (cm^{-1})) are likely due to parasite nucleic acids only. Further, differences in the peaks related to

the amide groups of the proteins were identified. Specifically, the band between 3500 and 3000 (cm^{-1}), commonly referred to as Amide A and associated with the stretching of N-H bonds; the band between 1700 and 1600 (cm^{-1}) (Amide I), primarily linked to the C=O stretching vibration and sensitive to the secondary structure of the protein; the band between 1600 and 1500 (cm^{-1}) (Amide II), mainly due to N-H in-plane bending and C-N stretching vibrations; and the band between 1350 and 1200(cm^{-1}) (Amide III), which is a combination of C-N stretching, N-H in-plane bending, and C-H in-plane bending vibrations, appear crucial in capturing the variations due to malaria infections. Also changes in the peaks associated with the C-H stretching modes of the lipids (2901, 2905, and 2859 (cm^{-1})) were observed.

Analysis of blank filter paper, compared to filter paper containing malaria-positive and -negative samples, indicated that the filter paper was adequately controlled for and did not affect the model performance. This is consistent with other reports that identified significant bands in the fingerprint region, which correspond to the presence of malaria parasites in blood samples [219, 222, 304, 327]. Spectral analysis of human blood has also revealed key features in the cellulose-overlapping region of 1100–500 (cm^{-1}), providing additional insights into distinguishing blood samples [185, 334–337]. For example, Mistek-Morabito et al. used the wavenumber ranges of 4000–2800 (cm^{-1}) and 1800–600(cm^{-1}) to differentiate human blood from other organisms, emphasizing the importance of the fingerprint region (below 1500 (cm^{-1})) [338]. Given the well-controlled experimental design of this study, which ensured standardization in the use of filter papers for both malaria-negative and malaria-positive samples, it is likely that the features observed in the fingerprint region offer valuable information for detecting malaria parasites, considering the characteristic peaks in human blood.

The advantage of using MIRs-ML for malaria parasite detection relies on its higher sensitivity and accuracy cost ratio, demonstrating potential applicability in low-income communities [174]. Standard low-cost maintenance, such as providing desiccants to limit humidity effects, is the only requirement for operation, with no need for additional reagents. This study demonstrated an added advantage of the approach, its capability to detect as low as one parasite/µL of blood in the presence and absence of anaemia, highlighting the potential use-case of MIRs-ML for malaria parasite detection in field settings. This technology has potential to be an easy-to-use method for screening parasite infections, and requires minimal training, specifically in sample handling, spectra acquisition, and result interpretation. This reduced training requirement is a major advantage over technologies like microscopy and PCR, which require high levels of expertise. This study, along with ongoing efforts to develop portable surveillance tools using similar technology [283, 339], suggests that this approach could be scalable, and might in future be integrated into routine health

facilities, or even adapted for population surveys in rural areas. Bench-top devices range in cost from $20,000 to $60,000 but are reagent-free and require minimal maintenance, with a lifespan exceeding 10 years. This operational cost advantage, combined with the sensitivity demonstrated in this study, makes them a viable alternative to more expensive PCR-based technologies. Even RDTs, which are more affordable, tend to have lower sensitivity and may be less reliable in low-transmission settings [174]. Additionally, there are now pocket-sized devices, which can cost as little as $2,000, which offer opportunities for non-invasive diagnostics through the skin, allowing for fast, real-time results for malaria [283]. However, to better integrate the methods, further investigations are needed to understand full needs [174].

One important question to consider is where MIRs-ML should be utilized, either as a point-of-care test or for population surveys. Using a field-collected dataset, this study revealed that MIRs-ML algorithms detected unseen field-collected specimens with a lower false-negative rate of 14% compared to a false-positive rate of 21%. This might primarily indicate a potential use case of MIRs-ML for population surveys that could complement PCR confirmation of positive MIRs-ML samples. However, these should be considered as preliminary observations and for the further integration of MIRs-ML into routine malaria surveillance, large-scale clinical trials are essential to validate the feasibility of MIRs-ML for malaria parasite detection in vertebrate hosts.

This study solely focused on detecting the *P. falciparum* parasite, prevalent in endemic regions. It is crucial to explore detection limits and infrared signals associated with infections from *Plasmodium ovale*, *Plasmodium vivax*, and *Plasmodium malariae*. Future studies may also explore the performance of MIRs-ML in detecting malaria infections across various epidemiological strata, as the current tools exhibit different performance characteristics based on transmission patterns, with RDTs and microscopy showing poor performance in low-transmission areas. Also, given the increasing threat of HRP2 gene deletions, future research should investigate whether HRP2 mutations could compromise the performance of MIRs-ML in detecting malaria infections. Moreover, the infrastructure requirements for IR-ML, including hardware and software configurations, training needs, and maintenance levels, should be addressed [174].

Additionally, it is important to further investigate malaria diagnostic interference of MIRs-ML due to other potential confounding factors, such as coinfection and nutritional factors. Exploring the potential of MIRs-ML to detect other blood infections common in malaria-endemic areas, such as typhoid fever, schistosomiasis, and viral infections like HIV, is also valuable, as these often co-occur with malaria.

3.6 Conclusion

To advance malaria elimination, there is a critical need for screening methods that combine cost-effectiveness with the ability to detect low-density parasitaemia, a gap not filled by current methods like RDTs, microscopy, or expensive PCR. This study demonstrated an AI-driven mid-infrared spectroscopy technique that excels in identifying malaria infections in dried blood spots, achieving high accuracy across various parasite densities. The detectable limit of malaria parasite by MIRs-ML is below the lowest concentration tested, which is 1 parasite per microlitre of blood. The performance of the technique was not compromised by anaemia, which is a frequent complication in malaria patients. Moreover, when MIRs-ML models initially trained on laboratory data were used to distinguish between infected and uninfected field samples collected from a field survey in rural Tanzania, the classification accuracies were maintained above 80%. These findings indicate the significant potential and viability of this AI-driven mid-infrared spectroscopy technique as an affordable and malaria-scalable screening tool in low-resource settings. Further validation in diverse areas and the consideration of additional confounders, such as co-infections, are necessary to further validate the approach in real-life settings.

Chapter 4: Comparison of Fine-Scale Malaria Strata Derived from Population Survey Data Collected Using mRDTs, Microscopy and qPCR in South-Eastern Tanzania

Published in Malaria Journal 2024:
https://doi.org/10.1186/s12936-024-05191-8

4.1 Abstract

Background: Malaria-endemic countries are increasingly adopting data-driven risk stratification, often at district or higher regional levels, to guide their intervention strategies. The data typically comes from population-level surveys collected by rapid diagnostic tests (RDTs), which unfortunately perform poorly in low transmission settings. Here, a high-resolution survey of *Plasmodium falciparum* prevalence rate (PfPR) was conducted in two Tanzanian districts using rapid diagnostic tests (RDTs), microscopy, and quantitative polymerase chain reaction (qPCR) assays, enabling the comparison of fine-scale strata derived from these different diagnostic methods.

Methods: A cross-sectional survey was conducted in 35 villages in Ulanga and Kilombero districts, south-eastern Tanzania between 2022 and 2023. We screened 7,628 individuals using RDTs (SD-BIOLINE) and microscopy, with two thirds of the samples further analyzed by qPCR. The data was used to categorize each district and village as having very low (*Pf*PR<1%), low (1%≤*Pf*PR<5%), moderate (5%≤*Pf*PR<30%), or high (*Pf*PR≥30%) parasite prevalence. A generalized linear model was used to analyse infection risk factors. Other metrics, including positive predictive value (PPV), sensitivity, specificity, parasite densities, and Kappa statistics were computed for RDTs or microscopy and compared to qPCR as reference.

Results: Significant fine-scale variations in malaria risk were observed within and between the districts, with village prevalence ranging from 0% to >50%. Prevalence varied by testing method: Kilombero was low risk by RDTs (*Pf*PR=3%) and microscopy (*Pf*PR=2%) but moderate by qPCR (*Pf*PR=9%); Ulanga was high risk by RDTs (*Pf*PR=39%) and qPCR (*Pf*PR=54%) but moderate by microscopy (*Pf*PR=26%). RDTs and microscopy classified majority of the 35 villages as very low

to low risk (18-21 villages). In contrast, qPCR classified most villages as moderate to high risk (29 villages). Using qPCR as the reference, PPV for RDTs and microscopy ranged from as low as <20% in very low transmission villages to >80% in moderate and high transmission villages. Sensitivity was 62% for RDTs and 41% for microscopy; specificity was 93% and 96%, respectively. Kappa values were 0.7 for RDTs and 0.5 for microscopy. School-age children (5-15years) had higher malaria prevalence and parasite densities than adults (P<0.001). High-prevalence villages also had higher parasite densities (Spearman r=0.77, P<0.001 for qPCR; r=0.55, P=0.003 for microscopy).

Conclusion: This study highlights significant fine-scale variability in malaria burden within and between the study districts and emphasizes the variable performance of the testing methods when stratifying risk at local scales. While RDTs and microscopy were effective in high-transmission areas, they performed poorly in low-transmission settings; and classified most villages as very low or low risk. In contrast, qPCR classified most villages as moderate or high risk. The findings emphasize that, where precise mapping and effective targeting of malaria are required in localized settings, tests must be both operationally feasible and highly sensitive. Furthermore, when planning microstratification efforts to guide local control measures, it is crucial to carefully consider both the strengths and limitations of the available data and the testing methods employed.

4.2 Background

Precise mapping of malaria prevalence is crucial for the eventual elimination of the disease from different localities. In line with World Health Organization (WHO) guidelines, National Malaria Control Programs (NMCPs) in Africa are increasingly adopting data-driven stratification of malaria burden, in most cases at either district or higher regional levels [340–342]. These stratifications involve assessing risk levels and burden in geographical areas at the subnational level (e.g. zones, regions, and districts) [341, 343, 344], and can include fine scale mapping (down to wards and villages levels) as countries progress towards elimination [345–347]. The data for such stratification may come from health facilities, active malaria screening during population surveys, or proxy data sources such as antenatal care clinic visits [345, 348, 349].

When developing country-level malaria strategies, the prevalence of malaria, representing the proportion of confirmed positive cases of *Plasmodium falciparum* (or other *Plasmodium* sp.) among all individuals tested [350, 351], can be classified into

various transmission categories. The WHO has previously used the following cutoff points for malaria endemicities: below 1% as very low, 1-10% as low, 10-35% as moderate, and above 35% as high burden malaria stratum [351]. Different NMCPs may adapt these criteria with slight adjustments based on local epidemiological insights. For instance, some countries, including Tanzania and Kenya, have used the parasite prevalence data to categorize their geographic zones as either very low risk (*Pf*PR < 1%), low risk (1% ≤ *Pf*PR < 5%), moderate risk (5% ≤ *Pf*PR < 30%), or high risk strata (*Pf*PR ≥ 30%) [341, 352]. Another measure that can be used for generating these strata is the annual parasite incidence (API), which is the number of diagnostically confirmed malaria cases per 1000 individuals per year and is usually obtained from health facilities data [351, 353]. API estimates are simpler to generate because they rely on facility-level data, but do not account for sub-clinical malaria infections, which can also contribute to transmission and impede malaria elimination effort [354].

National malaria programs usually rely on different actively and passively collected data to measure malaria burden and monitor the effectiveness of control measures [355–357]. For instance, Tanzania employs multiple platforms, including the District Health Information software (DHIS2) populated with data from routine health facility visits, the Malaria Indicator Surveys (MIS) and Tanzania Demographic and Health Surveys (TDHS), which are done every 4-5 years through household surveys, and the school malaria parasite surveillance (SMPS) targeting kids aged 5-16 years during [341, 358–360]. A common feature of these established systems is that most rely primarily on rapid diagnostic tests (RDTs) and microscopy [349, 361, 362], though samples are sometime also preserved for PCR assays.

Microscopy, long used in malaria diagnosis, can quantify parasite loads and identify different *Plasmodium* species, which are essential for precise treatment choices [224, 226]. However, its effectiveness depends significantly on the skill and experience of the microscopist, making it unreliable in some contexts, and it can miss a substantial number of true infections due to sub-optimal accuracy [308, 328, 363]. In contrast, Rapid Diagnostic Tests (RDTs) offer a consistent and user-friendly option, enabling quick, on-site diagnosis without specialized skills or equipment. RDTs have become widely used in both point-of-care settings and population surveys due to their operational simplicity and cost-effectiveness [103, 197, 231, 233, 364]. While the technique enhances access to diagnostics, especially in remote areas, RDTs have lower sensitivity for detecting low-level infections, such as those with <100 parasites/µL of blood, and cannot quantify parasite density. Additionally, current

RDTs may detect antigens for over three weeks post-treatment especially those targeting histidine-rich proteins 2 (HPR2), leading to poor specificity and potential overestimation of malaria cases in high transmission areas [103, 364, 365].

In contrast, polymerase chain reaction (PCR) assays are known for their high sensitivity and specificity [366]. While conventional PCR assays typically provide qualitative information on malaria infections, quantitative PCR (qPCR) can offer additional quantitative measures of malaria parasite density [296, 367]. Unfortunately, the widespread use of PCR assays for population surveys is hindered by cost constraints and the need for specialized expertise and infrastructure for implementation [246, 247, 366].

The increased focus on evidence-based strategies in malaria control also includes a transition from broad subnational stratifications to more granular, fine-scale approaches [345, 349]. However, although current methods like RDTs and microscopy are favored for their operational simplicity, their effectiveness in detailed risk stratification, which are critical for targeting both clinical and sub-clinical infections for malaria elimination, remains poorly understood. Some authors have also suggested that RDTs may have vastly reduced performance in settings where the malaria burden has been significantly reduced [368]. This calls for a rigorous evaluation and comparison of these methods against highly sensitive techniques such as qPCR to refine malaria stratification approaches for malaria elimination. Indeed, available evidence, including data from Kenya and Tanzania, suggest that PCR assays are generally better at pinpointing main malaria hotspots in communities than RDTs and microscopy [228, 369]. The study from Tanzania further showed that in subsequent treatment campaigns relying on RDT-based screening, 45% of infections remain untreated, even if treatment is offered to all members of households with an infected individual [369]. In the Kenyan study, the authors went further to suggest that since detection of hotspots depends on the sensitivity of diagnostic tools, health authorities working in malaria elimination settings should consider using PCR to guide detection of the residual hotspots, as this provides greatest opportunities to find asymptomatic individuals and sub-patent parasite reservoirs in the communities [228].

All these studies clearly show that while sub-national stratification may be the most effective approach to decide on how to allocate resources, the type of data used for such epidemiological profiling matters significantly; especially when the stratification is done at local-sub-district levels. In places like southeastern Tanzania, which has experienced decades of sustained malaria interventions and progress, and where robust entomological surveillance already exists [370], addition of detailed parasite prevalence data from population-level surveys is required to enable more precise, fine-scale stratifications at both district and sub-district levels.

The aim of this study was therefore to generate a high-resolution population-level survey map of *P. falciparum* prevalence in two districts in south-eastern Tanzania and to compare the fine-scale malaria strata obtained using data from different test methods, namely RDTs, microscopy, and qPCR. Additionally, the study evaluated the performance of RDTs and microscopy relative to qPCR in a range of transmission settings from high to very low. This study also sought to provide detailed population survey data on malaria burden to complement the ongoing entomological surveys in the study area.

4.3 Methods

4.3.1 Study site

The study was conducted in Morogoro region, in south-eastern Tanzania Figure 4.1, in the two districts of Kilombero (population: 583,000; 8.2414°S, 36.3349°E; elevation: 270m) and Ulanga (population: 233,000; 8.9889°S, 36.6133°E; elevation: 800m). The average malaria prevalence in the Morogoro region has previously been estimated to exceed 10%, with *P. falciparum* as the dominant malaria species [358, 359, 371]. The main economic activities for residents include rice farming, sugarcane farming and maize farming, though the area also has other food crops and large commercial tree plantations (teak). The known annual rainfall range is 1200-1400 mm in the lower-lying plains of Kilombero district, and 1400-2100 mm in the higher areas in Ulanga district [372]. Approximately 90% of the rainfall occurs during the wet seasons between December to April, with dry seasons typically lasting from June through September [372]. The annual mean daily temperature is around 27°C in the lowlands and approximately 23°C in the highlands. Relative humidity averages from 75% in the lowlands to 80% in the highlands.

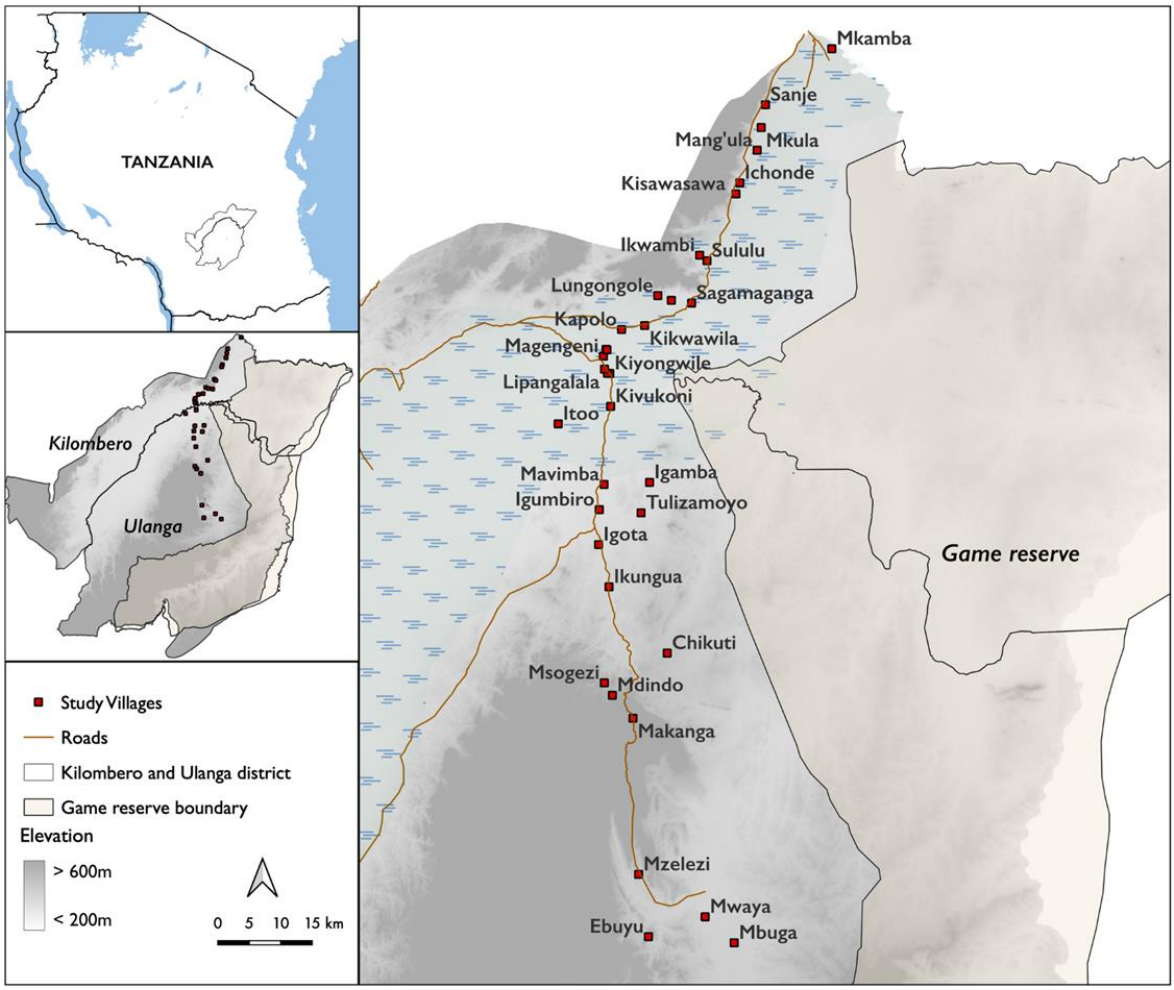

Figure 4.1: Study villages in Kilombero and Ulanga districts, south-eastern Tanzania

4.3.2 Study design, procedures and survey tools

The cross-sectional surveys were conducted once per village, and the entire surveillance spanned two consecutive years, from 2022 in Ulanga to 2023 in Kilombero, covering the months of April to September each year. Villages were randomly selected from each district, and sample sizes were proportionately determined based on the population of each village using the Cochran formula adjusted for finite populations [373–375]. The sample size aimed to achieve a 95% confidence interval with a precision of 5% for each specific village prevalence estimate see **supplementary table 3**.

The expected prevalence varied depending on the village and was derived from previous surveys and health centers within each village, These earlier surveys had covered a far smaller subset of the areas, and yielded prevalence rates from as low as 1% to as high as 45% (*Minja et al. 2019, unpublished*). However, for villages without these population surveys, health-facility data or prevalence estimates from

neighboring villages were utilized. Based on the estimated sample sizes per village, representative households were determined, assuming an average household size of three individuals. Households were selected by randomizing the names of all households obtained from the respective village administrations. This selection ensured equal representation of households from each sub-village, thereby covering all parts of the village. The selected households were visited and recruited if they consented.

The screening criteria included individuals aged 5-60 years who had not taken malaria medications in the preceding two weeks. This precaution aimed to prevent potential overestimation by RDTs, as they may detect residual traces post-treatment [376]. Individuals needing special medical attention, such as pregnant women, were excluded from the study. All eligible individuals in selected households were allowed to participate. Each participant who underwent malaria screening was assigned a unique identification number that was also linked to their corresponding household ID. On-site finger-prick blood samples were collected for three diagnostic tests: 1) RDTs, 2) creating thick and thin blood smears, and 3) collecting 3–5 dried blood spots (samples) on Whatman 903 protein saver cards. Subsequently, these samples were transported to the reference laboratory for microscopy and qPCR analysis.

4.3.3 Ethical considerations, survey team, and trainings

Permission to conduct this study was obtained from the Ifakara Health Institute Review Board (Ref: IHI/IRB/No: 1/2021) and the National Institute for Medical Research-NIMR (NIMR/HQ/R.8a/Vol. 1X/3735). Additionally, approvals were obtained from regional, district, ward, and respective selected village authorities before commencing the surveys, given the screening was done at centralized location in each village. Written informed consent was obtained from individual adult participants (and parents or guardians of those aged below 18) on the day before the actual testing. The study team consisted of 11 members, including three molecular laboratory technologists, four licensed medical laboratory microscopists, two licensed clinical officers, and two social scientists. Prior to the survey commencement, a five-day training session was conducted at the Ifakara Health Institute laboratory. This training covered explanations of the study protocols, pilot implementations, procedures for protecting human participants, quality assurance and training on data collection tools.

4.3.4 Tests using malaria rapid diagnostic tests (RDTs)

A small blood drop obtained through a finger prick was collected onto the RDTs (SD Bioline Ag *Pf*/Pan), following the manufacturer's instructions. The buffer solution was applied according to standard RDTs procedures and left on the bench surface for up to 20 minutes. The type RDT used were capable of detecting *P. falciparum* infections by targeting histidine-rich proteins 2, which react on the *Pf*-line. Additionally, they could detect *P. malariae*. *P. vivax*, and *P. ovale* by targeting glycolytic lactate dehydrogenase, expressed by the Pan-line on RDTs [103]. The RDT results were recorded on a paper form, and any individuals who tested positive for malaria were promptly treated with Arthemether Lumefantrine (ALu), following Tanzania's national malaria treatment guidelines [377].

4.3.5 Tests using microscopy

Thick and thin blood smears were created in the field, stained with 10% Giemsa for 15 minutes then examined for the presence of malaria parasites under oil immersion at 100X magnification [374, 378, 379]. Two experienced microscopists independently read the slides, and discrepancies between them were resolved by a third, more experienced microscopist. They read the thick smear first, and if an infection was detected, the thin smear was read to identify parasite species. The presence of both asexual and sexual malaria parasite stages discriminating *P. falciparum*, *P. malariae*, and *P. ovale* was recorded. Asexual stage parasites were counted per 200 white blood cells and assuming 8000 WBC/µL [380]. The mean count of malaria parasite by microscopy between the two readers was calculated and confirmed by the third reader.

4.3.6 Tests using real-time qPCR assays

A representative sample of approximately two thirds of all samples was randomly selected from each village and screened further by quantitative polymerase chain reaction (qPCR) i.e. 4905 samples out of the total 7628 samples. Out of the five spots on the Whatman protein saver card, three were punched using a handheld 6mm slot hole puncher. These punched spots were then used for DNA extraction with the Quick-DNA^{TM} Miniprep Plus Kit (Zymo Research, USA) [381], and eluted with50 µL of elution buffer, stored at -20°C for further detection and quantification of *P. falciparum* infections using probe-level allele-specific quantification (PlasQ)-multiplex qPCR assays protocols [367, 382, 383]. The detection and quantification of *P.*

falciparum parasites were performed using the Bio-Rad CFX96 real-time PCR system (Bio-Rad Laboratories, USA) [382] and analyzed with Bio-Rad CFX maestro software. The qPCR reaction, PlasQ primers and probes mix, are summarized in supplementary Table S4.1 & Figure S4.2. DNA amplification processes included: activation at 95°C for 1 min, denaturation at 95°C for 15 seconds, and annealing and elongation at 57°C for 45 seconds for 45 cycles, followed by melting [382].

The qPCR assays were run with positive controls (samples with confirmed *P. falciparum*) and a non-template control (samples with no *P. falciparum* as negative control). For absolute parasite quantification, the WHO international standard for *P. falciparum* nucleic acid amplification techniques were used (WHO reference from NIBSC#04/176) [367]. The standard was reconstituted following the manufacturer's instructions and serially diluted in the range of 100,000 parasites/µL to 0.01 and analyzed in triplicates.

During the qPCR assay, the prepared standards were run together with unknown samples, and at the end of the assay, the standard curve and samples were normalized and analyzed with Bio-Rad CFX maestro software. The obtained normalized Ct values of the samples and the linear regression equation derived from the standard curve were used to calculate the parasites density of the unknown samples, expressed as parasites per microlitre (parasites/µL) of blood.

4.3.7 Malaria stratifications (*PfPR*) categories

Malaria stratifications generally rely on predefined *Pf*PR categories, with NMCPs adopting WHO definitions. In this study, which focuses on fine-scale stratifications at the village level (the lowest administrative boundaries), *Pf*PR categories predefined in a study conducted in mainland Tanzania were adapted [341, 345]. These categories stratify malaria risk at the council level, which is also considered fine scale, as it is below the district level [345]. The arbitrary risk categories used are: very low risk (*Pf*PR <1%), low risk (1% ≤ *Pf*PR <5%), moderate risk (5% ≤ *Pf*PR <30%), and high risk (*Pf*PR ≥30%). In this study, the strata were defined as fine-scale because they were performed at the village level using data derived from village prevalence estimates.

4.3.8 Data analysis

All results from RDTs, microscopy, and qPCR were entered into the Open Data Kit (ODK) system [384], and subsequently downloaded as an excel file for further cleaning. The datasets for RDTs, microscopy, and qPCR results were merged based on the participant's ID using the Pandas Python package [385]. Generalized linear mixed models (GLMMs) with a binomial distribution were utilized to evaluate the relationship between malaria infection risk and the predictors age and gender. These models were implemented using the R statistical software, where random effects for both Village and House ID were incorporated to address the hierarchical structure and intra-cluster correlations within the dataset.

Additionally, to evaluate the performance of RDTs and microscopy in fine-scale malaria stratifications compared to qPCR, their agreement was tested using Kappa statistic [386], and the resulting Kappa values interpreted as follows: $\kappa < 0.20$ as poor agreement, 0.21–0.40 as fair, 0.41–0.60 as moderate, 0.61–0.80 as substantially good and 0.81–1 as almost perfect agreement [387]. In addition, the positive predictive value (PPV) for RDTs and microscopy was computed, using qPCR results as the reference, per village, as (proportion of positive test results that are actually true positives, estimated as PPV = True Positives / (True Positives + False Positives)). Fine-scale stratification by villages was performed using data from qPCR, RDT, and microscopy to generate prevalence maps with QGIS software version 3.26, enabling visualization of malaria prevalence across the study area. To further analyze this data, we employed Inverse Distance Weighting (IDW) interpolation techniques. IDW estimates values at unsampled locations by weighting observed data points inversely to their distance, creating a smooth, continuous surface [388]. This method was applied to the malaria prevalence data from RDTs, microscopy, and qPCR for each village, producing continuous surfaces that visually depict spatial variations in malaria risk across the study area.

The geometric mean of parasite density, estimated by microscopy and qPCR, was calculated for each village. These densities were also statistically compared across different gender and age groups within each village. The non-parametric Mann-Whitney statistics were used to compare the parasite densities between two categorical groups, while Kruskal-Wallis statistical tests were used to compare more than two categorical groups [389, 390]. For example, differences in parasite densities between age groups were tested using Kruskal-Wallis statistics, and if statistically significant, the Mann-Whitney statistics were applied for pairwise statistical significance tests. All analyses comparing parasite densities excluded the negative cases and focused solely on investigating parasite density distribution among malaria-positive patients within each respective village. Lastly, to test for statistical

correlations between parasite prevalence and parasite densities estimated by both qPCR and Microscopy, non-parametric Spearman's rank correlation tests were employed [391]. Additionally, a logistic regression model was used to evaluate the probability of detecting malaria infections (positive or negative) with both RDTs and microscopy at varying parasite densities estimated by qPCR.

4.4 Results

Baseline study population: This survey covered 35 villages across Ulanga and Kilombero districts. A total of 7,628 participants (>5 years) were recruited upon consent and tested for malaria using RDTs and microscopy. The number of participants tested per village ranged from over 160 to 449. Additionally, 64.3% of these participants (4,905) were also tested using qPCR Figure 4.2. Males comprised 38% of the study population, while females made up 62%. Among the participants, 35% were school-aged children (5-15 years), and 65% were aged 16 years and above Figure 4.1.

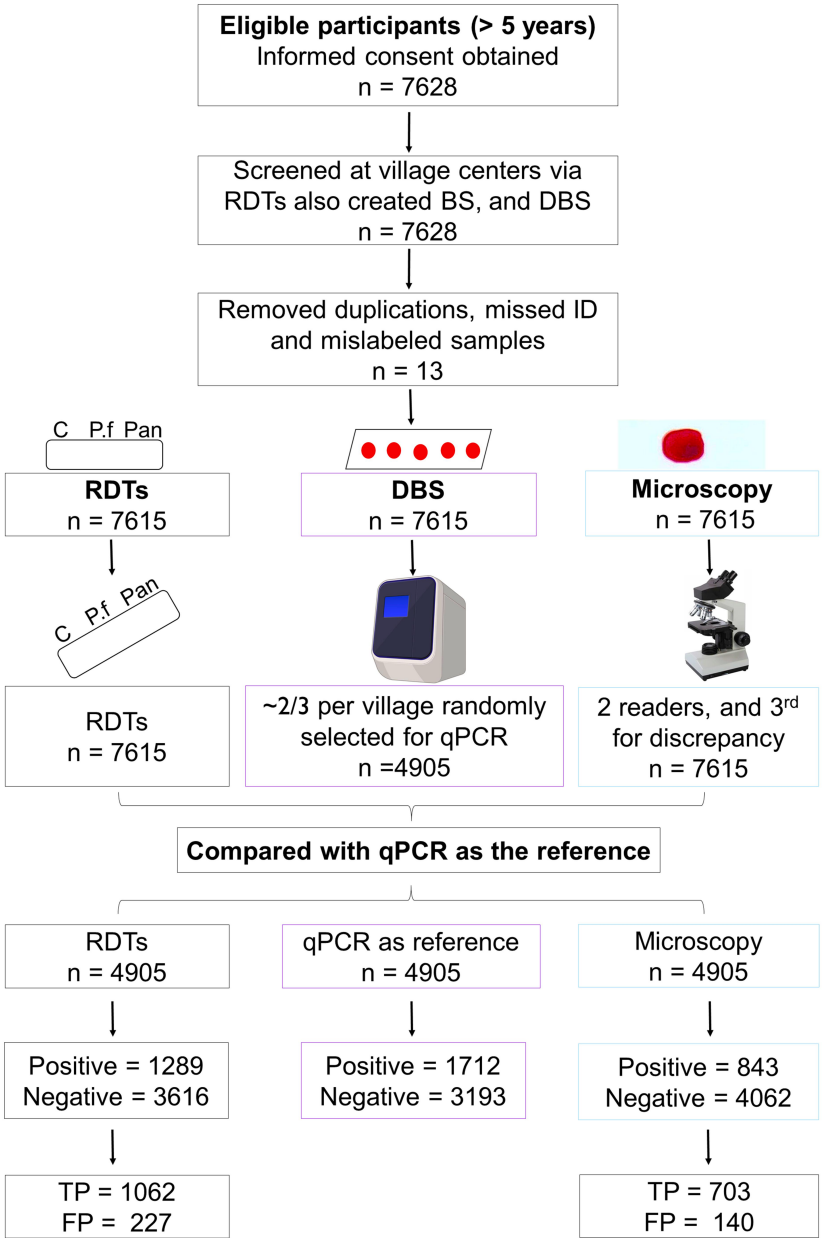

Figure 4.2: Schematic representation of the study sampling procedures

4.4.1 Malaria prevalence by RDTs, Microscopy and qPCR

In the Ulanga district, malaria transmission was found to be high by both qPCR and RDTs, with *P. falciparum* prevalence rates of 53.89% [95% CI, 52.06-55.72] and 38.35% [95% CI, 36.92-39.79] respectively. However, microscopy categorized it as moderate, with a prevalence rate of 26.07% [95% CI: 24.77-27.36] (Table 4.2). Within this moderate to high transmission strata in Ulanga, males had a significantly higher prevalence of malaria compared to females. The odds ratios of malaria infection in males compared to females were estimated as 1.6 [95% CI: 1.4-1.8] ($P < 0.001$) by RDTs, 1.4 [95% CI: 1.2-1.6] ($P < 0.001$) by microscopy, and 1.5 [95% CI: 1.2-1.7] (P

Table 4.1: Baseline characteristics of the study populations

	Kilombero District n (%)	Ulanga District n (%)	Total N (%)
Villages	19 (54.3)	16 (45.7)	35
Sub Villages	48 (51.6)	45 (48.4)	93
	Gender		
Female	2164 (67.4)	2573 (58.3)	4737 (62.1)
Male	1047 (32.6)	1844 (41.7)	2891 (37.9)
Total	**3211**	**4417**	**7628**
	Age Group		
5-10 years	519 (16.2)	935 (21.2)	1454 (19.1)
11-15 years	400 (12.5)	802 (18.2)	1202 (15.8)
16-20 years	198 (6.2)	333 (7.5)	531 (7.0)
>20 years	2094 (65.2)	2347 (53.1)	4441 (58.2)
Total	**3211**	**4417**	**7628**

< 0.001) by qPCR (Table 4.2). All tests - RDTs, microscopy, and qPCR - indicated that school-age children (5-15 years) had a significantly higher prevalence of malaria infections than the other age groups, (P<0.001), refer (Table 4.2).

In Ifakara council, within the Kilombero district, both RDTs and microscopy categorized the area as a low risk stratum, with observed prevalence rates of 2.68 [95% CI: 2.12-3.24] and 1.84 [95% CI: 1.37 – 2.30], respectively (Table 4.3). However, qPCR classified Kilombero district as a moderate risk stratum with a prevalence rate of 8.77 [95% CI: 7.55-9.99] (Table 4.3). Notably, there were no statistically significant differences in malaria infection risk between males and females in this low to moderate transmission setting, as indicated by both RDTs (Odds ratios 1.2% [95% CI; 0.8, 2.], P=0.361) and microscopy (Odds prevalence 1.33% [95% CI; 0.7, 2.0], P=0.521), as well as qPCR (Odds ratios 1.2% [95% CI: [0.7-1.4], P = 0.941). Additionally, school-age children (5-15 years) exhibited a significantly higher risk of malaria infections compared to those 16 years old and above, as demonstrated by both RDTs and microscopy (P<0.001). However, qPCR demonstrated no significant difference between the two groups (P<0.124) (Table 4.3).

Table 4.2: Malaria prevalence in Ulanga district by sex and age groups, as measured using RDTs, microscopy and qPCR

	RDTs				Microscopy				qPCR			
Attribute	**Positive/ Total tested**	**Prevalence (%) [95% CI]**	**Odds ratios [95%CI]**	**P-value**	**Positive/ Total tested**	**Prevalence (%) [95% CI]**	**Odds ratios [95%CI]**	**P-value**	**Positive/ Total tested**	**Prevalence (%) [95% CI]**	**Odds ratios [95%CI]**	**P-value**
Overall prevalence	1689/4404	38.4 [36.9-39.8]	-	-	1148/4404	26.1 [24.8–27.4]	-	-	1531/2841	53.9 [52.1-55.7]	**-**	**-**
Sex												
Female	874/2566	34.1 [32.2-35.9]	**Ref**		593/2566	23.1 [21.5–24.7]	**Ref**	-	830/1659	50.0 [47.6-52.4]	**Ref**	**-**
Male	815/1838	44.3 [42.1-46.6]	1.6 [1.4-1.8]	<0.001	555/1838	30.2 [28.1-32.3]	1.4 [1.2-1.6]	<0.001	701/1182	59.3 [56.5-62.1]	1.5 [1.2-1.7]	<0.001
Age group												
5-15 years	976/1734	56.3 [53.9 - 58.6]	**Ref**		699/1734	40.3 [38-42.7]	**Ref**	-	693/1156	59.9 [57.1-62.8]	**Ref**	**-**
≥ 16 years	713/2670	26.7 [25 - 28.4]	0.3 [0.2-0.3]	0.001	449/2670	16.8 [15.4-18.3]	0.3 [0.3-0.4]	<0.001	838/1685	49.7 [47.3-52.1]	0.3 [0.2-0.3]	<0.001

Table 4.3: Malaria prevalence in the Kilombero district by sex and age groups, as measured using RDTs, microscopy and qPCR

	RDTs				Microscopy				qPCR			
Attribute	**Positive/ Total tested**	**Prevalence (%) [95% CI]**	**Odds ratios [95%CI]**	**P-value**	**Positive/ Total tested**	**Prevalence (%) [95% CI]**	**Odds ratios [95%CI]**	**P-value**	**Positive/ Total tested**	**Prevalence (%) [95% CI]**	**Odds ratios [95%CI]**	**P-value**
Overall prevalence	86/3211	2.7 [2.1-3.2]	-	-	59/3211	1.8 [1.4 – 2.3]	**-**	-	181/2064	8.8 [7.6-10.0]	**-**	**-**
Sex												
Female	50/2164	2.3 [1.7-2.9]	Ref	-	36/2164	1.2 [1.1-2.2]	Ref	-	118/1385	8.5 [7.1-10.0]	Ref	**-**
Male	36/1047	3.4 [2.3-4.5]	1.2 [0.8-2.0]	0.361	23/1047	2.2 [1.3 – 3.1]	1.2 [0.7-2.1]	0.521	63/679	9.3 [7.1-11.5]	0.9 [0.7-1.4]	0.941
Age group												
5-15 years	38/919	4.1 [3-5.7]	**Ref**		26/919	2.8 [1.9-4.2]	**Ref**	-	61/599	10.2 [7.9-13]	**Ref**	**-**
≥ 16 years	48/2292	2.1 [1.6-2.8]	0.5 [0.3-0.8]	0.008	33/2292	1.4 [1-2.1]	0.5 [0.3-0.9]	<0.021	120/1465	8.2 [6.9-9.7]	0.6 [0.3-1.2]	<0.124

4.4.2 Micro-stratification of malaria risk using data collected by qPCR, RDTs, and microscopy.

Significant variability in malaria infections was observed at the individual village level, with prevalence rates ranging from 0% to over 50% across the study area (Figure 4.3 & Table 4.4). Additionally, the method used to test for malaria significantly impacted the risk categorization of villages. Among the 35 villages surveyed, qPCR data indicated that only one village (1.2% of all villages) had very low malaria prevalence (*Pf*PR < 1%). In contrast, RDTs identified 12 villages (34.3% of all villages) and microscopy identified 11 villages (31.4% of all villages) as having very low prevalence. For moderate transmission, qPCR, RDTs, and microscopy categorized 15, 9, and 8 villages, respectively. For high transmission, qPCR identified 14 villages, RDTs identified 8, and microscopy identified 6. Notably, qPCR detected more malaria infections than RDTs and microscopy, resulting in many villages being classified into higher transmission categories. Overall, using qPCR data, over 80% of the villages were classified as moderate to high risk, significantly higher than the 48% classified by RDTs and 40% by microscopy. Conversely, while only 17% of the villages were classifiable as having low or very low malaria risk based on qPCR data, as high as 51% and 60% of the villages were classified into these same categories based on RDT and microscopy data (Table 4.4 and Figure 4.4).

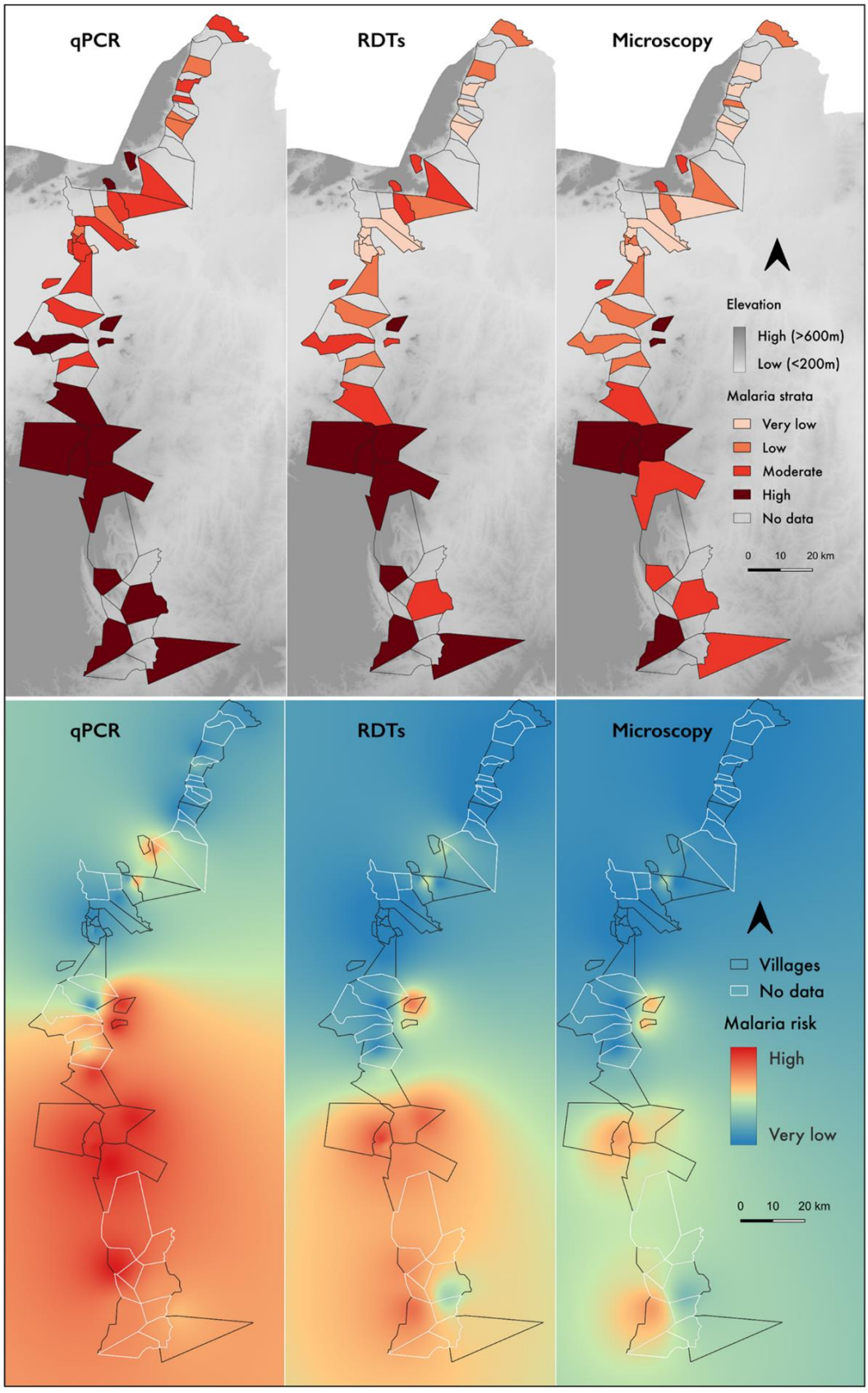

Figure 4.3: Fine-scale malaria mapping of 35 surveyed villages in the Ulanga and Kilombero districts using qPCR, RDTs, and microscopy data is shown in the top panel. The bottom panel indicates malaria risk generated by interpolating prevalence data obtained for each surveyed village by qPCR, RDTs, and Microscopy. Categories defined based on calculated prevalence rates as either very low risk (*Pf*PR <1%), low risk (1% ≤ *Pf*PR <5%), moderate risk (5% ≤ *Pf*PR <30%), or high risk (*Pf*PR ≥30%) (total number of villages = 35.

Table 4.4: Number of villages categorized into different risk strata based on the *P. falciparum* prevalence rate (*Pf*PR) data from qPCR, RDTs, and microscopy

Risk strata	0.98Prevalence	qPCR		RDTs		Microscopy	
		No.	%	No.	%	No.	%
Very low	*Pf*PR < 1%	1	2.9	12	34.3	11	31.4
Low	1% ≤ *Pf*PR < 5%	5	14.3	6	17.1	10	28.6
Moderate	5% ≤ *Pf*PR < 30%	15	42.9	9	25.7	8	22.9
High	*Pf*PR ≥ 30%	14	40.0	8	22.9	6	17.1
Total		35	100.0	35	100.0	35	100.0

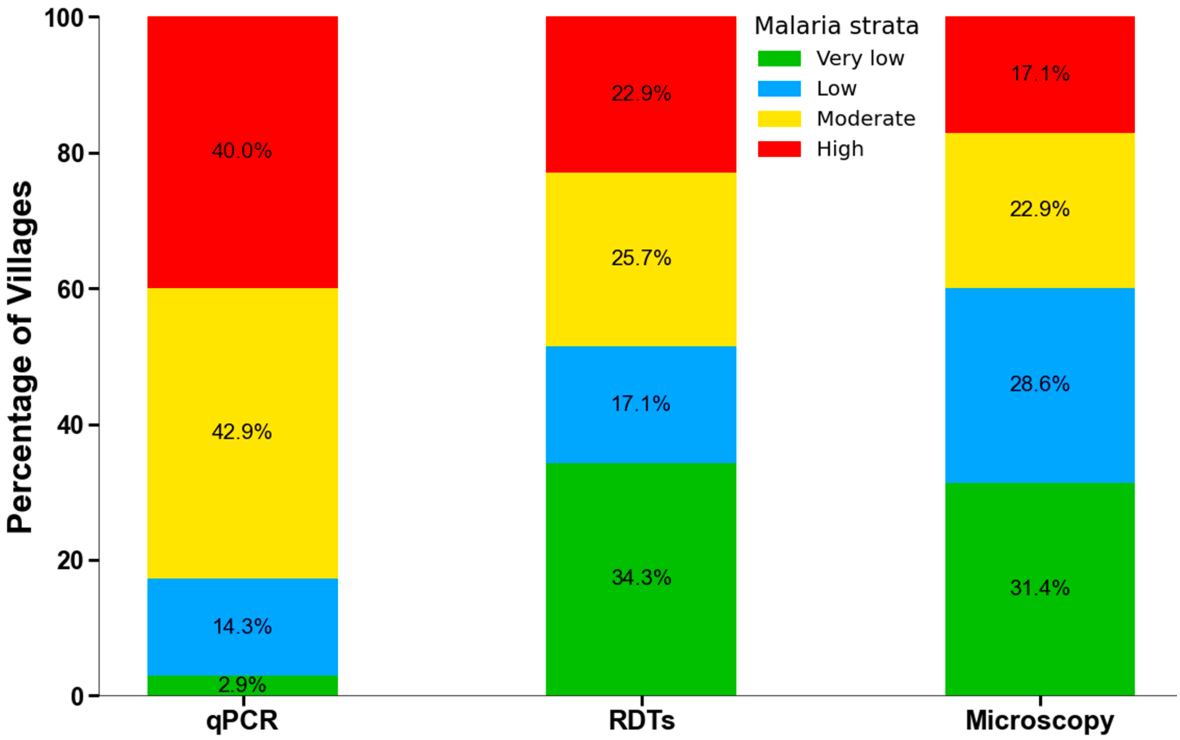

Figure 4.4: Percentage of villages categorized by different testing methods as either very low risk (*Pf*PR <1%), low risk (1% ≤ *Pf*PR <5%), moderate risk (5% ≤ *Pf*PR <30%), or high risk (*Pf*PR ≥30%) (total number of villages = 35)

4.4.3 Comparison of the perfomance of RDTs and microscopy relative to qPCR.

In this comparative analysis, only samples tested by all three methods—PCR, RDTs, and microscopy—were included (n = 4905). Among these, qPCR identified 1712 (34.9%) positives, respectively (Table 4.5 and Figure 4.5).

Table 4.5: Overall prevalence in the 35 surveyed villages estimated using qPCR, RDTs, and microscopy. Additionally, the table summarizes the proportion of malaria positive samples missed by RDTs and microscopy when qPCR is used as the reference.

	No. tested	**Pf. Positive**	**Prevalence**
qPCR	4905	1712	34.90%
RDTs	4905	1289	26.30%
Microscopy	4905	843	17.20%
Proportion of missed positives when qPCR is the reference			
	Total Positive by PCR	**Sample missed**	**(%) of missed Positive**
RDTs	1712	650	37.90%
Microscopy	1712	1009	58.90%

Both RDT and microscopy missed several infections otherwise identified by qPCR. This category of false negatives included cases where qPCR identified a sample as positive, but microscopy identified it as negative, cases classified as positive by qPCR but negative by RDTs, and cases where RDTs indicated positive results while microscopy indicated negative result. Out of the 1712 positives detected by qPCR, RDTs missed 650 (37.97%) and microscopy missed 1009 (58.9%) (Table 4.5). Additionally, when comparing microscopy to RDTs, microscopy failed to detect 45.46% (586/1289) of malaria infections detected by RDTs. RDTs correctly identified 1062 (62.03%) samples as true positives, while microscopy identified 703 (41.06%) as true positives (Table 4.6). Furthermore, RDTs misclassified 227 (7.10%) samples as false positives, while microscopy misclassified 140 (4.38%) (Table 4.6). More importantly, 56 samples were classified as positive by both RDTs and microscopy but were missed by qPCR Figure 4.5).

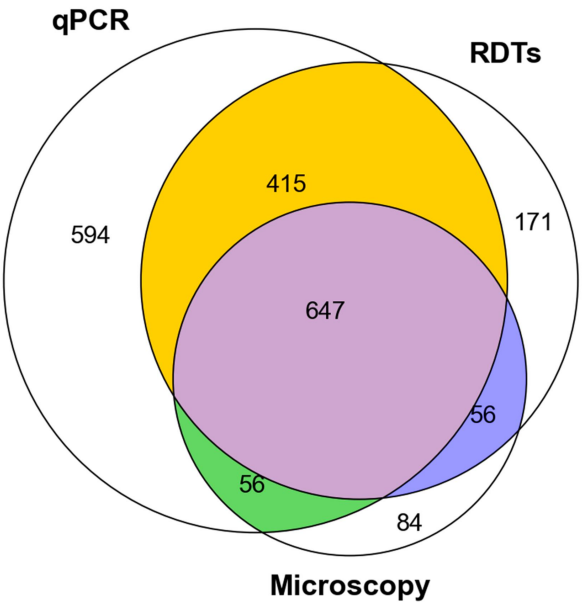

Figure 4.5: The Venn diagram illustrates positive samples detected exclusively by a specific tool while the other two missed them (qPCR only: 594 positive, RDT only: 171 positive, Microscopy only: 84 positive). Additionally, it shows intersections indicating positive detection by two tools when one detects negative (qPCR & RDT: 415 positive; qPCR & Microscopy: 56 positive; RDT & Microscopy: 56 positive). It also indicates intersections where all tools detect positive samples (qPCR, RDT, & Microscopy: 647 positive).

Table 4.6: Evaluation metrics for assessing the performance of RDTs and microscopy relative to qPCR during the fine-scale stratification of malaria risk in Ulanga and Kilombero districts, southeastern Tanzania. The evidence from other published studies serves only as a descriptive summary for comparison purposes.

Test characteristics	RDTs	Microscopy (Thick smear)
True Positives (PCR positive = 1712)	1062	703
False Positives (PCR negative)	227	140
True Negatives (PCR negative = 3193)	2966	3057
False Negatives (PCR positive)	650	1009
Sensitivity [95% CI]	62.0% [95% CI: 60.0-64.2]	41.0% [95% CI: 38.8-43.4]
Specificity [95% CI]	92.9% [95% CI: 92.0-93.7]	95.6% [95% CI: 94.9-96.3]
Positive Predictive Value [95% CI]	82.4% [95% CI: 80.3 -84.4]	83.4% [95% CI: 80.8-86.0]
Negative Predictive Value [95% CI]	82.0% [95% CI: 80.7-83.2]	75.2% [95% CI: 73.8-76.4]
Kappa value [95% CI]	0.7 [95% CI: 0.6-0.8]	0.5 [95% CI: 0.4-0.6]
Accuracy	82.1%	76.57%

4.4.4 Positive predictive values (PPVs), sensitivity, specificity, and agreement of RDTs and microscopy when compared to qPCR.

Considering qPCR as the benchmark, the sensitivity (the proportion of actual positives which were correctly identified as such) of RDTs was 62.0% [95% CI: 60.0-64.2], while that of microscopy was 41.0% [95% CI: 38.8 - 43.4]. The specificity (proportion of actual negatives which were correctly identified as such) was 92.9% [95% CI: 92.00-93.7] for RDTs and 95.6% [95% CI: 94.9- 96.3] for microscopy (Table 4.6). Overall, the positive predictive value (PPV), i.e. the probability that individuals with a positive test result actually have true infection, was 82.4% [95% CI: 80.3 -84.4] for RDTs and 83.4% [95% CI: 80.8-86.0] for microscopy (Table 4.6). Importantly however, the PPV for both RDTs and microscopy varied with malaria endemicity, generally increasing with prevalence, ranging from less than 20% in very low transmission areas to over 80% in high transmission areas (Figure Figure 4.6).

When considering the micro-strata generated using qPCR data, the PPV of RDTs and microscopy started at 0% in very low risk strata and gradually increased to >80% as villages shifted towards high risk strata (Figure 4.6A). However, when referring to the strata generated using RDTs data (Figure 4.6B), the PPV of both RDTs and microscopy started at 20% in very low risk strata and gradually increased to >80% in high-risk strata. The agreement between RDTs and qPCR was good (Kappa value = 0.58 [95% CI: 0.56-0.61]), while the agreement between microscopy and qPCR showed fair agreement (Kappa value = 0.42 [95%CI: 0.39-0.44]), (Table 4.6).

The sensitivity of both RDTs and microscopy varied by age, where RDTs sensitivity was higher for school-aged children (>80%) and dropped to 75% and 60% for 16-20 years and >20 years, respectively (Figure 4.6C). A similar trend of sensitivity was observed for microscopy (Figure 4.6C), indicating that RDTs and microscopy perform better in detecting malaria in school-aged children compared to adults.

The relationship between parasite density and the malaria detection probability by RDTs and microscopy was also examined. In this analysis, the probability of RDTs detecting positive malaria infections was maximized reaching 1 at 100 parasites/µL, where the logistic regression (logit (p)) model saturated (Figure 4.6D). At this density in contrast, the probability of microscopy to detect malaria infections was only 0.85% (Figure 4.6D), suggesting higher sensitivity of RDTs vs microscopy.

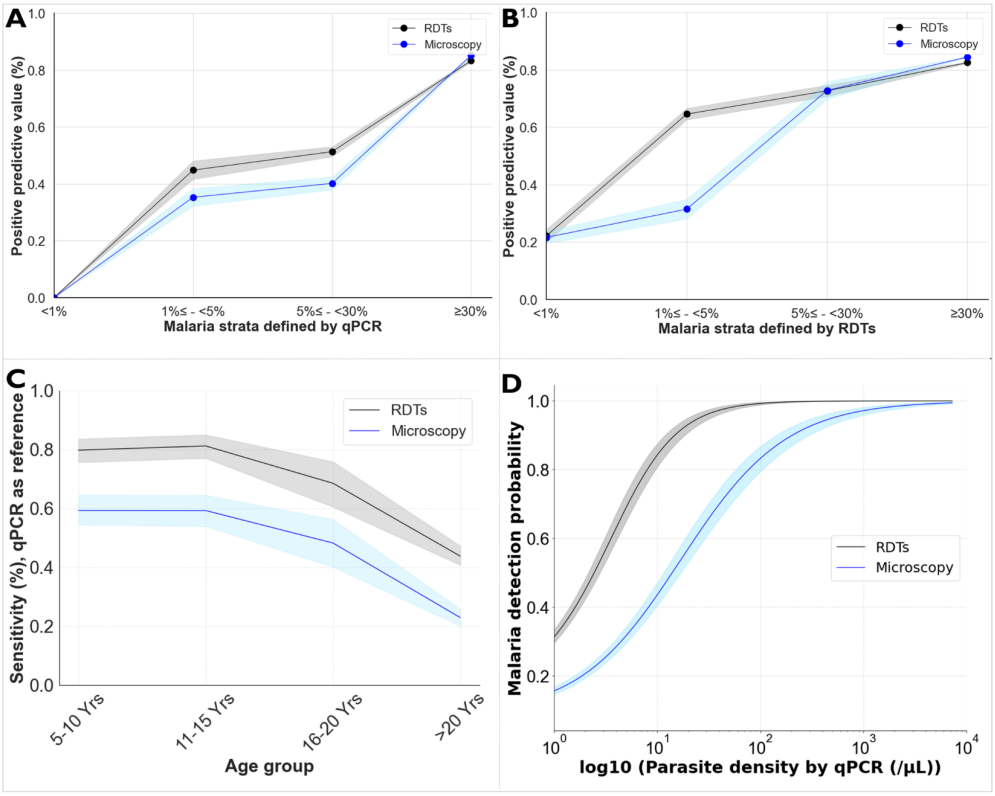

Figure 4.6: Estimates of the positive predictive values (PPVs) of RDTs and microscopy at different malaria endemicities across the study villages, defined based on either qPCR data (A) or RDT data (B). Panel C) illustrates the trend of sensitivity of both RDTs and microscopy relative to age groups. Panel D) displays the detection probability of both RDTs and microscopy relative to the parasite density estimated by qPCR.

4.4.5 Parasites density estimates and their correlations with *Plasmodium* prevalence

Further, asexual parasite densities estimated by both microscopy and qPCR were investigated and compared across different sex and age groups using Mann-Whitney statistics for two categories and the Kruskal-Wallis statistical test for more than two categories. Overall, PCR was capable of detecting approximately 100 fold lower parasite densities compared to microscopy. The geometric mean asexual parasite density estimated by microscopy was 2206.4 parasites/µL (95% CI: 1976.7-2462.8), while that estimated by PCR was 27.07 parasites/µL (95% CI: 23.23-31.54).

The asexual parasite density of infected individuals significantly differed between males and females as estimated by qPCR ($P < 0.001$), with males harboring a higher parasite density compared to females, though similar trend was observed by microscopy, this sex difference was not statistically detectable by microscopy ($P = 0.11$). Importantly, the geometric mean parasite density estimated by both microscopy and qPCR per village demonstrated a significant positive correlation with

the parasite prevalence of the respective village. Thus, villages with high malaria prevalence also had high malaria parasite densities compared to villages with lower prevalence (Figure 4.7C-F). Considering qPCR-estimated geometric mean parasite densities, the Spearman rank correlation score was 0.77 ($P < 0.001$) and 0.76 ($P < 0.001$) when the malaria prevalence of the villages was estimated by qPCR and RDTs, respectively (Figure 4.7C & Figure 4.7E). On the other hand, the Spearman rank correlation for the parasite density estimated by microscopy was 0.55 ($P < 0.003$) and 0.48 ($P < 0.012$) for qPCR and RDTs estimated prevalence of the villages, respectively (Figure 4.7D & Figure 4.7F). When parasite density by age groups were analyzed, both microscopy and qPCR revealed a significant difference in estimated malaria parasite densities between age groups based on Kruskal-Wallis statistics ($P < 0.001$). Pairwise tests by Mann-Whitney statistics revealed that school-aged children (5-15 years old) harbored a higher parasite density than those 16 years old and above ($P < 0.001$) as indicated by both microscopy and qPCR (Figure 4.7A & Figure 4.7B)

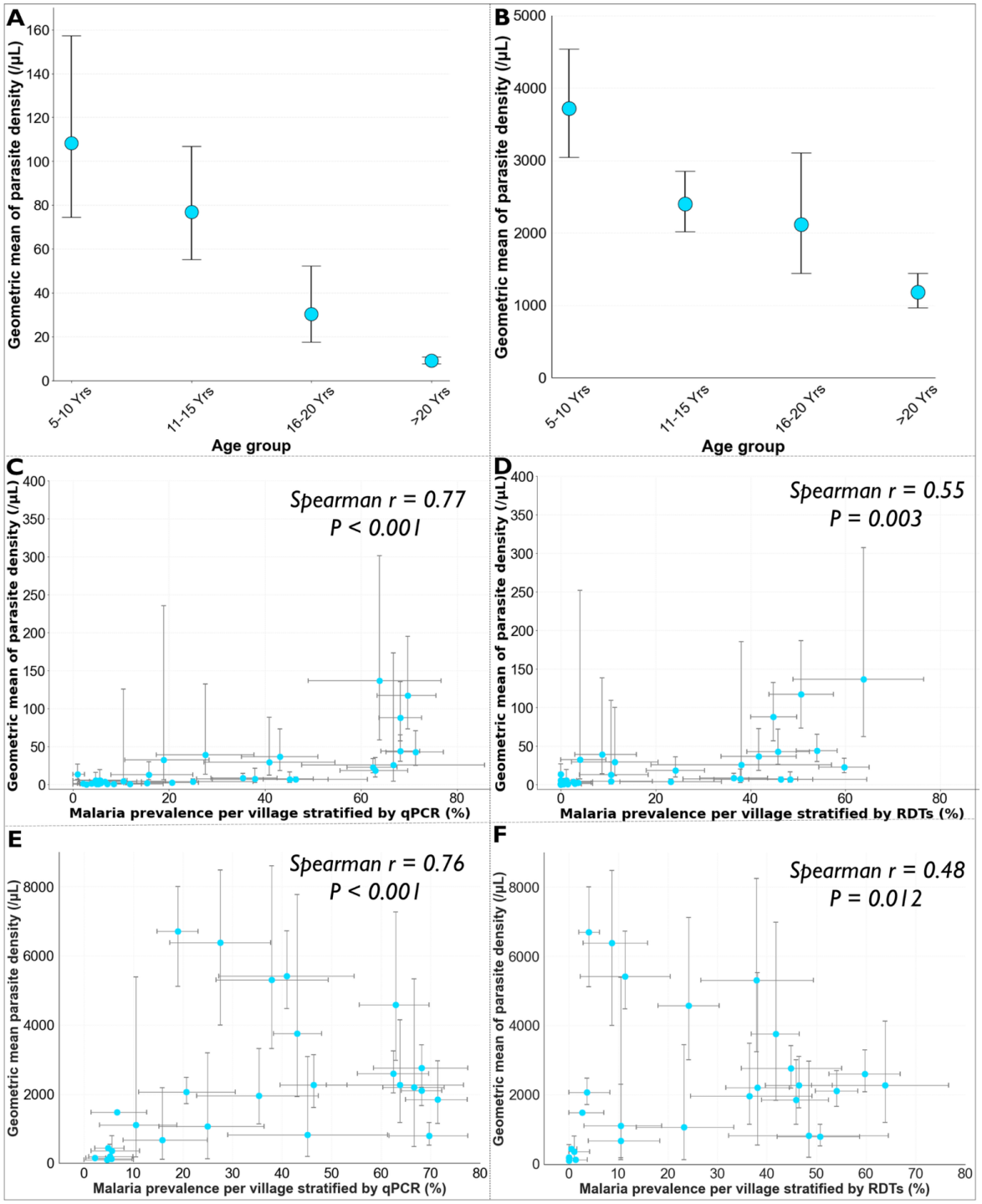

Figure 4.7: Geometric mean parasite densities per age group estimated by A) qPCR and B) microscopy. Panel C (density estimated by qPCR) and Panel D (density estimated by microscopy) show the correlation between parasite density and prevalence estimates by qPCR. Panels E (density estimated by qPCR) and F (density estimated by microscopy) show the correlation between parasite density and prevalence estimates by RDTs.

4.5 Discussion

In malaria-endemic countries, data-driven risk stratification is increasingly used at district or higher regional levels to guide intervention strategies and optimize resource allocation. Additionally, the geographical variations in levels of endemicities and the shift towards elimination in some settings necessitates finer resolution for optimal resource allocation [345, 349, 392]. In most settings in Africa, the data used for epidemiological stratification of malaria typically comes from rapid diagnostic tests (RDTs) or microscopy-based testing, which despite wide scale availability and low operational costs, often perform poorly in low transmission settings [228, 248, 393]. While direct comparisons of these diagnostic tools for fine-scale stratification are currently limited, selecting the most appropriate data sources and testing methods is crucial, as different methods can yield significantly different results depending on endemicity, particularly in elimination settings. Even without alternative testing methods, data users and decision-makers need to understand the limitations of their selected approaches, especially the weaknesses of current dominant data sources like RDTs or microscopy. In this study, we conducted a high-resolution survey of *P. falciparum* malaria in two Tanzanian districts, comparing fine-scale strata obtained using RDTs, microscopy, and qPCR assays.

The study showed significant variability in malaria risk at a fine scale. Within less than 150 kilometers, malaria prevalence estimates ranged from 0% to over 50% across contiguous villages in an area broadly classified as moderate risk (17% *Pf*PR) by recent government stratification [371]. Such fine-scale variability is not uncommon and has been observed in several other settings [394]. In one study in Madagascar, there was a tenfold difference of malaria prevalence within a radius of less than 50 kilometers [395]. For precise micro-stratifications, this study emphasizes the importance of carefully selecting diagnostic tools, especially for local malaria elimination efforts. Our findings indicate that RDTs and microscopy have poor positive predictive values, which can be even less than 20% in villages with very low and low transmission as the proportion of truly infected individuals is very small compared to non-infected persons. There were also significant discrepancies in the resulting micro-strata depending on the test method used. For instance, among the 35 surveyed villages, RDTs and microscopy classified 12 and 11 as very low and 6 and 10 as low risk strata, respectively, while qPCR identified only 1 village as very low and 5 as low transmission. This means RDTs and microscopy classified majority of the villages as very low to low risk while qPCR classified most villages as moderate to high risk (Table 4.4).

Clear demarcation of areas with very low to low risk versus those with moderate to high risk is essential, particularly in the push towards elimination. As countries increasingly adopt data-driven decision-making for malaria control, there is a risk of improper resource allocation or premature withdrawal of effective interventions from localities erroneously deemed as nearing elimination. Local authorities need to decide which data to use for local-level micro-stratification and whether RDTs, commonly used for broader-scale sub-national stratification, suffice for fine-scale local decision-making. Previous evidence has shown that hotspots identified by RDTs are less stable than those identified by microscopy and PCR [228]. Hotspots of febrile malaria infections are also generally unstable and variable over geographical spaces, while hotspots of asymptomatic cases tend to be more permanent and can be more practically targeted for transmission control [396]. In this current study, we also found significant positive correlations between malaria parasite densities and malaria prevalence in southeastern Tanzania, emphasizing the need to incorporate tests that depict sub-microscopic infections into malaria stratification and decision making to better target the hotspots. As already reported in other studies, villages in our study area, which were classified as low transmission areas had lower geometric mean parasite density compared to those with higher transmission rates.

Our findings, benchmarked against qPCR, reveal limited detection capabilities of RDTs and microscopy in overall fine-scale stratifications, especially in low transmission settings. Previous studies have emphasized the usefulness of routine hospital data for micro-stratifications [347, 349, 397, 398]. However, evidence indicates that both microscopy and RDTs are less effective in identifying stable febrile malaria hotspots, except for asymptomatic hotspots, which are reliably identified by microscopy [396], however still not stable when transmission is low [306]. Our research underscores the importance of identifying subclinical infections using sensitive tools to advance malaria elimination, particularly through fine-scale population surveys. Additionally, there is evidence suggesting potential benefits from integrating hospital and school-age children survey data or even antenatal care centers [341, 348]. Nevertheless, these approaches heavily rely on rapid diagnostic tests (RDTs) as the primary tool for malaria detection. While the World Health Organization (WHO) recommends monitoring RDT performance alongside microscopy, our study is particularly relevant as we have directly compared the fine-scale stratification capabilities of RDTs, microscopy, and qPCR at a fine scale.

This study demonstrated overall good agreement between RDTs and qPCR, while microscopy showed fair agreement. However, RDTs missed over 38% of malaria infections, particularly among adults over twenty years old, who were found to harbor lower parasite densities compared to those under twenty years old. However, RDTs remain useful in testing fever-positive malaria cases in hospitals and are widely

employed in population surveys due to their cost-effectiveness and ease of implementation [231]. As evidenced in this study, carefully re-consideration of using RDTs for finer-scale mapping and intervention planning at sub-district level should be a priority. Similarly, microscopy missed >50% of the malaria infections detected by qPCR, which is consistent with previous studies, including a meta-analysis of 42 studies, which showed that microscopy misses over 50% of malaria infections [308, 399]. Operational challenges, such as the level of expertise required for accurate detection and the need for electricity and precise sample handling procedures, contribute to these limitations. Interestingly, microscopy underestimated malaria risk by classifying more villages as low strata compared to qPCR. Nonetheless, microscopy still plays a crucial role when used in conjunction with tools like RDTs, providing valuable information about malaria parasite densities [174, 400, 401]. Here, we estimate a 100-fold higher parasite density when measured by microscopy compared to densities measured by qPCR, consistent with similar trends observed in previous studies [382]. The findings of this study also indicate that the false-negative rate of microscopy decreases with increasing parasite density, a pattern observed in other studies too [400].

The analysis also revealed variations in parasite densities across different age groups, with school-age children (5-15 years old) exhibiting higher parasite densities compared to individuals aged 16 and above. Notably, our study identified a reduced sensitivity of both RDTs and microscopy among adults aged over 16 years, consistent with findings from prior studies conducted before 2015 in various regions [402–409]. It is possible that this pattern is driven by age-related differences in malaria parasite prevalence, as observed in Table (Table 4.3), and may be confounded by unequal sampling of the age distribution. Furthermore, our findings suggest that this trend may be attributed to the lower parasite density estimates observed in adults within the study (Figure 4.7A & Figure 4.7B). Significantly, our research provides valuable insights, highlighting the potential implications of these trends, particularly in fine-scale mapping scenarios, where RDTs and microscopy may underestimate burden at very low and low transmission strata, with qPCR serving as the reference standard in this study.

When selecting a tool for a stratification exercise, it is crucial to consider several key operational factors. First, to assess whether transmission levels are sufficiently low to require a high-sensitivity tool capable of differentiating between locations with the lowest prevalence. This was exemplified in much of this study area, especially in the northern zones where qPCR was clearly more sensitive than RDTs and microscopy. Second, evaluate the logistical and cost implications associated with using each tool for testing individuals. Finally, consider the ethical requirements and the ability to provide immediate results and treatment when necessary. Ultimately, when aiming to

achieve more precise fine-scale mapping of malaria infections to facilitate more accurate resource allocation, the choice of testing tools should be based on the balance between sensitivity and operational feasibility.

Sensitive molecular tools like qPCR are available, but qPCR has operational challenges, including the need for well-designed infrastructure, high costs, and expertise, and it is not portable for remote areas. Efforts are underway to develop portable qPCR technologies, but cost and expertise remain significant barriers. To address these gaps, NMCPs should develop innovative plans, which might include: a) establishing centralized facilities for receiving and processing qPCR samples and conducting such surveys infrequently, such as every 3 years; b) partnering with local research organizations to support high-accuracy evaluations using nucleic acid-based tests; c) exploring alternative methods for micro-stratification, such as geo-spatial modeling that integrates information such as land use, elevations, and other environmental factors, and potentially combining facility and population survey data. A related point to emphasize is the overall need for highly sensitive, cost-effective, and potentially reagent-free tools that align with the economic context of malaria-endemic settings. Recent innovations such as high/ultra-sensitive RDTs, the saliva-based tests [410] or the use of Infrared spectroscopy (IR) and machine learning (ML) [174, 411] have shown promise in detecting malaria infections at sensitivities equivalent to PCR, but further research are needed before these technologies can be routinely deployed. Such reagent-free assays like the IR-AI based approaches would be particularly transformative for scaling up effective micro stratification of malaria risk in Africa.

It is important to recognize that prevalence rates obtained from different tests are not directly comparable; for example, a 5% prevalence detected by RDTs does not equate to 5% detected by PCR. Therefore, in some cases, the ranking of prevalence is more critical than the exact rates. In some cases, ranking prevalence may be more critical than the exact rates. Additionally, variations in sample sizes should be considered, especially in fine-scale stratifications, as confidence intervals (CIs) may cause overlap across strata. Therefore, it is important to assess stratifications based on prevalence CIs rather than relying solely on point estimates. In this study Despite some villages spanning two or three strata based on their CIs, RDTs and microscopy still classified more villages as very low to low risk, while qPCR frequently classified them as moderate to high (see Supplementary Table 4).

More importantly, the need for more detailed data becomes crucial when stratification occurs at local scales, such as comparing wards or villages within districts, as done in this paper, rather than at the national level, where regions or districts are compared. While most malaria stratifications are currently conducted at national and sub-national levels using RDTs and sometimes microscopy, this study highlights that

the choice of test methods can influence decision-making and overall control strategies, especially in finer-scale stratifications. Determining appropriate public health decisions was beyond the scope of this study and may vary depending on the scale of stratification. However, we emphasize that decision-making should consider the strengths and limitations of the available data when planning stratifications. Additionally, countries may therefore establish locally relevant thresholds for deciding which interventions to implement or withdraw.

This study also raised some important new questions. For example, it is interesting to observe that areas with low transmission also have persistently low parasite densities compared to those in higher transmission settings, which are usually reported to acquire immunity and become protective. Although this phenomenon of low parasite density in low transmission areas was not explored in detail in this study, it could suggest residual immunity among individuals due to recent declines in transmission or potential migration of participant [412]. Studies have demonstrated that in low transmission areas, highly virulent parasites are more exposed to facilitate malaria transmission by mosquitoes compared to low virulent ones [413]. Consequently, high virulent parasites are detected and treated, leading to their removal from the population [413]. This leaves behind low virulent parasites that are less exposed and maintain low densities, becoming symptomatic, undetectable, and untreated [414]. This phenomenon may contribute to long-term parasite transmission strategies, highlighting the importance of using highly sensitive tools for screening [382, 413, 415].

In interpreting the findings of this study, several limitations should be considered. The IDW technique used here is primarily intended for visualizing general trends in malaria risk rather than providing precise prevalence estimates or specific risk levels for each village (both sampled and unsampled). Unlike the exact data shown in the top panel of Figure 3, IDW interpolation is subject to smoothing effects, particularly in areas with fewer data points, which may reduce the accuracy of the maps. Villages without data may contribute to differences, such as the appearance of low-risk areas in the southern regions, where actual values could range from moderate to high. Nonetheless, this approach effectively visualizes likely malaria risk patterns in unsampled areas by using known data from sampled villages, based on the results of different screening methods. Furthermore, seasonal variations are expected to influence village-level prevalence estimates and, consequently, the distribution of malaria risk. However, seasonality does not affect the primary objective of this study, which is to evaluate the performance of qPCR, RDTs, and microscopy for fine-scale stratification.

This study also did not account for all factors that may contribute to the broader heterogeneity of malaria infections in southeastern Tanzania. It is crucial for future studies to also investigate how different categorizations of malaria prevalence-based strata impact the agreement between diagnostic tools. This will help determine the most appropriate categories for decision-making and resource allocation. Future investigations should also delve into potential environmental, geographical, immunological or genetic diversity of the parasite influences underlying this variability. Additionally, the biological significance of missed infections by both RDTs and microscopy was not explored. Consequently, the study did not estimate the transmission burden associated with these undetected positive samples, nor assess the parasite densities necessary to sustain transmission in the population.

4.6 Conclusion

As countries progress towards malaria elimination, fine-scale mapping of malaria risk becomes increasingly important. This study highlights significant variability in village-level malaria risk within and between districts in southeastern Tanzania, an area where the scale-up of effective interventions has led to substantial progress, yet cases persist despite high intervention coverage. Secondly, the study underscores the variable performance of different testing methods in stratifying risk. While RDTs and microscopy, the primary test methods used in low-income endemic settings and the main sources of data for ongoing epidemiological stratification efforts, were effective in high-transmission areas, they performed poorly in low-transmission settings, often classifying most villages as very low or low risk. In contrast, qPCR classified most villages as moderate or high risk. These findings demonstrate the importance of using appropriate testing methods for data-driven, fine-scale risk stratification to enhance targeted interventions aimed at reducing and eliminating malaria. The study underscores the need for proper choices of malaria testing approaches that are both operationally feasible and sufficiently sensitive to enable precise mapping and effective targeting of malaria in local contexts. More importantly, public health authorities must recognize the strengths and limitations of their available data when planning local stratification or making decisions. While innovation for more effective strategies is ongoing, sensitive molecular tools like qPCR, despite their operational challenges, will be crucial for accurate malaria risk mapping and intervention planning, especially in settings with significantly reduced risk. Going forward, developing new tools that balance operational costs and sensitivity, particularly in low transmission settings, will be essential for effective malaria control and eventual elimination.

Chapter 5: Performance of Mid-Infrared Spectroscopy and Machine Learning for Detecting Malaria Infections in High and Low Transmission Settings

5.1 Abstract

Background: Mid-infrared spectroscopy combined with machine learning (MIRs-ML) has emerged as a promising approach for detecting malaria parasites, with potential to achieve high sensitivity while balancing costs and operational efficiency. However, its performance across different malaria endemicities remains unexplored. We therefore evaluated the performance of MIRs-ML for malaria screening in blood samples collected from high and low transmission areas in south-eastern Tanzania, using qPCR as the reference standard.

Methods: We conducted a cross-sectional survey in south-eastern Tanzania, screening 7628 individuals across 35 villages with malaria *Plasmodium falciparum* prevalence ranging from less than 1% to over 50%. Additionally, we used qPCR to analyse dried blood spots (DBS) from 4,905 of these individuals, randomly selected from across the epidemiological strata. Mid-infrared spectra from these DBS were collected using ATR-FTIR spectrometer and used to train and validate machine-learning classifiers. The spectra were labelled based on the qPCR results, and two classifiers, Random forest and Logistic regression, were trained using: (i) data from all epidemiological strata, (ii) data from high transmission strata, (iii) data from individuals with the highest parasitaemia in high transmission strata, or (iv) a mix of laboratory-generated and field-collected data. These classifiers were validated and used to predict the qPCR results in unseen datasets of MIR spectra from low transmission villages (*Pf*PR < 5%) and high transmission villages (*Pf*PR >30%).

Results: Based on the qPCR results as the reference, classifiers trained on data from all epidemiological strata or high parasitaemia in high transmission areas achieved over 93% accuracy and >90% sensitivity (recall) in detecting malaria across both low and high transmission settings. However, classifiers trained exclusively on high transmission data demonstrated over 95% accuracy and 93.5% sensitivity in

high transmission areas but had reduced accuracy of 87% and sensitivity of 86.5% in low transmission areas. Moreover, classifiers incorporating both laboratory and field data achieved accuracy levels comparable to those trained exclusively on field data.

Conclusion: This study demonstrates the effectiveness of MIRs-ML across different transmission settings, showing strong performance for classifying infected versus non-infected individuals in both high and low transmission strata. The findings emphasize the importance of selecting appropriate training datasets for the ML models, and particularly highlight the suitability of laboratory data augmented with field data. Given that the approach is robust, reagent-free, and easy-to-perform, this study provides further evidence of its potential for broader application in large-scale parasitological surveys of malaria across a range of epidemiological settings.

5.2 Background

Over the past two decades, malaria control efforts have averted 2.1 billion cases and 11.7 million deaths globally [1]. This success is attributed to interventions including antimalarial drugs and vector control measures such as insecticide-treated bed nets (ITNs), indoor residual sprays (IRS), and larval source management [5, 416–418]. These successes inspired a trend to transition towards malaria elimination, with several countries planning to achieve this goal by 2030 [194]. However, several significant challenges persist, highlighting the need for inexpensive, scalable screening methods with high sensitivity, even at low levels of parasitaemia and prevalence. Conventional tools, such as RDTs and microscopy, are widely used but demonstrate limited sensitivity in detecting malaria infections, particularly in low transmission settings, despite being cost-effective [128, 419–421]. In these contexts, undetected infections can be very high, in some instances reaching even 50% , especially in low transmission settings [422]. This underscores the critical need for more sensitive diagnostic approaches, particularly during population screenings, that could span on being scalable, cost-effective and user-friendly [198].

Molecular assays, like polymerase chain reaction (PCR), demonstrate high sensitivity in detecting malaria infections [128, 366, 423], but their suitability for population-wide surveys is hindered by several factors, including the high cost of reagents, labour-intensive procedures, the need for specialized expertise, limited portability and not sufficiently robust for field laboratories in locations most affected by malaria [420, 424, 425]. As a result, PCR assays are not considered feasible for wide-scale implementation, particularly in remote areas. This emphasizes the need for alternative malaria screening methods capable of striking a balance between

sensitivity and operational viability [198, 426]. Such approaches are vital as core components of the broader evidence-based strategies endorsed by the WHO to ensure the accurate and timely detection of infections [416]. Indeed, the requirement for highly scalable and low-cost approaches for malaria surveillance is now considered one of the fundamental pillars of malaria elimination efforts as envisaged under the global strategy for malaria elimination by WHO, 2016-2030 [194].

Recently, mid-infrared spectroscopy combined with machine learning (MIRs-ML) have demonstrated potential for detecting malaria infections in human blood [174, 427]. This technology involves scanning the blood samples either wet or dried on paper cards with infrared light to obtain blood chemical signatures [217, 218, 222]. Computational approaches are used to identify and translate the spectra signatures into meaningful biological traits, such as the presence or absence of malaria infection [217, 218, 222, 428]. Under laboratory conditions, MIRs-ML could detect malaria parasites at ultra-low concentrations, of which are undetected by conventional tools such as RDT and microscopy, even in presence of confounders anaemia and varying parasite densities [222, 411]. The added advantage of using MIRs-ML for malaria screening is promising for balancing the cost of operations with sensitivity, especially when compared to PCR.

Despite the progress in MIRS-ML techniques, their practical application in field settings remains underexplored. Some studies using samples collected from population surveys have shown over 90% accuracy in detecting *P. falciparum* infections and greater than 80% accuracy for mixed infections of *P. falciparum* and *P. vivax* [217, 218]. Additionally, the approach achieved a sensitivity of 92% and a specificity of 97% in detecting malaria infections in blood samples, using samples collected from hospitals in Thailand [218]. Despite these demonstrations on applicability of the MIRs-ML for detecting malaria infections on realistic samples, there is no evidence of the performance of such technologies in detecting malaria infections in areas with varying malaria transmission endemicity.

It is crucial to test promising malaria screening tools in areas with varying levels of endemicity to determine their suitability for point-of-care diagnosis or screening in different transmission strata (low, moderate, and high) or exclusively in high transmission areas [174]. For instance, detailed fine-scale mapping of malaria in south eastern Tanzania revealed significant variability in malaria prevalence, ranging from <1% to 50% between local lowest administrative boundaries known as villages, as estimated by RDTs, microscopy, and qPCR [429]. In these settings, RDTs and microscopy showed poor positive predictive value (<20% PPV) compared to qPCR, while they performed better (>80% PPV) in high transmission areas [429]. Therefore,

evaluating novel malaria screening tools like MIRs-ML in such settings could help determine their effectiveness across different transmission strata, providing a clearer understanding of where these tools might be most suitable.

Laboratory demonstrations have shown the potential for optimizing algorithm development by using high-parasitaemia samples alongside negative ones in training sets while cover immunological and genetic variations. These algorithms trained with high-parasitaemia samples have successfully transitioned to field applications, underscoring the importance of assessing the best training datasets using realistic field samples [411]. This could involve using data from high transmission areas, combining various data types, or calibrating laboratory models with integrated field data to develop robust systems with minimal effort [174].

The aim of this study was therefore to evaluate the performance of MIRs-ML in detecting malaria infections across villages with different malaria prevalence levels. Using qPCR as a reference method, we compared the performance of this approach for malaria screening in blood samples collected from high prevalence (*Pf*PR $\geq$ 30% by qPCR) and low malaria ((*Pf*PR $<$5% by qPCR) areas.

5.3 Methods

5.3.1 Study area

This study was conducted in south eastern Tanzanian districts of Ulanga and Kilombero, in the Kilombero Valley (Figure 5.1), where malaria prevalence is significantly heterogeneous, with village-level malaria prevalence varying from $<$ 1% to $>$ 50% [429].

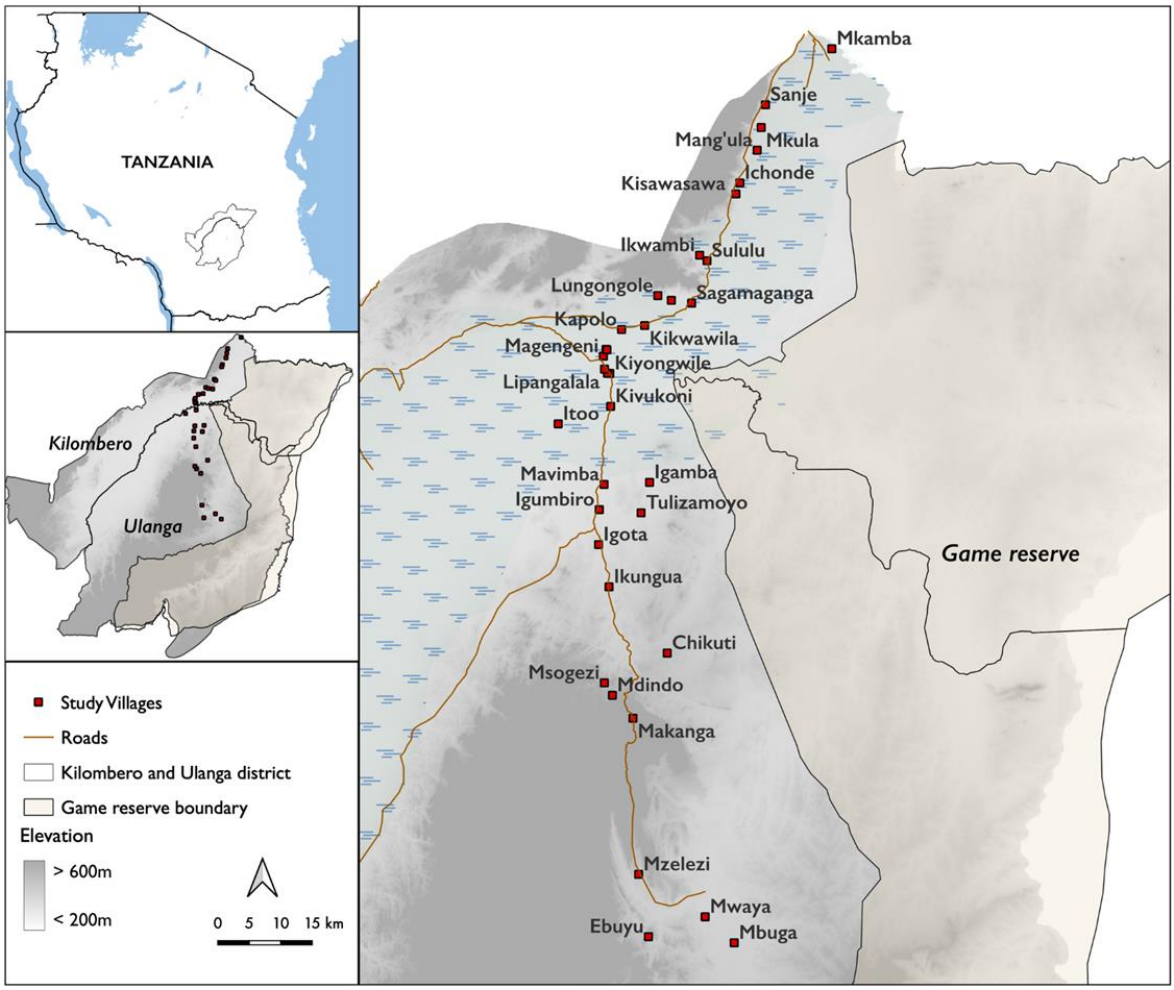

Figure 5.1: Map of the study area, encompassing 35 villages and over 100 sub-villages within the Kilombero and Ulanga districts

Ulanga District is situated at 8.9889°S, 36.6133°E and has a population exceeding 200,000 individuals while Kilombero District is located at 8.2414°S, 36.3349°E, has a population of over 500,000 [429, 430]. The study area has temperature range that fluctuates between 20°C and 35°C, influenced by both altitude and seasonal variations. The region experiences a rainy season typically from December through April, followed by a dry season from June to September. The primary economic activities include subsistence farming and large-scale agriculture. Most families engage in crop farming, with rice being the predominant crop. Additionally, there are extensive commercial operations, particularly large-scale teak and sugarcane plantations [372, 431, 432].

5.3.2 Study surveys, and creation of dried blood spots

A cross-sectional survey was carried out in 35 villages (Figure 5.1). The sample size for each village was calculated proportionally based on the village population and malaria prevalence estimates from prior surveys, as described in Mshani et al [429]. Households were selected using systematic random sampling, and written consent was obtained from each selected household before conducting surveys and recruiting participants. Consent was provided on a household basis, and all individuals in a consenting household were recruited. Each participant was assigned a unique identification number to link relevant information, including malaria test results from different tools, demographic data, and household characteristics.

Malaria screening was performed using RDTs (SD Bioline Ag-Pf/Pan) through finger pricks at temporary screening centers set up in each village. Additionally, both thin and thick blood smears were prepared and analysed using microscopy [224, 429]. For dried blood spots, approximately 50 µL of blood from each participant was applied to a single spot on Whatman^{TM} protein saver cards, totalling three to five spots per individual depending on the volume of blood available. These cards were left to air-dry and then stored. The blood smears and dried blood spots were transported to the Ifakara Health Institute's laboratory, where further analysis for malaria infections was performed using microscopy and quantitative polymerase chain reaction (qPCR), respectively.

5.3.3 DNA extraction and qPCR analysis

DNA extraction from dried blood samples was done using theQuick-DNA^{TM} Miniprep Plus Kit (Zymo Research, USA) [381]. The extracted DNA was dissolved in 50 µL of elution buffer and stored at −20°C until it was needed for detecting and quantifying *P. falciparum* infections with probe-level allele-specific quantification (PlasQ) multiplex qPCR assays, [367, 382, 383]. Detection and quantification of *P. falciparum* parasites were performed using the Bio-Rad CFX96 real-time PCR system (Bio-Rad Laboratories, USA), with data analysed using Bio-Rad CFX Maestro software. The qPCR reaction, PlasQ primers and probes mix, are summarized in supplementary Table S4.1 & Figure S4.2. The DNA amplification protocol included an initial activation step at 95°C for 1 minute, followed by 15 seconds of denaturation at 95 °C and 45 seconds of annealing/elongation at 57 °C, repeated for a total of 45 cycles, ending with a melting phase [367, 382, 383]. The quantitative polymerase chain reaction (qPCR) assays included both positive controls (samples known to contain *P. falciparum*) and a non-template control (samples free of *P. falciparum*). For unknown

samples, the result was considered positive for the target genes (*pf*varATS and 18S ribosomal RNA) if the cycle threshold (Ct) value was less than 37, and negative if the Ct value was greater than 37. Similarly, for the human ribonuclease P gene (extraction control), a Ct value less than 35 was considered positive, while values of 35 or higher were considered negative. For absolute quantification, the WHO international standard for *P. falciparum* nucleic acid amplification (WHO reference NIBSC#04/176) [367], was employed. This standard was prepared by serially dilutions from 100,000 parasites/µL to 0.01 parasites/µL, with each dilution tested in triplicate.

During qPCR assay, the prepared standards were analysed alongside the unknown samples. Following the assay, the standard curve and sample data were normalized and analysed using Bio-Rad CFX Maestro software. The normalized cycle threshold (Ct) values of the samples, along with the linear regression equation from the standard curve, were used to determine the parasite density in the unknown samples, expressed as parasites per microliter (parasites/µL) of blood.

5.3.4 Malaria heterogeneity in the study area

The villages were stratified based on the results from RDTs, microscopy, or qPCR. While the WHO provides standard guidelines for stratifying malaria risk, it allows countries to adjust these ranges according to their understanding of local transmission patterns. Therefore, the stratification categories used in this study were adapted from the Tanzania National Malaria Control Program [341]. Malaria prevalence was highly variable in the 35 surveyed villages, ranging from less than 1% to over 50% based on any of the three tests as reported in Mshani et al [429] and summarised in Table 5.1.

Table 5.1: Stratifications of study villages by *P. falciparum* prevalence (*Pf*PR), serving as benchmarks for evaluating MIRs-ML performance in malaria screening across different endemicity levels

Risk strata	Prevalence	qPCR		RDTs		Microscopy	
		No.	%	No.	%	No.	%
Very low	*Pf*PR < 1%	1	2.9	12	34.3	11	31.4
Low	1% ≤ *Pf*PR < 5%	5	14.3	6	17.1	10	28.6
Moderate	5% ≤ *Pf*PR < 30%	15	42.9	9	25.7	8	22.9
High	*Pf*PR ≥ 30%	14	40.0	8	22.9	6	17.1
Total		35	100.0	35	100.0	35	100.0

5.3.5 Acquisition and processing of mid-infrared spectra

For each participant, a single cycle of Whatman protein saver cards that was fully covered with blood was selected, resulting in one spectrum per individual. A punched cycle from the Whatman card was scanned using a Fourier Transform Infrared (FT-IR) spectrometer, which operated across the mid-infrared range, 4000–500 (cm^{-1}) with a resolution of 2 (cm^{-1}). The scanning equipment was a compact Bruker Alpha FTIR interferometer, equipped with a Platinum-Attenuated Total Reflectance (ATR) module featuring diamond crystals. To enhance light penetration, the card was positioned on the diamond crystal of the spectrometer, and pressure was applied using an anvil to ensure optimal contact between the sample and the crystal. Each scan was performed 32 times to produce an averaged spectrum, which was labelled with a unique ID assigned to each participant, along with the date of scanning. These unique IDs facilitated the linkage of the mid-infrared spectra with laboratory malaria status results by qPCR and other demographic data collected during field activities.

The spectra were first pre-processed to ensure that only high-quality data were used for machine learning analysis. Using a program adapted from Gonzalez-Jimenez et al. [212], low-quality spectra, such as those distorted by the anvil, were discarded. This program also corrected for atmospheric interference, including excess water and CO content.

5.3.6 Selection of machine learning algorithms

The processed mid-infrared spectra were linked with qPCR laboratory results using unique identity numbers, with the Pandas Python package [385]. After merging the datasets, the final dataset included wavenumbers and their corresponding absorption intensities, along with malaria screening results, which were classified as positive or negative based on the qPCR data. This dataset was then used for selecting, training, and evaluating the machine learning algorithms using Python version 3.9.

A supervised learning approach was used to evaluate six models through stratified k-fold cross-validation, selecting the best model based on accuracy, sensitivity, specificity, Receiver Operating Characteristic (ROC) curves, and Area Under the Curve (ROC-AUC). The models evaluated included K-Nearest Neighbours (KNN), Logistic Regression (LR), Support Vector Machine (SVM), Random Forest (RF), Gradient Boosting (XGB), and Multilayer Perceptron (MLP). To address class imbalance, random under-sampling was applied, and the data was standardized to

ensure uniformity. The dataset was divided such that 70% was used for model selection, training, and testing, while the remaining 30% was reserved to prevent data leakage and was used for validating the trained algorithms.

Using stratified K-fold cross validation, the selection of the models was conducted using datasets divided into four segments based on malaria strata defined by qPCR prevalence results (Table 5.1): (i) data from all epidemiological strata, (ii) data from high transmission strata, (iii) data from individuals with the highest parasitaemia in high transmission strata, or (iv) a mix of laboratory-generated and field-collected data.

5.3.7 Training and testing of machine learning algorithms

The stratifications based on the qPCR results were used as the benchmark for evaluating the performance of MIRs-ML in malaria screening (Table 5.1). The best-performed algorithms on cross validation were selected and trained to classify malaria infections from field-collected samples. The dataset was randomly shuffled and divided into 80% for training and 20% for testing model performance. Training was done using the four categories of datasets divided as explained during model selection by cross-validation above. For validation of the performance of the trained models, we used the 20% unseen datasets using data from: i) high malaria transmission villages (*Pf*PR>30%) and ii) low malaria transmission villages (*Pf*PR < 5%). The performance of the ML models on these validation sets was assessed using a range of metrics, including accuracy, F1-score, recall (sensitivity), and precision.

5.4 Results

5.4.1 Acquired infrared spectra

To assess the performance of MIRs-ML for malaria screening in areas with varying transmission levels, whether in high or low settings, 7,628 participants from the Kilombero Valley in south-eastern Tanzania were screened for malaria infections using RDTs and microscopy across 35 villages. From these, 4,905 participants were randomly selected, ensuring that each village was represented by at least two-thirds (approximately 65%) of the screened participants. These samples were then analysed using qPCR to detect and quantify malaria infections, and subsequently scanned using an MIR spectrometer. Thus, the obtained spectra where labelled either positive or negative based on the qPCR results. Significant peaks associated

with malaria infection were identified in the spectra of the scanned dried blood spots (Figure 5.2). These peaks corresponded to protein markers such as amide I, amide II, and amide A, as well as markers associated with hemozoin, lipids, and nucleic acids. These spectral features can be indicative of malaria parasites, either as by-products of their metabolic activity or as direct markers of their presence in human blood. Out of the 4,905 spectra acquired, 9 were excluded during pre-processing due to distortion from improper anvil placement on the diamond crystal. Additionally, 19 spectra were discarded due to low absorption intensity caused by high water content, atmospheric interference, and carbon dioxide absorption. Consequently, 4,877 spectra were retained for evaluating the performance of ML algorithms in malaria screening across villages with varying transmission.

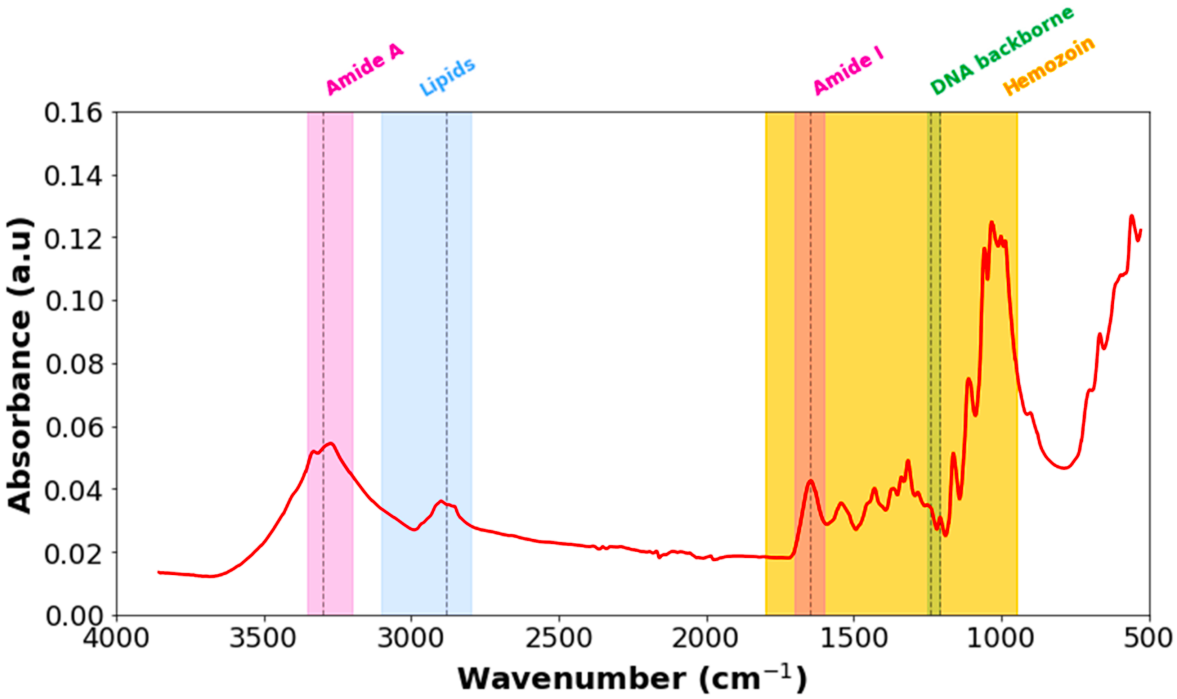

Figure 5.2: Mid-infrared spectra averaged over 4,877 dried blood spots (DBS) from samples collected across various villages with differing levels of malaria endemicity

5.4.2 Malaria strata for MIRs-ML analysis

As shown in Table 5.1, the categories were adapted from a previous study by Tanzania NMCPs [341]. In this study, to ensure enough negative and positive samples in each transmission category, we made slight adjustments. Consequently, we classified the 35 study villages into three main categories: low ($0 < Pf\text{PR} < 5\%$), moderate ($5\% \leq Pf\text{PR} < 30\%$), and high malaria transmission strata ($Pf\text{PR} \geq 30\%$) (see Table 5.2).

Table 5.2: New strata for training and validation of MIRs-ML, based on *P. falciparum* prevalence rate (*Pf*PR) estimate by qPCR, with ”Very Low” and ”Low” strata merged into a single “Low” stratum

Strata	Categories by prevalence	Total sample	Positive	Negative
Low transmission	$0 < Pf\text{PR} < 5\%$	769	19	750
Moderate	$5\% \leq Pf\text{PR} < 30\%$	1492	175	1317
High transmission	$Pf\text{PR} \geq 30\%$	2616	1514	1102

5.4.3 Selection, training and testing of machine learning algorithms

Of the six machine learning algorithms evaluated with data from all epidemiological strata, Random Forest (RF) outperformed the other evaluated classifiers, achieving an accuracy of 91.48% in classifying malaria infections in dried blood spots (Figure 5.3A), and was consequently selected for further training and fine-tuning to optimize its hyper parameters for generalizability and for avoiding overfitting. The optimized RF model achieved an accuracy of 90% when tested on 20% of the dataset from the same all epidemiological strata (Figure 5.3B). Additionally, this model attained an ROC-AUC score of 0.92 for malaria classification using the combined strata dataset (Figure 5.3C).

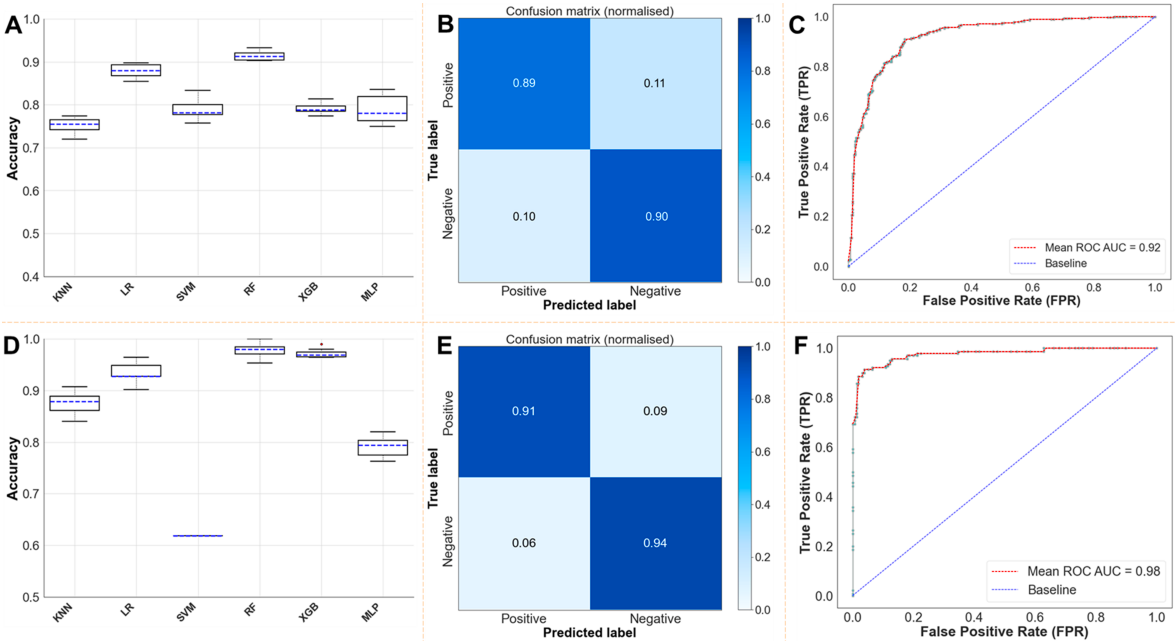

Figure 5.3: Performance of ML algorithms during cross-validation, training, and testing with an 80%-20% split. Panels A, B, and C show the performance metrics for models evaluated using datasets from all epidemiological strata (high, moderate, and low), while panels D, E, and F datasets derived from high transmission settings. A, D display cross-validation scores, B, E show performance on the test set from the same strata used for training, and C, F present the ROC-AUC scores.

5.4.4 Validation of models trained using combined data from across the full range of endemicities or data from high transmission settings on classifying malaria in low and high transmission settings.

The performance of two RF models was evaluated: one trained on data from all epidemiological strata (Model 1) and one trained exclusively with data from high transmission strata (Model 2). Both models were tested with completely unseen data from high and low malaria transmission settings. Model 1 (Trained on data from all epidemiological strata) achieved an accuracy of 93% (sensitivity: 93%) for classifying malaria-infected and uninfected samples in high transmission settings (274 positive and 274 negative samples) and 92.5% (Sensitivity: 92.5%) in low transmission settings (7 positive and 7 negative samples) (Figure 5.4). In contrast, Model 2 (trained on data from high transmission strata) showed 93.5% (sensitivity: 93.5%) accuracy when validated with high transmission data (274 positive and 274 negative samples) and 86.5% (Sensitivity: 86.5%) when tested with low transmission data (19 positive and 19 negative samples) (Figure 5.4). Table 5.3 summarizes the results of validating the two RF classifiers on classifying malaria infections from both high and low transmission settings.

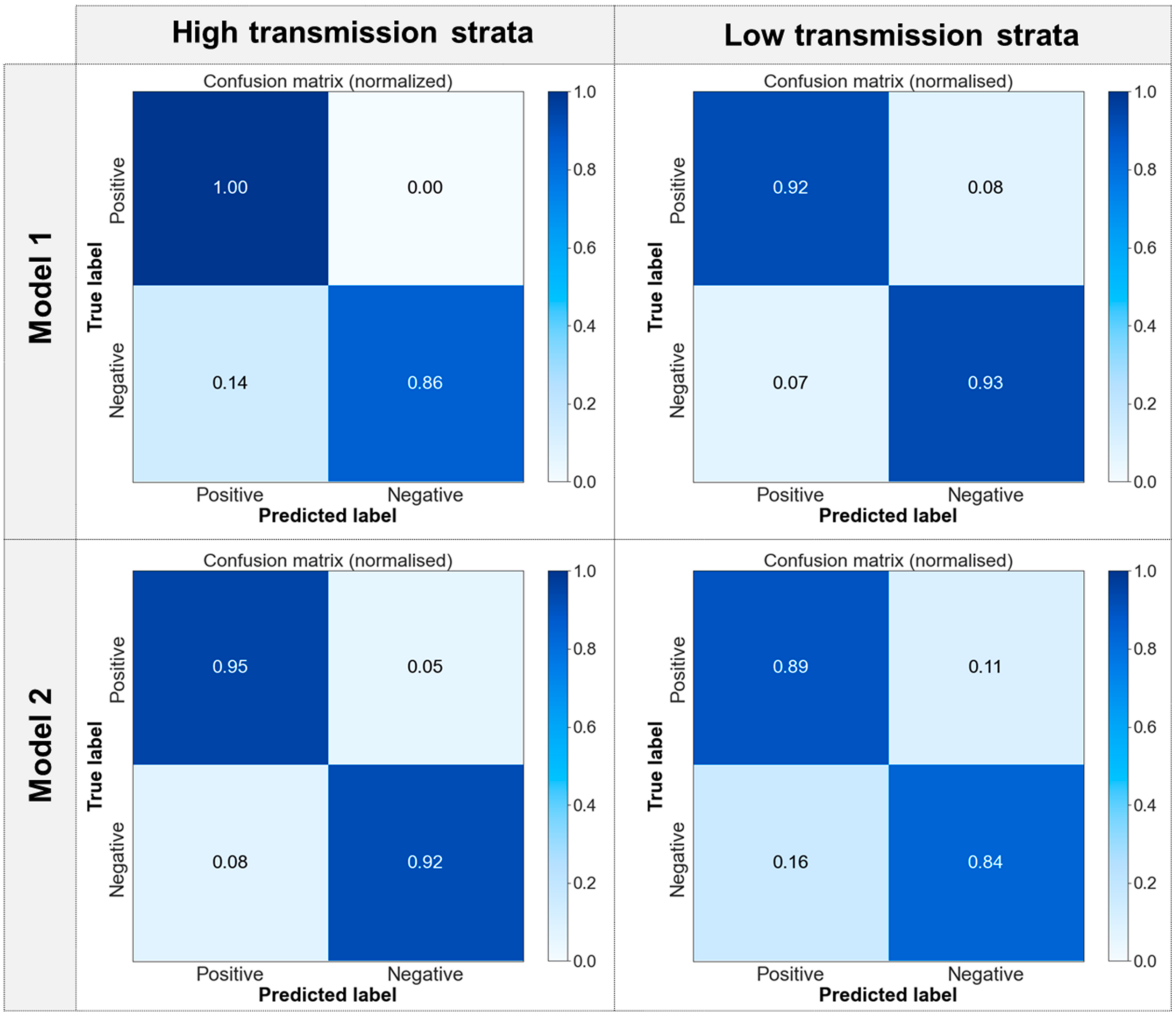

Figure 5.4: Performance of MIRs-ML models on unseen high and low transmission datasets. Model 1 was trained on data from all epidemiological strata, while Model 2 was trained on data from high transmission strata

Table 5.3: Summary of ML evaluation metrics (Recall, Precision, F1-score) and sample counts from high and low malaria transmission strata used for validation of classifiers trained on data from all epidemiological strata and from high transmission strata only.

Performance in high prevalence villages (*Pf*PR ≥ 30%))									
Model 1: Trained on data from all epidemiological strata					Model 2: Trained on data from high transmission strata				
Class	Precision	Recall	F1-score	Validation Sample size	Class	Precision	Recall	F1-score	Validation Sample size
Positive	0.88	1.00	0.93	274	Positive	0.92	0.95	0.93	186
Negative	1.00	0.86	0.92	274	Negative	0.94	0.92	0.93	186
Performance in low transmission villages (*Pf*PR < 5%))									
Model 1: Trained on data from all epidemiological strata					Model 2: Trained on data from high transmission strata				
Class	Precision	Recall	F1-score	Validation Sample size	Class	Precision	Recall	F1-score	Validation Sample size
Positive	0.92	0.92	0.93	7	Positive	0.85	0.89	0.87	19
Negative	0.93	0.93	0.92	7	Negative	0.89	0.84	0.86	19

5.4.5 Evaluating the influence of parasite densities on the performance of MIRs-ML models for malaria screening.

The distribution of parasite densities, estimated by qPCR, was analysed across 35 surveyed villages, revealing the highest densities in high transmission areas (Figure 5.5). We selected only the top 25% of samples with higher parasite densities from high transmission settings for MIRs-ML training. To ensure an adequate number of positive samples for validation—particularly given the limited number of positive samples (19) from low transmission settings—all samples from low transmission areas were kept separate for validation.

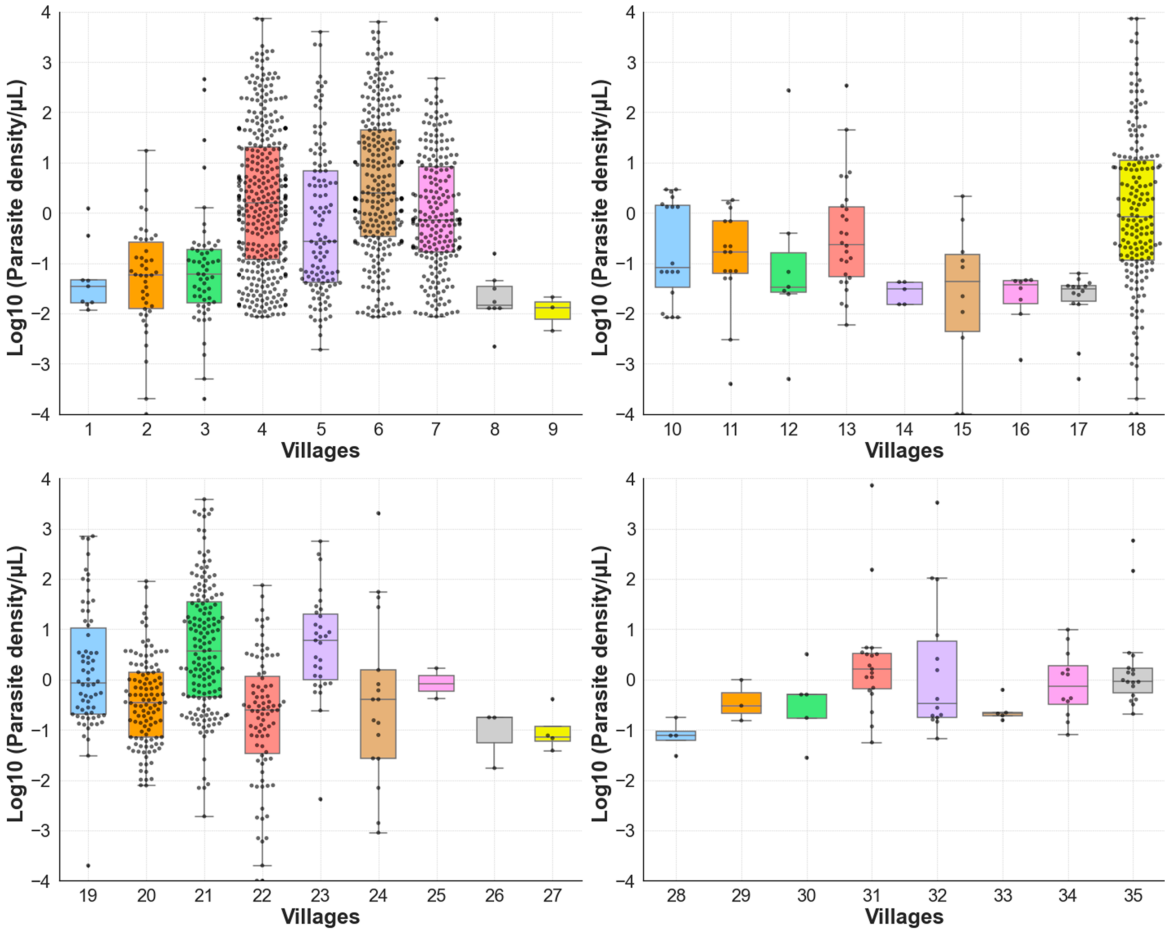

Figure 5.5: Distribution of parasite densities estimated by qPCR for positive samples across various surveyed villages. Negative samples are not depicted in this illustration.

Using stratified k-fold cross-validation, the Logistic Regression (LR) classifier outperformed other tested classifier, achieving an accuracy score of 96.54% (Figure 5.6A) for classifying malaria infections on data from individuals with the highest parasitaemia in high transmission strata against negative. Upon fine-tuning, the LR model achieved an accuracy of 96% in classifying malaria-positive and malaria-negative samples (Figure 5.6B) and an ROC-AUC score of 0.99 (Figure 5.6C).

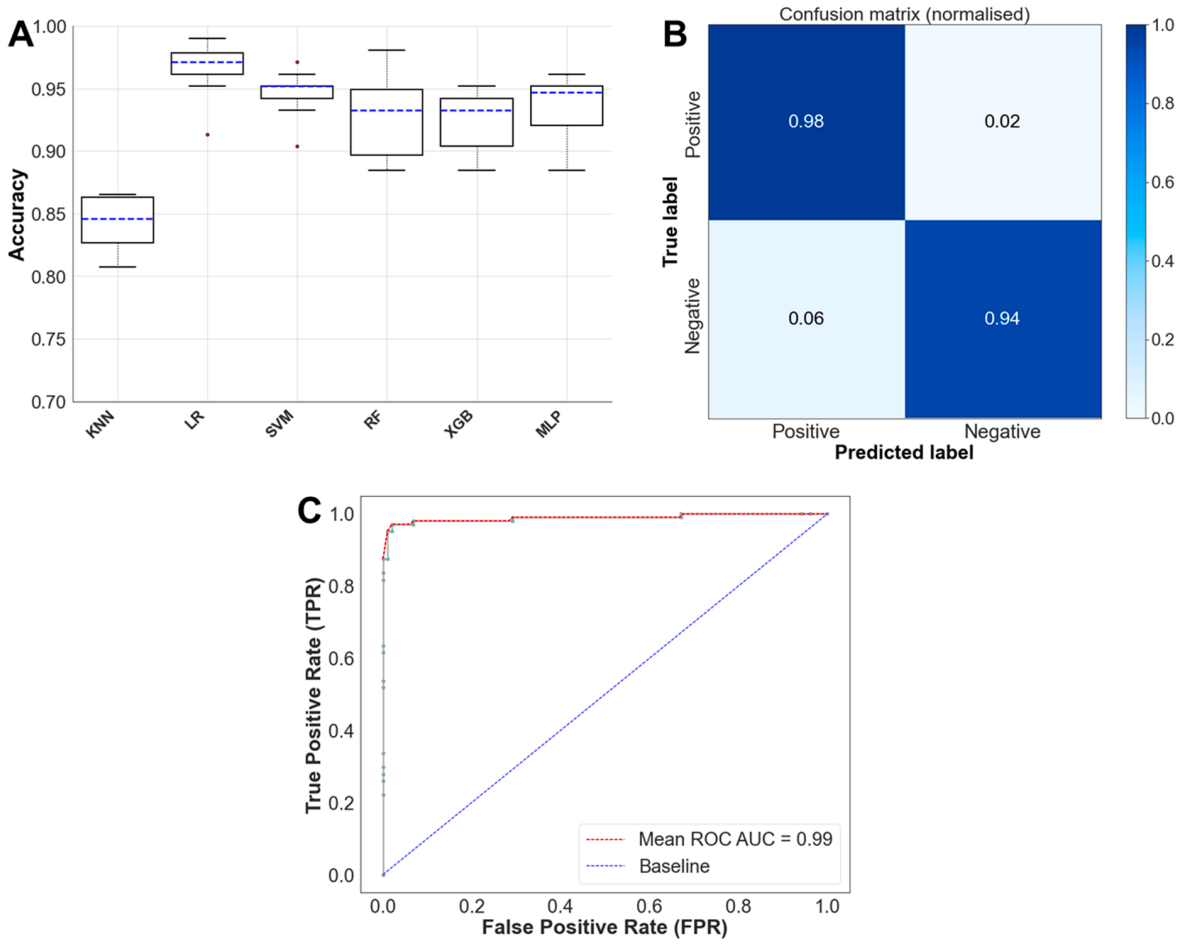

Figure 5.6: Performance of ML classifiers evaluated with the top 25% parasitaemia from high transmission settings across villages. Panel A shows k-fold cross-validation of ML classifiers, while Panels B and C display Logistic Regression (LR) performance on the 20% test set: Panel B shows the confusion matrix and Panel C shows the ROC-AUC curve

The LR model, trained on the highest parasitaemia from high transmission settings, achieved an accuracy of 97% for predicting malaria-positive samples and 96% for predicting malaria-negative samples when validated with unseen high transmission data (sensitivity: 96.5%) (Figure 5.7A). Conversely, when validated with unseen low transmission data, the model achieved 100% accuracy for predicting negative samples (19 samples) but 89% accuracy for predicting positive samples, (Sensitivity: 94.5; 19 samples) (Figure 5.7B). Table 5.4 summarizes other evaluation metrics for these classifiers in classifying malaria infections from both high and low transmission settings.

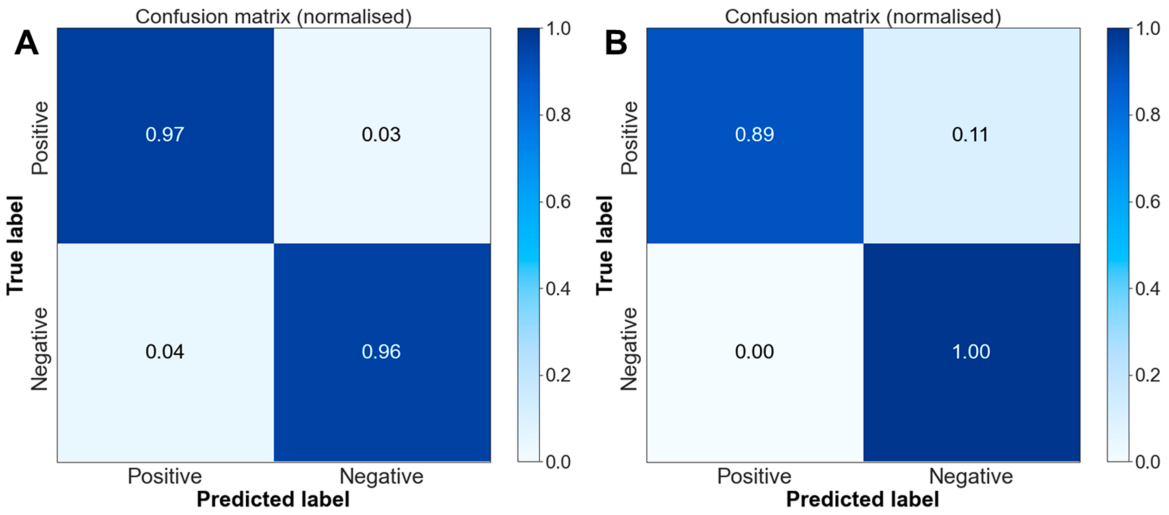

Figure 5.7: Validation of the Logistic Regression (LR) model trained using a dataset generated from the top 25% parasitaemia of high transmission strata. Panel A indicates performance in high transmission settings (159 positive and 159 negative samples), while Panel B shows performance in low transmission (19 positive and 19 negatives.)

5.4.6 Evaluating laboratory-developed algorithms for transition to field applications.

Previously, our MIRs-ML system, trained on samples produced in the laboratory, demonstrated over 80% accuracy in predicting unseen malaria infections in field datasets, with field results referenced against conventional PCR [411]. In this study, we evaluated the generalizability of these laboratory-trained algorithms using field samples analysed by qPCR – which is more sensitive than PCR - focusing on their performance in high and low transmission settings. The MIRs-ML system trained in the laboratory achieved accuracies of 68% and 64% for detecting malaria infections in high and low transmission field-collected datasets, respectively (Figure 5.8A).

Since the LR model, which performed best in the laboratory, does not support transfer or partial learning [213, 282], we retrained the MIRs-ML system by integrating both laboratory and field datasets, specifically from high transmission settings. We combined laboratory data (samples with 6% and 0% parasitaemia) with varying proportions of high transmission field data—10% from high transmission (262 samples), 20% (524 samples), and 30% (786 samples). The sample size used for training and testing these model when combining laboratory and field datasets are summarised in the supplementary Table S5.1. Additionally, we incorporated the top 100 highest parasitaemia samples from the field dataset. Here, LR achieved the highest stratified K-fold cross-validation accuracy in all scenarios, including when

combining laboratory data with 10%, 20%, and 30% of the high transmission dataset and when incorporating the top 100-parasitaemia samples from the field (Figure 5.8A-D).

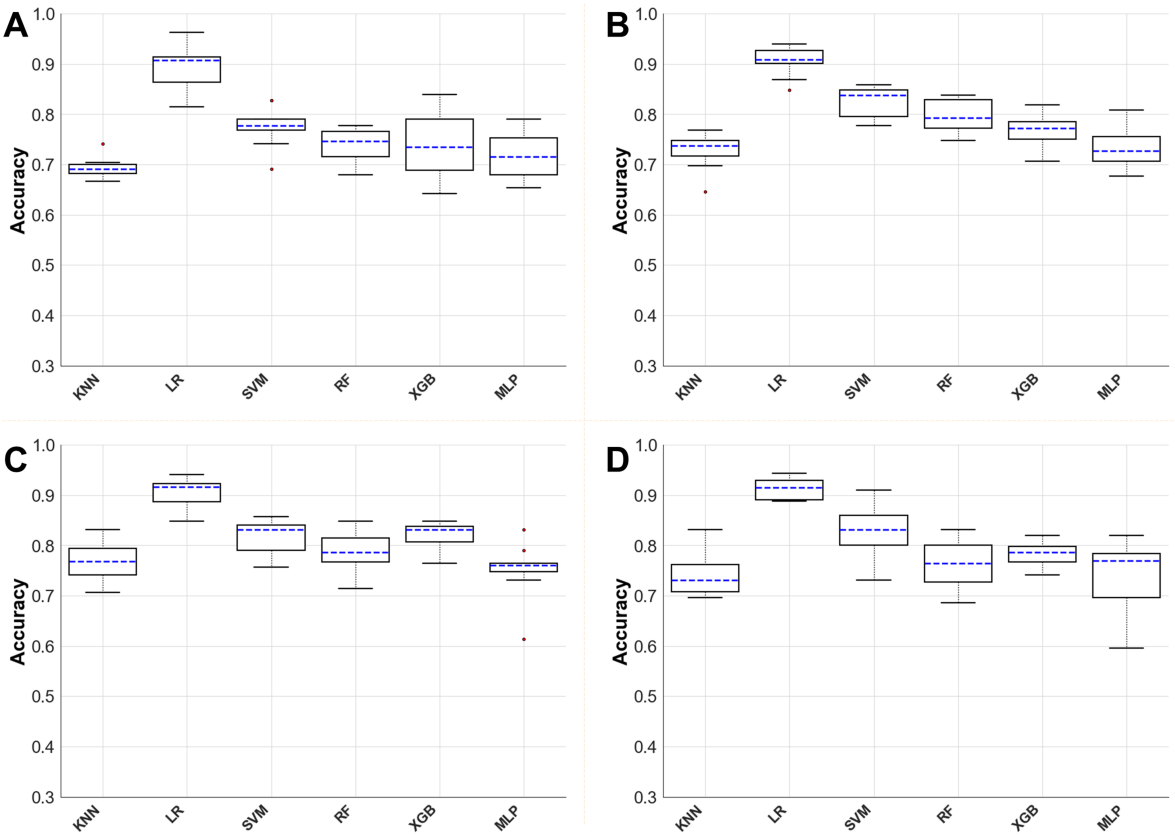

Figure 5.8: Algorithm performance evaluated with stratified K-fold cross-validation using lab combined with field datasets from high transmission settings: A) 10%; B) 20%; C) 30% of samples;, and D) the 100 highest parasitaemic field samples

The calibrated LR algorithms were then validated for their performance in detecting malaria infections using samples from both low and high transmission settings (Figure 5.9A). For instance, the LR model, calibrated with laboratory data (samples with 6% and 0% parasitaemia) combined with the top 100 highest parasitaemia samples from the field, achieved 100% accuracy for predicting malaria-positive samples (19 samples) and 89% accuracy for predicting malaria-negative samples in the low transmission strata (Sensitivity: 94.5%; 19 samples) (Figure 5.9B and Table 5.4).

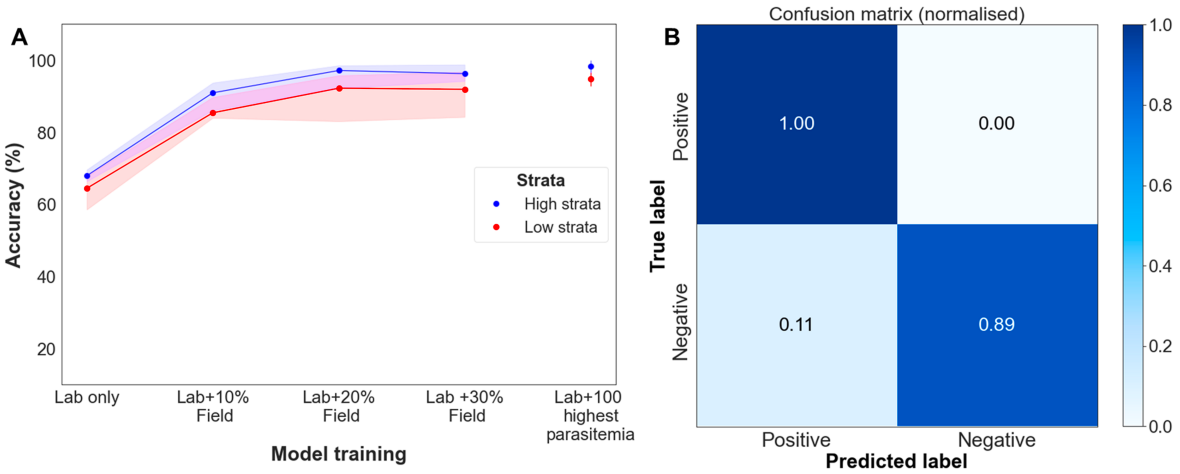

Figure 5.9: Validation of the laboratory-calibrated LR with unseen datasets: Panel A shows LR performance with lab data alone and when combined with 10%, 20%, 30%, and the top 100 parasitaemia field samples. Panel B presents the confusion matrix for LR re-trained with lab data and top 100 parasitaemia samples, validated on low transmission strata (38 samples).

Table 5.4: Summary of ML evaluation metrics (Recall, Precision, F1-score) and sample counts from high and low malaria transmission strata used for validation of models trained on to 25% of high parasitemia from high transmission strata and Lab combined with top 100 samples from the field.

Performance in high prevalence villages (*Pf*PR ≥ 30%)									
Trained on highest parasitaemia from high prevalence strata					Trained on lab (samples with 6% and 0% parasitaemia) combined with top 100 field samples with high parasitaemia				
Class	Precision	Recall	F1-score	Validation Sample size	Class	Precision	Recall	F1-score	Validation Sample size
Positive	0.96	0.97	0.96	159	Positive	0.95	1.00	0.97	274
Negative	0.97	0.96	0.96	159	Negative	1.00	0.95	0.97	274
Performance in low prevalence villages (*Pf*PR < 5%)									
Trained on highest parasitaemia from high prevalence strata					Trained on lab (samples with 6% and 0% parasitaemia) combined with top 100 field samples with high parasitaemia				
Class	Precision	Recall	F1-score	Validation Sample size	Class	Precision	Recall	F1-score	Validation Sample size
Positive	1.00	0.89	0.94	19	Positive	0.90	1.00	0.95	19
Negative	0.90	1.00	0.95	19	Negative	1.00	0.89	0.94	19

5.4.7 Major spectral features that influenced ML algorithms performance on classifying malaria positive and negative samples.

Based on the partitioning of the training datasets described above, we trained seven different models (either RF or LR algorithms) using various training datasets, ranging from field data alone to combinations of field and lab data. A key finding is that the wavenumber 1557 (cm^{-1}), which corresponds to NH bending in proteins (amide II band), significantly influenced the ability of classifiers to predict malaria infections across all seven models, regardless of whether LR or RF algorithms were used (Table 5.5). Additionally, the wavenumber 1565 (cm^{-1}), indicative of the amide I band due to C=O stretching in proteins, and the wavenumber 1081 (cm^{-1}), associated with C=O stretching in proteins, nucleic acids, or elevated carbohydrates, were present in at least five models. Wavenumbers 1230 (cm^{-1}), 1139 (cm^{-1}), and 1657 (cm^{-1}) were among the top informative features in at least three models each, representing nucleic acid proteins, lipids, and amide I bands, respectively. These findings underscore the consistent biochemical features captured across different models and provide insights into the molecular changes associated with malaria infection. The common wavenumbers and their band assignments are summarized in Table 5.5.

Table 5.5: The common MIRs wavenumbers that appear in various model-training approaches indicative of malaria parasite presence in human blood.

Wavenumber (cm^{-1})	ML model defined by datasets used for training	Typical Assignment	Possible explanation in-relation to malaria infections
1557 cm^{-1}	1,2,3,4,5,6,7	Amide II band (N-H bending in proteins)	Changes in protein content and structure, such as alterations in haemoglobin levels due to malaria infection.
1565 cm^{-1}	1, 4,5,6,7	Amide I band (C=O stretching in proteins)	Changes in protein secondary structures could be associated with changes in haemoglobin due to digestion by the parasite or other structural proteins.
1139 cm^{-1}	4,5,6	Phosphate stretching (nucleic acids), C-O stretching (carbohydrates)	Changes in nucleic acids (i.e parasite DNA) or glycoproteins.
1657 cm^{-1}	1,3,7	Amide I band (C=O stretching in proteins)	Related to protein secondary structures, particularly the presence of β-sheets in proteins. Changes can indicate alterations in protein structures, potentially including hemoglobin.
1723 cm^{-1}	3,5,6	Carbonyl stretching (lipids)	Reflects changes in lipid carbonyl groups. It can indicate alterations in lipid profiles or oxidative stress due to infection.
1081 cm^{-1}	3,4,5,6,7	C-O stretching (nucleic acids, carbohydrates)	Could be indicative of parasite's nucleic acids or host cell glycosylation.
1230 cm^{-1}	3,5,6,7	P-O stretching (nucleic acids)	Nucleic acid backbone structures. It can depict alterations or presence of DNA/RNA due to malaria parasite presence.

1. Trained on data from all epidemiological strata; 2. Data from high transmission strata; 3. Data from individuals with the highest parasitaemia in high transmission strata; 4. Lab +10% high strata; 5. Lab +20% high strata; 6. Lab +30% high strata; 7. Lab + top 100 highest parasitaemia from field.

5.5 Discussion

This study explored MIRs-ML techniques for malaria screening in different transmission settings. We analyzed mid-infrared spectra from dried blood spots collected in south-eastern Tanzania, where malaria prevalence ranges from <1% to over 50% [429]. Our MIR-ML system achieved over 92% accuracy in detecting malaria across both low and high transmission settings. Its performance depends on the training datasets: using samples from all epidemiological strata or high parasitaemia resulted in a robust system capable of accurate screening, even in low transmission settings where conventional tools might perform poorly.

In high transmission settings, all training methods achieved accuracy rates over 95%. This strong performance highlights the significant potential of these tools for malaria detection in areas with high endemicity. The high accuracy is likely due to the elevated parasite densities in these settings, which may improve the sensitivity and reliability of MIRs-ML systems. This is consistent with existing tools, such as RDTs and microscopy, which also perform better under high transmission [411, 426, 433]. Additionally, abundance of positive samples in these regions enabled robust training of the MIRs-ML systems.

The MIRs-ML system showed strong potential for detecting malaria in low transmission settings, an area where current diagnostic tools fall short [312, 420]. When trained on samples across all epidemiological strata, the system achieved over 90% sensitivity in detecting malaria in new samples. However, when trained solely on high transmission data, its sensitivity in low transmission settings dropped to 86% when compared to qPCR. This highlights the need to include low transmission samples during training. Such inclusion helps the system adapt to the specific malaria patterns of low transmission environments, improving its accuracy.

Performance variations of the MIRs-ML system can also be linked to parasitemia levels. High transmission areas have a range of parasitemia levels, which can affect system robustness. Conversely, low parasitemia in low transmission areas makes detection more challenging. Previous research has shown that training with high parasitemia samples is essential for developing a robust MIRs-ML system capable of detecting malaria effectively [411].

This study supports the finding that the MIRs-ML system, when trained on the highest parasitaemia from high transmission areas, showed improved performance in detecting malaria infections in low transmission settings, achieving an accuracy of over 90%. Specifically, the system detected positive cases with 89% accuracy and negative cases with 100% accuracy. Although the detection of positive cases was

slightly lower compared to models trained with combined datasets, these results suggest that the MIRs-ML system, when trained with high parasitaemia data from high transmission settings, can be effectively adapted for use in low transmission environments.

In addition to these findings, other studies have demonstrated the potentiality of similar approaches for malaria screening in field scenarios. For instance, Mwanga et al. developed a system that achieved over 90% accuracy in detecting malaria infections using field-collected samples, although their analysis did not account for varying endemicity levels [217]. Similarly, Heraud et al. validated approaches in high transmission settings, where MIRs-ML achieved a sensitivity of 92% and a specificity of 97% [218]. Building on these previous studies, this research provides the first evidence of the potential application of MIRs-ML in low transmission settings, highlighting its promise as a viable tool for malaria detection in such challenging environments.

In our previous study, ML models trained on laboratory datasets performed optimally when evaluated with field samples, as confirmed by nested PCR, achieving an accuracy of over 80% (with approximately 250 samples tested). However, when these models were tested on a new dataset referenced by qPCR in this study, which included around 4,877 spectra, the accuracy dropped to 66.17%. Several factors could explain this decline in performance and warrant further investigation. The discrepancy may be due to differences between the qPCR and nested PCR methods, which could result in variations in the reference standards used for positive and negative results, leading to differing outcomes [369].

To address these observations for the failure of laboratory data in predicting qPCR-referenced data, we incorporated field data into the training process to recalibrate the laboratory-trained models. This integration led to a notable improvement in the accuracy with qPCR-referenced samples. Our findings suggest that incorporating field data during training or applying transfer learning can significantly enhance the adaptability and performance of ML models across diverse transmission endemicities. The MIRs-ML approach has proven to be user-friendly, reagent-free, cost-effective, and fast in assessing various malaria indicators, including the presence of parasites in human blood [173, 434]. Additionally, we have previously demonstrated its ability to detect as few as one parasite/ul of blood of blood, a sensitivity not achieved by RDTs or microscopy. This study underscores its potential performance in low transmission settings, a significant advancement that had not been previously explored.

While the sensitivity of MIRs-ML tools is well-established, it's also crucial to consider the effort required for their development and optimization, including adaptation for national malaria control programs or creating country-specific algorithms. Our findings indicate that robust MIRs-ML systems can be developed in controlled laboratory settings and adapted for field use with minimal additional calibration. For instance, combining high parasitaemia samples from the lab with top parasitaemia samples from the field achieved performance levels similar to training with comprehensive field datasets. Therefore, considerations such as costs, time, and work force for dataset collection should be taken into account. Overall, once developed, MIRs-ML systems can balance high sensitivity with operational efficiency, requiring minimal training for end-users in basic computer skills, sample handling, and result interpretation.

Our analysis identified several key wavenumbers that appeared consistently across multiple models, reflecting common biochemical features associated with malaria infection. Notably, wavenumbers such as 1230 (cm^{-1}), which is indicative of nucleic acids; 1139 (cm^{-1}), associated with lipids; and 1657 (cm^{-1}), linked to the amide I band, were present in at least three of the models (defined based on training sets). These consistent features suggest their significant roles in the biochemical changes occurring during malaria infection. Further examination of model-specific wavenumbers revealed additional important signals. For proteins, several amide bands were prominent: 1557 (cm^{-1}), 1565 (cm^{-1}), 1455 (cm^{-1}), 1457 (cm^{-1}), and 1459 (cm^{-1}), along with C-H bending at 1417 (cm^{-1}), 1439 (cm^{-1}), and 1551 (cm^{-1}). These wavenumbers highlight changes in protein structure and composition that are characteristic of malaria infection and their ranges has been also reported with various study [217, 411, 427, 428, 434].

In the case of carbohydrates, significant C-O stretching bands were observed at 1033 (cm^{-1}), 1045 (cm^{-1}), 1049 (cm^{-1}), 1123 (cm^{-1}), and 1653 (cm^{-1}). For nucleic acids, phosphate stretching was evident at 1131 (cm^{-1}), 1133 (cm^{-1}), 1135 (cm^{-1}), 1137 (cm^{-1}), 1193 (cm^{-1}), and 1195 (cm^{-1}), while C-O stretching was seen at 1081 (cm^{-1}), 1230 (cm^{-1}), and 1241 (cm^{-1}). Lipid characteristics were identified by carbonyl stretching at 1723 (cm^{-1}), 1755 (cm^{-1}), and 1775 (cm^{-1}), and C-H bending at 1673 (cm^{-1}), 1675 (cm^{-1}), and 1679 (cm^{-1}). These findings underscore the complexity of biochemical changes associated with malaria infection, as reflected in the diverse wavenumber patterns captured by our models.

Despite the promising results demonstrating the applicability of MIRs-ML for malaria detection in both high and low transmission settings in this study, several critical limitations must be addressed. First, the influence of various biological factors—such as age, altitude, parasite densities, anaemia, and co-existing parasitic infections—on MIRs-ML performance needs further investigation. Understanding how these factors

influence malaria detection accuracy in realistic field conditions is essential and should be a focus of future research. Additionally, this study explored only *P. falciparum* infections; to enhance the robustness of MIRs-ML system, it is crucial to evaluate its effectiveness against other malaria species and in mixed infection conditions, which are prevalent in different regions. Furthermore, this research was conducted only in the Kilombero Valley of south-eastern Tanzania. For a more comprehensive assessment, it is necessary to validate MIRs-ML systems across a range of geographical areas. This broader validation will account for variations in geography, immunology, and genetic diversity, ensuring that the algorithms are both robust and adaptable to diverse epidemiological contexts.

5.6 Conclusion

This study demonstrates the high potential of MIRs-ML as a malaria screening tool, achieving >90% sensitivity in low transmission settings and >93% in high transmission areas. Its performance mainly depends on the selection of the training datasets, with a reduced sensitivity of 87% when trained exclusively on high transmission data and validated in low transmission settings. It is the first to show these capabilities across different transmission levels, addressing the limitations of conventional tools in low transmission regions. The study also underscores the feasibility of adapting laboratory-trained algorithms for field use, particularly by integrating both lab and field data during model training. Further validation across diverse settings is needed to ensure its broad effectiveness, positioning MIRs-ML as a valuable tool for improving malaria detection and control strategies.

Chapter 6: A Web-Based AI Platform for Real-Time Analysis of Infrared Spectral Data to Enhance Parasitological and Entomological Surveys of Malaria

6.1 Abstract

Mid-infrared spectroscopy combined with machine learning (MIRs-ML) shows promise for measuring key parasitological and entomological indicators of malaria. The approach is simple, reagent-free, robust, and fast, but its scalability is limited by the need for advanced AI programming expertise to interpret the data. To address this challenge, we introduce 'VectorPredictor,' the first web-based platform that provides access to pretrained ML models for instant interpretation of infrared data. The current Beta version of the platform is powered by models trained on over 5,000 human blood samples and 40,000 mosquitoes, with datasets continually expanding, from Tanzania, Burkina Faso, and the UK. This enables real-time malaria predictions, streamlining surveillance in low-resource settings. To demonstrate the functionality of the system, we show its perfomance in predicting malaria infections in field-collected human blood samples and identifying the species and age classes of field-collected mosquitoes. The platform is easy to use and potential to be a one-stop interface for assessing multiple malaria indicators by integrating additional predictive models.

6.2 Introduction

Effective monitoring of key parasitological and entomological indicators of malaria is crucial for tracking progress against the disease and evaluating the effectiveness of control measures [193]. Malaria control programs typically record mosquito-related indicators such as malaria vector species, their resistance status, and the entomological inoculation rate, which measures the number of infected mosquito bites a person might receive, on a daily, monthly, or annual basis [124, 174, 211]. Additionally, they measure parasitological indicators, which might include the

prevalence rate, which is the proportion of malaria-positive cases out of the total tested, and the annual parasite incidence (API), which represents the number of malaria-positive individuals per 1,000 tested populations [351, 353, 429].

Malaria prevalence and API are typically measured using rapid diagnostic tests (RDTs) or microscopy, though both methods show reduced sensitivity, especially in low-transmission settings [429]. Molecular assays like PCR offer greater sensitivity but are costly and less feasible in low-income regions for large scale surveys [174, 366]. Similarly, entomological techniques, including mosquito dissections and molecular methods, face limitations such as high operational costs and complexity, hindering their widespread application in malaria surveillance [174, 210, 268, 272, 274, 275].

Recent studies have highlighted the potential of infrared spectroscopy combined with machine learning (IR-ML) techniques for estimating key parasitological and entomological malaria indicators [173, 174]. This approach offers cost-effectiveness, speed, robustness and user-friendly making it highly promising for malaria surveillance and diagnosis. IR-ML techniques have demonstrated high accuracy, sensitivity, and specificity in predicting malaria infections in humans and mosquitoes, as well as in identifying mosquito species, age, blood meal histories, *Wolbachia* infections, and insecticide resistance [173, 212, 213, 216, 411, 435]. For instance, our models can detect malaria infections in human blood at densities as low as 1 parasite/µl with over 90% accuracy, even in cases of severe anaemia [411]. We have also developed models that can identify vertebrate blood-hosts for these mosquitoes, with accuracies above 90%, enabling rapid estimation of the degree of anthropophily in these vector species [216, 436].The approach readily extends to species identification, age-grading [212, 213, 437], and identification of endosymbionts like *Wolbachia* [173, 288, 290, 292, 435, 437] and protozoan pathogens including *Plasmodium falciparum* infections in mosquitoes.

Despite the significant potential that IR-ML have demonstrated for malaria surveillance, there is currently no readily accessible IR-ML platform available for researchers or National Malaria Control Programs (NMCPs) for predicting malaria indicators. The interpretation of infrared spectra and the training of ML algorithms can be quite complex, particularly for end-users. Consequently, there is a need for automated platforms to facilitate access to these technologies, enabling end-users to simply upload the obtained spectra and receive interpretable indicators of malaria transmission, such as infection status in humans and vectors, or the age and species of mosquitoes. These platforms could include trained ML algorithms deployed as applications for mobile devices, tablets, desktop software, and cloud-based online systems [174].

In response to these challenges, we introduce VectorPredictor, the first online platform that utilizes IR-ML approaches to simultaneously predict malaria infections in humans and identify the age and species of mosquitoes. The VectorPredictor web application is intended to be a public, open-source platform designed for scientists and NMCPs to leverage mid-infrared spectra for predicting malaria indicators. It is powered by two models: one trained on over 5,000 human samples from southeastern Tanzania for predicting malaria infections, and a deep convolutional neural network trained on over 40,000 mosquitoes from Tanzania, Burkina Faso, and the United Kingdom. To demonstrate the functionality of the system, we show its perfomance in predicting malaria infections in field-collected human blood samples and identifying the species and age classes of field-collected mosquitoes.

6.3 Implementation

6.3.1 Software architecture

The VectorPredictor platform has two main functionalities: 1) predicting malaria infections in humans and 2) predicting the age and species of mosquitoes. These are supported by four key components: a) User authentication: We use authentication functionalities from Django to ensure secure user registration, login, and session management. User roles and permissions can be used to restrict access to specific features based on user privilege; b) metadata input: we provide a user-friendly interface for users to input metadata associated with their spectra, such as collection site, sample storage conditions, collection date, and other relevant details; c) spectra uploading and filtering: the platform allows users to upload mid-infrared spectra data files, after which they can filter the data, such as by specifying a range of wavenumbers desired; and d) prediction outputs, the core functionality of the application, which used two pre-trained models: one for predicting malaria infections in human-derived samples and another for determining mosquito age groups and species.

When a user uploads a spectrum and initiates a prediction, the Django view sends the data to a RESTful API endpoint, receives the prediction results, and displays them within the application interface.

The web structure of the website is depicted in Figure 6.1, and source code accessible at: https://github.com/Issamshani17/VectorPredictor.

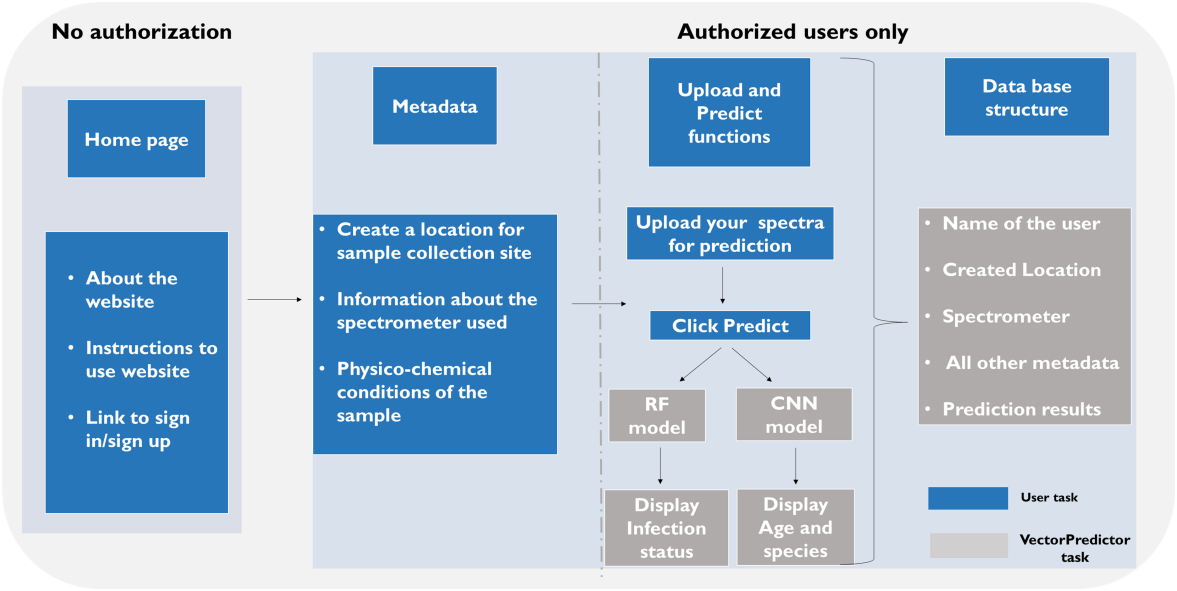

Figure 6.1: Schematic flow of the VectorPredictor built-in functionalities for predicting malaria infections in humans and determining the age and species of mosquitoes. Note: RF stands for Random Forest and CNN stands for Convolutional Neural Network.

6.3.2 Deployed machine learning algorithms

The platform is powered by two models: one trained on human samples and another on mosquito samples.

Random Forest Classifier : This classifier predicts malaria infections in blood samples by categorizing them as malaria-positive or malaria-negative. Trained on 4,905 dried blood spots from southeastern Tanzania and validated against qPCR results, the model was developed using samples from various transmission settings, with prevalence rates ranging from less than 1% to over 50% [429]. It achieved over 94% prediction accuracy for samples referenced by qPCR, across both low and high malaria transmission areas. This model is preliminary and will be updated with new samples and user feedback on the VectorPredictor platform.

Convolutional Neural Network (CNN): This deep learning model was trained on over 40,000 mosquitoes from Tanzania, Burkina Faso, and the Unitied Kingdom, UK to predict mosquito species and age groups [213]. The dataset incorporated laboratory, genetic, and environmental variability across three mosquito species: *An. gambiae*, *An. arabiensis*, and *An. coluzzii*. The CNN, which includes a 1-dimensional convolutional layer as the input (wavenumbers) and a dense layer with 500 features, predicts mosquito species and classifies them into three age groups: 1–4 days, 5–10 days, and 11–17 days. The model achieves >95% accuracy for age group predictions and >94% accuracy for species classification.

6.4 Key considerations for accurate predictions

6.4.1 Quality of the spectra

To ensure precise predictions of malaria infections in human blood samples or the age and species of mosquitoes, users must acquire mid-infrared spectra that align closely with the parameters used to train the models on the VectorPredictor platform.

For malaria infection predictions, spectra should be within the range of 4000-500 (cm^{-1}), scanned at a resolution of 2 (cm^{-1}) with 32 scans. For predicting mosquito age and species, spectra should also fall within the 4000-500 (cm^{-1}) range but scanned at a resolution of 1 (cm^{-1}) with 16 scans. Users can save their spectra in one of three formats, namely Opus, Mzz, or dpt. Adhering to these parameters significantly enhances the reliability of predictions made by VectorPredictor. Currently, high-quality spectra are those obtained from dried samples, such as dried blood spots or mosquitoes, to minimize water content (Figure 6.2A). For mosquito samples, this is achieved by storing them in silica gel-containing tubes, either individually or in pools. Mosquitoes should be stored and dried on silica gel for up to 10 days, although earlier-scanned mosquitoes are preferable (Figure 6.2A). For malaria predictions, the model was trained on spectra from dried blood spots. To prepare these, add approximately 50 µL of fingerprick or venous blood onto Whatman^{TM} protein saver cards, allow the sample to air-dry, then scan and use the obtained spectra for malaria predictions.

6.4.2 Sample storage and handling

Studies have shown that storage time does not affect MIRs-ML performance [295]. However, methods such as freezing and ethanol reduce MIRs-ML accuracy for predicting various entomological indicators [295]. It is recommended to carefully examine spectra peaks, as shown in Figure 6.2B-E, before uploading them to VectorPredictor.

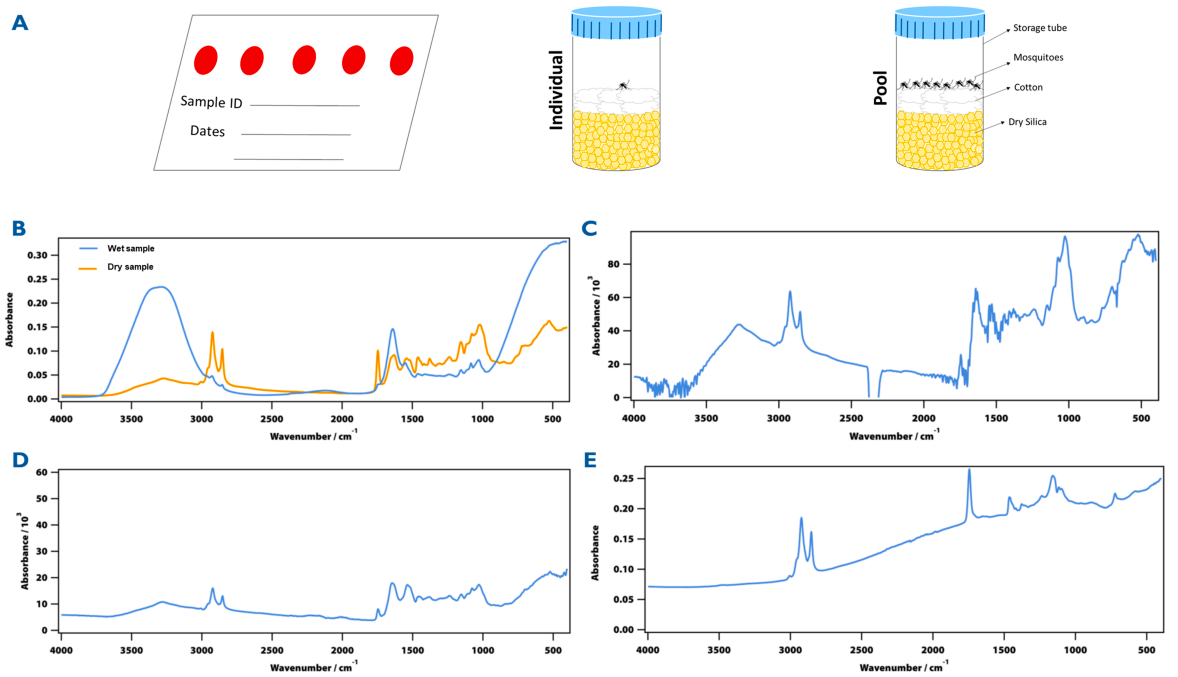

Figure 6.2: Illustrates the best specimen storage approaches and provides snapshots of quality spectra. **Panel A** shows the sample storage setup for drying purposes. **Panel B** depicts spectra from samples stored for 1-20 days, highlighting the importance of ensuring that spectra patterns closely resemble those of dry samples with clear peaks. **Panel C** presents an example of spectra affected by interference from atmospheric water and carbon dioxide. **Panel D** features spectra with low intensity, which may compromise prediction accuracy when using the VectorPredictor. Finally, **Panel E** displays spectra that are shifted due to poor sample positioning.

6.4.3 Considerations for scanning and labelling of spectra

For human-derived dried blood samples, standard Whatman papers are used to collect the dried blood spots. Here, it is crucial that the punched spot from the protein saver card is not less than 100mm cycle to fully cover the infrared crystal. Optimal spectra quality is achieved when the card is placed upside down, allowing the side where the blood was applied to directly contact the infrared crystal, and pressure is applied with the anvil to maximize light penetration [411]. For labeling, it is recommended to use a separator “-” between each block of information, such as in the format DD-UL-SN23-200324-230324. While the naming convention can be customized, maintaining the “-” separator is important so that the VectorPredictor can accurately extract the wavenumbers and absorption intensity of the respective spectra.

For mosquito samples, the scanning should be done on the approriate part of the mosquito body, relevant to the entomological indicators targeted for prediction. Previous studies have primarily demonstrated the efficacy of scanning three body

parts of mosquitoes using IR technologies. Mid-infrared is commonly employed on the head and thorax for predicting chronological age, species identity, and estimating resistance status [174, 212]; and also for detecting *plasmodium* infections since the infective stage of the parasite is usually lodged in the salivary glands in the head. The abdomen of mosquitoes has been shown to be useful for predicting blood meal histories [216]. On the other hand, near-infrared typically scans the head and thorax, with the light beam passing through a mosquito part via a probe [173].

To use the acquired spectra with VectorPredictor for predicting mosquito age and species, users should scan the head and thorax of the respective mosquitoes. They should begin by removing dried mosquitoes stored in silica gel tubes and placing them at room temperature for up to 10 minutes to allow evaporation of atmospheric water and gas interference. Subsequently, position the dried mosquitoes side by side on the ATR crystal, and apply pressure by squeezing an anvil to grind the head and thorax, optimizing light penetration depth. After each scanning batch, users must clean the ATR crystal with ethanol and tissue, allowing a few seconds for ethanol evaporation, and then use a dry tissue to absorb any remaining water and ethanol content before the next scans [212]. Considering the dataset used for the CNN deployed on this platform, users should ensure proper labeling and naming of the spectra, as outlined above, using the separator “-”. This practice ensures the CNN identifies similar spectra patterns in the intended mosquitoes for wavenumbers and absorption intensities, facilitating accurate predictions.

6.5 Results

6.5.1 Accessing the VectorPredictor homepage

Once users have acquired mid-infrared spectra of the intended samples, either dried blood spots (DBS) or mosquitoes, in Mzz, dpt, or Opus format, they should access the VectorPredictor platform at `https://vectorpredictor.com`and navigate to the homepage. We have purchased this domain, and its activation is currently in process. For thesis demonstrations, users should access the platform and refer to the instructions provided in the GitHub repository: `https://github.com/Issamshani17/VectorPredictor.`

The homepage provides an overview of the workflow, as shown in Figure 6.3. Initially, end-users must register for an account by clicking the ”Sign Up” button and providing required information, such as username, institution name, and email (see Figure 6.3C). Note that only registered users can access other sections of the

platform. Therefore, it is advisable for each project or group to create a single account for use by all team members. This account will be linked to the uploaded spectra and associated information. All samples collected within a single project and uploaded through this registered project account will share common information. Users can then follow simple on-screen instructions to navigate through the system (see Figure 6.3B). After logging in, users are directed to the welcome page, where they can choose to predict either mosquito age and species or malaria infections in human blood samples, as shown in Figure 6.4.

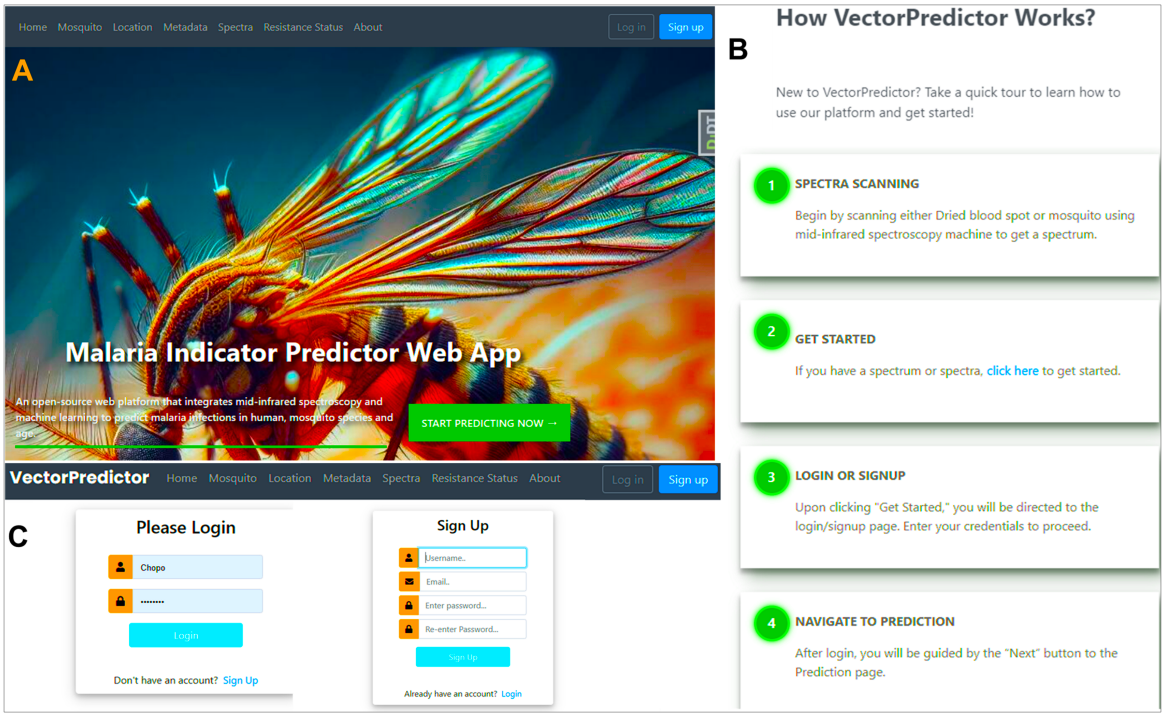

Figure 6.3: Screenshots of the homepage accessible to users: Panels A and B show general instructions, while Panel C displays the login and registration options for users to log in or create a new account.

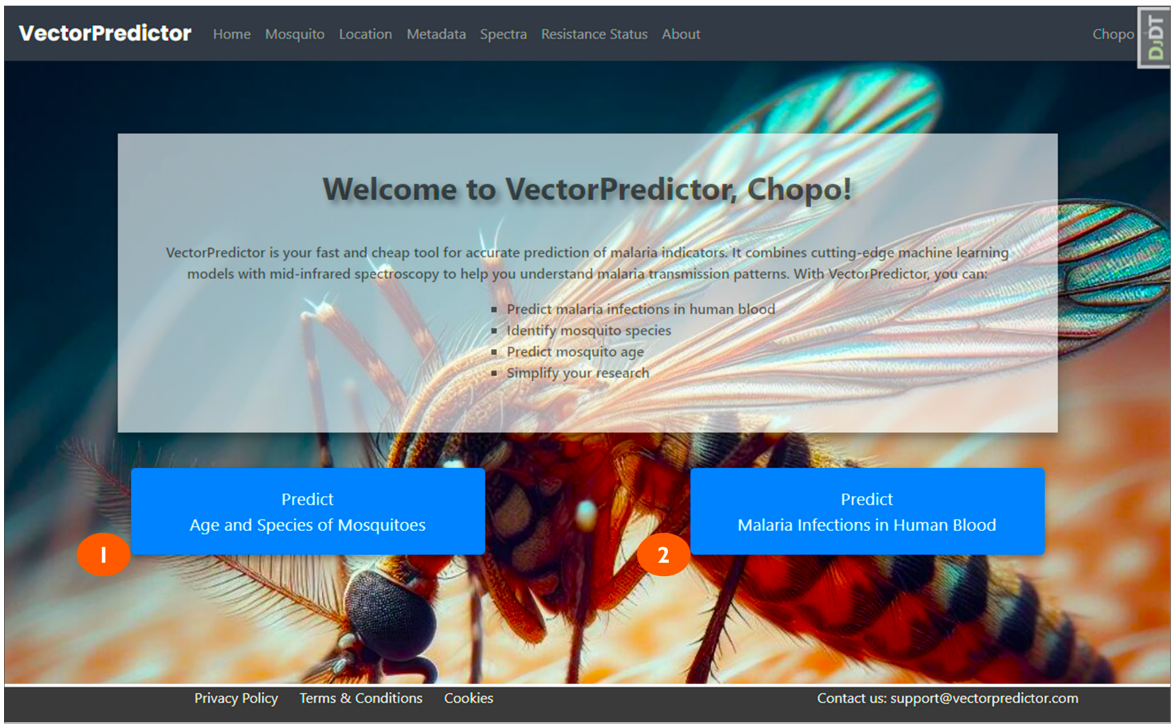

Figure 6.4: The web page screen where users can select either ”Predict Age and Species of Mosquitoes” or ”Predict Malaria Infections in Human Blood.

6.5.2 Section I: Predicting malaria infections in human

When the user presses the button to predict malaria infections, they will be directed to a page that provides instructions about the deployed model and offers options to predict malaria infections either from a single spectrum or from a batch of spectra. The key functionalities are illustrated in Table 6.1 and Figure 6.5:

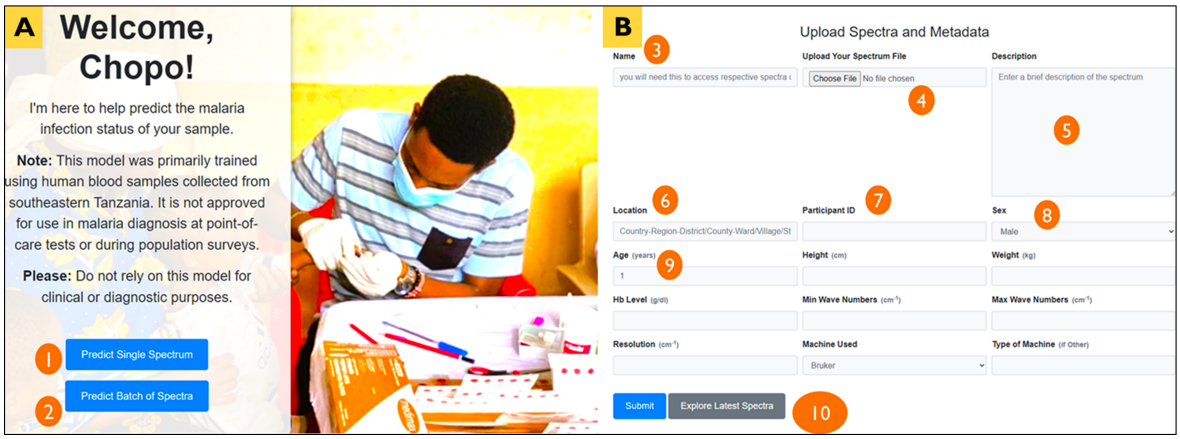

Figure 6.5: Screenshot of the malaria prediction page. Panel A shows the initial page where users click Button 1 to be directed to Panel B, which provides metadata entry functionalities. Numbered labels in Table 01 above.

Table 6.1: Overview of VectorPredictor functionalities when predicting malaria infections in human samples.

	Functionality	Details
1	Single spectrum predictions	Allows predictions from a single spectrum (Figure 5A/B).
2	Batch prediction	Supports single spectra predictions; batch predictions coming soon.
3	Metadata naming	Each spectrum requires a unique name for organization.
4	File upload requirements	Files must be in mzz, dpt, or opus format.
5	Description field	Optional description field to enhance data utility.
6	Sample collection location	Users must enter sample collection location.
7	Sample ID	Optional sample ID for tracking and model improvements.
8	Sex specification	Users select sex (male, female, other) for demographic data.
9	Age and other optional fields	Age required; height and weight fields appear for under 15 years; other fields optional.
10	Form submission and feedback	Users submit data, correct errors, and access prediction page; review spectra via 'View Spectra' page.

After submitting the metadata form and agreeing to the terms, including confirmation that the data were collected following the ethical guidelines of the respective country, users are automatically redirected to a page with various tools for interacting with the spectra. These functionalities allow users to view saved database details, download uploaded spectra, and predict malaria infections, as shown in Figure 6.6A. The page also displays the name of the spectrum in the prediction pipeline, such as 'Msogezi01' (Figure 6.6A). The functionalities of the Spectra interaction page are explained in Table 6.2 and figure Figure 6.6.

Table 6.2: Spectra interaction functionalities.

	Functionality	Details
1	Viewing spectrum metadata	Allows users to view metadata of the selected spectrum (Figure 6B).
2	Downloading spectra file	Users can download the spectrum file in its original format; restricted to logged-in users.
3	Spectra pre-processing and malaria prediction	Loads spectrum, cleans data, and predicts malaria status (positive/negative).
4	Returning to new spectrum entry	Users can navigate back to the spectrum entry page (Figure 6B).
5	Browsing other spectra	Enables users to browse and view other spectra entries (Figure 6C).

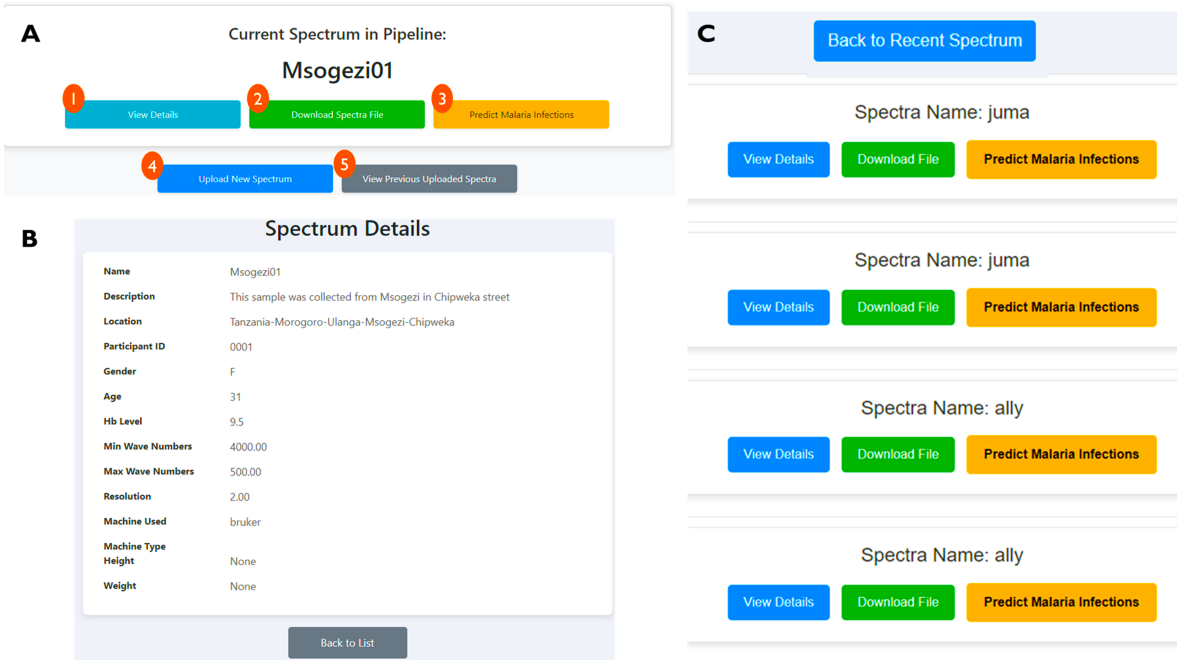

Figure 6.6: This figure illustrates the VectorPredictor pages and their functionalities for malaria infection prediction. Panel A shows options for downloading spectra files and making predictions, Panel B displays the metadata table with details stored for a specific spectrum, and Panel C demonstrates tools for inspecting, downloading, and predicting for multiple spectra simultaneously.

After the user clicks the ”Predict Malaria Infections” button, they will be directed to a results page displaying malaria prediction results based on the uploaded spectrum. This section provides various interactive features, as outlined in Table 6.3 and Figure 6.7:

Table 6.3: Functionalities for predicting malaria infections by VectorPredictor

	Functionality	**Details**
1	Spectrum name display	Allows users to track specific spectral information and link it with the corresponding results.
2	Predict malaria infections	Malaria status, either positive or negative, will be displayed here, reflecting the output from the machine learning model.
3	Line plot visualization	Line plot of extracted wavenumbers relative to their absorption intensity from the uploaded spectrum.
4	Download line plot	Allows the download of the line plot (wavenumber vs. intensity) as a PNG file.
5	Download dataset	Allows download of the dataset of the respective spectrum as a CSV file.
6	Data visualization	Display data in two columns, showing the wavenumbers and their corresponding intensity as shown in Figure 7B.
7	Download results	Allows download of the results in PDF format, as displayed in Figure 7C.

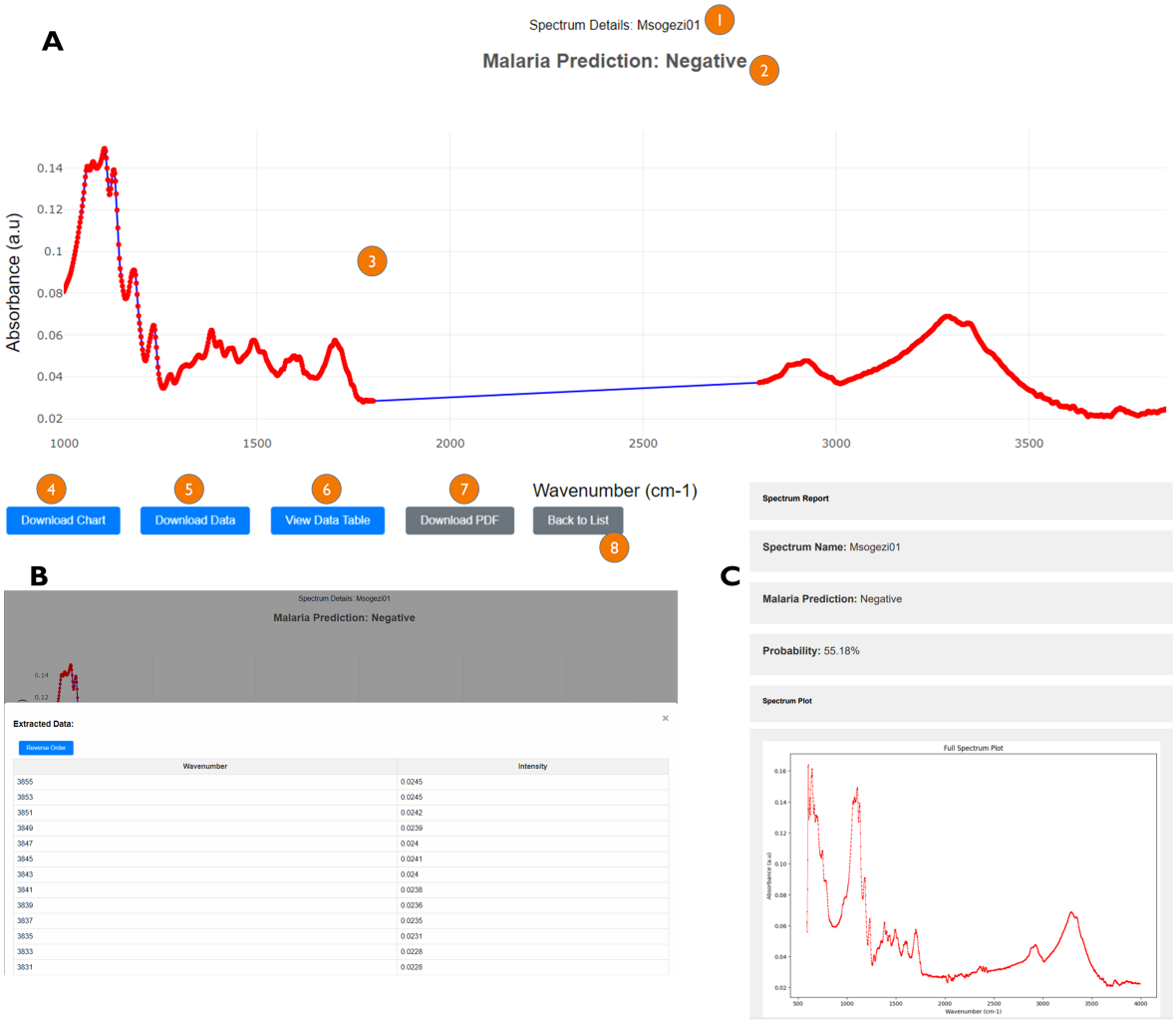

Figure 6.7: Screenshot of the malaria infection prediction results page. Panel A shows the general page with the results, plot, and various interactive functionalities. Panel B displays the extracted data, with wavenumbers and intensities for detailed examination. Panel C shows the PDF version of the results that users can download, including the spectrum name, malaria prediction results with probabilities, and the line plot for wavenumber vs. intensity.

6.5.3 Section II: Predicting mosquitoes age and species

In addition to predicting malaria infections in human samples, users can also predict the age and species of mosquitoes. From the homepage (Figure 6.5), clicking button 1 directs users to the species and age prediction functionalities. Upon accessing this section, users will follow the outlined steps: **Creating locations for mosquito collection:** In this step, users are required to create and save the collection site for mosquito samples (Table 6.4 and Figure 6.8). This information is essential for linking all uploaded mosquito spectra from the same location, which can improve the accuracy of the deployed machine learning model. Additionally, in the future, data such as temperature, humidity, malaria burden, and mosquito vectors could be

extracted from these locations for further analysis such as geospatial modeling. Below is a step-by-step guide to the location functionalitiesas dipected by Table 6.4 and Figure 6.8.

Table 6.4: Functionalities for creating locations where mosquito samples were collected.

	Functionality	Details
1	Location page	Access the location page at any time while navigating through the system or by clicking on 'Predict mosquito age and species' in Figure 4.
2	Create a new location	A search box will appear after clicking this button, allowing the entry of a new location name.
3	Enter the location name	Type the location name in the search box, and auto-suggestions will appear. The map will automatically update to show this location.
4	Map display	The intended location should match the one shown on the map to ensure accuracy.
5	Given name for the location	Confirmation that the created location is linked to the correct name provided.
6	Any other description	Allows input of any descriptions to enhance future utility of the data.
7	Coordinate display	The coordinates of the entered location are displayed here, providing additional confirmation.
8	Submit location	Allows the location to be saved in the database.

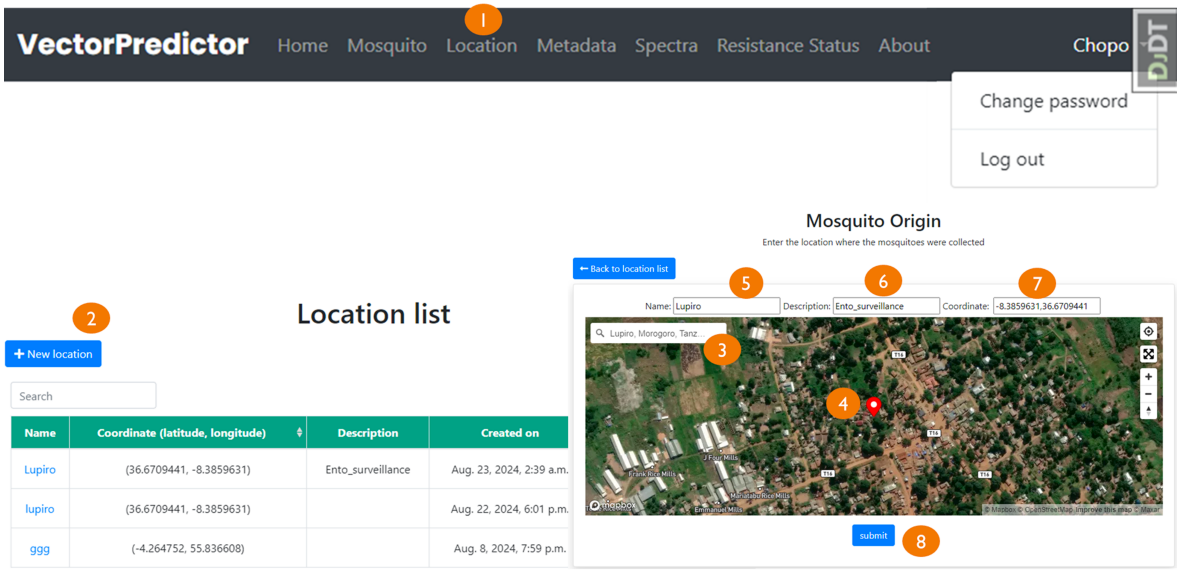

Figure 6.8: The pages depicts functionalities for entering mosquito samples collection site, as part of the metadata.

Key metadata entry: Once the user has created and submitted the mosquitoes' collection site, the system will navigate to the metadata form, requiring the user to fill the suggestion boxes with information such as the brand name of the spectrometer

used for scanning, the wavenumber range, the part of the mosquito's body scanned, morphological identification of the mosquitoes, and their resistance status (Figure 6.9). The user can access this metadata form at any time by clicking the location 'button 01', as shown in Figure 6.9. The primary purpose of this section is to link the uploaded spectra with this metadata, enabling incremental learning of the deployed algorithm in future.

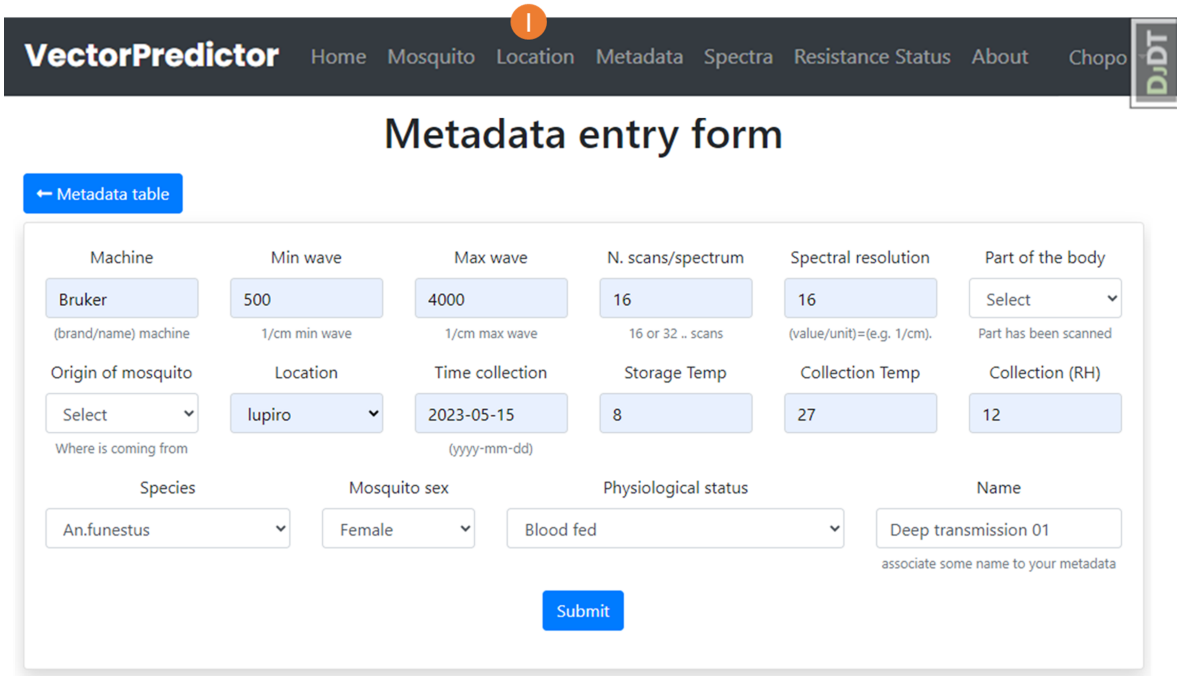

Figure 6.9: The metadata form entry for spectra used to predict the species and age of mosquitoes.

Spectra upload, quality check, and Age and Species Predictions: After completing the location and metadata forms, the VectorPredictor system navigates to the spectra upload page (Figure 6.10). Here, users can upload spectra either individually or in batches, and previously created metadata names will be available for selection. This section also provides quality-control measures for the uploaded spectra, assessing whether they meet criteria for intensity thresholds, background quality, and atmospheric interferences. The functionalities for spectra upload, filtering and predictions of mosquitoes age and species are depicted in Table 6.5 and figure Figure 6.10 below.

Table 6.5: Functionalities for Spectra upload, quality check, and Age and Species Predictions.

	Functionality	Details
1	Spectra upload	Allows access to the spectra upload page, as indicated in Figure 10A.
2	Choose File to upload	Files must be in MZZ, DPT, or OPUS format.
3	Select metadata name	Link each spectrum with its associated metadata name provided in the previous sections.
4	Upload button	Allows selected spectra to be saved in the database and display Figure 10C.
5	Load and view spectra	Pass the spectra through the filters and display the line plot with the filter results in Figure 10B.
6	Spectra filters	Indicates whether the spectra quality fails or passes; predictions will proceed regardless of the quality status (Figure 10B).
7	Line plot	Line plot of extracted wavenumbers relative to their absorption intensity for the uploaded spectrum.
8	Predict age and species of mosquitoes	Age class (either 1-4 days, 5-10 days, or 11-17 days) and species (either *An. gambiae*, *An. arabiensis*, or *An. coluzzii*) will be predicted.

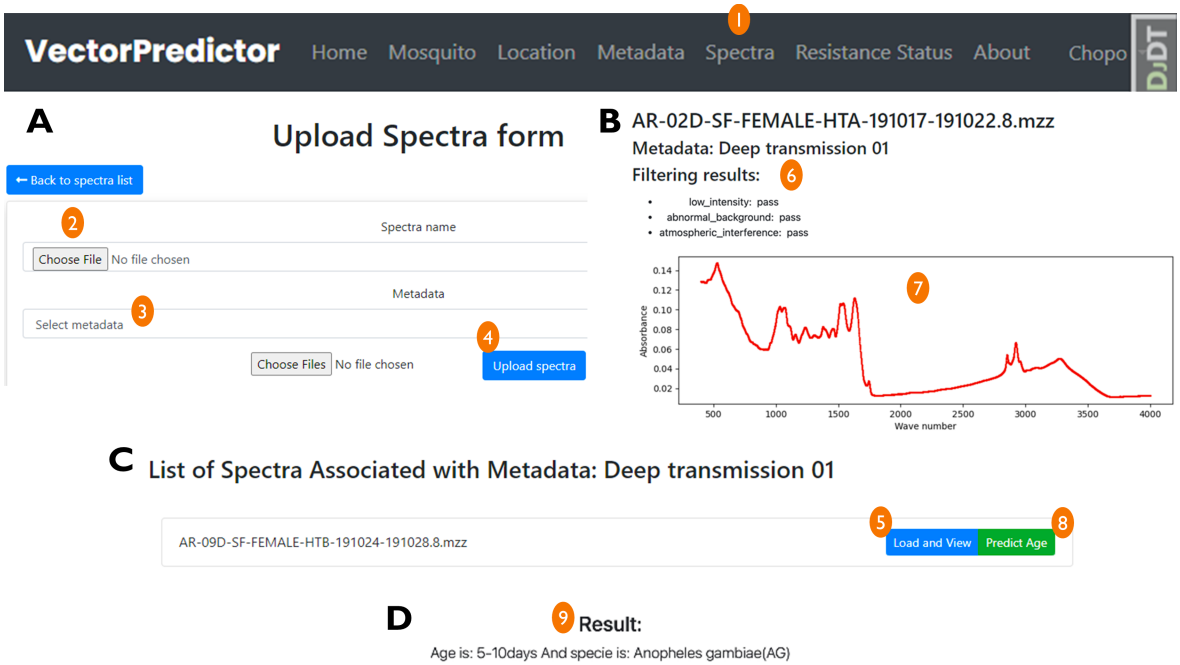

Figure 6.10: Panel A shows the spectra upload page. Panel B displays spectra details, including filtering results for atmospheric interference, abnormal backgrounds, and low intensity, along with line plots of wavenumbers versus absorption intensities. Panel C features functionalities for further spectrum investigation, including predictions for mosquito age and species. Panel D presents the prediction results.

6.6 Discussion

The development of the VectorPredictor, an AI-powered online platform for the simultaneous detection of malaria infections in human blood samples and mosquito vector profiling by age and species, represents a significant advancement in applying IR-ML based technologies to real-world scenarios and bringing them to end users. This platform could offer crucial support to malaria control programs and researchers, particularly for both parasitological and entomological malaria surveillance.

The platform simplifies the analysis of mid-infrared spectra and offers access to pre-trained machine learning algorithms, making them more accessible across various settings, including low-resource environments. Users benefit from an intuitive interface that enables simultaneous predictions of multiple malaria indicators. Traditionally, detecting malaria infections in humans required less sensitive tools such as RDTs and microscopy, or expensive methods such as PCR. Similarly, identifying mosquito species or classifying their age often required specialized expertise in morphological identification, PCR techniques, or microscopic dissections [174]. VectorPredictor consolidates all these tasks into a single, user-friendly platform.

The modular design of VectorPredictor is a significant advantage, allowing for the future integration of predictive models for additional indicators, thereby extending its utility beyond malaria surveillance. For instance, incorporating models to predict insecticide resistance, mosquito blood meal histories, sporozoites infection could evolve the platform into a comprehensive tool for disease surveillance [173, 174]. Furthermore, the ability to input metadata associated with spectra, such as collection site and sample conditions, facilitates more personalized and location-specific predictions, which could be essential for targeted intervention strategies in future.

Integrating such platform into malaria control programs holds great potential. By providing a standardized and automated method for monitoring malaria indicators, NMCPs could obtain more accurate and timely data, which is crucial for assessing the effectiveness of control measures and making informed decisions. Furthermore, adapting the platform for mobile and offline use would enhance its accessibility in remote areas with limited internet connectivity.

This platform should be regarded as an initial prototype with room for further development; therefore, its results should not be used for clinical purposes or decision-making at this stage. The machine learning models are still under refinement and have not been approved by any regulatory authorities. Several challenges must be addressed to ensure successful implementation and widespread adoption of the VectorPredictor. One critical challenge is the quality of the

mid-infrared spectra, which directly influences prediction accuracy. Adherence to recommended procedures for sample collection, storage, and scanning is essential. To this end, training and capacity-building efforts are necessary to ensure users understand the platform and the importance of following these standards. Another challenge is the ongoing need for model updates and validation. As new data becomes available and the platform is deployed across different geographic and epidemiological settings, retraining and validating the machine learning models will be crucial to maintain their accuracy and relevance. This will require continuous collaboration between researchers, public health officials, and users to integrate new data and insights into the system.

While the current focus of the VectorPredictor on malaria is appropriate given the global burden of the disease, expanding its capabilities to include other vector-borne diseases could significantly enhance its impact. For example, the ability to detect additional pathogens in mosquito vectors or assess the risk of emerging diseases in real time would make the platform an invaluable tool in global health surveillance.

6.7 Conclusion

The AI-powered online platform for malaria detection and mosquito vector profiling marks a significant advancement in the fight against malaria. By promising to offer a user-friendly, scalable, and cost-effective solution for monitoring key malaria indicators, it has the potential to enhance malaria surveillance, particularly in low-resource settings. Future developments should focus on expanding the capabilities of the platform, prioritizing user training, and ensuring the continuous update and validation of ML models to maintain high accuracy and reliability. If successfully integrated into existing malaria control programs, this platform could play a pivotal role in improving current malaria surveillance systems – including the estimation of key parasitological and entomological indicators- thereby accelerating progress toward malaria elimination in the future.

Chapter 7: General discussion

As malaria-endemic countries shift their focus toward elimination, the need for simplified, scalable, and cost-effective disease surveillance methods becomes increasingly urgent. These tools must possess sufficient sensitivity to detect malaria infections despite challenges such as low parasite densities or prevalence, and they must function reliably in environments with poor infrastructure or limited electricity access. Although several attempts have been made to develop such systems, including high-level advocacy by WHO for integrating surveillance as a core strategy, the challenges persist [194, 198].

7.1 Screening malaria infections using AI-Powered infrared spectroscopy

Research on new malaria screening tools has been ongoing for a while, aiming to simplify current approaches without limiting validity [312]. For example, there has been considerable interest in creating non-invasive techniques such as tests using saliva and urine [438, 439], and those that can overcome the growing issue of parasite mutations [243, 440], which render them undetectable by conventional malaria rapid diagnostic tests (mRDTs). These mutations pose a significant threat to ongoing malaria surveillance and control efforts [441–443]. These studies have achieved varied successes though so far, we have not found anything more scalable and more cost-effective than mRDTs and microscopy. Current tools also often fall short in sensitivity, particularly as the epidemiological profile approaches elimination [127, 406, 421]. While mRDTs and light microscopy are widely used and low-cost, their sensitivity significantly diminishes under conditions of low parasitemia, with predictive values dropping in regions where true positives are scarce compared to false positives [308, 444]. To be truly effective, new field-ready tools must operate under challenging conditions with unstable electricity availability and without requiring extensive technical training.

My PhD research therefore focused on improving malaria surveillance for evaluating a straightforward technique that utilizes mid-infrared spectroscopy, combined with machine learning algorithms (MIRs-ML), as a rapid, reagent-free method for detecting malaria infections in humans. This system was adapted from previous studies and developments in entomological studies, where similar technology has

been successfully employed to measure various parameters such as mosquito age, blood-feeding behavior (including whether mosquitoes feed on humans or other vertebrates), species identification, and detection of infective stages of malaria parasites [212, 213, 216, 217].

7.1.1 Establishing a target product profile for AI-Powered infrared spectroscopy as a tool for malaria screening

The ultimate goal of my research was to demonstrate that the same approach could be effectively used for rapidly screening malaria infections in human blood samples across varying parasite densities and in field settings with different levels of endemicity. We argued that this was essential to allow further development of the technology for real-life application in large-scale field surveys in areas targeting control or elimination of malaria. To achieve this, I began by conducting an in-depth review of the current state of the technology, evaluating its advantages and disadvantages compared to other existing screening tools such as PCR, RDTs, and microscopy. I also highlighted key research gaps that must be addressed before this infrared-based technology can become practically useful in malaria-endemic settings in sub-Saharan Africa. My analysis extended to both entomological and parasitological contexts of malaria screening, exploring multiple use cases and varying degrees of feasibility. Further, in addition to providing a general overview of the technological landscape, I aimed to identify critical research gaps that need to be bridged to maximize the potential of AI-enhanced infrared spectroscopy.

Many of the identified gaps aligned with those previously recognized by other experts, such as the need to fully understand the biochemical signals associated with distinctive spectra and the importance of optimizing sample processing methods [173, 217, 295]. However, unique gaps remain, which required significant advancements in the field. A key area of focus was establishing thresholds for detection and exploring the potential influence of confounding factors, such as anaemia, which is commonly observed in individuals infected with malaria and other parasites.

Another critical lesson was that new tools will need to meet certain specific criteria set by experts and authorities to be effectively integrated into public health practices. For the integration of MIRs-ML technology into routine malaria surveillance, it was therefore important to establish a target product profile to ensure both effectiveness and practical utility of the products. As a minimum, my analysis indicated that MIRs-ML technology must demonstrate high sensitivity and specificity, with performance at similar to or better than existing methods such as ELISA, PCR, and

microscopy for entomological indicators, and RDTs and microscopy for parasitological indicators. The technology should be robust, requiring minimal maintenance, and capable of operating on solar-powered batteries due to frequent power supply issues in malaria-endemic regions. Additionally, it must efficiently process dried samples from both mosquitoes and humans and function effectively at temperatures up to 35 °C, a requirement in line with prevailing environmental conditions in malaria-endemic settings, while remaining user-friendly with minimal training requirements. Although not strictly necessary, there are additional desirable, features that could significantly enhance the utility of MIRs-ML technology, such as versatility in handling various sample types and effectiveness across different malaria transmission settings, particularly in low-transmission areas. Portable spectrometers would be especially valuable in remote locations with limited electricity, and alternative energy sources would be advantageous. Balancing sensitivity with practical operational requirements is crucial to ensure the technology performs well even under resource constraints.

This target product profile served as a foundational guideline, and the work described in my thesis was part of the iterative process necessary to refine it further – through additional development and validation to fully realize the potential of this technology.

7.1.2 Screening of malaria infections in the context of varying parasite densities and anaemic conditions

Next, I conducted what is likely the most extensive analysis of its kind, where we recruited 65 healthy adult volunteers from local tertiary colleges and invited them to donate blood – generating hundreds of samples over the test durations. This blood was then spiked with cultured malaria parasites to generate a range of infection levels across different parasite densities. By simulating malaria infections as low as 1 parasite/µL of blood and as high as 6% parasitemia, we covered a full spectrum of infection levels (ranging from 0.00003%, 0.002%, 0.1%, to 6%). To introduce additional complexity and to mirror the likely scenarios in field settings, we adjusted hematocrit levels to simulate various degrees of anaemia: mild anaemia (50% hematocrit), moderate anaemia (20% hematocrit), and severe anaemia (12.5% hematocrit).

The dried blood spots were analyzed using Attenuated Total Reflection-Fourier Transform Infrared (ATR-FTIR) spectroscopy to acquire mid-infrared spectra for subsequent machine learning analysis. I partitioned the dataset into training and validation subsets, ensuring that the algorithms were validated on data that they had not previously encountered. The primary objective was to establish a robust, AI-driven, reagent-free, and user-friendly method for detecting malaria infections,

leveraging the mid-infrared spectra from dried blood spots. This approach was evaluated across a range of parasite densities and anaemic conditions to ensure broad applicability. In addition to traditional diagnostic metrics like sensitivity, specificity, and positive predictive value, I also included overall accuracy as a key performance metric.

Overall accuracy was defined as the percentage of cases where our method correctly identified the qPCR result, whether positive or negative, since qPCR is currently the most sensitive and widely accepted benchmark for parasite detection. In addition to accuracy, we also measured various metrics such as recall (corresponding to sensitivity), F1-score, and precision. While high sensitivity and specificity typically lead to high accuracy, it is important to note that high accuracy can be misleading if sensitivity and specificity are imbalanced. We addressed this issue by analyzing accuracy distributions per class (positive or negative) through confusion matrices. Our results were promising, demonstrating that the AI-powered mid-infrared spectroscopy technique offers a simplified and cost-effective method for malaria screening. This technique maintained high accuracy and sensitivity, even under varying parasite densities and anaemic conditions. Most importantly, the findings indicate that this approach has significant potential for rapid, high-throughput screening, which could be crucial for large-scale malaria control and elimination programs.

In this research, MIRs-ML technology emerged with considerable promise in laboratory settings, detecting as few as 1–3 parasites/µL of blood with over 90% accuracy. Therefore, the sensitivity of MIRs-ML, comparable to qPCR, suggests it could be valuable for large-scale surveys where detecting low levels of infection is essential. For example, MIRs-ML could be integrated into malaria elimination programs or used to support large-scale treat and test approaches for malaria elimination [445]. Additionally, capability of MIRs-ML to detect very low parasitemia makes it useful for border areas and malaria elimination zones, where detecting imported cases and preventing parasite circulation is critical [446].

7.1.3 Demonstrating performance of AI-powered infrared spectroscopy for large-scale field surveys of malaria

Once the laboratory evaluation and optimization was completed in controlled laboratory settings, we sought to validate its utility in the field using both lab-trained and field-trained ML algorithms to interpret the infrared spectra collected from thousands of dried blood-spots. To achieve this, we conducted a large-scale, intensive population survey at the household level in rural southeastern Tanzania,

specifically in the expansive Kilombero Valley. Before the year 2000, the valley was classified as holoendemic, characterized by intense malaria transmission throughout the year [447, 448]. During the 1990s, studies reported up to 1,400 infectious bites per person annually [449]. By 2009, however, ongoing malaria control efforts, including extensive bed net distribution campaigns, had achieved a reduction in malaria burden by up to 18-fold [449]. Further advancements, such as enhanced diagnostic access, distribution of bed nets, and availability of antimalarial drugs, played a crucial role in this decline [450]. For instance, by 2015, the widespread implementation of Long-Lasting Insecticidal Nets (LLINs) led to a 60% reduction in malaria transmission and contributed to the local disappearance of the primary vector, *Anopheles gambiae sensu stricto* [450].

In the present day, malaria infections in the semi-urban areas of the valley have markedly decreased, with only one infected mosquito captured over 3572 trap-nights [370]. The overall prevalence of *P. falciparum* in the region stands at approximately 10%, with the southeastern parts still identified as high transmission zones [358, 359]. Malaria transmission occurs both indoors and outdoors, with school-age children and adults particularly exposed to outdoor transmission during early evening hours (6 PM to 10 PM) and early morning hours (5 AM to 7 AM). Children under school age are more vulnerable to early evening transmission, as they are generally protected by bed nets during the early morning hours [451].

Our study covered 35 villages and 93 sub-villages in kilombero and Ulanga districts, where we screened 7,628 individuals from diverse demographics, ranging in age from 5 to 60 years, across 3,018 households. We employed three diagnostic methods: microscopy, RDTs, and qPCR (performed on approximately 65% of the samples). Additionally, we scanned each individual's blood samples (mounted on filter papers as dried blood spots), generating thousands of spectral signatures from these communities.

These data served two critical purposes: first, to generate a fine-scale stratification map of the entire study area, categorizing villages into very low, low, moderate, or high parasite prevalence based on the diagnostic results from RDTs, microscopy, and qPCR. Traditionally, such stratification heavily depends on mRDTs to create data layers that guide the deployment of major malaria interventions. However, we hypothesized that given the varying performance, sensitivity, and specificity of different diagnostic methods, the resulting stratification might vary significantly depending on the diagnostic tool employed. We argued that while RDT-based stratification might suffice for large-scale decision-making—such as determining which districts should receive specific interventions or be considered for a malaria

elimination push—more localized, fine-scale decisions, such as those at the district level, might require more refined diagnostic tests with higher sensitivity to better delineate differences and prevent the misallocation of resources.

Our findings confirmed this hypothesis, revealing that in regions where malaria has been substantially reduced, and where RDTs and microscopy are more likely to miss infected individuals, fine-scale stratification maps are more accurate when generated using data from qPCR. The superior sensitivity of qPCR in detecting low-density infections allows for more precise identification of transmission hotspots, which is critical in settings approaching malaria elimination. However, we caution that the interpretation of stratification data is highly context-dependent and resource-sensitive. Therefore, while our findings do not advocate for an immediate, widespread shift to qPCR-based stratification, they strongly suggest that users of stratification data must be acutely aware of the diagnostic methods underlying the data. This understanding is essential because the choice of screening tool could lead to significant differences in how areas are classified and, consequently, how resources are allocated. Furthermore, this insight underscores the need for a context-specific approach when applying stratification data, particularly in areas where malaria transmission is low and traditional diagnostics may underperform.

The second use of the field data was aligned with our key objective: to validate the performance of the AI-driven mid-infrared spectroscopy approach for field surveys of malaria in areas varying transmission endemicity either low or high. To achieve this, we employed machine learning models that were trained using either the lab data, as previously described, or a portion of the field data. The field-trained models were further diversified by training them on data from high-prevalence areas, low transmission settings, across the full spectrum of epidemiological risk, and from highly parasitemic individuals. With these models, we evaluated the suitability of this approach for rapid screening of individual cases in the field, determining whether they were infected or not. We achieved tremendous success, with both laboratory-trained and field-trained models accurately identifying infected samples. The accuracy of these models ranged from 88% to over 95% in both low and high transmission settings. While this was not the first time that such models have been applied to test human blood samples—previous studies in Australia and Tanzania have shown that infrared spectroscopy can achieve over 90% accuracy in parasite detection from human blood samples [217, 218], our work was the first to directly demonstrate the utility of this approach for field surveys.

However, these previous studies did not stratify samples based on malaria transmission endemicity. The primary contribution of my PhD research was the demonstration of the effectiveness of MIRs-ML in classifying malaria infections from samples derived from both high and low transmission settings, using qPCR as the

reference standard. The MIRs-ML system performed well in low transmission settings, although its accuracy varied depending on the selection of the training datasets. Further improvements in accuracy could be achieved by increasing the size of the training datasets or by employing alternative statistical approaches, such as transfer learning techniques, as demonstrated by Mwanga et al. and Siria et al. [213, 282]. The next step is to deploy this approach to generate different epidemiological strata and demonstrate that it can indeed serve as a low-cost surveillance method. Secondly, while the successes observed so far may be sufficient for field-level screening surveys, the validity of the tests remain inadequate for diagnostic uses. We therefore propose further development to evaluate and potentially improve performance in clinical settings.

Overall, these studies have demonstrated the significant potential of the AI-powered infrared spectroscopy approach for large-scale malaria screening in both laboratory and field settings. The technique is straightforward, involving the scanning of dried blood spots with a desktop mid-infrared scanner and the subsequent analysis of the spectra using pre-trained AI classifiers. When interpreted together with studies on entomological indicators, it can be concluded that these attributes make it highly adaptable to field conditions, particularly in low-resource settings. In this study, the approach was successfully adapted for field use, effectively predicting natural malaria infections in blood samples from a population-level survey in Tanzania. With further field trials and validation, this technique could substantially enhance malaria surveillance and contribute to accelerating malaria elimination efforts. Additionally, as a complementary outcome of this research, we were able to generate a large dataset to compare different malaria diagnostic methods. Our findings indicate that when these tools are used for stratifying malaria risk, the resulting strata can differ, potentially leading to different policy decisions regarding malaria interventions.

7.1.4 Delivering AI-Powered mid-infrared spectroscopy to users via web-based platform

While the first part of this thesis demonstrated the potential of MIRs-ML technologies for malaria screening, a significant challenge emerged in translating these technologies into accessible, real-world applications for non-expert users. This includes removing the need for users to create their own algorithms and providing a standardized approach for the applicability of MIRs-ML in malaria surveillance. Addressing this challenge led my research beyond proof-of-concept studies to the development of a functional prototype platform, which we named ‘VectorPredictor’. This novel web-based tool integrates various MIRs-ML models into a user-friendly

interface, allowing users to upload their infrared spectra and quickly receive malaria infection predictions. Importantly, the system requires only basic computer skills, eliminating the need for specialized expertise or complex laboratory workflows.

Prior to this PhD research, we had been developing machine-learning algorithms for predicting entomological indicators such as mosquito age, species, blood meal source, infections, and resistance status [212, 213, 216, 217]. For the first time, we have successfully integrated these pre-trained algorithms for entomological surveillance with the malaria-screening model developed during this PhD. Two critical lessons emerged from this integration: Firstly, this platform could function as a one-stop shop, capable of predicting malaria infections in human samples while simultaneously determining mosquito age and species within the same system. Traditionally, these tasks required separate, labor-intensive, and costly methods, such as molecular, microscopic, and serological tests [174]. Integrating these capabilities into a single, reagent-free, and rapid interface highlights the transformative potential of MIRs-ML technologies for overall malaria surveillance. Secondly, the advantage of using a platform like VectorPredictor its ability to support continuous improvement of the underlying machine learning models through incremental and batch learning techniques [452]. More importantly, the platform could facilitate the development of a spatial network for forecasting potential infections based on prior predictions, especially in low-transmission areas. This would support targeted, localized incremental learning of the algorithms, enhancing their effectiveness in specific localities. This feature not only enhances the performance of the deployed ML algorithms but also allows for a quick response to public health threats, such as parasite mutations. In the future, such tools will enable the system to learn from new data in real-time, providing timely updates to the trained ML models and facilitating prompt responses to potential threats such as mutations.

Upon approval for using MIRs-ML systems for malaria screening, countries might adopt the development of context-based algorithms tailored to specific areas. Thus, a platform like VectorPredictor could facilitate the creation of these localized systems, adapting to varying transmission intensities and biological threats in different regions. This platform should be considered a preliminary prototype, with further refinements needed to maximize its applicability and successfully transition to real-life applications, pending the improvement of ML models and approval from respective authorities before its deployment.

7.2 Questions arising and future directions

Despite the valuable findings, lessons, and conclusions drawn from the previous chapters of this PhD, several critical concerns emerged that warrant further investigation. First, in the analysis of Chapter 3, where I generated various levels of malaria parasitemia in laboratory experiments (6%, 0.1%, 0.002%, and 0.00003%), the findings revealed that training models with the highest parasitemia (6%) against negative samples produced more robust results compared to using a combination of all parasitemia levels or only low parasitemia (0.00003%) against negative samples. This raises questions about the underlying mechanisms: Why does the highest parasitemia yield more robust models, particularly for malaria screening? Is it due to the parasitemia level affecting the induced signals of malaria parasites, or does mixing different parasitemia levels introduce noise, thereby reducing machine-learning performance during training? Interestingly, in field datasets, similar trends were observed; training with high parasitemia levels produced robust models and mixing samples regardless of parasitemia levels in field conditions also led to robust algorithms. We argue that, future studies should delve into the infrared-induced signals by malaria parasites and how parasite density might influence these signals. Understanding this will be crucial in developing training datasets that consistently generate robust algorithms.

Secondly, a unique aspect of this study was the validation of ML models trained with laboratory data against field-collected samples. When field samples were referenced by nested PCR, the algorithms-maintained accuracy, achieving over 80% accuracy in transitioning from laboratory to field datasets (~250 samples). However, when the same algorithms were validated with samples I collected, as indicated in Chapter 4 and referenced by qPCR (~4900 samples), the performance dropped to 60% accuracy. This discrepancy likely arises from the different reference methods (qPCR vs. nested PCR), highlighting the importance of the reference standard in training robust machine learning models. Building on the rich datasets generated, I plan to investigate training algorithms using references from RDTs, microscopy, qPCR, and nested qPCR to determine which method yields the most generalizable algorithms. This will be a key focus for future research.

Thirdly, Chapter 4 focused on generating fine-scale malaria burden maps for the Kilombero Valley, covering 93 sub-villages. The findings revealed significant heterogeneity in malaria prevalence between neighboring villages, with rates ranging from 0% to over 50%, despite their proximity within a 150 km radius and shared temporal and spatial characteristics. Future studies should explore the underlying causes of this heterogeneity. Moreover, comparisons of fine-scale malaria burden

maps generated using RDTs, microscopy, and qPCR showed that RDTs and microscopy often underestimated malaria burden, particularly by categorizing a village as low transmission when qPCR indicated it as moderate or high risk. As countries move towards malaria elimination, the need for accurate fine-scale mapping becomes increasingly urgent. One pressing research question is: How would public health decisions be impacted when relying on fine-scale mapping using commonly used tools like RDTs and microscopy? This question remains unanswered, and future research should focus on investigating how low-resource countries can generate accurate surveillance data for proper resource allocation, given the high costs and sensitivity requirements of approaches like qPCR.

Lastly, considering that this research primarily focused on malaria screening using field-generated samples, a critical question is where MIRs-ML approaches should be applied either as point-of-care tests or as field screening tools. I have demonstrated that MIRs-ML could accurately detect parasite concentrations as low as 1 parasite/µL of blood, suggesting that while this sensitivity might not be necessary for hospital case management, it could be highly beneficial for large-scale surveys. However, this hypothesis requires further validation backed by evidence, and future studies should be designed to evaluate the performance of MIRs-ML in clinical settings. Additionally, as countries increasingly advocate for fine-scale mapping of malaria risk and face challenges using RDTs, microscopy, and PCR for that purpose as demonstrated in chapter 4, a pertinent question arises: How well would MIRs-ML perform in generating precise fine-scale risk maps compared to conventional approaches? This PhD advocates for future research to focus on demonstrating the effectiveness of MIRs-ML in generating fine-scale malaria maps and comparing them with RDTs, microscopy, and PCR.

7.3 Key implications and recommendations

This PhD research has revealed critical findings with substantial implications for advancing IR-ML approaches as a promising tool in malaria surveillance and risk stratification by control programs. Here, I have highlighted the key messages, implications, and recommendations. These recommendations are not limited to IR-ML but can also be adapted to other novel tools for malaria parasite detection in human samples.

7.3.1 Developing a roadmap for integrating IR-ML into routine surveillance

This PhD research provides the first roadmap for integrating IR-ML into routine malaria surveillance. In collaboration with experts, I have outlined the essential and desirable characteristics of IR-ML tools, identified key considerations, and highlighted research gaps that need addressing to facilitate the widespread adoption of these techniques. The developed TPP and identified research questions will guide future research aim to build evidence for applicability of IR-ML for malaria surveillance in general. These TPPs also ensure that stakeholders are aware of the crucial aspects that need further exploration.

Although my research has answered some of the initial questions raised in Chapter 1, I propose several recommendations for researchers and malaria control programs. First, collaboration between the research community and malaria control programs is vital for developing a comprehensive TPP. This TPP should outline the essential features that IR-ML must achieve for successful integration into malaria surveillance, ensuring input from a broad team of experts, stakeholders, and end-users. While my work has initiated the development of this TPP, I am aware of ongoing efforts by other teams to expand on these findings. These teams are conducting stakeholder mapping to identify potential users of the tools once developed (*Urio et al., 2024 unpublished*). They are also exploring the availability of portable spectrometers, focusing on prototypes suitable for areas with limited electricity, and investigating non-invasive spectrometers for skin-based malaria screening. The TPP should serve as a general roadmap for any novel malaria diagnostic tool introduced into routine surveillance, not just IR-ML and might be country-specific. Secondly, capacity building is also crucial, IR-ML pioneers should collaborate closely with malaria control programs and researchers to ensure a thorough understanding of IR-ML systems and assess the infrastructure needs for successful implementation. This involves evaluating spectrometer availability, identifying priority indicators, and fostering collaborations to accelerate technology adoption.

7.3.2 Malaria Screening under varying parasite densities and anemic conditions

This research demonstrates that MIRs-ML can detect malaria at levels as low as 1 parasite/µL of blood, a sensitivity unattainable by RDTs and microscopy. Notably, its performance remained consistent across different degrees of anaemia, whether moderate or severe. The conclusions derived from my PhD have greater implications

for understanding the potential of IR-ML for malaria screening. The unique design of this study, which considered various confounding factors, confirmed that MIRs-ML is not impacted by such variables, making it a reliable tool for screening malaria infections across diverse populations and demographic groups. Beyond this, I am aware of available studies that also show IR-ML technologies could detect more than one disease at once, such as diabetes [453]. However, based on these important conclusions, we preliminarily recommend that malaria control programs consider adopting MIRs-ML for large-scale field screening due to its demonstrable high sensitivity. Caution is warranted in hospital settings, especially in endemic areas, to prevent overestimation of cases and potential mismanagement of fever.

7.3.3 Fine-Scale mapping of malaria burden

Our research highlights significant malaria heterogeneity when stratification is performed at a fine-scale level such as wards, villages, and sub-villages. RDTs and microscopy underestimated malaria burden at this scale, misclassified villages as very low or low risk, while qPCR indicated these same villages as moderate or high risk. This discrepancy is particularly evident in low-prevalence villages where RDTs and microscopy exhibit poor positive predictive value. These findings are timely, as there is a concerted push for shifting towards fine-scale mapping of malaria risks by NMCPs. Thus, the implications of my findings might alert the NMCPs to the limitations of the designs and choice of diagnostic tools when assessing malaria risk stratifications at fine-scale. National malaria control programs should carefully design stratification approaches and select diagnostic tools that balance sensitivity with considerations of operational feasibility. Understanding the limitations and strengths of the collected data is crucial for effective malaria risk mapping and resource allocation.

7.3.4 Performance of MIRs-ML for malaria Screening in villages with varying parasite prevalence

MIRs-ML technologies have proven effective in accurately predicting malaria infections in both high and low prevalence villages, as confirmed by qPCR. This research marks a significant advancement, as there were previously no demonstrations of MIRs-ML performance in areas with varying malaria endemicity. These findings complement the results of Chapter 3 by highlighting the potential of MIRs-ML for large-scale malaria screening. MIRs-ML has the potential of addressing the challenges of conventional tools by balancing cost and sensitivity, even in low

transmission settings. Key recommendations include conducting further validation of MIRs-ML across different levels of endemicity and geographical settings to ensure its reliability and effectiveness.

7.3.5 Selection of training datasets for developing machine learning algorithms

The choice of training datasets significantly affects the performance of machine learning algorithms. This PhD research highlights three key findings: i) Training algorithms with high-parasitemia samples results in more robust MIRs-ML systems. ii) Incorporating samples from diverse settings, such as both high and low transmission villages, produces MIRs-ML systems that are more generalizable across various levels of malaria endemicity, including low-prevalence areas. iii) Calibrating laboratory-generated models with field data can further enhance the robustness of MIRs-ML systems.

These findings emphasize the importance of carefully considering the efforts and resources required by malaria control programs and researchers when developing MIRs-ML systems. Key factors include the extent of data collection, the expertise involved, and potential future improvements to the algorithms. While we cannot definitively conclude the best approach to training these algorithms, we recommend using high-parasite datasets whenever possible. Previous study by Dar et al.; 2021, also supports similar conclusions [292]. However, generalizability remains a challenge. Advanced techniques, such as transfer learning, may address this issue. For algorithms to perform effectively in low-transmission settings, it is crucial that training datasets include representative samples from these contexts, enabling accurate identification of true positives.

7.4 Limitations of the Study

This PhD research has demonstrated the potential applications of MIRs-ML techniques for malaria screening. Beyond validating these techniques in various settings, I have also shown how MIRs-ML can be delivered to end-users through the development of a prototype web-based platform. While specific chapters of this research discuss the limitations in detail, here are some general limitations.

Laboratory-generated samples revealed that training algorithms with high parasitemia levels resulted in more robust models compared to those trained on combined parasitemia levels or low concentrations. The parasitemia dilutions conducted had factors of 60, resulting in classes of 6%, 0.1%, 0.002%, and 0.00003%. The clear distinctions between these parasitemia classes may have influenced the poor model performance when parasitemia classes were combined for analysis. Further research could investigate this by employing smaller dilution factors, such as 10, 1, or less, to explore this phenomenon further. It should be noted that, even in field conditions where such high parasitemia levels (6%) are rare or almost impossible, selecting the highest available parasitemia still yielded robust models. Therefore, while our findings are genuine, we urge for detailed investigations into this specific issue.

Another limitation relates to the experimental design, where blood from donors was collected using EDTA tubes. Although standardized by ensuring all samples utilized the same tubes, the chemical components could introduce noise in the infrared spectra. Research indicates that EDTA tubes result in higher water content compared to heparin, which is significant given that mid-infrared spectrometers are sensitive to water content [301]. Although we dried the blood samples on protein saver cards before scanning, potentially mitigating the impact of water, we argue that future studies should account for any noise introduced by chemical compounds, such as those in anticoagulants or parasite culture materials.

This research also provides evidence of how the choice of diagnostic tools can impact the precision and strength of fine-scale malaria risk stratifications. On the other hand, the findings show that novel tools like MIRs-ML perform well in low-prevalence villages where RDTs and microscopy underperformed compared to qPCR. However, our analysis for MIRs-ML was limited to a pool of villages in low transmission settings. Future research should aim to generate fine-scale maps using MIRs-ML across all villages and compare them with those obtained by RDTs, microscopy, and qPCR. Additionally, incorporating environmental, geographical, and socio-economic variables could provide more robust MIRs-ML systems that might complement the challenges of conventional tools observed in this research for fine-scale mapping. Furthermore, the quantification of the parasite by MIRs-ML was not fully addressed, primarily due to limitations in the data generated from the laboratory. However, in future studies using our field-generated samples from 4,905 individuals, it will be possible to analyze and assess the quantification capabilities of MIRs-ML for malaria parasites in human blood samples. One notable challenge in applying AI in healthcare is addressing ethical issues, particularly concerning participant and data protection, including accountability in case of errors. This study did not explore in detail how the use of MIRs-ML might be influenced by these ethical

considerations. Therefore, it is crucial to emphasize the need for dedicated research on ethics, participant protection, and data security for application of MIRs-ML for malaria screening.

7.5 Conclusion

This thesis demonstrated the significant potential of MIRs-ML for malaria screening, especially in low-resource settings, as it promising to become reagent-free, user-friendly, fast, and robust. The research outlined the characteristics required to support the integration of MIRs-ML into routine surveillance, established the lowest reliable malaria parasite concentrations detectable by MIRs-ML, and evaluated the limitations and strengths of RDTs and microscopy for malaria fine-scale mapping through extensive cross-sectional surveys in southeastern Tanzania. These surveys provided malaria risk profiles that were used to validate the performance of MIRs-ML across varying levels of malaria endemicity. The developed TPP served as a roadmap not only for MIRs-ML but also for other novel malaria screening tools aiming for integration into routine surveillance. MIRs-ML showed high sensitivity, the ability to detect lower parasite concentrations, and high specificity in both laboratory and field samples, making it promising for large-scale malaria population surveys. Additionally, the findings related to fine-scale mapping emphasized the importance of proper design and the choice of diagnostic tools that considers high sensitivity and operational feasibility. Further studies should explore how novel tools like MIRs-ML could help NMCPs overcome diagnostic challenges. Additionally, research should evaluate how to best adapt these techniques in the future, as further validations are necessary.

Appendix for Chapter 3

Table S3.1: A two-way matrix of dried blood spots (DBS) generated in laboratory and used to train, test and validate machine-learning classifiers

Hematocrit concentrations that mimic anemic condition					
Malaria parasitemia (%)		Normal (40-50%)	Moderate anemia (25%)	Severe anemia (12.5%)	**Total**
	6%	335	335	335	1005
	0.10%	335	335	335	1005
	0.00%	335	335	335	1005
	0.00%	335	335	335	1005
	0%	335	150	150	635
Total DBS		1675	1490	1490	**4655**

Table S3.2: A summary of total spectra discarded due to either excessive water content, atmospheric water vapor and carbon dioxide interferences or bad intensity

Hematocrit concentrations that mimic anemic condition					
Malaria parasitemia (%)		Normal (40-50%)	Moderate anemia (25%)	Severe anemia (12.5%)	**Total**
	6%	4	5	11	20
	0.10%	2	10	8	20
	0.00%	1	6	16	23
	0.00%	2	3	6	11
	0%	3	11	7	22
Total DBS		12	35	49	**96**

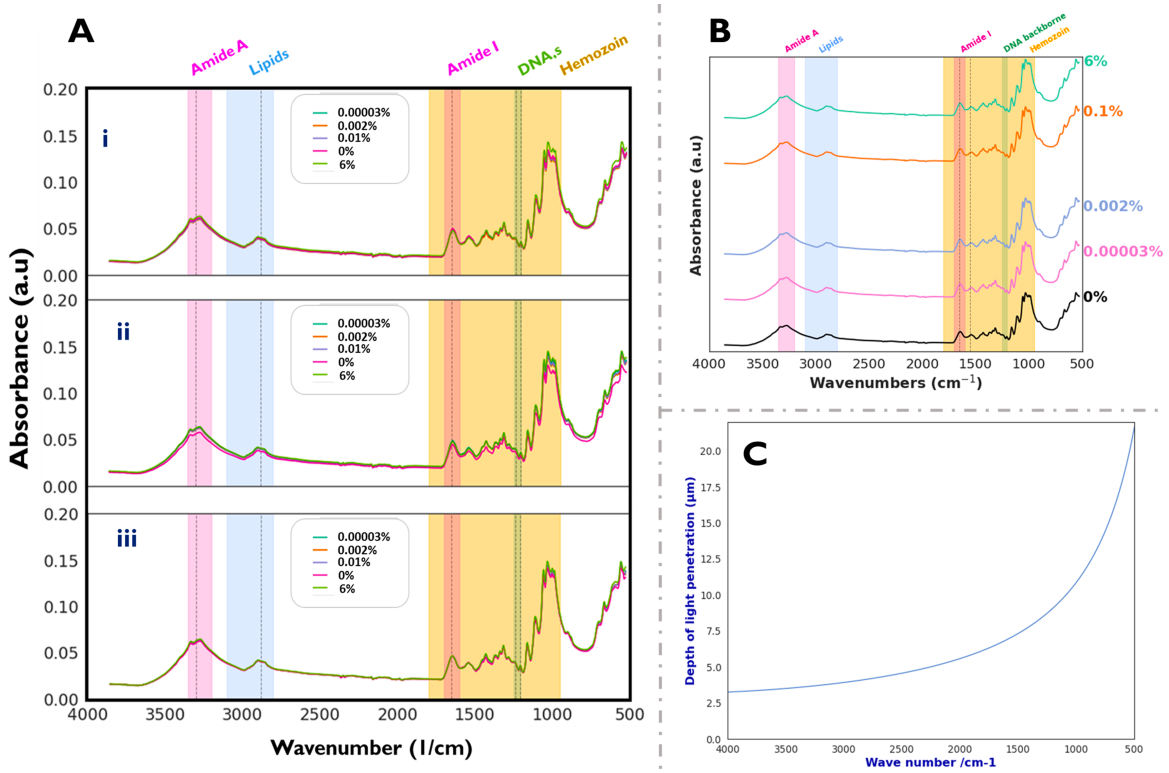

Figure S3.1: Average spectra of the generated anemic conditions, non-anemic (Ai), moderate (Aii), and severe anemia (Aiii) spectra. (B) Illustrates the magnified (Ai) for a better visualization of the average spectra of specific parasitemia in non-anemic samples. (C) Represent the estimated depth of light penetration to the DBS sample.

Figure S3.2: RDTs showing results when we tested the final dilutions sample as part of quality assurance processes

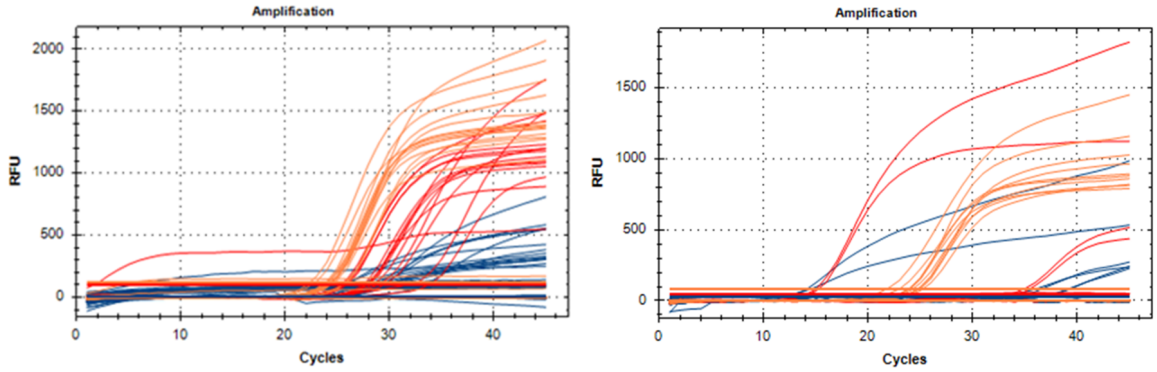

Figure S3.3: A representative PCR amplification cycles for the random samples generated in the laboratory as part of quality assurance processes

Appendix for Chapter 4

Table S4.1: Master Mix preparation

Component	Stock concentration	Final concentration	Reaction volume (µL)	Example for 100 reactions (µL)
Luna Universal Probe qPCR Master Mix	2x	1x	5	500
PlasQ Primer Mix	5x	1x	2	200
Molecular biology grade H_2O	-	-	1	100

Table S4.2: Preparation of 1 mL of 5x Oligo mix and their respective sequence

Oligo name	Species specificity	Target region	Oligo sequence	Oligo modification [5'-3']
***P. falciparum* (PlasQ assay)**				
Pspp18S F	*Plasmodium spp*	18S rDNA	GCT CTT TCT TGA TTT CTT GGA TG	-
Pspp18S R	*Plasmodium spp*	18S rDNA	AGC AGG TTA AGA TCT CG TTC G	-
Pspp18S probe	*Plasmodium spp*	18S rDNA	ATG GCC GTT TTT AGT TCG TG	Cy5-BHQ2
PfvarATS F	*P. falciparum*	varATS	CCC ATA CAC AAC CAA YTG GA	-
PfvarATS R	*P. falciparum*	varATS	TTC GCA CAT ATC TCT ATG TCT ATC T	-
PfvarATS probe	*P. falciparum*	varATS	TRT TCC ATA AAT GGT	FAM-NFQ/MGB
HsRNaseP F	*H. sapiens*	RnaseP gene	AGA TTT GGA CCT GCG AGC G	-
HsRNaseP R	*H. sapiens*	RnaseP gene	GAG CGG CTG TCT CCA CAA GT	-
HsRNaseP probe	*H. sapiens*	RnaseP gene	TTC TGA CCT GAA GGC TCT GCG CG	YakimaYellow-BHQ1

Table S4.3: Prevalence estimates for the 35 surveyed villages using three diagnostic methods.

					RDT		Microscopy		qPCR	
District	**Village Name**	**Latitude**	**Longitude**	**Survey Month**	No tested	Prevalence % [95% CI]	No tested	Prevalence % [95% CI]	No tested	Prevalence % [95% CI]
Kilombero	Ichonde	-7.88122	36.877098	July-2023	188	0.5 [0.1-2.9]	188	0.5 [0.1-2.9]	94	4.9 [2-11.3]
Kilombero	Ikwambi	-7.9859	36.819019	June-2023	143	25 [18.6-32.7]	143	9.6 [5.8-15.6]	92	45.2 [35.4-55.4]
Kilombero	Kapolo	-8.09353	36.7061085	August-2023	138	0.7 [0.1-3.9]	138	0 [0-2.7]	89	7.1 [3.4-14.4]
Kilombero	Kiyongwile	-8.1571	36.6891643	September-2023	212	0 [0-1.8]	212	0 [0-1.8]	106	0.9 [0.2-5.1]
Kilombero	Kikwawila	-8.08771	36.7395421	August-2023	146	0 [0-2.6]	146	0.8 [0.2-4]	92	4.7 [1.9-11.1]
Kilombero	Kisawasawa	-7.89719	36.8715262	June-2023	141	0 [0-2.7]	141	0 [0-2.7]	88	2.8 [0.9-8.7]
Kilombero	Lihami	-8.15684	36.6855141	September-2023	197	0 [0-1.9]	197	0 [0-1.9]	99	11.9 [6.9-19.7]
Kilombero	Lipangalala	-8.1508	36.6813302	September-2023	147	0 [0-2.5]	147	0 [0-2.5]	89	8.5 [4.3-16.1]
Kilombero	Lungongole	-8.04441	36.7584786	August-2023	180	7.2 [4.3-11.9]	180	3.9 [1.9-7.8]	90	10.5 [5.7-18.5]
Kilombero	Magengeni	36.68213	244.1016846	September-2023	183	0.6 [0.1-3.1]	183	2.7 [1.2-6.2]	183	5.6 [3.1-10]
Kilombero	Mang'ula	-7.8339	36.9022122	June-2023	270	0 [0-1.4]	270	2.6 [1.3-5.3]	135	5.3 [2.6-10.5]
Kilombero	Minarani	-8.12218	36.6835894	September-2023	139	0 [0-2.7]	139	0.7 [0.1-3.9]	92	2.2 [1-7.6]

(Continued)

District	Village Name	Latitude	Longitude	Survey Month	RDT		Microscopy		qPCR	
					No tested	Prevalence % [95% CI]	No tested	Prevalence % [95% CI]	No tested	Prevalence % [95% CI]
Kilombero	Mkamba	-7.68703	37.0102679	May-2023	147	1.4 [0.4-4.9]	147	2 [0.7-5.8]	147	5.6 [2.9-10.6]
Kilombero	Mkochi	-8.05123	36.7780487	August-2023	136	28.6 [21.7-36.7]	136	22.9 [16.6-30.6]	89	37.9 [28.5-48.3]
Kilombero	Mkula	-7.8011	36.9080764	June-2023	231	0.4 [0.1-2.4]	231	0 [0-1.6]	116	15.4 [10-23.1]
Kilombero	Sagamaganga	-8.05523	36.8074578	July-August 2023	218	4.1 [2.2-7.6]	218	0.5 [0.1-2.6]	109	20.6 [14.1-29.1]
Kilombero	Sanje	-7.76816	36.9143145	May 2023	205	1.5 [0.5-4.3]	205	0.5 [0.1-2.7]	103	3.9 [1.5-9.6]
Kilombero	Sululu	-7.99394	36.8296639	June 2023	149	13.4 [8.9-19.8]	149	4 [1.8-8.5]	96	25 [17.4-34.5]
Kilombero	Utaifa A	-8.12283	36.6848243	September-2023	212	0.9 [0.2-3.3]	212	2.4 [1-5.5]	106	5.8 [2.7-11.9]
Ulanga	Chikuti	-8.56194	36.7720928	May 2022	449	53.3 [48.7-57.9]	449	30.1 [26-34.5]	449	68.2 [63.8-72.3]
Ulanga	Ebuyu	-8.97243	36.7449489	June 2022	385	51.6 [46.6-56.6]	385	42 [37.2-46.9]	193	46.4 [39.5-53.4]
Ulanga	Mbuga	-8.9813	36.8690018	July 2022	349	30.9 [26.3-35.9]	349	20.5 [16.6-25]	175	35.4 [28.7-42.7]
Ulanga	Igota	-8.40479	36.6727855	April-2022	142	4.2 [1.9-8.9]	142	2 [0.7-5.9]	94	27.5 [19.5-37.3]
Ulanga	Igumbiro	-8.35423	36.6738147	April 2023	134	5.7 [2.9-10.1]	134	3.4 [1.4-8]	92	40.9 [31.4-51.1]

(Continued)

District	Village Name	Latitude	Longitude	Survey Month	RDT		Microscopy		qPCR	
					No tested	Prevalence % [95% CI]	No tested	Prevalence % [95% CI]	No tested	Prevalence % [95% CI]
Ulanga	Ikungua	-8.46596	36.6878861	January 2023	181	25.4 [19.6-32.2]	181	15.5 [11-21.5]	91	62.9 [52.6-72]
Ulanga	Itoo	-8.23007	36.6143815	April-2023	148	6.1 [3.2-11.2]	148	6.8 [3.7-12]	92	15.8 [9.7-24.6]
Ulanga	Kivukoni	-8.20477	36.690195	February-2023	147	2 [0.7-5.8]	147	3.4 [1.5-7.7]	92	18.9 [12.2-28.1]
Ulanga	Makanga	-8.65621	36.72257092	April 2022	367	46.3 [41.3-51.4]	367	25.7 [21.5-30.4]	184	71.4 [64.5-77.4]
Ulanga	Mavimba	-8.31773	36.6807224	February 2023	148	1.4 [0.4-4.9]	148	1.4 [0.4-4.9]	96	6.7 [3.2-13.5]
Ulanga	Igamba	-8.31479	36.7465093	April 2023	149	48.7 [40.8-56.7]	149	34.7 [27.5-42.6]	96	63.8 [53.8-72.7]
Ulanga	Mdindo	-8.62298	36.6927682	April-2022	406	45 [40.23-49.9]	406	36.8 [32.3-41.6]	406	68.2 [63.5-72.5]
Ulanga	Msogezi	-8.60496	36.6811327	April-2022	408	61.4 [56.6-66]	408	42 [37.3-46.8]	401	62.4 [57.6-67]
Ulanga	Mwaya	-8.94368	36.8269591	June-2022	304	20.7 [16.5-25.6]	304	15.1 [11.5-19.6]	152	43.1 [35.5-51.1]
Ulanga	Mzelezi	-8.88216	36.7308193	July-2022	384	45.3 [40.4-50.3]	384	28 [23.7-32.7]	192	69.7 [62.9-75.8]
Ulanga	Tulizamoyo	-8.35886	36.7342939	April-2022	132	28.6 [21.6-36.8]	132	33.3 [25.8-41.7]	88	66.7 [56.3-75.7]

Table S4.4: Number of villages categorized into different risk strata based on the *P. falciparum* prevalence rate (PfPR) data including the 95% Lower and upper Confidence interval (LCI UCI) from qPCR, RDTs and microscopy

Risk strata	Prevalence	qPCR			RDTs			Microscopy		
		LCI	Observed	UCI	LCI	Observed	UCI	LCI	Observed	UCI
Very low	PfPR < 1%	2	1	0	16	12	0	14	11	0
Low	1% ≤ PfPR < 5%	11	5	0	5	6	16	8	10	12
Moderate	5% ≤ PfPR < 30%	9	15	18	7	9	6	10	8	13
High	PfPR ≥ 30%	13	14	17	7	8	13	3	6	10
Total		**35**	**35**	**35**	**35**	**35**	**35**	**35**	**35**	**35**

Appendix for Chapter 5

Table S5.1: A summary of sample size distributions used when evaluating the performance of MIRs-ML trained on combined laboratory and field datasets for malaria screening

Model type	Lab samples	Field samples	Training size	Test size	Balanced positive class	Balanced negative class
Lab only	657	-	460	92	230	230
Lab + 10%	657	262	644	162	403	403
Lab + 20%	657	524	792	198	495	495
Lab + 30%	657	786	950	238	594	594
Lab + 100 highest parasitemia from the field	657	100	502	126	314	314

Bibliography

[1] World Health Organization (WHO), *World malaria report*. 2023.

[2] L. M. Cohee, J. I. Nankabirwa, B. Greenwood, A. Djimde, and D. P. Mathanga, "Time for malaria control in school-age children.," *The Lancet Child & Adolescent Health*, vol. 5, no. 8, pp. 537–538, 2021.

[3] J. E. Coalson, L. M. Cohee, A. G. Buchwald, A. Nyambalo, J. Kubale, K. B. Seydel, D. Mathanga, T. E. Taylor, M. K. Laufer, and M. L. Wilson, "Simulation models predict that school-age children are responsible for most human-to-mosquito plasmodium falciparum transmission in southern malawi," *Malaria journal*, vol. 17, pp. 1–12, 2018.

[4] World Health Organization (WHO), "High burden to high impact: a targeted malaria response," tech. rep., 2018.

[5] S. Bhatt, D. J. Weiss, E. Cameron, D. Bisanzio, B. Mappin, U. Dalrymple, K. E. Battle, C. L. Moyes, A. Henry, P. A. Eckhoff, E. A. Wenger, O. Briët, M. A. Penny, T. A. Smith, A. Bennett, J. Yukich, T. P. Eisele, J. T. Griffin, C. A. Fergus, M. Lynch, F. Lindgren, J. M. Cohen, C. L. Murray, D. L. Smith, S. I. Hay, R. E. Cibulskis, and P. W. Gething, "The effect of malaria control on Plasmodium falciparum in Africa between 2000 and 2015," *Nature*, vol. 526, no. 7572, 2015.

[6] A.-K. Heuschen, G. Lu, O. Razum, A. Abdul-Mumin, O. Sankoh, L. Von Seidlein, U. D'Alessandro, and O. Müller, "Public health-relevant consequences of the COVID-19 pandemic on malaria in sub-Saharan Africa: a scoping review," *Malaria journal*, vol. 20, pp. 1–16, 2021.

[7] V. Moin-Vaziri and M. Badakhshan, "The Impact of COVID-19 Pandemic on Arthropod-Related Diseases.," *Journal of arthropod-borne diseases*, vol. 17, pp. 28–35, Mar. 2023.

[8] World Health Organization, "Vector alert: Anopheles stephensi invasion and spread in Africa and Sri Lanka," *https://iris.who.int/bitstream/handle/10665/365710/9789240067714-eng.pdf*, no. 2, p. 4, 2022.

[9] World Health Organization (WHO), "Vector Borne Diseases," 2020.

[10] N. Becker, D. Petric, M. Zgomba, C. Boase, M. Madon, C. Dahl, and A. Kaiser, *Mosquitoes and their control*. Springer Science& Business Media, 2010.

[11] M. A. Phillips, J. N. Burrows, C. Manyando, R. H. van Huijsduijnen, W. C. Van Voorhis, and T. N. C. Wells, “Malaria.,” *Nature reviews. Disease primers*, vol. 3, p. 17050, Aug. 2017.

[12] F. Verra, A. Angheben, E. Martello, G. Giorli, F. Perandin, and Z. Bisoffi, “A systematic review of transfusion-transmitted malaria in non-endemic areas,” *Malaria Journal*, vol. 17, pp. 1–14, 2018.

[13] F. Rosso, O. L. Agudelo Rojas, C. C. Suarez Gil, J. A. Lopez Vargas, J. E. Gó mez-Mesa, D. C. Carrillo Gomez, L. Meza Ramirez, and L. A. Caicedo Rusca, “Transmission of malaria from donors to solid organ transplant recipients: A case report and literature review,” *Transplant Infectious Disease*, vol. 23, no. 4, p. e13660, 2021.

[14] D. A. Milner, “Malaria pathogenesis,” *Cold Spring Harbor Perspectives in Medicine*, vol. 8, no. 1, pp. 1–12, 2018.

[15] A. F. Cowman, J. Healer, D. Marapana, and K. Marsh, “Malaria: Biology and Disease.,” *Cell*, vol. 167, pp. 610–624, Oct. 2016.

[16] R. Sendor, C. L. Mitchell, F. Chacky, A. Mohamed, L. E. Mhamilawa, F. Molteni, S. Nyinondi, B. Kabula, H. Mkali, and E. J. Reaves, “Similar Prevalence of Plasmodium falciparum and Non–P. falciparum Malaria Infections among Schoolchildren, Tanzania,” *Emerging infectious diseases*, vol. 29, no. 6, p. 1143, 2023.

[17] R. N. Price, R. J. Commons, K. E. Battle, K. Thriemer, and K. Mendis, “Plasmodium vivax in the era of the shrinking P. falciparum map,” *Trends in parasitology*, vol. 36, no. 6, pp. 560–570, 2020.

[18] J. Hawadak, R. R. Dongang Nana, and V. Singh, “Global trend of Plasmodium malariae and Plasmodium ovale spp. malaria infections in the last two decades (2000–2020): a systematic review and meta-analysis,” *Parasites& vectors*, vol. 14, no. 1, p. 297, 2021.

[19] S. Antinori, L. Galimberti, L. Milazzo, and M. Corbellino, “Biology of human malaria plasmodia including Plasmodium knowlesi,” *Mediterranean journal of hematology and infectious diseases*, vol. 4, no. 1, 2012.

[20] M. M. Cova, M. H. Lamarque, and M. Lebrun, “How apicomplexa parasites secrete and build their invasion machinery,” *Annual Review of Microbiology*, vol. 76, no. 1, pp. 619–640, 2022.

[21] V. J. M. J., M. Markus, and K. T. W. A., “Organelle Dynamics in Apicomplexan Parasites,” *mBio*, vol. 12, pp. 10.1128/mbio.01409–21, Aug. 2021.

[22] B. J. Foth and G. I. McFadden, “The apicoplast: a plastid in Plasmodium falciparum and other Apicomplexan parasites,” *International review of cytology*, vol. 224, pp. 57–110, 2003.

[23] S. A. Ralph, G. G. Van Dooren, R. F. Waller, M. J. Crawford, M. J. Fraunholz, B. J. Foth, C. J. Tonkin, D. S. Roos, and G. I. McFadden, “Metabolic maps and functions of the Plasmodium falciparum apicoplast,” *Nature Reviews Microbiology*, vol. 2, no. 3, pp. 203–216, 2004.

[24] I. M. Lamb, I. C. Okoye, M. W. Mather, and A. B. Vaidya, “Unique Properties of Apicomplexan Mitochondria,” *Annual review of microbiology*, vol. 77, no. 1, pp. 541–560, 2023.

[25] A. F. Cowman and B. S. Crabb, “Invasion of red blood cells by malaria parasites,” *Cell*, vol. 124, no. 4, pp. 755–766, 2006.

[26] C. R. Harding and F. Frischknecht, “The riveting cellular structures of apicomplexan parasites,” *Trends in Parasitology*, vol. 36, no. 12, pp. 979–991, 2020.

[27] A. Amambua-Ngwa, L. Amenga-Etego, E. Kamau, R. Amato, A. Ghansah, L. Golassa, M. Randrianarivelojosia, D. Ishengoma, T. Apinjoh, and O. Maïga-Ascofaré, “Major subpopulations of Plasmodium falciparum in sub-Saharan Africa,” *Science*, vol. 365, no. 6455, pp. 813–816, 2019.

[28] R. E. Howes, A. P. Patil, F. r. B. Piel, O. A. Nyangiri, C. W. Kabaria, P. W. Gething, P. A. Zimmerman, C. Barnadas, C. M. Beall, and A. Gebremedhin, “The global distribution of the Duffy blood group,” *Nature communications*, vol. 2, no. 1, p. 266, 2011.

[29] R. E. Howes, K. E. Battle, K. N. Mendis, D. L. Smith, R. E. Cibulskis, J. K. Baird, and S. I. Hay, “Global Epidemiology of Plasmodium vivax.,” *The American journal of tropical medicine and hygiene*, vol. 95, pp. 15–34, Dec. 2016.

[30] D. Ménard, C. Barnadas, C. Bouchier, C. Henry-Halldin, L. R. Gray, A. Ratsimbasoa, V. Thonier, J.-F. ç. Carod, O. Domarle, and Y. Colin, “Plasmodium vivax clinical malaria is commonly observed in Duffy-negative Malagasy people,” *Proceedings of the National Academy of Sciences*, vol. 107, no. 13, pp. 5967–5971, 2010.

[31] P. A. Zimmerman, “Plasmodium vivax Infection in Duffy-Negative People in Africa.,” Sept. 2017.

[32] T. G. Woldearegai, P. G. Kremsner, J. r. F. J. Kun, and B. Mordmüller, “Plasmodium vivax malaria in Duffy-negative individuals from Ethiopia,” *Transactions of the Royal Society of Tropical Medicine and Hygiene*, vol. 107, no. 5, pp. 328–331, 2013.

[33] C. S. Chu and N. J. White, “Management of relapsing Plasmodium vivax malaria.,” *Expert review of anti-infective therapy*, vol. 14, pp. 885–900, Oct. 2016.

[34] K. E. Battle, T. C. D. Lucas, M. Nguyen, R. E. Howes, A. K. Nandi, K. A. Twohig, D. A. Pfeffer, E. Cameron, P. C. Rao, D. Casey, H. S. Gibson, J. A. Rozier, U. Dalrymple, S. H. Keddie, E. L. Collins, J. R. Harris, C. A. Guerra, M. P. Thorn, D. Bisanzio, N. Fullman, C. K. Huynh, X. Kulikoff, M. J. Kutz, A. D. Lopez, A. H. Mokdad, M. Naghavi, G. Nguyen, K. A. Shackelford, T. Vos, H. Wang, S. S. Lim, C. J. L. Murray, R. N. Price, J. K. Baird, D. L. Smith, S. Bhatt, D. J. Weiss, S. I. Hay, and P. W. Gething, “Mapping the global endemicity and clinical burden of Plasmodium vivax, 2000-17: a spatial and temporal modelling study.,” *Lancet (London, England)*, vol. 394, pp. 332–343, July 2019.

[35] D. A. Moreno-Pérez, J. A. Ruíz, and M. A. Patarroyo, “Reticulocytes: Plasmodium vivax target cells,” *Biology of the Cell*, vol. 105, no. 6, pp. 251–260, 2013.

[36] M. Ginouves, V. Veron, L. Musset, E. Legrand, A. Stefani, G. Prevot, M. Demar, F. Djossou, P. Brousse, and M. Nacher, “Frequency and distribution of mixed Plasmodium falciparum-vivax infections in French Guiana between 2000 and 2008,” *Malaria journal*, vol. 14, pp. 1–6, 2015.

[37] W. E. Collins and G. M. Jeffery, “Plasmodium malariae: parasite and disease,” *Clinical microbiology reviews*, vol. 20, no. 4, pp. 579–592, 2007.

[38] S. Sato, “Plasmodium—a brief introduction to the parasites causing human malaria and their basic biology,” *Journal of physiological anthropology*, vol. 40, no. 1, p. 1, 2021.

[39] A. S. Badiane, K. Diongue, S. Diallo, A. A. Ndongo, C. K. Diedhiou, A. B. Deme, D. Ma, M. Ndiaye, M. C. Seck, and T. Dieng, “Acute kidney injury associated with Plasmodium malariae infection,” *Malaria Journal*, vol. 13, pp. 1–5, 2014.

[40] G. B. da Silva Junior, J. R. Pinto, E. J. G. Barros, G. M. N. Farias, and E. D. F. Daher, “Kidney involvement in malaria: an update,” *Revista do Instituto de Medicina Tropical de São Paulo*, vol. 59, p. e53, 2017.

[41] W. E. Collins and G. M. Jeffery, “Plasmodium ovale: parasite and disease,” *Clinical microbiology reviews*, vol. 18, no. 3, pp. 570–581, 2005.

[42] C. J. Sutherland, N. Tanomsing, D. Nolder, M. Oguike, C. Jennison, S. Pukrittayakamee, C. Dolecek, T. T. Hien, V. E. Do Rosário, and A. P. Arez, “Two nonrecombining sympatric forms of the human malaria parasite Plasmodium ovale occur globally,” *The Journal of infectious diseases*, vol. 201, no. 10, pp. 1544–1550, 2010.

[43] M. C. Oguike, M. Betson, M. Burke, D. Nolder, J. R. Stothard, I. Kleinschmidt, C. Proietti, T. Bousema, M. Ndounga, and K. Tanabe, “Plasmodium ovale curtisi and Plasmodium ovale wallikeri circulate simultaneously in African communities,” *International journal for parasitology*, vol. 41, no. 6, pp. 677–683, 2011.

[44] M. A. Abdulraheem, M. Ernest, I. Ugwuanyi, H. M. Abkallo, S. Nishikawa, M. Adeleke, A. E. Orimadegun, and R. Culleton, “High prevalence of Plasmodium malariae and Plasmodium ovale in co-infections with Plasmodium falciparum in asymptomatic malaria parasite carriers in southwestern Nigeria,” *International journal for parasitology*, vol. 52, no. 1, pp. 23–33, 2022.

[45] J. Cox-Singh, T. M. E. Davis, K.-S. Lee, S. S. G. Shamsul, A. Matusop, S. Ratnam, H. A. Rahman, D. J. Conway, and B. Singh, “Plasmodium knowlesi malaria in humans is widely distributed and potentially life threatening,” *Clinical infectious diseases*, vol. 46, no. 2, pp. 165–171, 2008.

[46] B. Singh and C. Daneshvar, “Plasmodium knowlesi malaria in Malaysia,” *Med J Malaysia*, vol. 65, no. 3, pp. 166–172, 2010.

[47] W. Chin, P. G. Contacos, G. R. Coatney, and H. R. Kimball, “A naturally acquired quotidian-type malaria in man transferable to monkeys,” *Science*, vol. 149, no. 3686, p. 865, 1965.

[48] Y. L. Fong, F. C. Cadigan, and G. R. Coatney, “A presumptive case of naturally occurring Plasmodium knowlesi malaria in man in Malaysia.,” 1971.

[49] R. Knowles and A. S. B. M. D. Gupta, “A study of monkey-malaria, and its experimental transmission to man,” *The Indian medical gazette*, vol. 67, no. 6, p. 301, 1932.

[50] A. L. Luzolo and D. M. Ngoyi, “Cerebral malaria.,” *Brain research bulletin*, vol. 145, pp. 53–58, Feb. 2019.

[51] M. E. Sinka, M. J. Bangs, S. Manguin, Y. Rubio-Palis, T. Chareonviriyaphap, M. Coetzee, C. M. Mbogo, J. Hemingway, A. P. Patil, and W. H. Temperley, “A global map of dominant malaria vectors,” *Parasites& vectors*, vol. 5, pp. 1–11, 2012.

[52] M. Gillies, “The Anophelinae of Africa south of Sahara (Ethiopian Zoogeographical Region),” *The South Africa Institute for Medical Research*, vol. 54, pp. 1–343, 1968.

[53] M. T. Gillies and M. Coetzee, “A supplement to the Anophelinae of Africa South of the Sahara,” *Publ S Afr Inst Med Res*, vol. 55, pp. 1–143, 1987.

[54] E. O. Ochomo, S. Milanoi, B. Abong’o, B. Onyango, M. Muchoki, D. Omoke, E. Olanga, L. Njoroge, E. Juma, and J. D. Otieno, “Molecular surveillance leads to the first detection of Anopheles stephensi in Kenya.,” 2023.

[55] M. E. Sinka, S. Pironon, N. C. Massey, J. Longbottom, J. Hemingway, C. L. Moyes, and K. J. Willis, “A new malaria vector in Africa: predicting the expansion range of Anopheles stephensi and identifying the urban populations at risk,” *Proceedings of the National Academy of Sciences*, vol. 117, no. 40, pp. 24900–24908, 2020.

[56] T. E. Carter, S. Yared, A. Gebresilassie, V. Bonnell, L. Damodaran, K. Lopez, M. Ibrahim, S. Mohammed, and D. Janies, “First detection of Anopheles stephensi Liston, 1901 (Diptera: culicidae) in Ethiopia using molecular and morphological approaches,” *Acta tropica*, vol. 188, pp. 180–186, 2018.

[57] A. Mnzava, A. C. Monroe, and F. Okumu, “Anopheles stephensi in Africa requires a more integrated response,” *Malaria journal*, vol. 21, no. 1, pp. 1–6, 2022.

[58] M. E. Sinka, “Global distribution of the dominant vector species of malaria,” in *Anopheles mosquitoes-New insights into malaria vectors*, IntechOpen, 2013.

[59] M. E. Sinka, M. J. Bangs, S. Manguin, M. Coetzee, C. M. Mbogo, J. Hemingway, A. P. Patil, W. H. Temperley, P. W. Gething, C. W. Kabaria, R. M. Okara, T. Van Boeckel, H. C. J. Godfray, R. E. Harbach, and S. I. Hay, “The dominant Anopheles vectors of human malaria in Africa, Europe and the Middle East: occurrence data, distribution maps and bionomic précis.,” *Parasites& vectors*, vol. 3, p. 117, Dec. 2010.

[60] M. Coetzee, “Key to the females of Afrotropical Anopheles mosquitoes (Diptera: Culicidae),” *Malaria Journal*, vol. 19, no. 1, pp. 1–20, 2020.

[61] S. K. Dadzie, R. Brenyah, and M. A. Appawu, “Role of species composition in malaria transmission by the Anopheles funestus group (Diptera: Culicidae) in Ghana.,” *Journal of vector ecology : journal of the Society for Vector Ecology*, vol. 38, pp. 105–110, June 2013.

[62] G. B. White, “Anopheles gambiae complex and disease transmission in Africa.,” *Transactions of the Royal Society of Tropical Medicine and Hygiene*, vol. 68, no. 4, pp. 278–301, 1974.

[63] I. Tirados, C. Costantini, G. Gibson, and S. J. Torr, “Blood-feeding behaviour of the malarial mosquito Anopheles arabiensis: implications for vector control.,” *Medical and veterinary entomology*, vol. 20, pp. 425–437, Dec. 2006.

[64] A. Mahande, F. Mosha, J. Mahande, and E. Kweka, “Feeding and resting behaviour of malaria vector, Anopheles arabiensis with reference to zooprophylaxis.,” *Malaria journal*, vol. 6, p. 100, July 2007.

[65] E. Chirebvu and M. J. Chimbari, “Characteristics of Anopheles arabiensis larval habitats in Tubu village, Botswana.,” *Journal of vector ecology : journal of the Society for Vector Ecology*, vol. 40, pp. 129–138, June 2015.

[66] L. C. Gouagna, M. Rakotondranary, S. Boyer, G. Lempérière, J.-S. é. Dehecq, and D. Fontenille, “Abiotic and biotic factors associated with the presence of Anopheles arabiensis immatures and their abundance in naturally occurring and man-made aquatic habitats.,” *Parasites& vectors*, vol. 5, p. 96, May 2012.

[67] M. Yohannes and E. Boelee, “Early biting rhythm in the Afro-tropical vector of malaria, Anopheles arabiensis, and challenges for its control in Ethiopia.,” *Medical and veterinary entomology*, vol. 26, pp. 103–105, Mar. 2012.

[68] M. W. Service, “Studies on sampling larval populations of the Anopheles gambiae complex.,” *Bulletin of the World Health Organization*, vol. 45, no. 2, pp. 169–180, 1971.

[69] E. W. Kaindoa, N. S. Matowo, H. S. Ngowo, G. Mkandawile, A. Mmbando, M. Finda, and F. O. Okumu, “Interventions that effectively target Anopheles funestus mosquitoes could significantly improve control of persistent malaria transmission in south-eastern Tanzania,” *PLoS ONE*, vol. 12, no. 5, 2017.

[70] R. S. McCann, E. Ochomo, M. N. Bayoh, J. M. Vulule, M. J. Hamel, J. E. Gimnig, W. A. Hawley, and E. D. Walker, “Reemergence of Anopheles funestus as a vector of Plasmodium falciparum in western Kenya after long-term implementation of insecticide-treated bed nets.,” *The American journal of tropical medicine and hygiene*, vol. 90, pp. 597–604, Apr. 2014.

[71] N. F. Kahamba, M. Finda, H. S. Ngowo, B. J. Msugupakulya, F. Baldini, L. L. Koekemoer, H. M. Ferguson, and F. O. Okumu, “Using ecological observations to improve malaria control in areas where Anopheles funestus is the dominant vector.,” *Malaria journal*, vol. 21, p. 158, June 2022.

[72] J. E. Gimnig, M. Ombok, L. Kamau, and W. A. Hawley, “Characteristics of larval anopheline (Diptera: Culicidae) habitats in Western Kenya.,” *Journal of medical entomology*, vol. 38, pp. 282–288, Mar. 2001.

[73] I. H. Nambunga, H. S. Ngowo, S. A. Mapua, E. E. Hape, B. J. Msugupakulya, D. S. Msaky, N. T. Mhumbira, K. R. Mchwembo, G. Z. Tamayamali, S. V. Mlembe, R. M. Njalambaha, D. W. Lwetoijera, M. F. Finda, N. J. Govella, D. Matoke-Muhia, E. W. Kaindoa, and F. O. Okumu, "Aquatic habitats of the malaria vector Anopheles funestus in rural south-eastern Tanzania.," *Malaria journal*, vol. 19, p. 219, June 2020.

[74] S. M. Muriu, E. J. Muturi, J. I. Shililu, C. M. Mbogo, J. M. Mwangangi, B. G. Jacob, L. W. Irungu, R. W. Mukabana, J. I. Githure, and R. J. Novak, "Host choice and multiple blood feeding behaviour of malaria vectors and other anophelines in Mwea rice scheme, Kenya," *Malaria Journal*, vol. 7, pp. 1–7, 2008.

[75] C. Garros, R. E. Harbach, and S. Manguin, "Morphological assessment and molecular phylogenetics of the Funestus and Minimus groups of Anopheles (Cellia).," *Journal of medical entomology*, vol. 42, pp. 522–536, July 2005.

[76] A. Cohuet, J.-C. Toto, F. Simard, P. Kegne, D. Fontenille, and M. Coetze, "Species Identification Within the Anopheles Funestus Group of Malaria Vectors in Cameroon and Evidence for a New Species," *The American Journal of Tropical Medicine and Hygiene*, vol. 69, no. 2, pp. 200–205, 2018.

[77] S. A. Mapua, E. E. Hape, J. Kihonda, H. Bwanary, K. Kifungo, M. Kilalangongono, E. W. Kaindoa, H. S. Ngowo, and F. O. Okumu, "Persistently high proportions of plasmodium-infected Anopheles funestus mosquitoes in two villages in the Kilombero valley, South-Eastern Tanzania.," *Parasite epidemiology and control*, vol. 18, p. e00264, Aug. 2022.

[78] J. Tavares, P. Formaglio, S. Thiberge, E. Mordelet, N. Van Rooijen, A. Medvinsky, R. Ménard, and R. Amino, "Role of host cell traversal by the malaria sporozoite during liver infection.," *The Journal of experimental medicine*, vol. 210, pp. 905–915, May 2013.

[79] F. E. G. Cox, "History of the discovery of the malaria parasites and their vectors," *Parasites& Vectors*, vol. 3, no. 1, p. 5, 2010.

[80] T. Ishino, K. Yano, Y. Chinzei, and M. Yuda, "Cell-passage activity is required for the malarial parasite to cross the liver sinusoidal cell layer.," *PLoS biology*, vol. 2, p. E4, Jan. 2004.

[81] C. D. Rodrigues, M. Hannus, M. Prudêncio, C. Martin, L. A. Gonçalves, S. Portugal, S. Epiphanio, A. Akinc, P. Hadwiger, K. Jahn-Hofmann, I. Röhl, G.-J. van Gemert, J.-F. Franetich, A. J. F. Luty, R. Sauerwein, D. Mazier, V. Koteliansky, H.-P. Vornlocher, C. J. Echeverri, and M. M. Mota, "Host Scavenger Receptor SR-BI Plays a Dual Role in the Establishment of Malaria Parasite Liver Infection," *Cell Host& Microbe*, vol. 4, no. 3, pp. 271–282, 2008.

[82] L. H. Miller, H. C. Ackerman, X. Z. Su, and T. E. Wellems, “Malaria biology and disease pathogenesis: Insights for new treatments,” *Nature Medicine*, vol. 19, no. 2, pp. 156–167, 2013.

[83] M. M. Mota, G. Pradel, J. P. Vanderberg, J. C. Hafalla, U. Frevert, R. S. Nussenzweig, V. Nussenzweig, and A. Rodriguez, “Migration of Plasmodium sporozoites through cells before infection ,” *Science*, vol. 291, no. 5501, pp. 141–144, 2001.

[84] N. J. White, “Determinants of relapse periodicity in Plasmodium vivax malaria,” *Malaria Journal*, vol. 10, no. October, 2011.

[85] S. Besteiro, J.-F. Dubremetz, and M. Lebrun, “The moving junction of apicomplexan parasites: a key structure for invasion.,” *Cellular microbiology*, vol. 13, pp. 797–805, June 2011.

[86] N. D. Geoghegan, C. Evelyn, L. W. Whitehead, M. Pasternak, P. McDonald, T. Triglia, D. S. Marapana, D. Kempe, J. K. Thompson, M. J. Mlodzianoski, J. Healer, M. Biro, A. F. Cowman, and K. L. Rogers, “4D analysis of malaria parasite invasion offers insights into erythrocyte membrane remodeling and parasitophorous vacuole formation,” *Nature Communications*, vol. 12, no. 1, p. 3620, 2021.

[87] A. S. Paul, S. Saha, K. Engelberg, R. H. Jiang, B. I. Coleman, A. L. Kosber, C.-T. Chen, M. Ganter, N. Espy, T. W. Gilberger, M.-J. Gubbels, and M. T. Duraisingh, “Parasite Calcineurin Regulates Host Cell Recognition and Attachment by Apicomplexans,” *Cell Host& Microbe*, vol. 18, no. 1, pp. 49–60, 2015.

[88] L. H. Miller, D. I. Baruch, K. Marsh, and O. K. Doumbo, “The pathogenic basis of malaria.,” *Nature*, vol. 415, pp. 673–679, Feb. 2002.

[89] N. M. Anstey, N. M. Douglas, J. R. Poespoprodjo, and R. N. Price, “Plasmodium vivax: clinical spectrum, risk factors and pathogenesis.,” *Advances in parasitology*, vol. 80, pp. 151–201, 2012.

[90] R. E. Sinden, “Sexual Development of Malarial Parasites,” vol. 22, pp. 153–216, Academic Press, 1983.

[91] G. A. Josling and M. Llinás, “Sexual development in Plasmodium parasites: Knowing when it’s time to commit,” *Nature Reviews Microbiology*, vol. 13, no. 9, pp. 573–587, 2015.

[92] F. K. Acquah, J. Adjah, K. C. Williamson, and L. E. Amoah, “Transmission-Blocking Vaccines: Old Friends and New Prospects.,” *Infection and immunity*, vol. 87, June 2019.

[93] L.-M. Birkholtz, P. Alano, and D. Leroy, “Transmission-blocking drugs for malaria elimination.,” *Trends in parasitology*, vol. 38, pp. 390–403, May 2022.

[94] A. Ruecker, D. K. Mathias, U. Straschil, T. S. Churcher, R. R. Dinglasan, D. Leroy, R. E. Sinden, and M. J. Delves, “A male and female gametocyte functional viability assay to identify biologically relevant malaria transmission-blocking drugs.,” *Antimicrobial agents and chemotherapy*, vol. 58, pp. 7292–7302, Dec. 2014.

[95] R. E. Sinden, “The biology of malaria transmission,” *Recent Advances in Malaria*, pp. 87–124, 2016.

[96] R. Joice, S. K. Nilsson, J. Montgomery, S. Dankwa, E. Egan, B. Morahan, K. B. Seydel, L. Bertuccini, P. Alano, K. C. Williamson, M. T. Duraisingh, T. E. Taylor, D. A. Milner, and M. Marti, “Plasmodium falciparum transmission stages accumulate in the human bone marrow.,” *Science translational medicine*, vol. 6, p. 244re5, July 2014.

[97] S. Bennink, M. J. Kiesow, and G. Pradel, “The development of malaria parasites in the mosquito midgut.,” *Cellular microbiology*, vol. 18, pp. 905–918, July 2016.

[98] A. N. Clements, *The biology of mosquitoes.* , vol. 1. 1992.

[99] J. R. Ohm, F. Baldini, P. Barreaux, T. Lefevre, P. A. Lynch, E. Suh, S. A. Whitehead, and M. B. Thomas, “Rethinking the extrinsic incubation period of malaria parasites,” 2018.

[100] M. S. Oakley, N. Gerald, T. F. McCutchan, L. Aravind, and S. Kumar, “Clinical and molecular aspects of malaria fever,” *Trends in parasitology*, vol. 27, no. 10, pp. 442–449, 2011.

[101] J. L. Miller, *Principles of infrared technology*. Springer, 1994.

[102] J. Nyataya, J. Waitumbi, V. A. Mobegi, A. Noreddin, and M. E. El Zowalaty, “Plasmodium falciparum histidine-rich protein 2 and 3 gene deletions and their implications in malaria control,” *Diseases*, vol. 8, no. 2, p. 15, 2020.

[103] A. Moody, “Rapid diagnostic tests for malaria parasites,” *Clinical microbiology reviews*, vol. 15, no. 1, pp. 66–78, 2002.

[104] World Health Organization, *WHO malaria terminology*. 2021.

[105] G. C. Kelly, J. Hii, W. Batarii, W. Donald, E. Hale, J. Nausien, S. Pontifex, A. Vallely, M. Tanner, and A. Clements, “Modern geographical reconnaissance of target populations in malaria elimination zones.,” *Malaria journal*, vol. 9, p. 289, Oct. 2010.

[106] World Health Organization (WHO), “WHO guidelines for malaria, 3 June 2022,” tech. rep., 2022.

[107] J.-A. A. Tangena, C. M. J. Hendriks, M. Devine, M. Tammaro, A. E. Trett, I. Williams, A. J. DePina, A. Sisay, R. Herizo, and H. T. Kafy, “Indoor residual spraying for malaria control in sub-Saharan Africa 1997 to 2017: an adjusted retrospective analysis,” *Malaria journal*, vol. 19, pp. 1–15, 2020.

[108] K. D. Konlan, N. Kossi Vivor, I. Gegefe, and L. Hayford, “Factors associated with ownership and utilization of insecticide treated nets among children under five years in sub-Saharan Africa,” *BMC Public Health*, vol. 22, no. 1, p. 940, 2022.

[109] A. Monroe, S. Moore, B. Olapeju, A. P. Merritt, and F. Okumu, “Unlocking the human factor to increase effectiveness and sustainability of malaria vector control,” *Malaria Journal*, vol. 20, pp. 1–6, 2021.

[110] M. Saito, R. Mansoor, K. Kennon, A. R. Anvikar, E. A. Ashley, D. Chandramohan, L. M. Cohee, U. D’Alessandro, B. Genton, M. E. Gilder, E. Juma, L. Kalilani-Phiri, I. Kuepfer, M. K. Laufer, K. M. Lwin, S. R. Meshnick, D. Mosha, V. Mwapasa, N. Mwebaza, M. Nambozi, J.-L. A. Ndiaye, F. Nosten, M. Nyunt, B. Ogutu, S. Parikh, M. K. Paw, A. P. Phyo, M. Pimanpanarak, P. Piola, M. J. Rijken, K. Sriprawat, H. K. Tagbor, J. Tarning, H. Tinto, I. Valéa, N. Valecha, N. J. White, J. Wiladphaingern, K. Stepniewska, R. McGready, and P. J. Guérin, “Efficacy and tolerability of artemisinin-based and quinine-based treatments for uncomplicated falciparum malaria in pregnancy: a systematic review and individual patient data meta-analysis.,” *The Lancet. Infectious diseases*, vol. 20, pp. 943–952, Aug. 2020.

[111] C. J. M. Whitty, C. Chandler, E. Ansah, T. Leslie, and S. G. Staedke, “Deployment of ACT antimalarials for treatment of malaria: challenges and opportunities,” *Malaria journal*, vol. 7, pp. 1–7, 2008.

[112] C. A. Scott, A. K. Yeshiwondim, B. Serda, C. Guinovart, B. H. Tesfay, A. Agmas, M. T. Zeleke, G. S. Guesses, A. L. Ayenew, and W. M. Workie, “Mass testing and treatment for malaria in low transmission areas in Amhara Region, Ethiopia,” *Malaria journal*, vol. 15, pp. 1–13, 2016.

[113] R. M. Chico and D. Chandramohan, “Intermittent preventive treatment of malaria in pregnancy: at the crossroads of public health policy.,” *Tropical medicine& international health : TM& IH*, vol. 16, pp. 774–785, July 2011.

[114] E. B. Esu, C. Oringanje, and M. M. Meremikwu, “Intermittent preventive treatment for malaria in infants.,” *The Cochrane database of systematic reviews*, vol. 7, p. CD011525, July 2021.

[115] A. Monroe, N. A. Williams, S. Ogoma, C. Karema, and F. Okumu, “Reflections on the 2021 World Malaria Report and the future of malaria control,” *Malaria Journal*, vol. 21, no. 1, p. 154, 2022.

[116] B. Balikagala, N. Fukuda, M. Ikeda, O. T. Katuro, S.-I. Tachibana, M. Yamauchi, W. Opio, S. Emoto, D. A. Anywar, and E. Kimura, “Evidence of artemisinin-resistant malaria in Africa,” *New England Journal of Medicine*, vol. 385, no. 13, pp. 1163–1171, 2021.

[117] WHO, *Vector alert: Anopheles stephensi invasion and spread in Africa and Sri Lanka*. Geneva, 2022.

[118] World Health Organization (WHO), “False-negative RDT results and implications of new reports of P. falciparum histidine-rich protein 2/3 gene deletions,” tech. rep., 2017.

[119] World Health Organization, “Malaria vaccine: WHO position paper – March 2022,” *Weekly epidemiological record*, no. 9, p. 76, 2022.

[120] M. S. Datoo, M. H. Natama, A. Som, O. Traor, T. Rouamba, D. Bellamy, P. Yameogo, D. Valia, M. Tegneri, and F. Ouedraogo, “Efficacy of a low-dose candidate malaria vaccine, R21 in adjuvant Matrix-M, with seasonal administration to children in Burkina Faso: a randomised controlled trial,” *The Lancet*, vol. 397, no. 10287, pp. 1809–1818, 2021.

[121] T. Nolan, “Control of malaria-transmitting mosquitoes using gene drives.,” *Philosophical transactions of the Royal Society of London. Series B, Biological sciences*, vol. 376, p. 20190803, Feb. 2021.

[122] G. F. Killeen, P. P. Chaki, T. E. Reed, C. L. Moyes, and N. J. Govella, “Entomological surveillance as a cornerstone of malaria elimination: a critical appraisal,” *Towards malaria elimination-a leap forward. Manguin S, Vas D, Eds. IntechOpen*, pp. 403–429, 2018.

[123] N. J. Govella, P. P. Chaki, and G. F. Killeen, “Entomological surveillance of behavioural resilience and resistance in residual malaria vector populations,” *Malaria Journal*, vol. 12, pp. 1–9, 2013.

[124] T. L. Russell, R. Farlow, M. Min, E. Espino, A. Mnzava, and T. R. Burkot, “Capacity of National Malaria Control Programmes to implement vector surveillance: a global analysis,” *Malaria Journal*, vol. 19, no. 1, pp. 1–9, 2020.

[125] M. Mubi, A. Janson, M. Warsame, A. Må rtensson, K. Källander, M. G. Petzold, B. Ngasala, G. Maganga, L. L. Gustafsson, and A. Massele, “Malaria rapid testing by community health workers is effective and safe for targeting malaria treatment: randomised cross-over trial in Tanzania,” *PloS one*, vol. 6, no. 7, p. e19753, 2011.

[126] A. Epstein, J. F. Namuganga, E. V. Kamya, J. I. Nankabirwa, S. Bhatt, I. Rodriguez-Barraquer, S. G. Staedke, M. R. Kamya, G. Dorsey, and B. Greenhouse, “Estimating malaria incidence from routine health facility-based surveillance data in Uganda.,” *Malaria journal*, vol. 19, p. 445, Dec. 2020.

[127] A. Mbanefo and N. Kumar, “Evaluation of Malaria Diagnostic Methods as a Key for Successful Control and Elimination Programs.,” *Tropical medicine and infectious disease*, vol. 5, June 2020.

[128] L. E. Fitri, T. Widaningrum, A. T. Endharti, M. H. Prabowo, N. Winaris, and R. Y. B. Nugraha, “Malaria diagnostic update: From conventional to advanced method,” *Journal of Clinical Laboratory Analysis*, vol. 36, no. 4, p. e24314, 2022.

[129] M. Dagen, “History of malaria and its treatment,” in *Antimalarial agents*, pp. 1–48, Elsevier, 2020.

[130] R. Varo, N. Balanza, A. Mayor, and Q. Bassat, “Diagnosis of clinical malaria in endemic settings,” *Expert Review of Anti-Infective Therapy*, vol. 0, no. 0, 2020.

[131] World Health Organization (WHO), “Malaria rapid diagnostic test performance: results of WHO product testing of malaria RDTs: round 8 (2016–2018),” 2018.

[132] T. Theophanides, “Introduction to Infrared Spectroscopy,” p. Ch. 0, Rijeka: IntechOpen, 2012.

[133] P. Larkin, *Infrared and Raman spectroscopy: principles and spectral interpretation*. Elsevier, 2017.

[134] W. Minkina, “How infrared radiation was discovered—Range of this discovery and detailed, unknown information,” *Applied Sciences*, vol. 11, no. 21, p. 9824, 2021.

[135] W. Herschel, “XIV. Experiments on the refrangibility of the invisible rays of the sun,” *Philosophical Transactions of the Royal Society of London*, no. 90, pp. 284–292, 1800.

[136] E. F. J. Ring, “The discovery of infrared radiation in 1800,” *The Imaging Science Journal*, vol. 48, no. 1, pp. 1–8, 2000.

[137] J. Maas, “Basic infrared spectroscopy,” *Hyen& Son, Ltd*, 1972.

[138] D. L. Pavia, G. M. Lampman, G. S. Kriz, and J. R. Vyvyan, “Introduction to spectroscopy,” 2015.

[139] G. F. Monnier, “A review of infrared spectroscopy in microarchaeology: Methods, applications, and recent trends,” *Journal of Archaeological Science: Reports*, vol. 18, pp. 806–823, 2018.

[140] B. Schrader, *Infrared and Raman spectroscopy: methods and applications*. John Wiley& Sons, 2008.

[141] N. Tsoulfanidis and S. Landsberger, *Measurement and detection of radiation*. CRC press, 2021.

[142] J. Coates, “Interpretation of infrared spectra, a practical approach,” *Encyclopedia of analytical chemistry*, vol. 12, pp. 10815–10837, 2000.

[143] M. El-Azazy, “Infrared Spectroscopy: Principles, Advances, and Applications,” 2019.

[144] M. El-Azazy, “Introductory chapter: infrared spectroscopy-A synopsis of the fundamentals and applications,” *Infrared spectroscopy-principles, advances, and applications*, pp. 1–10, 2018.

[145] B. C. Smith, *Infrared spectral interpretation: a systematic approach*. CRC press, 2018.

[146] G. R. Fowles, *Introduction to modern optics*. Courier Corporation, 1989.

[147] H. H. Telle, A. G. Ureņa, and R. J. Donovan, *Laser chemistry: spectroscopy, dynamics and applications*. John Wiley& Sons, 2007.

[148] J. Workman Jr and A. Springsteen, *Applied spectroscopy: a compact reference for practitioners*. Academic Press, 1998.

[149] B. C. Smith, *Fundamentals of Fourier transform infrared spectroscopy*. CRC press, 2011.

[150] Y. Ozaki, “Infrared spectroscopy—Mid-infrared, near-infrared, and far-infrared/terahertz spectroscopy,” *Analytical Sciences*, vol. 37, no. 9, pp. 1193–1212, 2021.

[151] J. L. Koenig, *Infrared and Raman spectroscopy of polymers*, vol. 12. iSmithers Rapra Publishing, 2001.

[152] C. N. Banwell and E. M. McCash, *Fundamentals of molecular spectroscopy*. Indian Edition, 2017.

[153] B. H. Stuart, *Infrared spectroscopy: fundamentals and applications*. John Wiley& Sons, 2004.

[154] PA Atkins, “Physical Chemistry,” 2006.

[155] Y. Ozaki, C. Huck, S. Tsuchikawa, and S. B. Engelsen, *Near-infrared spectroscopy: theory, spectral analysis, instrumentation, and applications*. Springer, 2021.

[156] C. Pasquini, “Near infrared spectroscopy: A mature analytical technique with new perspectives – A review,” *Analytica Chimica Acta*, vol. 1026, pp. 8–36, 2018.

[157] J. Haas and B. Mizaikoff, “Advances in mid-infrared spectroscopy for chemical analysis,” *Annual Review of Analytical Chemistry*, vol. 9, no. 1, pp. 45–68, 2016.

[158] S. De Bruyne, M. M. Speeckaert, and J. R. Delanghe, “Applications of mid-infrared spectroscopy in the clinical laboratory setting,” *Critical Reviews in Clinical Laboratory Sciences*, vol. 55, pp. 1–20, Jan. 2018.

[159] HC Sherman, “Handbook of Instrumental Techniques for Analytical Chemistry,” *New Jersey: Prentice Hall*, 1997.

[160] S. Prati, G. Sciutto, I. Bonacini, and R. Mazzeo, “New frontiers in application of FTIR microscopy for characterization of cultural heritage materials,” *Analytical Chemistry for Cultural Heritage*, pp. 129–160, 2017.

[161] H. Buijs, “Infrared Spectroscopy,” *Springer Handbooks*, vol. 71, no. 12, pp. 607–613, 2006.

[162] J. P. Keogh, “Instrumental advances and applications in millimeter/submillimeter-wave spectroscopy,” 2018.

[163] R. A. Millikan, “Albert Abraham Michelson,” *National Academy Biographical Memoirs*, vol. 19, 1939.

[164] B. Jaleh and P. Fakhri, “Infrared and Fourier transform infrared spectroscopy for nanofillers and their nanocomposites,” in *Spectroscopy of polymer nanocomposites*, pp. 112–129, Elsevier, 2016.

[165] G. Ramer and B. Lendl, “Attenuated Total Reflection F ourier Transform Infrared Spectroscopy,” *Encyclopedia of analytical chemistry: applications, theory and instrumentation*, 2006.

[166] F. M. Mirabella, *Internal reflection spectroscopy: theory and applications*. CRC Press, 2020.

[167] M. Milosevic, “Internal reflection and ATR spectroscopy,” *Applied Spectroscopy Reviews*, vol. 39, no. 3, pp. 365–384, 2004.

[168] J. Grdadolnik, “ATR-FTIR spectroscopy: Its advantage and limitations,” *Acta Chimica Slovenica*, vol. 49, no. 3, pp. 631–642, 2002.

[169] K. Vishwanath, K. Chang, D. Klein, Y. F. Deng, V. Chang, J. E. Phelps, and N. Ramanujam, “Portable, fiber-based, diffuse reflection spectroscopy (DRS) systems for estimating tissue optical properties,” *Applied spectroscopy*, vol. 65, no. 2, pp. 206–215, 2011.

[170] J. Torrent and V. Barrón, “Diffuse reflectance spectroscopy,” *Methods of Soil Analysis Part 5—Mineralogical Methods*, vol. 5, pp. 367–385, 2008.

[171] P. B. Coleman, *Practical sampling techniques for infrared analysis*. CRC Press, 2020.

[172] S. R. Culler, “Diffuse reflectance infrared spectroscopy: Sampling techniques for qualitative/quantitative analysis of solids,” in *Practical sampling techniques for infrared analysis*, pp. 93–105, CRC Press, 2020.

[173] B. Goh, K. Ching, R. J. Soares Magalhães, S. Ciocchetta, M. D. Edstein, R. Maciel-De-freitas, and M. T. Sikulu-Lord, “The application of spectroscopy techniques for diagnosis of malaria parasites and arboviruses and surveillance of mosquito vectors: A systematic review and critical appraisal of evidence,” *PLoS Neglected Tropical Diseases*, vol. 15, no. 4, pp. 1–24, 2021.

[174] I. H. Mshani, D. J. Siria, E. P. Mwanga, B. B. D. Sow, R. Sanou, M. Opiyo, M. T. Sikulu-Lord, H. M. Ferguson, A. Diabate, K. Wynne, M. González-Jiménez, F. Baldini, S. A. Babayan, and F. Okumu, “Key considerations, target product profiles, and research gaps in the application of infrared spectroscopy and artificial intelligence for malaria surveillance and diagnosis,” *Malaria Journal*, vol. 22, no. 1, p. 346, 2023.

[175] W. Ertel, *Introduction to artificial intelligence*. Springer, 2018.

[176] G. Oppy and D. Dowe, “The turing test,” 2003.

[177] IBM Data and AI Team, “Understanding the different types of artificial intelligence,” *https://www.ibm.com/think/topics/artificial-intelligence-types*, 2023.

[178] G. James, D. Witten, T. Hastie, and R. Tibshirani, *An Introduction to Statistical Learning: with Applications in R*. Springer Science & Business Media, 2nd ed., 2023.

[179] M. Mohammed, M. B. Khan, and E. B. M. Bashier, *Machine learning: algorithms and applications*. Crc Press, 2016.

[180] J. G. Greener, S. M. Kandathil, L. Moffat, and D. T. Jones, “A guide to machine learning for biologists.,” *Nature reviews. Molecular cell biology*, vol. 23, pp. 40–55, Jan. 2022.

[181] J. E. Van Engelen and H. H. Hoos, “A survey on semi-supervised learning,” *Machine learning*, vol. 109, no. 2, pp. 373–440, 2020.

[182] M. A. Wiering and M. Van Otterlo, “Reinforcement learning,” *Adaptation, learning, and optimization*, vol. 12, no. 3, p. 729, 2012.

[183] N. M. Ralbovsky and I. K. Lednev, “Towards development of a novel universal medical diagnostic method: Raman spectroscopy and machine learning,” *Chemical Society Reviews*, vol. 49, no. 20, pp. 7428–7453, 2020.

[184] C. A. Meza Ramirez, M. Greenop, L. Ashton, and I. U. Rehman, “Applications of machine learning in spectroscopy,” *Applied Spectroscopy Reviews*, vol. 56, no. 8-10, pp. 733–763, 2021.

[185] M. Paraskevaidi, B. J. Matthew, B. J. Holly, B. J. Hugh, C. P. V. Thulya, C. Loren, C. StJohn, G. Peter, G. Callum, and K. G. Sergei, “Clinical applications of infrared and Raman spectroscopy in the fields of cancer and infectious diseases,” *Applied Spectroscopy Reviews*, vol. 56, no. 8-10, pp. 804–868, 2021.

[186] A. Sohail, S. Khan, R. Ullah, S. A. Qureshi, M. Bilal, and A. Khan, “Analysis of hepatitis C infection using Raman spectroscopy and proximity based classification in the transformed domain,” *Biomedical optics express*, vol. 9, no. 5, pp. 2041–2055, 2018.

[187] T. Mahmood, H. Nawaz, A. Ditta, M. I. Majeed, M. A. Hanif, N. Rashid, H. N. Bhatti, H. F. Nargis, M. Saleem, F. Bonnier, and H. J. Byrne, “Raman spectral analysis for rapid screening of dengue infection,” *Spectrochimica Acta Part A: Molecular and Biomolecular Spectroscopy*, vol. 200, pp. 136–142, 2018.

[188] M. Laroche, L. Almeras, E. Pecchi, Y. Bechah, D. Raoult, A. Viola, and P. Parola, “Maldi-tof ms as an innovative tool for detection of plasmodium parasites in anopheles mosquitoes,” *Malaria Journal*, vol. 16, pp. 1–10, 2017.

[189] J. Murugaiyan and U. Roesler, “Maldi-tof ms profiling-advances in species identification of pests, parasites, and vectors,” *Frontiers in cellular and infection microbiology*, vol. 7, p. 184, 2017.

[190] S. Angeletti, “Matrix assisted laser desorption time of flight mass spectrometry (maldi-tof ms) in clinical microbiology,” *Journal of microbiological methods*, vol. 138, pp. 20–29, 2017.

[191] M. A. Stauning, C. S. Jensen, T. Staalsøe, and J. A. Kurtzhals, “Detection and quantification of plasmodium falciparum in human blood by matrix-assisted laser desorption/ionization time-of-flight mass spectrometry: A proof of concept study,” *Malaria Journal*, vol. 22, no. 1, p. 285, 2023.

[192] R. McGalliard, H. Muhamadali, N. AlMasoud, S. Haldenby, V. Romero-Soriano, E. Allman, Y. Xu, A. P. Roberts, S. Paterson, E. D. Carrol, *et al.*, “Bacterial discrimination by fourier transform infrared spectroscopy, maldi-mass spectrometry and whole-genome sequencing,” *Future Microbiology*, no. 0, 2024.

[193] World Health Organization (WHO), “Malaria surveillance, monitoring and evaluation: a reference manual,” 2018.

[194] World Health Organization (WHO), “Global technical strategy for malaria 2016-2030,” *World Health Organization*, 2015.

[195] World Health Organization (WHO), “Test, treat, track: scaling up diagnostic testing, treatment and surveillance for malaria,” tech. rep., 2012.

[196] MalERA:, *An updated research agenda for diagnostics, drugs, vaccines, and vector control in malaria elimination and eradication.*, vol. 14. 2017.

[197] UNITAID, “2015 Malaria Diagnostics Landscape Update,” no. February, 2015.

[198] malERA Refresh Consultative Panel on Characterising the Reservoir and M. Transmission, “malera: An updated research agenda for characterising the reservoir and measuring transmission in malaria elimination and eradication,” *PLoS medicine*, vol. 14, no. 11, p. e1002452, 2017.

[199] T. Bousema, L. Okell, S. Shekalaghe, J. T. Griffin, S. Omar, P. Sawa, C. Sutherland, R. Sauerwein, A. C. Ghani, and C. Drakeley, “Revisiting the circulation time of Plasmodium falciparum gametocytes: molecular detection methods to estimate the duration of gametocyte carriage and the effect of gametocytocidal drugs,” *Malaria journal*, vol. 9, no. 1, pp. 1–11, 2010.

[200] H. Lamptey, M. F. Ofori, K. A. Kusi, B. Adu, E. Owusu-Yeboa, E. Kyei-Baafour, A. T. Arku, S. Bosomprah, M. Alifrangis, and I. A. Quakyi, “The prevalence of submicroscopic Plasmodium falciparum gametocyte carriage and multiplicity of infection in children, pregnant women and adults in a low malaria transmission area in Southern Ghana,” *Malaria journal*, vol. 17, no. 1, pp. 1–12, 2018.

[201] J. I. Nankabirwa, A. Yeka, E. Arinaitwe, R. Kigozi, C. Drakeley, M. R. Kamya, B. Greenhouse, P. J. Rosenthal, G. Dorsey, and S. G. Staedke, “Estimating malaria parasite prevalence from community surveys in Uganda: a comparison of microscopy, rapid diagnostic tests and polymerase chain reaction,” *Malaria Journal*, vol. 14, no. 1, p. 528, 2015.

[202] D. L. Smith and F. E. McKenzie, “Statics and dynamics of malaria infection in Anopheles mosquitoes,” 2004.

[203] S. E. Bellan, “The importance of age dependent mortality and the extrinsic incubation period in models of mosquito-borne disease transmission and control,” *PLoS One*, vol. 5, no. 4, p. e10165, 2010.

[204] D. L. Smith, K. E. Battle, S. I. Hay, C. M. Barker, T. W. Scott, and F. E. McKenzie, “Ross, Macdonald, and a theory for the dynamics and control of mosquito-transmitted pathogens,” *PLoS pathogens*, vol. 8, no. 4, p. e1002588, 2012.

[205] N. Protopopoff, J. F. Mosha, E. Lukole, J. D. Charlwood, A. Wright, C. D. Mwalimu, A. Manjurano, F. W. Mosha, W. Kisinza, I. Kleinschmidt, and M. Rowland, “Effectiveness of a long-lasting piperonyl butoxide-treated insecticidal net and indoor residual spray interventions, separately and together, against malaria transmitted by pyrethroid-resistant mosquitoes: a cluster, randomised controlled, two-by-two fact,” *The Lancet*, 2018.

[206] C. Garrett-Jones and B. Grab, “The assessment of insecticidal impact on the malaria mosquito’s vectorial capacity, from data on the proportion of parous females.,” *Bulletin of the World Health Organization*, vol. 31, no. 1, pp. 71–86, 1964.

[207] C. Garrett-Jones, A. Dranga, R. Marinov, M. Mihai, and W. H. Organization, “Epidemiological entomology and its application to malaria,” tech. rep., 1968.

[208] J. C. Beier, P. V. Perkins, J. K. Koros, F. K. Onyango, T. P. Gargan, R. A. Wirtz, D. K. Koech, and C. R. Roberts, “Malaria sporozoite detection by dissection and ELISA to assess infectivity of afrotropical Anopheles (Diptera: Culicidae).,” *Journal of medical entomology*, vol. 27, no. 3, pp. 377–384, 1990.

[209] V. Chaumeau, C. Andolina, B. Fustec, N. Tuikue Ndam, C. Brengues, S. p. Herder, D. Cerqueira, T. Chareonviriyaphap, F. Nosten, and V. Corbel, “Comparison of the performances of five primer sets for the detection and quantification of Plasmodium in anopheline vectors by real-time PCR,” *PLoS One*, vol. 11, no. 7, p. e0159160, 2016.

[210] J. B. Silver, *Mosquito ecology: field sampling methods*. springer science& business media, 2007.

[211] T. R. Burkot, R. Farlow, M. Min, E. Espino, A. Mnzava, and T. L. Russell, “A global analysis of National Malaria Control Programme vector surveillance by elimination and control status in 2018,” *Malaria Journal*, vol. 18, no. 1, pp. 1–12, 2019.

[212] M. González Jiménez, S. A. Babayan, P. Khazaeli, M. Doyle, F. Walton, E. Reedy, T. Glew, M. Viana, L. Ranford-Cartwright, A. Niang, D. J. Siria, F. O. Okumu, A. Diabaté, H. M. Ferguson, F. Baldini, and K. Wynne, “Prediction of

mosquito species and population age structure using mid-infrared spectroscopy and supervised machine learning," *Wellcome Open Research*, vol. 4, no. May, p. 76, 2019.

[213] D. J. Siria, R. Sanou, J. Mitton, E. P. Mwanga, A. Niang, I. Sare, P. C. D. Johnson, G. M. Foster, A. M. G. Belem, K. Wynne, R. Murray-Smith, H. M. Ferguson, M. González-Jiménez, S. A. Babayan, A. Diabaté, F. O. Okumu, and F. Baldini, "Rapid age-grading and species identification of natural mosquitoes for malaria surveillance," *Nature Communications*, vol. 13, no. 1, p. 1501, 2022.

[214] M. P. Milali, M. T. Sikulu-Lord, S. S. Kiware, F. E. Dowell, G. F. Corliss, and R. J. Povinelli, "Age grading an. gambiae and an. arabiensis using near infrared spectra and artificial neural networks," *PloS one*, vol. 14, no. 8, p. e0209451, 2019.

[215] M. P. Milali, S. S. Kiware, N. J. Govella, F. Okumu, N. Bansal, S. Bozdag, J. D. Charlwood, M. F. Maia, S. B. Ogoma, F. E. Dowell, *et al.*, "An autoencoder and artificial neural network-based method to estimate parity status of wild mosquitoes from near-infrared spectra," *PloS one*, vol. 15, no. 6, p. e0234557, 2020.

[216] E. P. Mwanga, S. A. Mapua, D. J. Siria, H. S. Ngowo, F. Nangacha, J. Mgando, F. Baldini, M. González Jiménez, H. M. Ferguson, K. Wynne, *et al.*, "Using mid-infrared spectroscopy and supervised machine-learning to identify vertebrate blood meals in the malaria vector, anopheles arabiensis," *Malaria Journal*, vol. 18, pp. 1–9, 2019.

[217] E. P. Mwanga, E. G. Minja, E. Mrimi, M. G. Jiménez, J. K. Swai, S. Abbasi, H. S. Ngowo, D. J. Siria, S. Mapua, C. Stica, *et al.*, "Detection of malaria parasites in dried human blood spots using mid-infrared spectroscopy and logistic regression analysis," *Malaria journal*, vol. 18, pp. 1–13, 2019.

[218] P. Heraud, P. Chatchawal, M. Wongwattanakul, P. Tippayawat, C. Doerig, P. Jearanaikoon, D. Perez-Guaita, and B. R. Wood, "Infrared spectroscopy coupled to cloud-based data management as a tool to diagnose malaria: A pilot study in a malaria-endemic country ," *Malaria Journal*, 2019.

[219] G. T. Webster, K. A. de Villiers, T. J. Egan, S. Deed, L. Tilley, M. J. Tobin, K. R. Bambery, D. McNaughton, and B. R. Wood, "Discriminating the Intraerythrocytic Lifecycle Stages of the Malaria Parasite Using Synchrotron FT-IR Microspectroscopy and an Artificial Neural Network," *Analytical Chemistry*, vol. 81, pp. 2516–2524, Apr. 2009.

[220] M. F. Maia, M. Kapulu, M. Muthui, M. G. Wagah, H. M. Ferguson, F. E. Dowell, F. Baldini, and L. Ranford-Cartwright, “Detection of Plasmodium falciparum infected Anopheles gambiae using near-infrared spectroscopy,” *Malaria Journal*, vol. 18, no. 1, pp. 1–11, 2019.

[221] A. Fried and D. Richter, “Infrared absorption spectroscopy,” *Analytical Techniques for Atmospheric Measurement*, vol. 1, pp. 72–146, 2006.

[222] A. Khoshmanesh, M. W. A. Dixon, S. Kenny, L. Tilley, D. McNaughton, and B. R. Wood, “Detection and Quantification of Early-Stage Malaria Parasites in Laboratory Infected Erythrocytes by Attenuated Total Reflectance Infrared Spectroscopy and Multivariate Analysis,” *Analytical Chemistry*, vol. 86, pp. 4379–4386, May 2014.

[223] J. N. Fernandes, L. M. B. Dos Santos, T. Chouin-Carneiro, M. G. Pavan, G. A. Garcia, M. R. David, J. C. Beier, F. E. Dowell, R. Maciel-de Freitas, and M. T. Sikulu-Lord, “Rapid, noninvasive detection of Zika virus in Aedes aegypti mosquitoes by near-infrared spectroscopy,” *Science advances*, vol. 4, no. 5, p. eaat0496, 2018.

[224] World Health Organization (WHO) and Regional Office for the Western Pacific, “Giemsa Staining of Malaria Blood Films,” 2016.

[225] World Health Organization (WHO), “Policy recommendation on malaria diagnostics in low transmission settings . March 2014.,” *March*, 2014.

[226] N. Tangpukdee, C. Duangdee, P. Wilairatana, and S. Krudsood, “Malaria diagnosis: a brief review,” *The Korean journal of parasitology*, vol. 47, no. 2, p. 93, 2009.

[227] L. M. Milne, M. S. Kyi, P. L. Chiodini, and D. C. Warhurst, “Accuracy of routine laboratory diagnosis of malaria in the United Kingdom.,” *Journal of clinical pathology*, vol. 47, no. 8, pp. 740–742, 1994.

[228] P. Mogeni, T. N. Williams, I. Omedo, D. Kimani, J. M. Ngoi, J. Mwacharo, R. Morter, C. Nyundo, J. Wambua, G. Nyangweso, M. Kapulu, G. Fegan, and P. Bejon, “Detecting Malaria Hotspots: A Comparison of Rapid Diagnostic Test, Microscopy, and Polymerase Chain Reaction,” *The Journal of Infectious Diseases*, vol. 216, pp. 1091–1098, Nov. 2017.

[229] N. M. Pham, W. Karlen, H. P. Beck, and E. Delamarche, “Malaria and the ’last’ parasite: How can technology help?,” *Malaria Journal*, vol. 17, no. 1, pp. 1–16, 2018.

[230] F. Odhiambo, A. M. Buff, C. Moranga, C. M. Moseti, J. O. Wesongah, S. A. Lowther, W. Arvelo, T. Galgalo, T. O. Achia, and Z. G. Roka, “Factors associated with malaria microscopy diagnostic performance following a pilot quality-assurance programme in health facilities in malaria low-transmission areas of Kenya, 2014,” *Malaria journal*, vol. 16, no. 1, pp. 1–10, 2017.

[231] J. Cunningham, S. Jones, M. L. Gatton, J. W. Barnwell, Q. Cheng, P. L. Chiodini, J. Glenn, S. Incardona, C. Kosack, J. Luchavez, D. Menard, S. Nhem, W. Oyibo, R. R. Rees-Channer, I. Gonzalez, and D. Bell, “A review of the WHO malaria rapid diagnostic test product testing programme (2008-2018): Performance, procurement and policy,” *Malaria Journal*, vol. 18, no. 1, 2019.

[232] “New perspectives : malaria diagnosis : report of a joint WHO/USAID informal consultation, 25-27 October 1999.”

[233] S. Shillcutt, C. Morel, C. Goodman, P. Coleman, D. Bell, C. J. Whitty, and A. Mills, “Cost-effectiveness of malaria diagnostic methods in sub-Saharan Africa in an era of combination therapy,” *Bulletin of the World Health Organization*, vol. 86, no. 2, pp. 101–110, 2008.

[234] P. J. Rosenthal, “How do we best diagnose malaria in Africa?,” *The American journal of tropical medicine and hygiene*, vol. 86, no. 2, p. 192, 2012.

[235] P. Bualombai, W. Satimai, D. Rodnak, P. Ruangsirarak, K. Congpuong, and S. Boonpheng, “Detecting Malaria Using SD Bioline Malaria Pf/PAN (HRP2, pLDH),” *Journal of Health Research*, vol. 27, no. 3, pp. 135–138, 2013.

[236] D. Gamboa, M.-F. Ho, J. Bendezu, K. Torres, P. L. Chiodini, J. W. Barnwell, S. Incardona, M. Perkins, D. Bell, J. McCarthy, and Q. Cheng, “A Large Proportion of P. falciparum Isolates in the Amazon Region of Peru Lack pfhrp2 and pfhrp3: Implications for Malaria Rapid Diagnostic Tests,” *PLOS ONE*, vol. 5, p. e8091, Jan. 2010.

[237] S. Mihreteab, K. Anderson, C. Pasay, D. Smith, M. L. Gatton, J. Cunningham, A. Berhane, and Q. Cheng, “Epidemiology of mutant Plasmodium falciparum parasites lacking histidine-rich protein 2/3 genes in Eritrea 2 years after switching from HRP2-based RDTs,” *Scientific Reports*, vol. 11, no. 1, pp. 1–12, 2021.

[238] S. M. Feleke, E. N. Reichert, H. Mohammed, B. G. Brhane, K. Mekete, H. Mamo, B. Petros, H. Solomon, E. Abate, and C. Hennelly, “Plasmodium falciparum is evolving to escape malaria rapid diagnostic tests in Ethiopia,” *Nature microbiology*, vol. 6, no. 10, pp. 1289–1299, 2021.

[239] R. Thomson, K. B. Beshir, J. Cunningham, F. Baiden, J. Bharmal, K. J. Bruxvoort, C. Maiteki-Sebuguzi, S. Owusu-Agyei, S. G. Staedke, and H. Hopkins, “pfhrp2 and pfhrp3 gene deletions that affect malaria rapid diagnostic tests for Plasmodium falciparum: analysis of archived blood samples from 3 African countries,” *The Journal of infectious diseases*, vol. 220, no. 9, pp. 1444–1452, 2019.

[240] J. Maltha, D. Gamboa, J. Bendezu, L. Sanchez, L. Cnops, P. Gillet, and J. Jacobs, “Rapid diagnostic tests for malaria diagnosis in the Peruvian Amazon: impact of pfhrp2 gene deletions and cross-reactions,” 2012.

[241] O. A. Koita, O. K. Doumbo, A. Ouattara, L. K. Tall, A. Konaré, M. Diakité, M. Diallo, I. Sagara, G. L. Masinde, and S. N. Doumbo, “False-negative rapid diagnostic tests for malaria and deletion of the histidine-rich repeat region of the hrp2 gene,” *The American journal of tropical medicine and hygiene*, vol. 86, no. 2, p. 194, 2012.

[242] J. B. Parr, R. Verity, S. M. Doctor, M. Janko, K. Carey-Ewend, B. J. Turman, C. Keeler, H. C. Slater, A. N. Whitesell, and K. Mwandagalirwa, “Pfhrp2-deleted Plasmodium falciparum parasites in the Democratic Republic of the Congo: a national cross-sectional survey,” *The Journal of infectious diseases*, vol. 216, no. 1, pp. 36–44, 2017.

[243] K. B. Beshir, N. Epúlveda, J. Bharmal, A. Robinson, J. Mwanguzi, A. O. Busula, J. G. De Boer, C. Sutherland, J. Cunningham, and H. Hopkins, “Plasmodium falciparum parasites with histidine-rich protein 2 (pfhrp2) and pfhrp3 gene deletions in two endemic regions of Kenya,” *Scientific reports*, vol. 7, no. 1, pp. 1–10, 2017.

[244] T. Hänscheid and M. P. Grobusch, “How useful is PCR in the diagnosis of malaria?,” *Trends in parasitology*, vol. 18, pp. 395–398, Sept. 2002.

[245] L. C. Okell, A. C. Ghani, E. Lyons, and C. J. Drakeley, “Submicroscopic infection in plasmodium falciparum-endemic populations: A systematic review and meta-analysis,” *Journal of Infectious Diseases*, vol. 200, no. 10, pp. 1509–1517, 2009.

[246] G. Snounou, “Detection and identification of the four malaria parasite species infecting humans by PCR amplification.,” *Methods in molecular biology (Clifton, N.J.)*, vol. 50, pp. 263–291, 1996.

[247] F. Perandin, N. Manca, A. Calderaro, G. Piccolo, L. Galati, L. Ricci, M. C. Medici, M. C. Arcangeletti, G. Snounou, and G. Dettori, “Development of a real-time PCR assay for detection of Plasmodium falciparum, Plasmodium vivax, and Plasmodium ovale for routine clinical diagnosis,” *Journal of clinical microbiology*, vol. 42, no. 3, pp. 1214–1219, 2004.

[248] D. Sumari, F. Mwingira, M. Selemani, J. Mugasa, K. Mugittu, and P. Gwakisa, “Malaria prevalence in asymptomatic and symptomatic children in Kiwangwa, Bagamoyo district, Tanzania,” *Malaria journal*, vol. 16, no. 1, pp. 1–7, 2017.

[249] G. Cottrell, A. Moussiliou, A. J. F. Luty, M. Cot, N. Fievet, A. Massougbodji, P. Deloron, and N. Tuikue Ndam, “Submicroscopic Plasmodium falciparum infections are associated with maternal anemia, premature births, and low birth weight,” *Clinical Infectious Diseases*, vol. 60, no. 10, pp. 1481–1488, 2015.

[250] U. Morris, W. Xu, M. I. Msellem, A. Schwartz, A. Abass, D. Shakely, J. Cook, A. Bhattarai, M. Petzold, and B. Greenhouse, “Characterising temporal trends in asymptomatic Plasmodium infections and transporter polymorphisms during transition from high to low transmission in Zanzibar, 2005–2013,” *Infection, genetics and evolution*, vol. 33, pp. 110–117, 2015.

[251] E. Baum, J. Sattabongkot, J. Sirichaisinthop, K. Kiattibutr, D. H. Davies, A. Jain, E. Lo, M.-C. Lee, A. Z. Randall, and D. M. Molina, “Submicroscopic and asymptomatic Plasmodium falciparum and Plasmodium vivax infections are common in western Thailand-molecular and serological evidence,” *Malaria journal*, vol. 14, no. 1, pp. 1–11, 2015.

[252] S. Karl, D. Gurarie, P. A. Zimmerman, C. H. King, T. G. St. Pierre, and T. M. E. Davis, “A sub-microscopic gametocyte reservoir can sustain malaria transmission,” *PloS one*, vol. 6, no. 6, p. e20805, 2011.

[253] M. T. Makler, C. J. Palmer, and A. L. Ager, “A review of practical techniques for the diagnosis of malaria,” *Annals of tropical medicine and parasitology*, vol. 92, no. 4, pp. 419–434, 1998.

[254] O. Ogunfowokan, A. I. Nwajei, and B. A. Ogunfowokan, “Sensitivity and specificity of malaria rapid diagnostic test (mRDT CareStatTM) compared with microscopy amongst under five children attending a primary care clinic in southern Nigeria,” *African Journal of Primary Health Care and Family Medicine*, vol. 12, no. 1, pp. 1–8, 2020.

[255] T. T. Timbrook, J. B. Morton, K. W. McConeghy, A. R. Caffrey, E. Mylonakis, and K. L. LaPlante, “The effect of molecular rapid diagnostic testing on clinical outcomes in bloodstream infections: a systematic review and meta-analysis,” *Clinical Infectious Diseases*, p. ciw649, 2016.

[256] M. A. C. Dowling and G. T. Shute, “A comparative study of thick and thin blood films in the diagnosis of scanty malaria parasitaemia,” *Bulletin of the World health Organization*, vol. 34, no. 2, p. 249, 1966.

[257] L. Kamau, M. Coetzee, R. H. Hunt, and L. L. Koekemoer, “A cocktail polymerase chain reaction assay to identify members of the Anopheles funestus (Diptera: Culicidae) group.,” *The American Journal of Tropical Medicine and Hygiene*, vol. 66, no. 6, pp. 804–811, 2017.

[258] A. S. Bell and L. C. Ranford-Cartwright, “A real-time PCR assay for quantifying Plasmodium falciparum infections in the mosquito vector,” *International Journal for Parasitology*, vol. 34, no. 7, pp. 795–802, 2004.

[259] M. W. Service and M. W. Service, “Estimation of the Mortalities of the Immature Stages and Adults,” *Mosquito ecology: field sampling methods*, pp. 752–889, 1993.

[260] G. Davidson, “Estimation of the survival-rate of anopheline mosquitoes in nature ,” *Nature*, vol. 174, no. 4434, pp. 792–793, 1954.

[261] T. S. Detinova, “Age-grouping methods in Diptera of medical importance with special reference to some vectors of malaria.,” *Monograph series. World Health Organization*, 1962.

[262] V. P. Polovodova, “The determination of the physiological age of female Anopheles by the number of gonotrophic cycles completed,” *Meditsinskaia parazitologiia i parazitarnye bolezni*, 1949.

[263] W. N. Beklemishev, T. S. Detinova, and V. P. Polovodova, “Determination of physiological age in anophelines and of age distribution in anopheline populations in the USSR.,” *Bulletin of the World Health Organization*, 1959.

[264] T. Hoc and J. Charlwood, “Age determination of Aedes cantans using the ovarian oil injection technique,” *Medical and Veterinary Entomology*, 1990.

[265] J. C. Beier, P. V. Perkins, R. A. Wirtz, R. E. Whitmire, M. Mugambi, and W. T. Hockmeyer, “Field evaluation of an enzyme-linked immunosorbent assay (ELISA) for Plasmodium falciparum sporozoite detection in anopheline mosquitoes from Kenya,” *American Journal of Tropical Medicine and Hygiene*, vol. 36, no. 3, pp. 459–468, 1987.

[266] A. Tassanakajon, V. Boonsaeng, P. Wilairat, and S. Panyim, “Polymerase chain reaction detection of Plasmodium falciparum in mosquitoes,” *Transactions of the Royal Society of Tropical Medicine and Hygiene*, vol. 87, no. 3, pp. 273–275, 1993.

[267] C. Bass, D. Nikou, A. M. Blagborough, J. Vontas, R. E. Sinden, M. S. Williamson, and L. M. Field, “PCR-based detection of Plasmodium in Anopheles mosquitoes: a comparison of a new high-throughput assay with existing methods,” *Malaria journal*, vol. 7, no. 1, pp. 1–9, 2008.

[268] E. Erlank, L. L. Koekemoer, and M. Coetzee, “The importance of morphological identification of African anopheline mosquitoes (Diptera: Culicidae) for malaria control programmes,” *Malaria Journal*, vol. 17, no. 1, pp. 1–7, 2018.

[269] L. L. Koekemoer, L. Kamau, R. H. Hunt, M. Coetzee, R. H. Hunt, L. L. Koekemoer, L. Kamau, R. H. Hunt, and M. Coetzee, “A cocktail polymerase chain reaction assay to identify members of the Anopheles funestus (Diptera: Culicidae) group.,” *The American journal of tropical medicine and hygiene*, vol. 66, no. 6, pp. 804–811, 2002.

[270] J. A. Scott, W. G. Brogdon, and F. H. Collins, “Identification of single specimens of the Anopheles gambiae complex by the polymerase chain reaction,” *American Journal of Tropical Medicine and Hygiene*, vol. 49, no. 4, pp. 520–529, 1993.

[271] F. Jourdain, M. Picard, T. Sulesco, N. Haddad, Z. Harrat, S. S. Sawalha, F. Günay, K. Kanani, T. Shaibi, and D. Akhramenko, “Identification of mosquitoes (Diptera: Culicidae): an external quality assessment of medical entomology laboratories in the MediLabSecure Network,” *Parasites& vectors*, vol. 11, no. 1, pp. 1–7, 2018.

[272] R. A. Wirtz, F. Zavala, Y. Charoenvit, G. H. Campbell, T. R. Burkot, I. Schneider, K. M. Esser, R. L. Beaudoin, and R. G. Andre, “Comparative testing of monoclonal antibodies against Plasmodium falciparum sporozoites for ELISA development,” *Bulletin of the World Health Organization*, vol. 65, no. 1, p. 39, 1987.

[273] T. R. Burkot, F. Zavala, R. W. Gwadz, F. H. Collins, R. S. Nussenzweig, and D. R. Roberts, “Identification of malaria-infected mosquitoes by a two-site enzyme-linked immunosorbent assay.,” *The American journal of tropical medicine and hygiene*, vol. 33, no. 2, pp. 227–231, 1984.

[274] J. C. Beier, P. V. Perkins, R. A. Wirtz, J. Koros, D. Diggs, T. P. Gargan II, and D. K. Koech, “Bloodmeal Identification by Direct Enzyme-Linked Immunosorbent Assay (Elisa), Tested on Anopheles (Diptera: Culicidae) in Kenya12,” *Journal of Medical Entomology*, vol. 25, pp. 9–16, Jan. 1988.

[275] R. J. Kent, “Molecular methods for arthropod bloodmeal identification and applications to ecological and vector-borne disease studies,” *Molecular ecology resources*, vol. 9, no. 1, pp. 4–18, 2009.

[276] B. J. Johnson, L. E. Hugo, T. S. Churcher, O. T. Ong, and G. J. Devine, “Mosquito Age Grading and Vector-Control Programmes,” 2020.

[277] R. Farlow, T. L. Russell, and T. R. Burkot, “Nextgen Vector Surveillance Tools: sensitive, specific, cost-effective and epidemiologically relevant,” *Malaria Journal*, vol. 19, no. 1, pp. 1–13, 2020.

[278] G. Davidson and C. C. Draper, “Field studies of some of the basic factors concerned in the transmission of malaria,” *Transactions of the Royal Society of Tropical Medicine and Hygiene*, vol. 47, no. 6, pp. 522–535, 1953.

[279] World Health Organization (WHO), “Global report on insecticide resistance in malaria vectors: 2010–2016,” 2018.

[280] F. Okumu, M. Gyapong, N. Casamitjana, M. C. Castro, M. A. Itoe, F. Okonofua, and M. Tanner, “What Africa can do to accelerate and sustain progress against malaria,” *PLOS Global Public Health*, vol. 2, no. 6, p. e0000262, 2022.

[281] M. Sikulu, G. F. Killeen, L. E. Hugo, P. A. Ryan, K. M. Dowell, R. A. Wirtz, S. J. Moore, and F. E. Dowell, “Near-infrared spectroscopy as a complementary age grading and species identification tool for African malaria vectors,” *Parasites& vectors*, vol. 3, no. 1, pp. 1–7, 2010.

[282] E. P. Mwanga, D. J. Siria, J. Mitton, I. H. Mshani, M. G. Jimenez, P. Selvaraj, K. Wynne, F. Baldini, F. O. Okumu, S. A. Babayan, M. González-Jiménez, P. Selvaraj, K. Wynne, F. Baldini, F. O. Okumu, and S. A. Babayan, “Using transfer learning and dimensionality reduction techniques to improve generalisability of machine-learning predictions of mosquito ages from mid-infrared spectra,” *BMC Bioinformatics*, vol. 24, no. 1, p. 11, 2023.

[283] G. A. Garcia, T. N. Kariyawasam, A. R. Lord, C. F. da Costa, L. B. Chaves, J. d. C. Lima-Junior, R. Freitas, and M. T. Sikulu-Lord, “Malaria absorption peaks acquired through the skin of patients with infrared light can detect patients with varying parasitemia,” *PNAS Nexus*, 2022.

[284] J. Grabska, C. W. Huck, K. B. Beć, J. Grabska, and C. W. Huck, “Near-Infrared Spectroscopy in Bio-Applications.,” *Molecules (Basel, Switzerland)*, vol. 25, June 2020.

[285] E. Y. K. Ng and M. Etehadtavakol, *Application of infrared to biomedical sciences*. Springer, 2017.

[286] B. B. Tarimo, V. O. Nyasembe, B. Ngasala, C. Basham, I. J. Rutagi, M. Muller, S. B. Chhetri, R. Rubinstein, J. J. Juliano, and M. Loya, “Seasonality and transmissibility of Plasmodium ovale in Bagamoyo District, Tanzania,” *Parasites& Vectors*, vol. 15, no. 1, pp. 1–6, 2022.

[287] L. Sroute, B. D. Byrd, and S. W. Huffman, “Classification of Mosquitoes with Infrared Spectroscopy and Partial Least Squares-Discriminant Analysis.,” *Applied spectroscopy*, vol. 74, pp. 900–912, Aug. 2020.

[288] A. Khoshmanesh, D. Christensen, D. Perez-Guaita, I. Iturbe-Ormaetxe, S. L. O'Neill, D. McNaughton, and B. R. Wood, "Screening of Wolbachia Endosymbiont Infection in Aedes aegypti Mosquitoes Using Attenuated Total Reflection Mid-Infrared Spectroscopy," *Analytical Chemistry*, 2017.

[289] D. Christensen, A. Khoshmanesh, D. Perez-Guaita, I. Iturbe-Ormaetxe, S. O'Neill, and B. Wood, "EXPRESS: Detection and Identification of Wolbachia pipientis Strains in Mosquito Eggs Using Attenuated Total Reflection Fourier Transform Infrared (ATR FT-IR) Spectroscopy," *Applied Spectroscopy*, p. 00037028211027140, 2021.

[290] L. M. B. Santos, M. Mutsaers, G. A. Garcia, M. R. David, M. G. Pavan, M. T. Petersen, J. Corrêa-Antônio, D. Couto-Lima, L. Maes, and F. Dowell, "High throughput estimates of Wolbachia, Zika and chikungunya infection in Aedes aegypti by near-infrared spectroscopy to improve arbovirus surveillance," *Communications biology*, vol. 4, no. 1, pp. 1–9, 2021.

[291] P. M. Esperança, A. M. Blagborough, D. F. Da, F. E. Dowell, and T. S. Churcher, "Detection of Plasmodium berghei infected Anopheles stephensi using near-infrared spectroscopy," *Parasites and Vectors*, vol. 11, no. 1, 2018.

[292] D. F. Da, R. McCabe, B. M. Somé, P. M. Esperan ça, K. A. Sala, J. Blight, A. M. Blagborough, F. Dowell, S. R. Yerbanga, and T. Lefèvre, "Detection of Plasmodium falciparum in laboratory-reared and naturally infected wild mosquitoes using near-infrared spectroscopy," *Scientific reports*, vol. 11, no. 1, pp. 1–8, 2021.

[293] B. J. Krajacich, J. I. Meyers, H. Alout, R. K. Dabiré, F. E. Dowell, and B. D. Foy, "Analysis of near infrared spectra for age-grading of wild populations of Anopheles gambiae," *Parasites and Vectors*, vol. 10, no. 1, pp. 1–13, 2017.

[294] M. P. Milali, S. S. Kiware, N. J. Govella, F. Okumu, N. Bansal, S. Bozdag, J. D. Charlwood, M. F. Maia, S. B. Ogoma, and F. E. Dowell, "An autoencoder and artificial neural network-based method to estimate parity status of wild mosquitoes from near-infrared spectra ," *PLoS One*, vol. 15, no. 6, p. e0234557, 2020.

[295] J. N. Mgaya, D. J. Siria, F. E. Makala, J. P. Mgando, J.-M. M. Vianney, E. P. Mwanga, and F. O. Okumu, "Effects of sample preservation methods and duration of storage on the performance of mid-infrared spectroscopy for predicting the age of malaria vectors," *Parasites& Vectors*, vol. 15, no. 1, p. 281, 2022.

[296] G. Snounou, S. Viriyakosol, W. Jarra, S. Thaithong, and K. Brown, “Identification of the four human malaria parasite species in field samples by the polymerase chain reaction and detection of a high prevalence of mixed infections,” *Molecular and Biochemical Parasitology*, vol. 58, no. 2, pp. 283–292, 1993.

[297] D. E. Goldberg, A. F. Slater, A. Cerami, and G. B. Henderson, “Hemoglobin degradation in the malaria parasite Plasmodium falciparum: an ordered process in a unique organelle.,” *Proceedings of the National Academy of Sciences*, vol. 87, no. 8, pp. 2931–2935, 1990.

[298] S. Roy, D. Perez-Guaita, D. W. Andrew, J. S. Richards, D. McNaughton, P. Heraud, and B. R. Wood, “Simultaneous ATR-FTIR Based Determination of Malaria Parasitemia, Glucose and Urea in Whole Blood Dried onto a Glass Slide,” *Analytical Chemistry*, vol. 89, pp. 5238–5245, May 2017.

[299] G. Lippi, “Machine learning in laboratory diagnostics: valuable resources or a big hoax?,” *Diagnosis*, vol. 8, no. 2, pp. 133–135, 2021.

[300] J. A. Adegoke, K. Kochan, P. Heraud, and B. R. Wood, “A Near-Infrared “Matchbox Size” Spectrometer to Detect and Quantify Malaria Parasitemia,” *Analytical Chemistry*, vol. 93, pp. 5451–5458, Apr. 2021.

[301] M. Martin, D. Perez-Guaita, D. W. Andrew, J. S. Richards, B. R. Wood, and P. Heraud, “The effect of common anticoagulants in detection and quantification of malaria parasitemia in human red blood cells by atr-ftir spectroscopy,” *Analyst*, vol. 142, no. 8, pp. 1192–1199, 2017.

[302] S. De Bruyne, M. M. Speeckaert, W. Van Biesen, and J. R. Delanghe, “Recent evolutions of machine learning applications in clinical laboratory medicine,” *Critical Reviews in Clinical Laboratory Sciences*, vol. 58, pp. 131–152, Feb. 2021.

[303] D. Perez-Guaita, D. Andrew, P. Heraud, J. Beeson, D. Anderson, J. Richards, and B. R. Wood, “High resolution FTIR imaging provides automated discrimination and detection of single malaria parasite infected erythrocytes on glass,” *Faraday Discussions*, vol. 187, no. 0, pp. 341–352, 2016.

[304] B. R. Wood, K. R. Bambery, M. W. A. Dixon, L. Tilley, M. J. Nasse, E. Mattson, and C. J. Hirschmugl, “Diagnosing malaria infected cells at the single cell level using focal plane array Fourier transform infrared imaging spectroscopy,” *Analyst*, vol. 139, no. 19, pp. 4769–4774, 2014.

[305] J. A. Adegoke, A. De Paoli, I. O. Afara, K. Kochan, D. J. Creek, P. Heraud, and B. R. Wood, “Ultraviolet/Visible and Near-Infrared Dual Spectroscopic Method for Detection and Quantification of Low-Level Malaria Parasitemia in Whole Blood,” *Analytical Chemistry*, vol. 93, no. 39, pp. 13302–13310, 2021.

[306] D. T. Kangoye, A. Noor, J. Midega, J. Mwongeli, D. Mkabili, P. Mogeni, C. Kerubo, P. Akoo, J. Mwangangi, and C. Drakeley, “Malaria hotspots defined by clinical malaria, asymptomatic carriage, PCR and vector numbers in a low transmission area on the Kenyan Coast,” *Malaria journal*, vol. 15, no. 1, pp. 1–13, 2016.

[307] M. N. Moyeh, I. M. Ali, D. L. Njimoh, A. M. Nji, P. M. Netongo, M. S. Evehe, B. Atogho-Tiedeu, S. M. Ghogomu, and W. F. Mbacham, “Comparison of the Accuracy of Four Malaria Diagnostic Methods in a High Transmission Setting in Coastal Cameroon,” *Journal of Parasitology Research*, vol. 2019, 2019.

[308] L. C. Okell, T. Bousema, J. T. Griffin, A. L. Ouédraogo, A. C. Ghani, and C. J. Drakeley, “Factors determining the occurrence of submicroscopic malaria infections and their relevance for control,” *Nature Communications*, vol. 3, pp. 1–9, 2012.

[309] M. Tetteh, D. Dwomoh, A. Asamoah, E. K. Kupeh, K. Malm, and J. Nonvignon, “Impact of malaria diagnostic refresher training programme on competencies and skills in malaria diagnosis among medical laboratory professionals: evidence from Ghana 2015–2019,” *Malaria Journal*, vol. 20, no. 1, pp. 1–12, 2021.

[310] A. Bazoumana BD Sow, Issa Mshani, Zephania Neema, Roger Sanou, Emmanuel Mwanga, Fredros O. Okumu and S. A. B. Diabaté, Jessica Enright, Simon Rogers, Francesco Baldini, “PAMCA Conference,” vol. ABS-416, pp. 67–68, 2022.

[311] F. E. Dowell, A. E. M. Noutcha, and K. Michel, “The effect of preservation methods on predicting mosquito age by near infrared spectroscopy,” *The American journal of tropical medicine and hygiene*, vol. 85, no. 6, p. 1093, 2011.

[312] D. Bell, A. E. Fleurent, M. C. Hegg, J. D. Boomgard, and C. C. McConnico, “Development of new malaria diagnostics: matching performance and need,” *Malaria Journal*, vol. 15, no. 1, pp. 1–12, 2016.

[313] B. Abuaku, L. E. Amoah, N. Y. Peprah, A. Asamoah, E. O. Amoako, D. Donu, G. A. Adu, and K. L. Malm, “Malaria parasitaemia and mRDT diagnostic performances among symptomatic individuals in selected health care facilities across Ghana,” *BMC Public Health*, vol. 21, p. 239, Dec. 2021.

[314] M. L. Wilson, “Malaria rapid diagnostic tests,” *Clinical Infectious Diseases*, vol. 54, no. 11, pp. 1637–1641, 2012.

[315] Y. Ge, D. Liang, J. Cao, R. Gosling, V. Mushi, and J. Huang, “How socioeconomic status affected the access to health facilities and malaria diagnosis in children under five years: findings from 19 sub-Saharan African countries,” *Infectious Diseases of Poverty*, vol. 12, no. 1, p. 29, 2023.

[316] M. L. Gatton, A. Chaudhry, J. Glenn, S. Wilson, Y. Ah, A. Kong, R. L. Ord, R. R. Rees-Channer, P. Chiodini, S. Incardona, Q. Cheng, M. Aidoo, and J. Cunningham, “Impact of Plasmodium falciparum gene deletions on malaria rapid diagnostic test performance,” *Malaria Journal*, vol. 19, no. 1, pp. 1–11, 2020.

[317] O. J. Watson, T. N.-A. Tran, R. J. Zupko, T. Symons, R. Thomson, T. Visser, S. Rumisha, P. A. Dzianach, N. Hathaway, I. Kim, *et al.*, “Global risk of selection and spread of plasmodium falciparum histidine-rich protein 2 and 3 gene deletions,” *medrxiv*, 2023.

[318] C. K. Murray, R. A. Gasser Jr, A. J. Magill, and R. S. Miller, “Update on rapid diagnostic testing for malaria,” *Clinical microbiology reviews*, vol. 21, no. 1, pp. 97–110, 2008.

[319] N. J. White, “Anaemia and malaria,” *Malaria Journal*, vol. 17, no. 1, p. 371, 2018.

[320] J. C. J. Calis, K. S. Phiri, and M. B. van Hensbroek, “Severe anemia in Malawian children-Reply,” *New England Journal of Medicine*, vol. 358, no. 21, p. 2291, 2008.

[321] J. Crawley, “Reducing the burden of anemia in infants and young children in malaria-endemic countries of Africa: from evidence to action,” *The Intolerable Burden of Malaria II: What’s New, What’s Needed: Supplement to Volume 71 (2) of the American Journal of Tropical Medicine and Hygiene*, 2004.

[322] W. Trager and J. B. Jensen, “Human malaria parasites in continuous culture,” *Journal of Parasitology*, vol. 91, no. 3, pp. 484–486, 2005.

[323] E. Hitz, A. C. Balestra, M. Brochet, and T. S. Voss, “Pfmap-2 is essential for male gametogenesis in the malaria parasite plasmodium falciparum,” *Scientific reports*, vol. 10, no. 1, p. 11930, 2020.

[324] C. Lambros and J. P. Vanderberg, “Synchronization of Plasmodium falciparum erythrocytic stages in culture,” *The Journal of parasitology*, pp. 418–420, 1979.

[325] United Republic of Tanzania, Ministry of Health and Social Welfare, National Malaria Control Programme, *National guidelines for malaria diagnosis, treatment and preventive therapies*, 2020. Accessed: 2024-09-17.

[326] S. Liu, Z. Deng, J. Li, J. Wang, N. Huang, R. Cui, Q. Zhang, J. Mei, W. Zhou, C. Zhang, Q. Ye, and J. Tian, "Measurement of the refractive index of whole blood and its components for a continuous spectral region.," *Journal of biomedical optics*, vol. 24, pp. 1–5, Mar. 2019.

[327] A. M. Banas, K. Banas, T. T. T. Chu, R. Naidu, P. E. Hutchinson, R. Agrawal, M. K. F. Lo, M. Kansiz, A. Roy, R. Chandramohanadas, and M. B. H. Breese, "Comparing infrared spectroscopic methods for the characterization of Plasmodium falciparum-infected human erythrocytes," *Communications Chemistry*, vol. 4, no. 1, p. 129, 2021.

[328] D. Payne, "Use and limitations of light microscopy for diagnosing malaria at the primary health care level," *Bulletin of the World Health Organization*, vol. 66, no. 5, p. 621, 1988.

[329] N. Ranadive, S. Kunene, S. Darteh, N. Ntshalintshali, N. Nhlabathi, N. Dlamini, S. Chitundu, M. Saini, M. Murphy, A. Soble, A. Schwartz, B. Greenhouse, and M. S. Hsiang, "Limitations of Rapid Diagnostic Testing in Patients with Suspected Malaria: A Diagnostic Accuracy Evaluation from Swaziland, a Low-Endemicity Country Aiming for Malaria Elimination," *Clinical Infectious Diseases*, vol. 64, pp. 1221–1227, May 2017.

[330] R. D. Kaaya, R. A. Kavishe, F. F. Tenu, J. J. Matowo, F. W. Mosha, C. Drakeley, C. J. Sutherland, and K. B. Beshir, "Deletions of the Plasmodium falciparum histidine-rich protein 2/3 genes are common in field isolates from north-eastern Tanzania," *Scientific reports*, vol. 12, no. 1, p. 5802, 2022.

[331] D. Schellenberg, C. Menendez, E. Kahigwa, F. Font, C. Galindo, C. Acosta, J. A. Schellenberg, J. J. Aponte, J. Kimario, and H. Urassa, "African children with malaria in an area of intense Plasmodium falciparum transmission: features on admission to the hospital and risk factors for death.," *The American journal of tropical medicine and hygiene*, vol. 61, no. 3, pp. 431–438, 1999.

[332] E. Kahigwa, D. Schellenberg, S. Sanz, J. J. Aponte, J. Wigayi, H. Mshinda, P. Alonso, and C. Menendez, "Risk factors for presentation to hospital with severe anaemia in Tanzanian children: a case–control study," *Tropical medicine& international health*, vol. 7, no. 10, pp. 823–830, 2002.

[333] L. F. V. Furtado, W. P. Alves, V. J. da Silva, and É. M. L. Rabelo, "Hookworm infection as a model for deepen knowledge of iron metabolism and erythropoiesis in anemia," *Cytokine*, vol. 177, p. 156559, 2024.

[334] C. P. Sharma, S. Sharma, and R. Singh, “Species discrimination from blood traces using ATR FT-IR spectroscopy and chemometrics: Application in wildlife forensics,” *Forensic Science International: Animals and Environments*, vol. 3, p. 100060, 2023.

[335] E. Mistek and I. K. Lednev, “FT-IR spectroscopy for identification of biological stains for forensic purposes,” 2018.

[336] E. Mistek, L. Halámková, and I. K. Lednev, “Phenotype profiling for forensic purposes: Nondestructive potentially on scene attenuated total reflection Fourier transform-infrared (ATR FT-IR) spectroscopy of bloodstains,” *Forensic Chemistry*, vol. 16, p. 100176, 2019.

[337] B. R. Wood, “Correction: The importance of hydration and DNA conformation in interpreting infrared spectra of cells and tissues,” *Chemical Society Reviews*, vol. 45, no. 7, p. 1999, 2016.

[338] E. Mistek-Morabito and I. K. Lednev, “Discrimination between human and animal blood by attenuated total reflection Fourier transform-infrared spectroscopy,” *Communications Chemistry*, vol. 3, no. 1, p. 178, 2020.

[339] M. P. Betancourth, A. Boldin, V. Ochoa-Gutierrez, R. Hogg, F. Baldini, M. G. Jiménez, K. Wynne, and D. Childs, “Towards fast quantum cascade laser spectrometers for high-throughput and cost-effective disease surveillance,” 2024.

[340] W. H. Organization, *WHO malaria policy advisory group (MPAG) meeting report, 18–20 April 2023*. World Health Organization, 2023.

[341] S. G. Thawer, F. Chacky, M. Runge, E. Reaves, R. Mandike, S. Lazaro, S. Mkude, S. F. Rumisha, C. Kumalija, and C. Lengeler, “Sub-national stratification of malaria risk in mainland Tanzania: a simplified assembly of survey and routine data,” *Malaria journal*, vol. 19, no. 1, pp. 1–12, 2020.

[342] D. Mategula, C. Mitambo, W. Sheahan, N. Masingi Mbeye, A. Gumbo, C. Kwizombe, J. Kawonga, B. Banda, G. Hamuza, A. Kalanga, D. Kamowa, J. Kafulafula, A. Banda, H. Twaibi, E. Musa, A. Kapito-Tembo, T. Ntwere, J. Chirombo, P. K. Kalonde, M. Masambuka, L. Munthali, M. Sakala, A. Bangoura, J. Gichuki, M. G. Chipeta, B. Galatas Adrade, M. Kayange, and D. J. Terlouw, “Malaria Burden Stratification in Malawi- A report of a consultative workshop to inform the 2023-2030 Malawi Malaria Strategic Plan.,” *Wellcome open research*, vol. 8, p. 178, 2023.

[343] M. I. Djaskano, M. Cissoko, M. S. I. Diar, D. K. Israel, K. H. é. Clément, A. M. Ali, M. Dormbaye, I. M. Souleymane, A. Batrane, and I. Sagara, “Stratification and adaptation of malaria control interventions in Chad,” *Tropical Medicine and Infectious Disease*, vol. 8, no. 9, p. 450, 2023.

[344] M. Cissoko, M. Magassa, V. Sanogo, A. Ouologuem, L. Sangaré, M. Diarra, C. S. Bationo, M. Dolo, M. D. Bah, S. Doumbia, M. B. Coulibaly, D. Traoré, B. Sidibé, J. Landier, I. Cissé, M. Sacko, J. Gaudart, and I. Sagara, “Stratification at the health district level for targeting malaria control interventions in Mali,” *Scientific Reports*, vol. 12, no. 1, p. 8271, 2022.

[345] S. G. Thawer, M. Golumbeanu, K. Munisi, S. Aaron, F. Chacky, S. Lazaro, A. Mohamed, N. Kisoka, C. Lengeler, F. Molteni, A. Ross, R. W. Snow, and E. Pothin, “The use of routine health facility data for micro-stratification of malaria risk in mainland Tanzania,” *Malaria Journal*, vol. 21, no. 1, p. 345, 2022.

[346] K. R. Rijal, B. Adhikari, N. Adhikari, S. P. Dumre, M. S. Banjara, U. T. Shrestha, M. R. Banjara, N. Singh, L. Ortegea, B. K. Lal, G. D. Thakur, and P. Ghimire, “Micro-stratification of malaria risk in Nepal: implications for malaria control and elimination,” *Tropical Medicine and Health*, vol. 47, no. 1, p. 21, 2019.

[347] S. G. Thawer, M. Golumbeanu, S. Lazaro, F. Chacky, K. Munisi, S. Aaron, F. Molteni, C. Lengeler, E. Pothin, R. W. Snow, and V. A. Alegana, “Spatio-temporal modelling of routine health facility data for malaria risk micro-stratification in mainland Tanzania,” *Scientific Reports*, vol. 13, no. 1, p. 10600, 2023.

[348] C. Kitojo, J. R. Gutman, F. Chacky, E. Kigadye, S. Mkude, R. Mandike, A. Mohamed, E. J. Reaves, P. Walker, and D. S. Ishengoma, “Estimating malaria burden among pregnant women using data from antenatal care centres in Tanzania: a population-based study,” *The Lancet Global Health*, vol. 7, no. 12, pp. e1695–e1705, 2019.

[349] V. A. Alegana, L. Suiyanka, P. M. Macharia, G. Ikahu-Muchangi, and R. W. Snow, “Malaria micro-stratification using routine surveillance data in Western Kenya,” *Malaria Journal*, vol. 20, pp. 1–9, 2021.

[350] J. E. Buring, *Epidemiology in medicine*, vol. 515. Lippincott Williams& Wilkins, 1987.

[351] World Health Organization (WHO), “A framework for malaria elimination,” tech. rep., 2017.

[352] V. A. Alegana, P. M. Macharia, S. Muchiri, E. Mumo, E. Oyugi, A. Kamau, F. Chacky, S. Thawer, F. Molteni, D. Rutazanna, C. Maiteki-Sebuguzi, S. Gonahasa, A. M. Noor, and R. W. Snow, "Plasmodium falciparum parasite prevalence in East Africa: Updating data for malaria stratification," *PLOS Global Public Health*, vol. 1, p. e0000014, Dec. 2021.

[353] J. Ssempiira, J. Kissa, B. Nambuusi, C. Kyozira, D. Rutazaana, E. Mukooyo, J. Opigo, F. Makumbi, S. Kasasa, and P. Vounatsou, "The effect of case management and vector-control interventions on space–time patterns of malaria incidence in Uganda," *Malaria journal*, vol. 17, pp. 1–11, 2018.

[354] P. Yekutiel, "Problems of epidemiology in malaria eradication.," *Bulletin of the World Health Organization*, vol. 22, no. 6, pp. 669–683, 1960.

[355] S. Brooker, J. H. Kolaczinski, C. W. Gitonga, A. M. Noor, and R. W. Snow, "The use of schools for malaria surveillance and programme evaluation in Africa," *Malaria journal*, vol. 8, pp. 1–9, 2009.

[356] C. Smith Gueye, G. Newby, J. Tulloch, L. Slutsker, M. Tanner, and R. D. Gosling, "The central role of national programme management for the achievement of malaria elimination: a cross case-study analysis of nine malaria programmes," *Malaria journal*, vol. 15, pp. 1–21, 2016.

[357] Bakar S, A. Holzschuh, A. Ross, L. Stuck, R. Abdul, A.-W. H. Al-Mafazy, I. Irema, A. Mbena, S. G. Thawer, S. J. Shija, S. M. Aliy, A. Ali, G. Fink, J. Yukich, and M. W. Hetzel, "Risk of imported malaria infections in Zanzibar: a cross-sectional study," *Infectious Diseases of Poverty*, vol. 12, no. 1, p. 80, 2023.

[358] ICF, "Tanzania demographic and health survey 2022 - final report ," 2023.

[359] F. Chacky, M. Runge, S. F. Rumisha, P. Machafuko, P. Chaki, J. J. Massaga, A. Mohamed, E. Pothin, F. Molteni, R. W. Snow, C. Lengeler, and R. Mandike, "Nationwide school malaria parasitaemia survey in public primary schools, the United Republic of Tanzania," *Malaria Journal*, vol. 17, no. 1, p. 452, 2018.

[360] R. A. Ashton, A. Bennett, A.-W. Al-Mafazy, A. K. Abass, M. I. Msellem, P. McElroy, S. P. Kachur, A. S. Ali, J. Yukich, and T. P. Eisele, "Use of routine health information system data to evaluate impact of malaria control interventions in Zanzibar, Tanzania from 2000 to 2015," *EClinicalMedicine*, vol. 12, pp. 11–19, 2019.

[361] G. J. H. Bastiaens, T. Bousema, and T. Leslie, "Scale-up of malaria rapid diagnostic tests and artemisinin-based combination therapy: challenges and perspectives in sub-Saharan Africa," *PLoS medicine*, vol. 11, no. 1, p. e1001590, 2014.

[362] A. M. Noor, P. W. Gething, V. A. Alegana, A. P. Patil, S. I. Hay, E. Muchiri, E. Juma, and R. W. Snow, “The risks of malaria infection in Kenya in 2009,” *BMC infectious diseases*, vol. 9, pp. 1–14, 2009.

[363] A. Manjurano, L. Okell, T. Lukindo, H. Reyburn, R. Olomi, C. Roper, T. G. Clark, S. Joseph, E. M. Riley, and C. Drakeley, “Association of sub-microscopic malaria parasite carriage with transmission intensity in north- eastern Tanzania,” pp. 1–8, 2011.

[364] C. Drakeley and H. Reyburn, “Out with the old, in with the new: the utility of rapid diagnostic tests for malaria diagnosis in Africa,” *Transactions of the Royal Society of Tropical Medicine and Hygiene*, vol. 103, no. 4, pp. 333–337, 2009.

[365] World Health Organization (WHO), “Universal access to malaria diagnostic testing: an operational manual,” *WHO Press*, vol. 12, no. 1, p. 31A, 2011.

[366] J. M. Roth, D. A. Korevaar, M. M. G. Leeflang, and P. F. Mens, “Molecular malaria diagnostics: a systematic review and meta-analysis,” *Critical reviews in clinical laboratory sciences*, vol. 53, no. 2, pp. 87–105, 2016.

[367] E. Kamau, S. Alemayehu, K. C. Feghali, D. Saunders, and C. F. Ockenhouse, “Multiplex qPCR for detection and absolute quantification of malaria,” *PloS one*, vol. 8, no. 8, p. e71539, 2013.

[368] B. Moonen, J. M. Cohen, R. W. Snow, L. Slutsker, C. Drakeley, D. L. Smith, R. R. Abeyasinghe, M. H. Rodriguez, R. Maharaj, M. Tanner, and G. Targett, “Operational strategies to achieve and maintain malaria elimination.,” *Lancet (London, England)*, vol. 376, pp. 1592–1603, Nov. 2010.

[369] J. F. Mosha, H. J. W. Sturrock, B. Greenhouse, B. Greenwood, C. J. Sutherland, N. Gadalla, S. Atwal, C. Drakeley, G. Kibiki, and T. Bousema, “Epidemiology of subpatent Plasmodium falciparum infection: implications for detection of hotspots with imperfect diagnostics,” *Malaria journal*, vol. 12, pp. 1–9, 2013.

[370] M. F. Finda, A. J. Limwagu, H. S. Ngowo, N. S. Matowo, J. K. Swai, E. Kaindoa, and F. O. Okumu, “Dramatic decreases of malaria transmission intensities in Ifakara, south-eastern Tanzania since early 2000s,” *Malaria Journal*, vol. 17, pp. 1–18, 2018.

[371] MoHCDGEC, “Ministry of Health, Community Development, Gender, Elderly and Children (MoHCDGEC). The 2021 school malaria and nutrition survey (SMNS) report Mainland Tanzania.,” 2022.

[372] E. P. Ruth, J. J. Kashaigili, and A. E. Majule, “Availability, Access and Use of Weather and Climate Information by Smallholder Farmers in the Kilombero River Catchment, Tanzania,” *Climate Impacts on Agricultural and Natural Resource Sustainability in Africa*, pp. 489–506, 2020.

[373] V. Kasiulevičius, V. Šapoka, and R. Filipavičiūtė, “Sample size calculation in epidemiological studies,” *Gerontologija*, vol. 7, no. 4, pp. 225–231, 2006.

[374] R. Arya, B. Antonisamy, and S. Kumar, “Sample size estimation in prevalence studies,” *The Indian Journal of Pediatrics*, vol. 79, pp. 1482–1488, 2012.

[375] W. G. Cochran, *Sampling Techniques*. Wiley publication in applied statistics, Wiley, 1977.

[376] J. C. Mouatcho and J. P. D. Goldring, “Malaria rapid diagnostic tests: challenges and prospects,” *Journal of medical microbiology*, vol. 62, no. 10, pp. 1491–1505, 2013.

[377] “National guidelines for malaria diagnosis and treatment, 2006 / United Republic of Tanzania, Ministry of Health and Social Welfare. [Dar es Salaam] : National Malaria Control Programme, [2006].”

[378] J. W. Bailey, J. Williams, B. J. Bain, J. Parker-Williams, P. L. Chiodini, and G. H. T. F. o. t. B. C. f. S. in Haematology, “Guideline: the laboratory diagnosis of malaria,” *British journal of haematology*, vol. 163, no. 5, pp. 573–580, 2013.

[379] World Health Organization (WHO), *Basic malaria microscopy*. World Health Organization, 2010.

[380] World Health Organization (WHO), “Malaria parasite counting,” tech. rep., 2016.

[381] “Quick-DNA™ Miniprep Kit, Rapid and simple isolation of ultra-pure DNA from biological liquids and cells,”

[382] L. M. Hofer, P. A. Kweyamba, R. M. Sayi, M. S. Chabo, S. L. Maitra, S. J. Moore, and M. M. Tambwe, “Malaria rapid diagnostic tests reliably detect asymptomatic Plasmodium falciparum infections in school-aged children that are infectious to mosquitoes,” *Parasites& Vectors*, vol. 16, no. 1, p. 217, 2023.

[383] N. Hofmann, F. Mwingira, S. Shekalaghe, L. J. Robinson, I. Mueller, and I. Felger, “Ultra-Sensitive Detection of Plasmodium falciparum by Amplification of Multi-Copy Subtelomeric Targets,” *PLOS Medicine*, vol. 12, p. e1001788, Mar. 2015.

[384] C. Hartung, A. Lerer, Y. Anokwa, C. Tseng, W. Brunette, and G. Borriello, "Open data kit: tools to build information services for developing regions," in *Proceedings of the 4th ACM/IEEE international conference on information and communication technologies and development*, pp. 1–12, 2010.

[385] W. McKinney, *Python for data analysis: Data wrangling with Pandas, NumPy, and IPython*. " O'Reilly Media, Inc.", 2012.

[386] J. R. Landis and G. G. Koch, "The Measurement of Observer Agreement for Categorical Data Published by : International Biometric Society Stable URL : https://www.jstor.org/stable/2529310," vol. 33, no. 1, pp. 159–174, 1977.

[387] S. R. Munoz and S. I. Bangdiwala, "Interpretation of Kappa and B statistics measures of agreement," *Journal of Applied Statistics*, vol. 24, no. 1, pp. 105–112, 1997.

[388] O. Babak and C. V. Deutsch, "Statistical approach to inverse distance interpolation," *Stochastic Environmental Research and Risk Assessment*, vol. 23, no. 5, pp. 543–553, 2009.

[389] P. E. McKight and J. Najab, "Kruskal-wallis test," *The corsini encyclopedia of psychology*, p. 1, 2010.

[390] P. E. McKnight and J. Najab, "Mann-Whitney U Test," *The Corsini encyclopedia of psychology*, p. 1, 2010.

[391] P. Sedgwick, "Spearman's rank correlation coefficient," *Bmj*, vol. 349, 2014.

[392] I. D. Ozodiegwu, A. O. Ogunwale, O. Surakat, J. O. Akinyemi, E. A. Bamgboye, A. F. Fagbamigbe, M. M. Bello, A.-M. Y. Adamu, P. Uhomobhi, C. Ademu, C. Okoronkwo, M. Adeleke, and I. O. Ajayi, "Description of the design of a mixed-methods study to assess the burden and determinants of malaria transmission for tailoring of interventions (microstratification) in Ibadan and Kano metropolis," *Malaria Journal*, vol. 22, no. 1, p. 255, 2023.

[393] A. I. Jiram, C. H. Ooi, J. M. Rubio, S. Hisam, G. Karnan, N. M. Sukor, M. M. Artic, N. P. Ismail, and N. W. Alias, "Evidence of asymptomatic submicroscopic malaria in low transmission areas in Belaga district, Kapit division, Sarawak, Malaysia," *Malaria journal*, vol. 18, pp. 1–12, 2019.

[394] P. Amratia, P. Psychas, B. Abuaku, C. Ahorlu, J. Millar, S. Oppong, K. Koram, and D. Valle, "Characterizing local-scale heterogeneity of malaria risk: a case study in Bunkpurugu-Yunyoo district in northern Ghana," *Malaria journal*, vol. 18, pp. 1–14, 2019.

[395] B. L. Rice, C. D. Golden, H. J. Randriamady, A. A. N. A. Rakotomalala, M. A. Vonona, E. J. G. Anjaranirina, J. Hazen, M. C. Castro, C. J. E. Metcalf, and D. L. Hartl, “Fine-scale variation in malaria prevalence across ecological regions in Madagascar: a cross-sectional study,” *BMC public health*, vol. 21, no. 1, p. 1018, 2021.

[396] P. Bejon, T. N. Williams, A. Liljander, A. M. Noor, J. Wambua, E. Ogada, A. Olotu, F. H. A. Osier, S. I. Hay, and A. Färnert, “Stable and unstable malaria hotspots in longitudinal cohort studies in Kenya,” *PLoS medicine*, vol. 7, no. 7, p. e1000304, 2010.

[397] V. A. Alegana, E. A. Okiro, and R. W. Snow, “Routine data for malaria morbidity estimation in Africa: challenges and prospects,” *BMC medicine*, vol. 18, pp. 1–13, 2020.

[398] A. R. Oduro, K. A. Bojang, D. J. Conway, T. Corrah, B. M. Greenwood, and D. Schellenberg, “Health centre surveys as a potential tool for monitoring malaria epidemiology by area and over time,” *PloS one*, vol. 6, no. 11, p. e26305, 2011.

[399] K. O. Mfuh, O. A. Achonduh-Atijegbe, O. N. Bekindaka, L. F. Esemu, C. D. Mbakop, K. Gandhi, R. G. F. Leke, D. W. Taylor, and V. R. Nerurkar, “A comparison of thick-film microscopy, rapid diagnostic test, and polymerase chain reaction for accurate diagnosis of Plasmodium falciparum malaria,” *Malaria journal*, vol. 18, no. 1, pp. 1–8, 2019.

[400] W. Oyibo, V. Latham, O. Oladipo, G. Ntadom, P. Uhomoibhi, N. Ogbulafor, C. Okoronkwo, F. Okoh, A. Mahmoud, E. Shekarau, O. Oresanya, Y. J. Cherima, I. Jalingo, B. Abba, M. Audu, and D. J. Conway, “Malaria parasite density and detailed qualitative microscopy enhances large-scale profiling of infection endemicity in Nigeria,” *Scientific Reports*, vol. 13, no. 1, p. 1599, 2023.

[401] P. Bejon, L. Andrews, A. Hunt-Cooke, F. Sanderson, S. C. Gilbert, and A. V. S. Hill, “Thick blood film examination for Plasmodium falciparum malaria has reduced sensitivity and underestimates parasite density,” *Malaria journal*, vol. 5, pp. 1–4, 2006.

[402] T. D. Swarthout, H. Counihan, R. K. K. Senga, and I. Van den Broek, “Paracheck-Pf® accuracy and recently treated Plasmodium falciparum infections: is there a risk of over-diagnosis? ,” *Malaria journal*, vol. 6, pp. 1–6, 2007.

[403] H. Reyburn, H. Mbakilwa, R. Mwangi, O. Mwerinde, R. Olomi, C. Drakeley, and C. J. M. Whitty, “Rapid diagnostic tests compared with malaria microscopy for guiding outpatient treatment of febrile illness in Tanzania: randomised trial,” *Bmj*, vol. 334, no. 7590, p. 403, 2007.

[404] T. A. Abeku, M. Kristan, C. Jones, J. Beard, D. H. Mueller, M. Okia, B. Rapuoda, B. Greenwood, and J. Cox, “Determinants of the accuracy of rapid diagnostic tests in malaria case management: evidence from low and moderate transmission settings in the East African highlands,” *Malaria journal*, vol. 7, pp. 1–10, 2008.

[405] H. Hopkins, W. Kambale, M. R. Kamya, S. G. Staedke, G. Dorsey, and P. J. Rosenthal, “Comparison of HRP2-and pLDH-based rapid diagnostic tests for malaria with longitudinal follow-up in Kampala, Uganda.,” *The American journal of tropical medicine and hygiene*, vol. 76, no. 6, pp. 1092–1097, 2007.

[406] I. Harris, W. W. Sharrock, L. M. Bain, K.-A. Gray, A. Bobogare, L. Boaz, K. Lilley, D. Krause, A. Vallely, and M.-L. Johnson, “A large proportion of asymptomatic Plasmodium infections with low and sub-microscopic parasite densities in the low transmission setting of Temotu Province, Solomon Islands: challenges for malaria diagnostics in an elimination setting,” *Malaria journal*, vol. 9, pp. 1–8, 2010.

[407] A. Laurent, J. Schellenberg, K. Shirima, S. C. Ketende, P. L. Alonso, H. Mshinda, M. Tanner, and D. Schellenberg, “Performance of HRP-2 based rapid diagnostic test for malaria and its variation with age in an area of intense malaria transmission in southern Tanzania,” *Malaria journal*, vol. 9, pp. 1–9, 2010.

[408] G. Mtove, B. Nadjm, B. Amos, I. C. E. Hendriksen, F. Muro, and H. Reyburn, “Use of an HRP2-based rapid diagnostic test to guide treatment of children admitted to hospital in a malaria-endemic area of north-east Tanzania,” *Tropical medicine& international health*, vol. 16, no. 5, pp. 545–550, 2011.

[409] D. J. Fryauff, E. Gomez-Saladin, I. Sumawinata, M. A. Sutamihardja, S. Tuti, B. Subianto, and T. L. Richie, “Comparative performance of the ParaSight F test for detection of Plasmodium falciparum in malaria-immune and nonimmune populations in Irian Jaya, Indonesia.,” *Bulletin of the World Health Organization*, vol. 75, no. 6, p. 547, 1997.

[410] D. Tao, B. McGill, T. Hamerly, T. Kobayashi, P. Khare, A. Dziedzic, T. Leski, A. Holtz, B. Shull, and A. E. Jedlicka, “A saliva-based rapid test to quantify the infectious subclinical malaria parasite reservoir,” *Science translational medicine*, vol. 11, no. 473, p. eaan4479, 2019.

[411] I. H. Mshani, F. M. Jackson, R. Y. Mwanga, P. A. Kweyamba, E. P. Mwanga, M. M. Tambwe, L. M. Hofer, D. J. Siria, M. González-Jimé nez, and K. Wynne, "Screening of malaria infections in human blood samples with varying parasite densities and anaemic conditions using AI-Powered mid-infrared spectroscopy," *Malaria Journal*, vol. 23, no. 1, p. 188, 2024.

[412] T. Bousema, L. Okell, I. Felger, and C. Drakeley, "Asymptomatic malaria infections: detectability, transmissibility and public health relevance," *Nature Reviews Microbiology*, vol. 12, no. 12, pp. 833–840, 2014.

[413] A. B. Björkman, "Asymptomatic low-density malaria infections: a parasite survival strategy?," *The Lancet infectious diseases*, vol. 18, no. 5, pp. 485–486, 2018.

[414] A. Björkman and U. Morris, "Why Asymptomatic Plasmodium falciparum Infections Are Common in Low-Transmission Settings.," *Trends in parasitology*, vol. 36, pp. 898–905, Nov. 2020.

[415] T.-N. Nguyen, L. von Seidlein, T.-V. Nguyen, P.-N. Truong, S. Do Hung, H.-T. Pham, T.-U. Nguyen, T. D. Le, M. Mukaka, and N. P. J. Day, "The persistence and oscillations of submicroscopic Plasmodium falciparum and Plasmodium vivax infections over time in Vietnam: an open cohort study," *The Lancet Infectious Diseases*, vol. 18, no. 5, pp. 565–572, 2018.

[416] W. H. Organization *et al.*, "Who guidelines for malaria, 14 march 2023," tech. rep., World Health Organization, 2023.

[417] World Health Organization (WHO), *Operational manual on indoor residual spraying*. 2024.

[418] Y. A. Williams, L. S. Tusting, S. Hocini, P. M. Graves, G. F. Killeen, I. Kleinschmidt, F. O. Okumu, R. G. A. Feachem, A. Tatarsky, and R. D. Gosling, "Chapter Six - Expanding the Vector Control Toolbox for Malaria Elimination: A Systematic Review of the Evidence," vol. 99, pp. 345–379, Academic Press, 2018.

[419] O. O. Oyegoke, L. Maharaj, O. P. Akoniyon, I. Kwoji, A. T. Roux, T. S. Adewumi, R. Maharaj, B. T. Oyebola, M. A. Adeleke, and M. Okpeku, "Malaria diagnostic methods with the elimination goal in view," *Parasitology research*, vol. 121, no. 7, pp. 1867–1885, 2022.

[420] M. Tedla, "A focus on improving molecular diagnostic approaches to malaria control and elimination in low transmission settings: Review," *Parasite Epidemiology and Control*, vol. 6, p. e00107, 2019.

[421] M. L. McMorrow, M. Aidoo, and S. P. Kachur, “Malaria rapid diagnostic tests in elimination settings—can they find the last parasite?,” *Clinical Microbiology and Infection*, vol. 17, no. 11, pp. 1624–1631, 2011.

[422] C. Whittaker, H. Slater, R. Nash, T. Bousema, C. Drakeley, A. C. Ghani, and L. C. Okell, “Global patterns of submicroscopic Plasmodium falciparum malaria infection: insights from a systematic review and meta-analysis of population surveys,” *The Lancet Microbe*, vol. 2, no. 8, pp. e366–e374, 2021.

[423] M. S. Cordray and R. R. Richards-Kortum, “Emerging nucleic acid–based tests for point-of-care detection of malaria,” *The American journal of tropical medicine and hygiene*, vol. 87, no. 2, p. 223, 2012.

[424] P. Mens, N. Spieker, S. Omar, M. Heijnen, H. Schallig, and P. A. Kager, “Is molecular biology the best alternative for diagnosis of malaria to microscopy? A comparison between microscopy, antigen detection and molecular tests in rural Kenya and urban Tanzania,” *Tropical Medicine& International Health*, vol. 12, no. 2, pp. 238–244, 2007.

[425] B. Gitta and N. Kilian, “Diagnosis of malaria parasites Plasmodium spp. in endemic areas: current strategies for an ancient disease,” *BioEssays*, vol. 42, no. 1, p. 1900138, 2020.

[426] C. Wongsrichanalai, M. J. Barcus, S. Muth, A. Sutamihardja, and W. H. Wernsdorfer, “A review of malaria diagnostic tools: microscopy and rapid diagnostic test (RDT),” *Defining and Defeating the Intolerable Burden of Malaria III: Progress and Perspectives: Supplement to Volume 77 (6) of American Journal of Tropical Medicine and Hygiene*, 2007.

[427] A. Fadlelmoula, S. O. Catarino, G. Minas, and V. Carvalho, “A Review of Machine Learning Methods Recently Applied to FTIR Spectroscopy Data for the Analysis of Human Blood Cells.,” *Micromachines*, vol. 14, May 2023.

[428] K. Kochan, D. E. Bedolla, D. Perez-Guaita, J. A. Adegoke, T. Chakkumpulakkal Puthan Veettil, M. Martin, S. Roy, S. Pebotuwa, P. Heraud, and B. R. Wood, “Infrared Spectroscopy of Blood,” *Applied Spectroscopy*, vol. 75, pp. 611–646, Dec. 2020.

[429] I. H. Mshani, F. M. Jackson, E. G. Minja, S. Abbas, N. S. Lilolime, F. E. Makala, A. B. Lazaro, I. S. Mchola, L. N. Mukabana, and N. Kahamba, “Comparison of Fine-Scale Malaria Strata Derived from Population Survey Data Collected Using mRDTs, Microscopy and qPCR in South-Eastern Tanzania,” *medRxiv*, pp. 2006–2024, 2024.

[430] T. The United Republic of Tanzania (URT), Ministry of Finance and Planning, O. of the National Bureau of Statistics and President's Office - Finance and Planning, and Z. Chief Government Statistician, "The 2022 Population and Housing Census: Administrative Units Population Distribution Report; Tanzania, December 2022.,"

[431] F. Kato, "Development of a major rice cultivation area in the Kilombero Valley, Tanzania," *African study monographs. Supplementary issue.*, vol. 36, pp. 3–18, 2007.

[432] D. B. Mosha and G. Boniface, "The impact of rice commercialisation on livelihoods in Kilombero Valley, Tanzania: anybody left behind?," *Tanzania Journal of Agricultural Sciences*, vol. 21, no. 1, pp. 252–262, 2022.

[433] J. R. Forney, C. Wongsrichanalai, A. J. Magill, L. G. Craig, J. Sirichaisinthop, C. T. Bautista, R. S. Miller, C. F. Ockenhouse, K. E. Kester, N. E. Aronson, E. M. Andersen, H. A. Quino-Ascurra, C. Vidal, K. A. Moran, C. K. Murray, C. C. DeWitt, D. G. Heppner, K. C. Kain, W. R. Ballou, and R. A. Gasser, "Devices for rapid diagnosis of malaria: Evaluation of prototype assays that detect Plasmodium falciparum histidine-rich protein 2 and a Plasmodium vivax-specific antigen," *Journal of Clinical Microbiology*, 2003.

[434] D. Perez-guaita, K. M. Marzec, A. Hudson, C. Evans, T. Chernenko, C. Mattha, M. Miljkovic, M. Diem, P. Heraud, J. S. Richards, D. Andrew, D. A. Anderson, C. Doerig, J. Garcia-bustos, D. Mcnaughton, and B. R. Wood, "Parasites under the Spotlight : Applications of Vibrational Spectroscopy to Malaria Research," 2018.

[435] M. T. Sikulu-lord, M. F. Maia, M. P. Milali, M. Henry, G. Mkandawile, E. A. Kho, R. A. Wirtz, L. E. Hugo, F. E. Dowell, and G. J. Devine, "Rapid and Non-destructive Detection and Identification of Two Strains of Wolbachia in Aedes aegypti by Near-Infrared Spectroscopy," pp. 1–12, 2016.

[436] E. P. Mwanga, I. S. Mchola, F. E. Makala, I. H. Mshani, D. J. Siria, S. H. Mwinyi, S. Abbasi, G. Seleman, J. N. Mgaya, and M. G. Jiménez, "Rapid assessment of the blood-feeding histories of wild-caught malaria mosquitoes using mid-infrared spectroscopy and machine learning," *Malaria Journal*, vol. 23, no. 1, p. 86, 2024.

[437] E. P. Mwanga, D. J. Siria, I. H. Mshani, S. H. Mwinyi, S. Abbasi, M. G. Jimenez, K. Wynne, F. Baldini, S. A. Babayan, and F. O. Okumu, "Rapid classification of epidemiologically relevant age categories of the malaria vector, Anopheles funestus," *Parasites& Vectors*, vol. 17, no. 1, p. 143, 2024.

[438] Z. G. Najafabadi, H. Oormazdi, L. Akhlaghi, A. R. Meamar, M. Nateghpour, L. Farivar, and E. Razmjou, “Detection of Plasmodium vivax and Plasmodium falciparum DNA in human saliva and urine: loop-mediated isothermal amplification for malaria diagnosis,” *Acta tropica*, vol. 136, pp. 44–49, 2014.

[439] C. J. Sutherland and R. Hallett, “Detecting malaria parasites outside the blood,” *Journal of Infectious Diseases*, vol. 199, no. 11, pp. 1561–1563, 2009.

[440] A. Kong, S. A. Wilson, Y. Ah, D. Nace, E. Rogier, and M. Aidoo, “HRP2 and HRP3 cross-reactivity and implications for HRP2-based RDT use in regions with Plasmodium falciparum hrp2 gene deletions,” *Malaria Journal*, vol. 20, no. 1, p. 207, 2021.

[441] I. Molina-de la Fuente, A. Pastor, Z. Herrador, A. Benito, and P. Berzosa, “Impact of Plasmodium falciparum pfhrp2 and pfhrp3 gene deletions on malaria control worldwide: a systematic review and meta-analysis,” *Malaria journal*, vol. 20, no. 1, p. 276, 2021.

[442] M. Gendrot, R. Fawaz, J. Dormoi, M. Madamet, and B. Pradines, “Genetic diversity and deletion of Plasmodium falciparum histidine-rich protein 2 and 3: a threat to diagnosis of P. falciparum malaria.,” *Clinical microbiology and infection : the official publication of the European Society of Clinical Microbiology and Infectious Diseases*, vol. 25, pp. 580–585, May 2019.

[443] O. J. Watson, T. N.-A. Tran, R. J. Zupko, T. Symons, R. Thomson, T. Visser, S. Rumisha, P. A. Dzianach, N. Hathaway, I. Kim, J. J. Juliano, J. A. Bailey, H. Slater, L. Okell, P. Gething, A. Ghani, M. F. Boni, J. B. Parr, and J. Cunningham, “Global risk of selection and spread of Plasmodium falciparum histidine-rich protein 2 and 3 gene deletions,” *medRxiv*, p. 2023.10.21.23297352, Jan. 2024.

[444] E. Lo, G. Zhou, W. Oo, Y. Afrane, A. Githeko, and G. Yan, “Low parasitemia in submicroscopic infections significantly impacts malaria diagnostic sensitivity in the highlands of Western Kenya,” *PloS one*, vol. 10, no. 3, p. e0121763, 2015.

[445] Y. P. Mlacha, D. Wang, P. P. Chaki, T. Gavana, Z. Zhou, M. G. Michael, R. Khatib, G. Chila, H. M. Msuya, and E. Chaki, “Effectiveness of the innovative 1, 7-malaria reactive community-based testing and response (1, 7-mRCTR) approach on malaria burden reduction in Southeastern Tanzania,” *Malaria journal*, vol. 19, pp. 1–12, 2020.

[446] M. D. Corbacho-Loarte, C. Crespillo-Andújar, S. Chamorro-Tojeiro, F. Norman, J. A. Pérez-Molina, O. Martín, J. M. Rubio, B. Gullón-Peña, R. López-Vélez, and B. Monge-Maillo, “Screening of imported malaria infection in asymptomatic migrants from Sub-Saharan Africa: A retrospective analysis of a 2010–2019 cohort,” *Travel Medicine and Infectious Disease*, vol. 49, p. 102411, 2022.

[447] T. Smith, J. D. Charlwood, J. Kihonda, S. Mwankusye, P. Billingsley, J. Meuwissen, E. Lyimo, W. Takken, T. Teuscher, and M. Tanner, “Absence of seasonal variation in malaria parasitaemia in an area of intense seasonal transmission,” *Acta Tropica*, vol. 54, no. 1, pp. 55–72, 1993.

[448] T. Smith, J. D. Charlwood, A. Y. Kitua, H. Masanja, S. Mwankusye, P. L. Alonso, and M. Tanner, “Relationships of malaria morbidity with exposure to Plasmodium falciparum in young children in a highly endemic area.,” *The American journal of tropical medicine and hygiene*, vol. 59, no. 2, pp. 252–257, 1998.

[449] T. L. Russell, D. W. Lwetoijera, D. Maliti, B. Chipwaza, J. Kihonda, J. D. Charlwood, T. A. Smith, C. Lengeler, M. A. Mwanyangala, R. Nathan, B. G. Knols, W. Takken, and G. F. Killeen, “Impact of promoting longer-lasting insecticide treatment of bed nets upon malaria transmission in a rural Tanzanian setting with pre-existing high coverage of untreated nets,” *Malaria Journal*, vol. 9, no. 1, pp. 1–14, 2010.

[450] F. Okumu and M. Finda, “Key characteristics of residual malaria transmission in two districts in south-eastern Tanzania—implications for improved control,” *The Journal of infectious diseases*, vol. 223, no. Supplement 2, pp. S143–S154, 2021.

[451] M. F. Finda, I. R. Moshi, A. Monroe, A. J. Limwagu, A. P. Nyoni, J. K. Swai, H. S. Ngowo, E. G. Minja, L. P. Toe, and E. W. Kaindoa, “Linking human behaviours and malaria vector biting risk in south-eastern Tanzania,” *PloS one*, vol. 14, no. 6, p. e0217414, 2019.

[452] H. Wang, Y. Qiang, C. Chen, W. Liu, T. Hu, Z. Li, and G. Chen, “Online partial label learning,” in *Machine Learning and Knowledge Discovery in Databases: European Conference, ECML PKDD 2020, Ghent, Belgium, September 14–18, 2020, Proceedings, Part II*, pp. 455–470, Springer, 2021.

[453] L. Roy, S. Mondal, N. Bhattacharyya, R. Ghosh, A. Banerjee, S. Singh, A. Chattopadhyay, S. A. Ahmed, R. S. Jassas, M. M. Al-Rooqi, Z. Moussa, I. I. Althagafi, D. Bhattacharya, K. Bhattacharya, A. K. Mallick, and S. K. Pal, “A spectroscopy based prototype for the noninvasive detection of diabetes from human saliva using nanohybrids acting as nanozyme,” *Scientific Reports*, vol. 13, no. 1, p. 17306, 2023.